THE UNIVERSITY
of EDINBURGH

Characterisation of skeletal development and the use of anabolic agents in murine models of Duchenne muscular dystrophy

---

Claire Wood

This thesis is presented for the degree of Doctor of Philosophy at the University of Edinburgh

2019

Declaration

I declare that this thesis has been composed entirely by the candidate, Claire Louise Wood. This work has not been previously been submitted for a Doctor of Philosophy degree or any professional qualification. I have done all the work, unless acknowledged otherwise. All sources of information have been acknowledged.

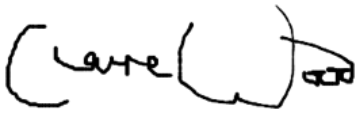

Claire Wood

Acknowledgements

Firstly I would like to thank Colin Farquharson for his outstanding and unwavering support as my main supervisor and also to Faisal Ahmed, Jarod Wong and Volker Straub for their valuable contributions throughout my studies.

I would also like to thank my mentors in Newcastle, Tim Cheetham and Simon Pearce, for their encouragement and help in securing my fellowship and to the MRC and MDUK for co-funding and giving me the opportunity to design and carry out this project.

Thank you to everyone in the Bone Biology group at Roslin for their advice and friendship during my PhD and in particular Elaine Seawright for helping me get established in the lab.

I would also like to acknowledge the help of Gemma Charlesworth and Rob van ‘t Hof at the University of Liverpool for their technical support with the micro-CT and to Karla Suchaki and Will Cawthorn at the QMRI for helping me to analyse the bone marrow adiposity data.

Thanks also to all the staff in the BRF for the organisation and care of the mice during these studies, without whom this project would not be possible.

Finally, my family and friends have been a huge support throughout my career and I would like to thank in particular Charlie and Imogen for their patience, understanding and encouragement over the past 3 years.

I would like to dedicate this thesis to my mum.

Abstract

Short stature and osteoporosis are common in Duchenne muscular dystrophy (DMD) and its pathophsyiology may include an abnormality of the growth hormone/insulin-like growth factor 1 (GH/IGF-1) axis, which is further exacerbated by glucocorticoid (GC) treatment. The mechanisms that underlie the undesirable effects of GCs on skeletal development are unclear and there is no proven intervention. Investigation of compounds to treat the defect in growth and skeletal development in GC treated DMD boys necessitates an appropriate pre-clinical model, but at present there is no established animal model to investigate GC effects on skeletal development. The *mdx* mouse is commonly used but its phenotype is mild and few medications that have shown benefit in the *mdx* mouse have also shown efficacy in clinical trials. The *mdx*:*cmah* mouse carries a human-like mutation in the *Cmah* gene and has a more severe muscle phenotype, but its growth and bone characteristics have never been investigated.

This thesis tested the overall hypothesis that "GC- treated mouse models of Duchenne muscular dystrophy (DMD) have an abnormality of linear growth and skeletal development that can be rescued by modulation of the growth hormone (GH)/ insulin-like growth factor-1 (IGF-1) axis.

Firstly the growth and bone phenotype of the *mdx*, *mdx:utr* and *mdx:cmah* muscular dystrophy mouse models were characterised. No clear intrinsic skeletal defect were observed in the *mdx* or *mdx:utr* mice. Furthermore, *mdx:cmah* mice showed clear evidence of catch-up growth that was also associated with an increase in bone development. This pattern does not mimic the typical DMD growth trajectory. Whilst the utility of the *mdx:cmah* mouse for studying growth and skeletal development in DMD may be limited, further studies of this model may shed light on the phenomenon of catch-up growth.

In the second part of the project, the aim was to identify a suitable GC regimen to induce both growth retardation and osteoporosis in juvenile *mdx and mdx:cmah* mice and their wildtype C57BL10 controls. C57BL10 mice appeared fairly resistant to GC challenge; despite high doses no biomechanical or trabecular architecture changes were noted. Prednisolone 20mg/kg body weight given by oral gavage appeared to be

the most effective regimen to induce growth retardation and osteoporosis over a 28-day period. A GC-sparing agent, VBP-6 was also examined as an alternative to GC, with the aim of further characterising its effects on skeletal development. This thesis has provided extra data to support the clinical trials that are currently investigating the use of VBP-15 (a VBP-6 analogue) as a GC-sparing agent in DMD and provides further evidence that VBP-6 is able to improve muscle function without the deleterious skeletal side-effects. VBP-6 could potentially be used as an alternative in other childhood conditions that necessitate the use of long-term GCs.

The final part of the project explored the potential of GH and IGF-1 given in combination to rescue the growth retardation and cortical bone defect seen during 4 weeks of prednisolone treatment in *mdx* mice. This intervention study determined that growth retardation could be rescued by combined GH/IGF-1 treatment but the osteopenia phenotype could not. As short stature remains one of the most significant concerns for boys with DMD as their life expectancy increases, it may now be appropriate to design a pilot clinical study to evaluate the safety and tolerability of combination GH and IGF-1 therapy in a small group of patients with DMD.

Lay abstract

Duchenne muscular dystrophy (DMD) is a severe and ultimately fatal disease. It affects up to 1 in 4000 males and there is no cure. Steroids are the only treatment that can help slow down muscle weakness but they have many side effects including growth failure and low bone mass (osteoporosis). The reasons for these unwanted side effects are unclear, but even boys who are not treated with steroids tend to be short and have weak bones. It may be that because DMD is a chronic inflammatory process, this disrupts the growth hormone (GH) /insulin-like growth factor (IGF-1) pathway. GH is produced by the anterior pituitary gland. It can act directly on the skeleton, but mainly acts indirectly, through IGF-1. Together the GH/IGF-1 pathway plays a crucial role in regulating normal bone growth and bone mass during childhood, and children with either GH or IGF-1 deficiency are short and may have low bone mass. There are no treatments available to help bone growth in DMD but new treatment regimens may be identified by studying mouse models of DMD.

The mouse model commonly used in DMD research is the X-linked Muscular Dystrophy (*mdx*) mouse, but it has significant limitations because the disease process is not as severe as in patients with Duchenne. Very few medications that are effective in the *mdx* mouse have shown to be useful in patients. Therefore I have tested a new mouse model, the *mdx:cmah* mouse. This mouse is bred from the *mdx* mouse, but also has an additional gene deletion to make it more 'human' and therefore I had hoped that it would behave in similar way to patients with Duchenne. I have looked, for the first time, at bone and growth in the *mdx:cmah* mouse and compared it both to the *mdx* and a healthy 'wildtype' mouse. Instead of finding impaired growth and skeletal development, I actually demonstrated that the *mdx:cmah* mouse shows catch-up growth and no evidence of impaired bone development. Although it does not appear to be an appropriate model to investigate bone and growth in DMD it may prove to be a useful model to study catch-up growth.

During the second part of the project, I gave both DMD mouse models and wildtype mice different regimens of steroids to determine which was the most effective at impairing their growth and bone development. I also tested a new steroid-sparing agent, known as VBP-6 and proved that it was able to improve muscle strength without causing the other steroid side-effects on the skeleton. This information will be

helpful to provide extra evidence to support the use of VBP-6 in clinical trials of childhood conditions, where steroids are usually used.

After finding an effective steroid regimen, the final part of the project involved testing whether the GC-treated *mdx* mice responded to a combination of GH and IGF-1. I found that the combination of GH and IGF-1 was able to rescue the growth retardation but not the bone defect. This work is very important because both GH and IGF-1 are readily available and are already used in children, so this work could now be carried out as a clinical trial in patients with DMD to see if the combination of GH and IGF-1 are also able to lessen the short stature in steroid-treated patients with DMD.

Publications

1. **Wood CL**, Straub V. Bone in muscular dystrophies- what do we know? Curr Opin Neurol 2018. PMID: 30080716
2. **Wood CL**, Soucek O, Wong SC et al. Animal Models for Exploring the Adverse Effects of Glucocorticoids on Bone Growth and Glucocorticoid-Induced Osteoporosis. J Endocrinol 2017. PMID: 29051192
3. **Wood CL**, Ahmed SF. Bone protective agents in childhood. Arch Dis Child 2017 PMID: 29066521
4. **Wood CL**, Cheetham T. Treatment of Duchenne muscular dystrophy: first small steps Lancet 2017. PMID: 28728957
5. **Wood CL,** Wood CL, Suchaki K, van 't Hof R, Cawthorn W, Dillon S, Straub V, Wong SC, Ahmed SF, Farquharson C. The utility of the *mdx:cmah* mouse as a model for assessing skeletal development in Duchenne muscular dystrophy. Submitted to DMM May 2019.

Prizes

1. **April 2019**: Second prize oral presentation at Roslin Institute student research day.
2. **March 2019:** Birrell-Gray travelling scholarship, awarded to attend ENDO.
3. **December 2018:** First prize poster at Edinburgh Musculoskeletal Group Winter Symposium.
4. **April 2018:** First prize poster at Roslin Institute student research Day.
5. **November 2017:** British Society for Paediatric Endocrinology Research Award.

Presentations

1. **April 2019:** Oral presentation, "Insulin-like growth factor 1 and growth hormone given in combination can overcome the growth retardation in glucocorticoid treated *mdx* mice but not the osteoporosis." Roslin Institute Student Research day, Edinburgh.
2. **April 2019:** Poster presentation, " The utility of *mdx:cmah* as a model for assessing skeletal development in Duchenne muscular dystrophy (DMD). A comparison of the *mdx* and the *mdx:cmah* models". Neuromuscular Translational Research Conference, Newcastle.

3. **March 2019:** Poster presentation, **"**Establishment of a Glucocorticoid (GC) Regimen to Induce both Growth Retardation and Osteoporosis in C57BL10 Muscular Dystrophy Mouse Models.**"** ENDO, New Orleans.
4. **December 2018:** Poster presentation, "Establishment of a Glucocorticoid (GC) Regimen to Induce both Growth Retardation and Osteoporosis in C57BL10 Muscular Dystrophy Mouse Models." Musculoskeletal Group Winter Symposium, Edinburgh.
5. **April 2018:** Poster presentation, "Characterisation of skeletal development in mouse models of Duchenne Muscular Dystrophy. " Roslin Institute student research day, Edinburgh.
6. **November 2017:** Oral presentation, "Characterisation of skeletal development in mouse models of Duchenne Muscular Dystrophy." British Society for Paediatric Endocrinology and Diabetes, Newcastle.

Invited talks

1. **April 2019:** Bones and growth in DMD- from bench to bedside. Muscular Dystrophy UK English Conference.
2. **November 2017:** Growth and development of muscle and bone in neuromuscular disorders. Muscular Dystrophy UK Scottish Conference.
3. **November 2017:** Skeletal actions of glucocorticoids: In vivo models. At British Endocrine Society conference.
4. **January 2017:** Osteopaenia of Prematurity at Northern Skeletal Bone Health day.
5. **November 2016:** Chair of vitamin D symposium at British Endocrine Society conference
6. **May 2016:** Bone Health in children and young adults with DMD at Update in Neuromuscular Disorders course (run by UCL),

Abbreviations

ADP	Adenosine diphosphate
ALP	Alkaline phosphatase
ALS	Acid labile subunit
αMEM	Alpha minimum essential media
ANOVA	Analysis of variance
ASBMR	American Society of Bone and Mineral Research
ATP	Adenosine triphosphate
BGP	Beta glycerophosphate
BMD	Bone mineral density
BMP	Bone morphogenetic protein
BrdU	5- Bromo 2'-deoxyuridine
BRF	Biological Research Facility
BVTV	Bone volume/tissue volume
BW	Bodyweight
C/EBP	CAAT enhancer binding protein
CK	Creatine Kinase
cmah	Cytidine monophosphate-N-acetylneuraminic acid hydroxylase
cMAT	Constitutive marrow adipose tissue
Ct.Ar	Cortical area
CT	Computed tomography
Ct.Th	Cortical thickness
CTx	Beta-crosslaps
DAB	3,3'- diaminobenzidine
DAPI	4',6-diamidino-2-phenylindole
DXA	Dual x-ray absorpiometry
DMD	Duchenne muscular dystrophy
DNA	Deoxyribonucleic acid
ECM	Extracellular matrix
EDTA	Ethylenediaminetetraacetic acid
FBS	Fetal bovine serum
GC	Glucocorticoid
GH	Growth hormone
GHR	Growth hormone receptor
GHRH	Growth hormone releasing hormone
GIO	Glucocorticoid-induced osteoporosis

GP	Growth plate
GR	Glucocorticoid receptor
GRE	Glucocorticoid response element
H& E	Haematoxylin and eosin
IGF-1	Insulin-like growth factor 1
IGF-1R	Insulin-like growth factor 1 receptor
IGFBP	Insulin-like growth factor binding protein
IHC	Immunohistochemistry
JAK	Janus tyrosine kinase
JWMDRC	John Walton Muscular Dystrophy Research Centre
MAT	Marrow adipose tissue
$MgCl_2$	Magnesium chloride
Micro CT or μCT	Micro computed tomography
MiRNAs	Micro ribonucleic acids
MR	Mineralocorticoid receptor
Ms:Bs	Mineralisign surface: bone surface
NBF	Neutral buffered formalin
Neu5GC	N-glycolyneuraminic acid
NFKβ	Nuclear factor kappa beta
NH_4	Ammonium
OPG	Osteoprotegrin
PBS	Phosphate buffered saline
PCNA	Proliferating cell nuclear antigen
PCR	Polymerase chain reaction
%	Percentage
PFA	Paraformaldeyde
PHOSPHO 1	Phosphoethanolamine/ phosphocholine phosphatase1
PI3K	Phosphoinositide-3-kinase
POC	Primary ossification centre
PPARγ2	Peroxisome proliferator-activated receptor gamma
PTH	Parathyroid hormone
qPCR	Quantitative polymerase chain reaction
RANKL	Receptor activator of nuclear factor kappa beta ligand
rMAT	Regulated marrow adipose tissue
RNA	Ribonucleic acid
RT	Room temperature
Runx2	Runt-related transcription factor 2
SMI	Structural model index

SOC	Secondary ossification centre
STAT	Signal transducer and activator
TA	Tibialis anterior
Tb. Sp	Trabecular separation
Tb.Th	Trabecular thickness
TGFβ	Transforming growth factor beta
TMB	3,3' 5,5' tetramethylbenzidine
TMD	Tissue mineral density
TRAP	Tartrate-resistant acid phosphatase
TNAP	Tissue non-specific alkaline phosphatase
TNF	Tumour necrosis factor
TRIS	Trisaminomethane
TREAT-NMD	Treat Neuromuscular Disease
TUNEL	TdT-mediated dUTP nick-end labelling
VEGF	Vascular endothelial growth factor
Wnt	Wingless/integrated
WT	Wildtype

Table of Contents

CHAPTER 1

Introduction and literature review

1 Introduction and literature review

1.1. Bone structure

The bony skeleton not only provides physical support and protection for vital organs but is also a crucial storage site for bone marrow and essential ions such as calcium and phosphorus. In addition, bone is a highly dynamic endocrine organ and undertakes continual modelling or remodelling in response to its environment (Crockett *et al.* 2011). The structure of bone varies dependent on its site and function within the body. Cortical bone forms approximately 80% of the mature skeleton (Clarke 2008). In long bones the diaphysis comprises almost exclusively cortical bone, whilst vertebral bodies and the metaphysis of long bones contain mainly trabecular bone. Cortical and trabecular bone have the same basic structure but the density and corresponding compressive strength of cortical bone is much greater (Sommerfeldt *et al.* 2001). Within the cortex, osteons form concentric layers, or lamellae of compact bone with inner Haversian canals containing blood vessels and nerves (Figure 1-1). Trabeculae make up a three dimensional structure of bony processes. The larger surface area and proximity of trabeculae to blood vessels in the bone marrow enable greater deformation to occur and a rapid response to changes in load and the environment.

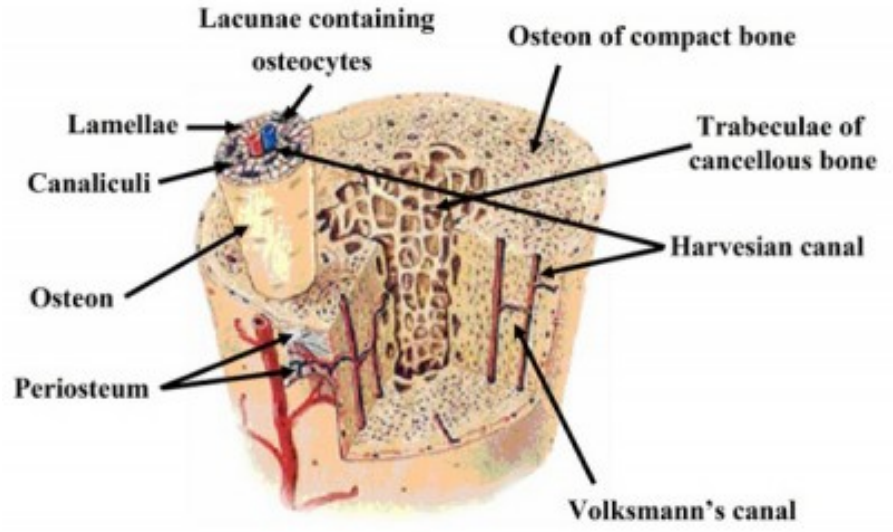

Figure 1-1 The differences between trabecular (cancellous) and cortical (compact) bone. Reproduced from (Cowin *et al.* 2015)

Bone is made up of inorganic salts and an organic matrix. The inorganic material comprises mainly calcium and phosphate ions which complex together to form hydroxyapatite crystals. The organic matrix is made predominantly of collagenous proteins and in particular type I collagen and also non-collagenous proteins, including osteocalcin, osteopontin, bone morphogenetic proteins (BMPs), and growth factors such as platelet-derived growth factor and IGF-1 and IGF-2. (Robey 2008). Bone cells comprise four main types: osteocytes, osteoblasts, osteoclasts and lining cells.

1.1.1 Osteocytes

Osteocytes account for 95% of all bone cells and have a lifespan of up to 25 years (Florencio-Silva *et al.* 2015). They resemble dendrites and are found in lacunae surrounded by the matrix of mineralised bone. Although osteocytes were previously thought to be passive cells, their dynamic nature and vital role in gatekeeping during bone remodelling has now been established. They are formed during the terminal differentiation of osteoblasts and their main role is to convert mechanical stimuli into a biological response (Aubin 1998, Kogianni *et al.* 2007). Load-induced strain causes micro-damage and initiates apoptosis of osteocytes and results in the release of receptor activator of nuclear factor kappa beta ligand (RANKL), which stimulates osteoclast formation and activity. Osteocytes also produce sclerostin, which is an inhibitor of wingless/integrated (Wnt) signalling and bone formation.

1.1.2 Osteoclasts

Osteoclasts are large multinucleated cells that originate from haematopoietic stem cells, which also give rise to macrophages. The osteoclast precursor cells fuse at the bone surface to form multi-nucleated osteoclasts which reside in specialised cavities known as Howship's lacunae. Their function is to resorb bone and they have a specialised cell membrane, known as the ruffled border, which is essential for their resorptive activity (Teitelbaum 2007). The osteoclast also expresses enzymes such as cathepsin K and matrix metalloprotease-9, which are important for matrix degradation (Delaissé *et al.* 2003). The osteoclast precursor expresses a RANK receptor which is activated by the binding of the cell membrane bound RANKL to stimulate osteoclast formation. Expression of RANKL occurs when cells are exposed to certain hormones and other factors such as parathyroid hormone (PTH). However,

osteoprotegrin (OPG) can act as a decoy receptor and bind RANKL, therefore preventing osteoclast formation.

1.1.3 Osteoblasts

Osteoblasts are cuboidal cells found along the surface of the bone and are predominantly responsible for bone formation (Karsenty *et al.* 2009). They are characterised by their unique ability to secret extracellular matrix (ECM) that is rich in type I collagen, which gives bones their tensile strength. Osteoblasts originate from multipotent mesenchymal stem cells, which have the capacity to differentiate into osteoblasts, adipocytes, chondrocytes, myoblasts, or fibroblasts (Figure 1-2). The transcription factor, runt-related transcription factor-2 (Runx2) is required for progenitor cells to differentiate into osteoblasts (Komori 2009); *Runx2* gene deletions in mice are lethal as their skeleton is unmineralised and the mice are unable to breathe (Takarada *et al.* 2013). Osterix is another transcription factor which acts downstream of Runx2 to aid osteoblast differentiation (Sinha *et al.* 2013). *Msx1* also regulates osteoblast differentiation in young animals (Figure 1-2). Mature osteoblasts also express osteocalcin, which is thought to be a key regulator of bone turnover and mineralisation as well as playing a role in glucose and fat metabolism (Ferron *et al.* 2008).

1.1.4 Bone lining cells

Bone lining cells cover the areas of bone surface in which neither formation or resorption are occurring (Everts *et al.* 2002). Their role is less clear but they probably aid coupling of the bone formation and resorption processes.

1.1.5 Bone marrow

The bone marrow micro-environment also regulates bone homeostasis and helps control the balance between bone formation and resorption. Bone marrow consists of two separate and distinct stem cell populations. The mesenchymal stem cells constitute the bone marrow stroma and are the progenitor cells for osteoblasts and adipocytes depending on the presence of key regulators such as peroxisome proliferated-activated receptor (PPAR)ϒ, CAAT enhancer binding protein (C/EBP), Runx2, Wnt and IGF-1 (Tencerova *et al.* 2016). Adipocytes in the bone marrow of the mouse are present throughout the long bones and also in the lumbar vertebrae but

most numerous in the epiphyses (Rosen *et al.* 2009). The haematopoetic stem cell population gives rise to blood cells or osteoclasts and is regulated by key factors such as RANKL and nuclear factor kappa beta (NFϰ β). The regulation of bone marrow adipogenesis is not fully understood but it is thought that an increase in bone marrow adipose tissue is associated with a reduction in bone mass (Shanmugam *et al.* 2018).

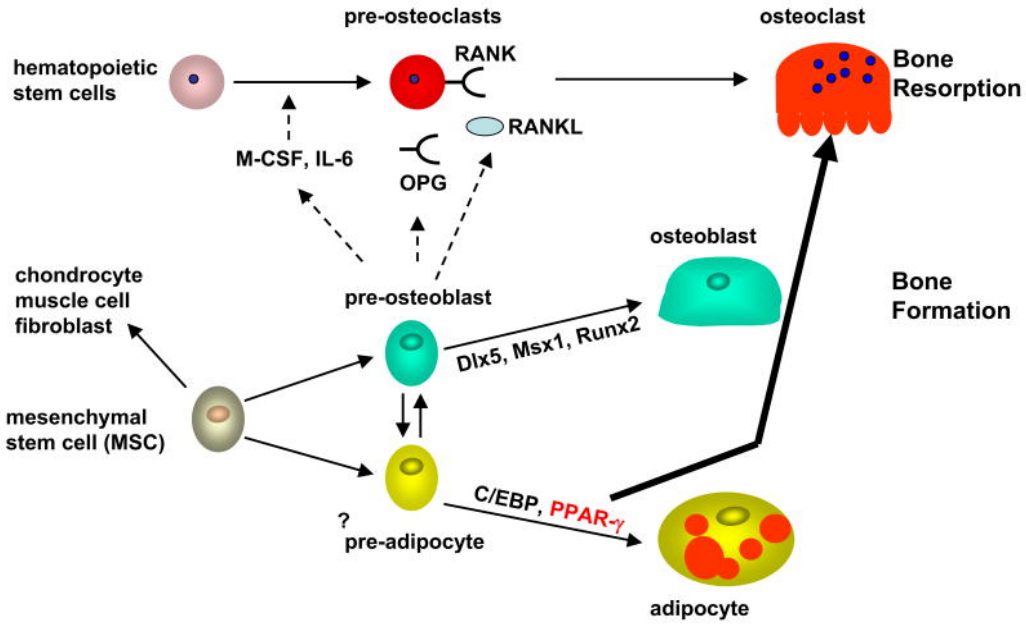

Figure 1-2 Factors controlling the fate of the mesenchymal stem cell and haematopoetic stem cell populations. Reproduced from (Rosen *et al.* 2009)

1.2 Skeletal development

The foetal skeleton develops in two distinct ways; intramembranous ossification occurs within flat bones such as those of the skull and facial bones, while endochondral ossification accounts for the development of all long bones of the skeleton such as the tibia and femur. In this thesis the focus is on endochondral ossification, which involves a cartilaginous intermediate phase, as this process is responsible for bone formation and longitudinal growth of the majority of the skeleton. During the initial, patterning phase of skeletal development, mesenchymal cells condense into tissue elements at specific sites that form the structure of future bones (Karsenty *et al.* 2002). By embryonic day 12 (E12) in mice, these pre-cartilaginous anlagen reflect the shape, size, position and number of skeletal elements that will be present in the mature skeleton (Maes *et al.* 2016). Following this, differentiation to

either chondrocytes or osteoblasts occurs within the condensations. Chondrocytes in the centre become hypertrophic, whilst cells in the perichondrium differentiate into osteoblasts and capillaries invade to form the bone collar, and subsequently the periosteal cortical bone. Between E14-16 (Figure 1-3) the hypertrophic chondrocytes start to secrete collagen X, become invaded by blood vessels and mineralisation of the cartilage matrix occurs. As apoptosis of the hypertrophic chondrocytes occurs, the cartilaginous ECM is gradually replaced by a bony ECM (rich in type I collagen), and osteoclasts partially resorb the mineralised cartilage surrounding the hypertrophic chondrocytes. The osteoblasts lay down osteoid on the cartilage remnants and the primary ossification centre forms. As osteoblasts continue to lay down new bone, the primary ossification centre expands towards the ends of the cartilage model and metaphyseal trabecular bone forms. In long bones of mice by post-natal day 5 (P5), epiphyseal blood vessels invade the avascular cartilage at each end of the bone and secondary ossification centres subsequently form. Layers of cartilaginous growth plates are left in between the epiphyseal and metaphyseal ossification centres, which enables further growth to occur.

1.2.1 The growth plate

The epiphyseal growth plate (GP) lies between the metaphysis and epiphysis of all developing long bones. It consists of chondrocytes embedded in ECM rich in collagen type II. The chondrocytes are arranged in vertical columns that lie parallel to the direction of bone growth. Each column is composed of discrete layers of chondrocytes that 'move' through their associated orderly pattern of resting, proliferative and hypertrophic phases (Mackie *et al.* 2011), Figure 1-3.

The resting zone contains small, scattered chondrocytes that are not actively involved in bone growth and replenish the pool of proliferative chondrocytes when required (Hunziker 1994). The proliferative zone chondrocytes are neatly stacked and are able to rapidly replicate. During the hypertrophic phase, chondrocytes increase their height between 5 to 10-fold but remain orientated in columns (Farnum *et al.* 2002). They secrete collagen type X which is unique to this cell type and also the phosphatases, alkaline phosphatase (ALP) and PHOSPHO1 which are essential for the mineralisation of the ECM surrounding the hypertrophic chondrocytes (Roberts *et al.* 2007). Once they reach the hypertrophic phase, chondrocytes promote invasion of

blood vessels via the production of vascular endothelial growth factor (VEGF), from the underlying metaphysis. This results in the delivery of osteoclasts to the chondro-osseous junction where they partially resorb the growth plate cartilage, forming a template for the deposition of osteoid by osteoblasts. This primary spongiosa is eventually fully remodelled to remove the cartilage cores and after mineralisation of the osteoid, the secondary spongiosa is formed.

The size of hypertrophic chondrocyte and rate of bone growth is highly correlated. It takes 2 days for chondrocyte differentiation from a proliferative to hypertrophic chondrocyte to occur in mice (Kember *et al.* 1976). The greatest height velocity in humans occurs during infancy and then height velocity subsequently declines until a further growth spurt at puberty. After puberty, once the primary ossification centre fuses with the secondary ossification centre via the formation of bony bridges, the GP becomes replaced by bone and cessation of growth occurs. Growth in the mouse slows down after puberty, but the GP does not completely fuse (Emons *et al.* 2011).

1.2.2 Bone remodelling

After birth, a continuing cycle of modelling (or remodelling in adults when it occurs without a change in bone shape) occurs and there is a fine balance between bone formation and bone resorption so that old bone is continually replaced by new tissue to sense and adapt to alterations in functional, metabolic and mechanical demands and repair microdamage within the matrix. (Frost 1990, Hofbauer *et al.* 2009).

Bone remodelling involves three phases: resorption, during which osteoclasts resorb old bone; reversal, when mononuclear cells appear on the bone surface; and formation, when osteoblasts lay down new bone until the resorbed bone is completely replaced (Hadjidakis *et al.* 2006). The modelling cycle is tightly regulated by the RANKL/OPG system (Boyce *et al.* 2007). RANKL interacts with the RANK receptor on osteoclast precursors, so that they begin the process of resorption. The effects of RANKL are blocked by OPG, a secretory dimeric glycoprotein belonging to the TNF receptor family (Hofbauer *et al.* 2000). OPG is produced mainly by osteoblasts and acts as a decoy receptor for RANKL. It regulates bone resorption by inhibiting the final differentiation and activation of osteoclasts and by inducing their apoptosis. The role of the OPG/RANK/RANKL coupling in regulation of bone remodelling can be demonstrated by RANKL knockout mice which show osteopetrosis and OPG-deficient

or RANKL overexpression mice which have osteoporosis (Bucay *et al.* 1998, Pettit *et al.* 2001).

1.2.3 Endocrine regulation of longitudinal bone growth

Bone is a highly complex endocrine organ and both local and systemic signals contribute to the delicate balance between either bone formation or resorption. Longitudinal bone growth is primarily influenced by the growth hormone/insulin-like growth factor-1 (GH/IGF-1) axis at both the endocrine and autocrine/paracrine level, but other hormones also contribute, including the thyroid and parathyroid glands, sex steroids and endogenous glucocorticoids.

1.3 The Growth hormone/ Insulin-like growth factor axis

Growth hormone (GH) and Insulin-like growth factor-1 (IGF-1) are fundamental regulators of longitudinal bone growth and have interdependent roles in the regulation of growth and skeletal function. Data from both humans and animals with GH/IGF-1 deficiency or deficient receptor signalling have shown the importance of the GH/IGF-1 axis in skeletal development (Lupu *et al.* 2001, Giustina *et al.* 2008, Cohen *et al.* 2014). GH is secreted by the anterior pituitary gland under the control of hypothalamic peptides; growth hormone-releasing hormone (GHRH) and ghrelin stimulate GH release whereas somatostatin release inhibiting factor inhibits GH release (Hartman *et al.* 1993). Whilst it was previously thought that GH only acted through IGF-1, it has now been shown that both hormones exert independent effects as well as acting in combination. Consistent with this theory, mice with combined GH and IGF-1 receptor deletion are smaller than mice with a single mutation only (Lupu *et al.* 2001). The precise mechanism of the action of GH and IGF-I on the epiphyseal GP remains unknown, however, and there are conflicting data regarding the relative contribution of each hormone on overall bone growth (Sims *et al.* 2000, Lupu *et al.* 2001, Hutchison *et al.* 2007).

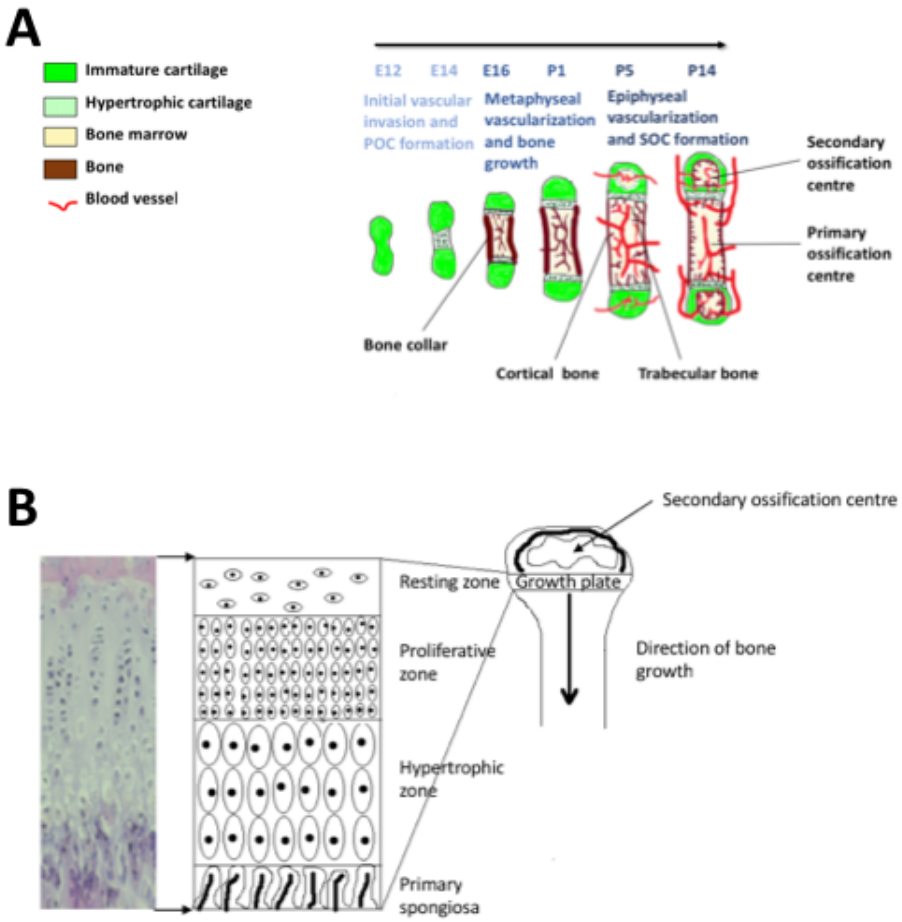

Figure 1-3 Endochondral ossification and growth plate (GP) in a mouse long bone. **A)** shows a schematic representation of endochondral ossification in a mouse long bone. Adapted from (Maes *et al.* 2016). At embryonic day 12-14 (E12-14): mesenchymal stem cells condense to form the cartilage analgen. Between E16 and P1: A bony collar is formed by osteoblasts to support bone growth. Invasion of blood vessels allows infiltration of osteoblasts and osteoclasts and the primary ossification centre forms: P5: The primary ossification centre expands to both ends of the diaphysis and the secondary ossification centre begins to form. P14: a discrete layer of chondrocytes (the GP) remains.
B) shows a H&E stained section of a GP from a mouse tibia and pictorial representation of the same region to demonstrate the zones within a GP and its epiphyseal location within a long bone.

The initial somatomedin hypothesis proposed in 1957 (Salmon *et al.* 1957) suggested that GH acted via a systemic intermediary substance, somatomedin -which was later renamed IGF-1, to initiate its effects on bone. Revised hypotheses have now been proposed, however, to account for the discovery of additional pathways. According to 'the dual effector theory'; in addition to causing an increase in systemic IGF-1 levels via a feedback loop, GH is also able to induce the expression and action of local IGF-1 at the level of the GP (Green *et al.* 1985). The presence of local GH recruits resting chondrocytes into a proliferative state and stimulates local IGF-1 production. Once activated, the chondrocytes also become responsive to IGF-1 enabling clonal expansion of chondrocyte columns to form (Zezulak *et al.* 1986). Flaws in the dual effector theory have now been highlighted, however, by data showing that GH also has direct effects on chondrocytes; the local injection of GH directly into the GP of the limbs of hypophysectomised rats produced a significant increase in length of the injected limb compared with the non-injected contralateral limb, which is suggestive of a direct effect of GH on growth regulation (Baron *et al.* 1992). The addition of IGF-1 to GH in female rats augments cortical bone mass (Sundström *et al.* 2014) without an effect on linear bone growth, which was considered to be best explained by the local effects of GH in combination with the synergistic effect of systemic IGF-1.

Direct GH effects are mainly mediated via the GH receptor (GHR). The GHR is a member of the class 1 cytokine receptor superfamily and comprises extracellular, transmembrane and intracellular domains. Activation of the GHR occurs by ligand-induced dimerization, mainly through activation of Janus Tyrosine Kinase 2 (JAK) (Argetsinger *et al.* 1993). Autophosphorylation and phosphorylation of the internalized GHR occurs. Intracellular protein activation results in the activation of transcription factors, especially through the signal transducer and activator (STAT) pathway. GH binds to its membrane receptor and activates signal transduction pathways to regulate transcription of GH target genes, such as IGF-1 (Chia 2014). The JAK/STAT signalling pathway is needed for GH induction of IGF-1 and GH activates chondrocyte STAT signalling (Pass *et al.* 2012). STAT5 is particularly influential within the GP . GH also affects the fate of mesenchymal precursor cells which can differentiate into adipocytes, chondrocytes or osteoblasts dependent on conditions (Pittenger *et al.* 1999, Hu *et al.*, 2018)). IGF is a single chain polypeptide that is similar in structure to pro-insulin. It is mainly produced by the liver under GH control, but also in skeletal

muscle and cartilage. IGF-1 is more important in post-natal growth while IGF-2 is predominantly responsible for foetal growth (D'Ercole *et al.* 1980). IGF's mainly travel in complex, almost entirely bound to one of six insulin-like growth factor binding proteins (IGFBPs). More than 95% of IGF-1 is bound to IGFBP3, which combines with an acid labile subunit (ALS) in a 150kDa ternary complex (Baxter 1988, Laron 2001). IGFBPs are produced by many tissues and are regulated mainly by GH, but also by IGF-1 itself. These complexes prolong the life of IGF in circulation and, depending on their concentration, can either inhibit the action of IGFs or enhance effectiveness (Clemmons 1993). IGF1 can only bind the receptor in its free form so release from ALS and IGFBP3 is required before it can be activated. However, without ternary complex half-life of free IGF1 is very short and has only a very short duration of action after release in the circulation. IGF-1 has both paracrine/autocrine and endocrine effects; the indirect effects of GH are mediated mainly via IGF-1 and IGFBPs. IGF-1 exerts its actions through the type 1 IGF receptor, a tyrosine kinase receptor that is structurally related to the insulin receptor and is present on the cell surface of all chondrocytes, particularly in the proliferative zone (Verschure *et al.* 1995).

IGF-1 is anabolic to bone; through the phosphoinositide-3-kinase (PI3K) pathway, it enhances Wnt- dependent activity and probably increases both osteoblast proliferation and osteoblast differentiation (Oh *et al.* 2003, Tahimic *et al.* 2013). IGF-1 has been conditionally deleted in osteoblasts at various stages of development and a reduction in bone formation and overall decrease in bone mass were noted. Mice with an osteoblast specific deletion of IGF-1R also demonstrate decreased trabecular bone volume, number, connectivity and spacing (Zhang *et al.* 2002). Conversely, mice with overexpression of IGF-1 in osteoblasts show increased bone mass and volume and increased activity of resident osteoblasts and bone formation rate (Zhao *et al.* 2000). Specific knockout of IGF-1 expression in osteocytes also caused a reduction in both appositional and longitudinal growth, alongside a shorter GP and smaller hypertrophic chondrocytes (Sheng *et al.* 2013). IGF-1R are expressed on osteoclasts, but it is unclear as yet if osteoclasts themselves secrete IGF-1 (Cooper *et al.* 2013). IGF-1 disruption in the liver leads to low bone mass and reduced bone formation rates (Yakar *et al.* 2002). In keeping with this, systemic IGF-1 administration can partially rescue the bone phenotype in the GH receptor deficient mouse by improving cortical bone thickness without an impact on trabecular bone (Yakar *et al.* 2002). IGF-1 also

has an important role in anabolic pathways in muscle (Fryburg 1994). It causes myocyte differentiation and via proliferation of muscle satellite cells, also has a role in muscle maintenance and repair (Song *et al.* 2013).

IGF-1 is mainly produced by cells in the perichondrium surrounding the GP chondrocytes, and acts predominantly on the hypertrophic zone (Parker *et al.* 2007). The overall contribution of hepatic generated IGF-1 to epiphyseal bone growth remains unclear and extra-hepatic IGF-1 certainly plays a role; liver specific conditional knockouts of IGF-1 have a 75% reduction in circulating IGF-1 but bone length and body size are unchanged from wild type (Yakar *et al.* 1999). Conversely, mice with targeted IGF1 chondrocyte deletion had normal systemic IGF-1 values but 40% reduction in local IGF1 and 27% reduction in body size (Govoni *et al.* 2007). Systemic IGF-1 can rescue growth impairment in IGF1 null mice, suggesting a role of systemic IGF-1 on autocrine/ paracrine IGF-1 actions (Wu *et al.* 2009). Overall it appears that IGF-1, either produced locally or systemically, regulates many of the key processes within the chondrocyte, including proliferation, differentiation, hypertrophy and survival and also matrix synthesis.

1.4 Duchenne muscular dystrophy (DMD)

DMD is the most common muscular dystrophy of childhood. It affects 1 in 4000 live male births (Emery 1991) and is a severe and ultimately fatal, X-linked recessive disease. DMD occurs as a result of mutations in the gene at 21p on the X chromosome, with the resulting reduction or complete loss of dystrophin protein. Absence of dystrophin leads to increased muscle cell fragility and an ongoing cycle of degeneration and repair with associated inflammatory change and eventually replacement of muscle fibres with fibrosis and fatty change (Deconinck *et al.* 2007). It is associated with progressive muscle weakness and untreated individuals lose ambulation by a mean age of 10 years (Bello *et al.* 2015). Respiratory, cardiac or orthopaedic complications usually cause premature death in the second or third decade. Whilst there is still no cure for DMD, therapeutic advances such as the routine use of GC and coordinated multidisciplinary care have dramatically improved the natural course of the disease (Moxley *et al.* 2010) so that patients with DMD now regularly survive into their thirties (Wagner *et al.* 2007).

Unfortunately, the use of GC in DMD comes at a heavy price. The side-effects of GC are well recognised, frequently encountered, and can be very serious. Glucocorticoid receptors (GRs) are present in many target organs and tissues and adverse effects can be varied, including insulin resistance, hypertension, behavioural problems, cataracts (Bonifati *et al.* 2000), adrenal suppression, growth retardation (Biggar *et al.* 2006), bone hypo-mineralisation thus increasing risk of vertebral and lower limb fractures (Larson & Henderson 2000; Bothwell et al. 2003; King et al. 2007) and pubertal delay (Wood et al. 2015). As a result, clinicians face new challenges in the follow-up and supportive care of those with DMD. Families are increasingly seeking an endocrine specialist opinion to discuss possible treatment options for problems including short stature, osteoporosis and pubertal delay. This is not a straightforward consultation due to the likely multifactorial nature of the problem and the need to consider concomitant GC use and potential interactions with any therapy initiated.

1.4.1 Glucocorticoid treatment in DMD

Glucocorticoids are currently the mainstay of treatment in DMD and are the only pharmacological intervention proven to stabilise muscle strength. Almost 50 years ago, a study of 14 patients with DMD was published which concluded that steroids may have some palliative benefit (Drachman *et al.* 1974). By 2004, it was agreed that " the evidence for the use of daily steroids in DMD is now established and that trials of other treatments should be against this *gold standard* (Bushby *et al.* 2004)" and a Cochrane review published in 2008 demonstrated that GC could stabilise muscle strength for up to three years (Manzur *et al.* 2008). The precise mechanism by which GC act to preserve muscle strength is however unclear. During the disease process, inflammatory mediators are released, and GC are thought to have an anti-inflammatory/ immunosuppressive effect, possibly related to their inhibitory action on the NFkβ pathway (Hoffman *et al.* 2012). Continuing longitudinal follow-up of GC-treated cohorts has found that long-term, regular use of GC improves skeletal muscle and allow up to a further 3 years of independent ambulation, cardiac function and respiratory function (Daftary *et al.* 2007). They delay the onset of scoliosis (Lebel *et al.* 2013) and contractures and also preserve upper extremity function, thus improving quality of life. GCs are offered when muscle function starts to plateau, this is usually by 5 years of age. Therefore by adulthood, most patients with DMD have been on high dose GCs for over 10 years.

1.5 Glucocorticoid-induced osteoporosis

It is estimated that, at any one time, over 250,000 people in the UK are exposed to systemic GC (Walsh *et al.* 1996). Approximately 10% of children will require GC at some stage during their childhood (Mushtaq *et al.* 2002) and 5% of the population aged 80 years or over have used GC in the past (Kanis *et al.* 2004). Long-term GCs are effective in many conditions, such as inflammatory bowel disease (Sbrocchi et al. 2010; Pappa et al. 2011) chronic renal disorders (Olgaard *et al.* 1992), lung conditions, haematological malignancies (El-Hajj Fuleihan *et al.* 2012) and connective tissue disease (Feber *et al.* 2012), and in DMD in particular, they are the mainstay of long-term treatment (Matthews *et al.* 2016). As discussed in Chapter 1, GCs are associated with frequent and wide-ranging side-effects, many of which are dose-related and associated with considerable morbidity. Of these, two of the potentially most serious and challenging to manage are glucocorticoid-induced osteoporosis (GIO) and growth retardation. Osteoporosis is characterised by a reduction in bone mass and loss of bone microarchitecture, leading to impaired bone strength and increased fracture risk (Reinwald *et al.* 2008). GIO is the most prevalent type of secondary osteoporosis and accounts for about 25% of cases (Eastell *et al.* 1998). The General Practice Research Database has shown that total daily prednisolone doses of as little as 2.5mg can cause an increased risk of fracture (Van Staa *et al.* 2000). Putting this into context, the recommended dose for prednisolone in DMD is 0.75mg/kg.

As healthy children have high rates of bone growth, their skeleton is particularly vulnerable to the adverse effects of GC on bone formation. GC-induced growth failure was first described 60 years ago after an equivalent cortisone dose of only 1.5mg/kg/day (Blodgett *et al.* 1956), equivalent to 0.3mg of prednisolone. GC-induced growth failure has been reported following GC exposure by several alternative routes including inhaled GC in asthma (Allen *et al.* 1994) and intra-articular steroid injections in juvenile arthritis (Umlawska *et al.* 2010). GC-induced growth failure is dose-dependent and alternate-day or weekend dosing is associated with less growth retardation (Escolar et al. 2011; Ricotti et al. 2013) . In children, although compensatory catch up growth may occur after cessation of GC therapy (Crofton *et*

al. 1998), prolonged exposure may reduce the potential for this catch up (Simon *et al.* 2002).

1.5.1 Mechanisms of glucocorticoid-induced osteoporosis

The aetiology of GC-induced osteoporosis is complex and a detailed review of the underlying mechanisms as recently reported (Henneicke *et al.* 2014) is beyond the scope of this literature review. Instead, I will summarise the key mechanisms and the differing effects of GCs in osteoblasts, osteoclasts and osteocytes. There are two distinct phases of GC-induced bone loss, resulting from the suppressive effects of GCs on both osteoblastogenesis and osteoclastogenesis. The initial acute period of increased bone resorption is followed by a more indolent phase of bone loss caused by a reduction in bone formation (Canalis *et al.* 2004). Indirect effects of GCs on the skeleton such as decreased calcium absorption, increased renal calcium clearance, reduced GH secretion and suppression of sex steroid metabolism were previously thought to play a fundamental role, but whilst these factors do contribute, the main mechanisms underlying GIO are now known to result from the direct effect of GCs on the resident bone cells (Figure 1-4) (Canalis *et al.* 2007).

GCs and mineralocorticoids act through corticosteroid receptors - the mineralocorticoid receptor (MR) and the GR. These receptors have often been referred to as Type 1 and Type 2 corticosteroid receptors, respectively (Eberwine 1999, Stewart 2007). The GR is a member of the nuclear receptor superfamily of ligand-dependent transcription factors and is expressed in nearly every cell in the body. In particular, the GR is expressed in many bone cells, including osteoblasts, osteoclasts and osteocytes (Bouvard *et al.* 2009) and also in chondrocytes within the GP. Once GCs bind to the GR in the cytoplasm, the GR translocates to the nucleus, where it acts as a transcription factor and modifies gene expression, via the GC-response element (GRE), either by causing transactivation or transrepression. Transactivation accounts for most of the GC-associated adverse effects and *in-vitro* and murine studies demonstrate that selective GR modulators can alter the extent of these adverse effects (Owen *et al.* 2007, Thiele *et al.* 2012). However, studies using transgenic mice with a GR gene mutation that prevents dimerization and therefore transactivation still have reduced bone formation. This suggests that transrepression is probably also partly responsible (Rauch *et al.* 2010). Polymorphism of the GR gene

is associated with varying susceptibility to GCs (Huizenga *et al.* 1998) which may in part explain the heterogeneity in GC-associated fracture rates in humans.

Micro RNAs (miRNAs) are endogenous RNAs made up of 18-25 nucleotides that interact with messenger RNA to change protein expression (Selbach *et al.* 2008). Recent work has shown that several miRNAs have differential expression in GC-treated bone (Ko et al. 2013; Wang et al. 2013a; Shi et al. 2015). For example, a reduction in miRNA-29a expression, which interacts with Wnt signalling components and dickopf-related protein 1 during osteoblast differentiation was associated with GC-associated bone loss. Gain of miRNA-29a function by a miRNA-29a precursor (Wang *et al.* 2013) attenuated the deleterious effects of GC treatment on bone mass, microarchitecture, and biomechanical strength.

1.5.2 Effects of GC on osteoblasts

The chronic bone loss in GIO predominantly results from the ability of GCs to decrease both the number and functionality of osteoblasts. Osteoblasts and adipocytes are both derived from mesenchymal stem cells (Caplan 1991). By changing the fate of osteoprogenitor cells, GCs effectively reduce the pool of cells that can become mature, differentiated osteoblasts and bone marrow stromal cells are instead directed along the adipogenesis pathway (Chen *et al.* 2016). This has been shown to occur via the transactivation of C/EBP in murine stromal cells (Pereira *et al.* 2002), which increases expression of PPARγ2 and suppresses expression of Runx2 (Canalis *et al.* 2004, 2007). GCs may, therefore, increase bone marrow adipose tissue at the expense of mature osteoblasts and cancellous bone (Weinstein *et al.* 2000). Outside of bone, GCs also promote pre-adipocyte conversion to mature adipocytes and thus cause hyperplasia of adipose tissue. A 2-fold increase in cancellous adipocyte area in GC-treated mice compared to placebo has been reported, alongside a significant increase in adipocyte production in bone marrow cultures (Weinstein *et al.* 2000). The precise mechanisms underlying the reduction in osteoblastogenesis that occurs upon GC administration is unclear, however, it is known that GCs cause suppression of bone anabolic factors such as BMPs (Pereira *et al.* 2002), osteoblast-specific factor 2, IGF-1 (Clemmons, 2018) and transforming growth factor beta (TGF-β) which activate osteoblastic transcription factors such as Runx2 and β-catenin. In cultured human osteoblasts, exogenous GC administration

also results in suppression of the canonical Wnt-β-catenin signalling pathway which can prevent osteoblast apoptosis and encourages progression through the osteoblast cell cycle and thus proliferation (Ohnaka *et al.* 2005). Furthermore, murine GC exposure has been shown to upregulate sclerostin gene expression, which antagonises Wnt stimulation of osteoblast differentiation and thereby inhibiting bone formation (Yao *et al.* 2016). Using a transgenic mouse line, GCs have also been shown to suppress interleukin 11 expression, which further inhibits osteoblast differentiation (Rauch *et al.* 2010). As well as inhibiting osteoblast differentiation, GCs also prevent bone matrix synthesis by inhibiting osteoblast-driven synthesis of type I collagen and osteocalcin (Canalis 2005). GC administration to mice has also been shown to induce osteoblast apoptosis and suppress terminal differentiation (Weinstein *et al.* 1998).

1.5.3 Effects of GC on osteoclasts and osteocytes

Osteoclasts are derived from haematopoietic stem cells and resorb bone by creating an acidic environment and producing collagen-degrading enzymes such as cathepsin K and matrix metalloproteinases (Delaissé *et al.* 2003). GCs exert an early direct effect on osteoclasts by increasing both their number and activity, with a corresponding increase in bone resorption, seen after only 7 days of GC treatment in mice (Jia *et al.* 2006). Intriguingly, this overall increase in osteoclast number occurs despite a reduction in osteoclast production in the bone marrow, suggesting that GC treatment increases the lifespan of pre-existing osteoclasts (Weinstein *et al.* 2002). However, the longer term role of the osteoclast in GIO remains controversial; despite an initial increase in bone resorption, prolonged GC excess appears to suppress osteoclast number and function. For example, after 4 weeks of prednisolone treatment in mice, bone resorption fell to or below normal levels (Weinstein *et al.* 1998). GCs also directly block the induction of cytoskeletal changes in the osteoclast required for the resorptive capabilities of the cell (Kim *et al.* 2007). There is also evidence that GCs suppress the proliferation of osteoclast precursors (Kim *et al.* 2006). However, GCs also cause an increase in RANKL (Hofbauer *et al.* 2009), which is produced by both osteoblasts and osteocytes

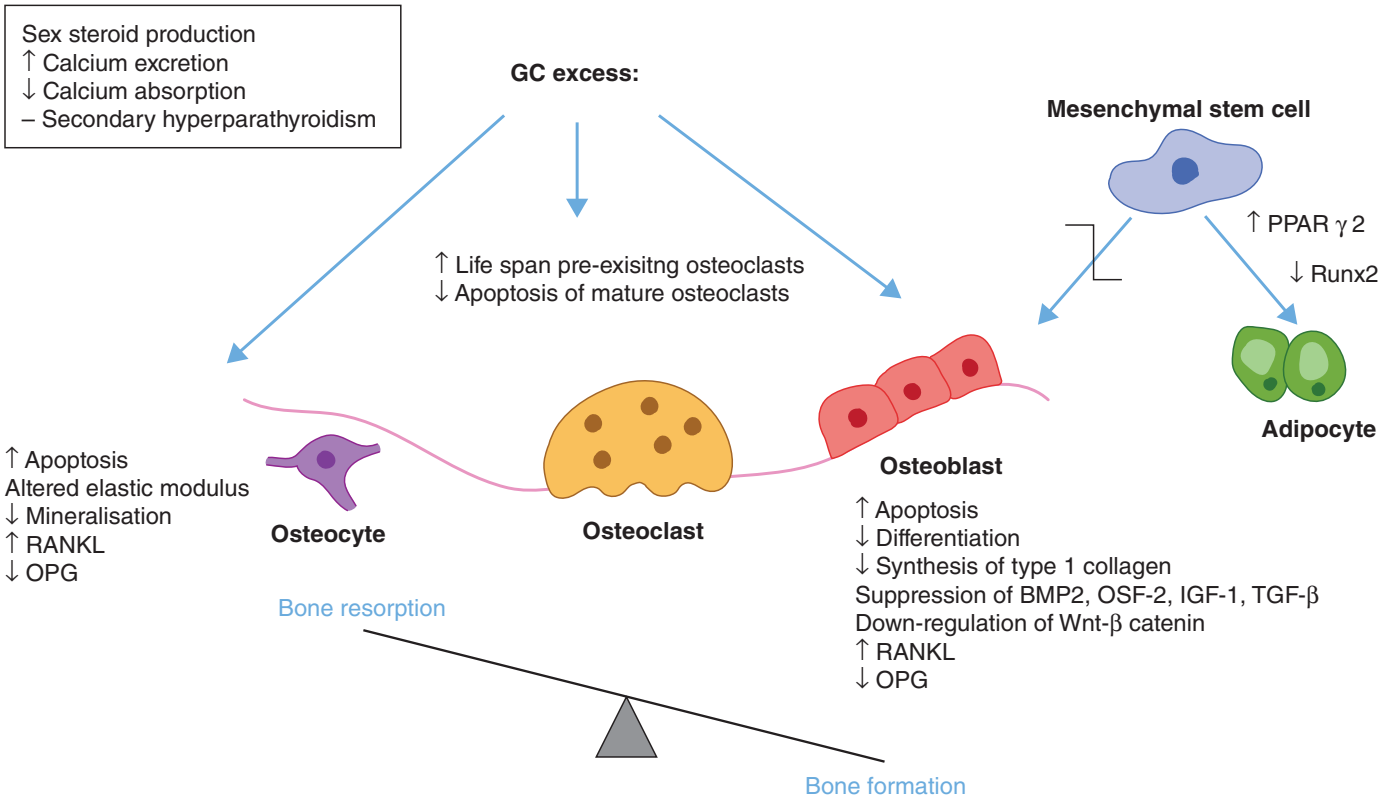

Figure 1-4 Glucocorticoid-induced mechanisms of GIO

(Nakashima *et al.* 2011, Xiong *et al.* 2011) and down-regulation of OPG. This skews the RANKL:OPG ratio towards osteoclastogenesis. Overall, the long-term effect of exogenous GCs on osteoclastogenesis still requires clarification but it appears that the osteoblast is the main target of exogenous GCs.

Osteocytes are terminally differentiated osteoblasts that play an important role in the repair of bone micro-damage (Rochefort *et al.* 2010). GCs alter the osteocyte-canalicular network by changing the elastic modulus surrounding the lacunae of osteocytes resulting in reduced mineralisation (Lane *et al.* 2006). Autophagy may be responsible for these observed localised osteocyte peri-lacunar changes, occurring as a self-protection mechanism during GC treatment (Xia *et al.* 2010). High dose GC therapy in several animal models and humans has also been shown to induce osteocyte apoptosis (Zalavras *et al.* 2003).

1.6 Glucocorticoid-induced growth retardation

The growth-suppressing effects of GCs are multifactorial and result from both systemic and local actions. The GH/IGF-1 axis is the main determinant of postnatal longitudinal growth and GH and IGF-1 have interdependent roles in growth regulation, see Section 1.2. The rate of longitudinal bone growth is principally controlled through the regulation of chondrocyte proliferation, differentiation and hypertrophy at the GP (Wong *et al.* 2016). GH promotes chondrocyte differentiation, the secretion of IGF-1 by liver cells and the amplification of local IGF-1 synthesis by chondrocytes, which induces clonal expansion of chondrocyte columns within the GP (Zezulak *et al.* 1986).

GCs affect the expression at multiple levels of the GH/IGF-1 axis (Price *et al.* 1992, Jux *et al.* 1998, Klaus *et al.* 2000, Smink *et al.* 2002). Seven days of dexamethasone treatment in pre-pubertal mice reduced *Igf-1* gene expression throughout chondrocytes in all phases within the GP (Smink *et al.* 2003) as well as causing a significant increase in the number of apoptotic cells within the hypertrophic zone. Different mechanisms of GC-induced apoptosis have been proposed such as activation of caspase-3 and suppression of Bcl-2 (Chrysis *et al.* 2003, Espina *et al.* 2008). GCs also reduce IGF-1 and GH receptor expression by chondrocytes (Jux *et al.* 1998). In addition, they impair IGF-1 signalling, mainly via the PI3K pathway within

the GP. Furthermore, GCs suppress prostaglandin E2 synthesis (Harada *et al.* 1995) as well as VEGF expression in chondrocytes, thus preventing blood vessel invasion of the ossification centre, which is crucial for degradation of the ECM and subsequent ossification and growth (Smink *et al.* 2003). The intrinsic effect of GCs on the mouse GP was evident when the local infusion of dexamethasone significantly reduced tibial growth compared to the contralateral limb (Baron *et al.* 1992). GCs also act systemically to inhibit the pulsatile secretion of GH from the anterior pituitary gland by increasing somatostatin tone (Mazziotti *et al.* 2013).

1.7 Glucocorticoid-induced osteoporosis in DMD

As quality of life and survival rates continue to improve in DMD as a result of advances in supportive care and treatment options, bone health has become an increasingly important issue in DMD (Buckner *et al.* 2015, Wong *et al.* 2019) . The presence of, and risk factors for, osteoporosis and fractures in this population have been well documented (Larson & Henderson 2000; King et al. 2007; McAdam et al. 2012; Joseph et al. 2019) and the recently updated standards of care for DMD include comprehensive information for the monitoring of bone health (Birnkrant *et al.* 2018). Bone pain and fractures (both long bone and vertebral) are common, frequently occur after minimal or no trauma and can be very challenging to manage (Birnkrant *et al.* 2018).

Specific data regarding the effects of GC on the growing skeleton in DMD is conflicting; GC use appears to be a definite risk factor for vertebral fractures (Bothwell *et al.* 2003, King *et al.* 2007) but data is not as compelling for long bone fractures. For example, one study found that the percentage of boys who sustained long bone fractures was similar in both GC treated or untreated cohorts. There were no details regarding steroid regimens, however, and much of the available data pre-dates the routine use of daily GC and therefore is not applicable to the contemporary population (McDonald *et al.* 2012). One Canadian study of DMD patients treated with daily deflazacort found that 25% had suffered a long bone fracture, 19% had a vertebral fracture (VF) and lumbar spine Z-scores declined with increasing GC treatment duration (McAdam *et al.* 2012). Symptomatic vertebral compression fractures have been described in 32% of DMD boys on long-term daily GC (King *et al.* 2007) but other data using modelling (Bothwell *et al.* 2003) predicts that by 100 months of high

dose daily GC therapy as many as 75% would have at least one VF. The recently published retrospective study which analysed 91 boys treated within the Scottish Muscle Network found the probability of developing a first symptomatic fracture (including VF) was 50% after 6.5 years of GC exposure (Joseph *et al.* 2019). This is still likely to be an underestimate of the true fracture rate, because only symptomatic VF were included and many boys were using 10 days on/off regimens. If routine spinal imaging was carried out, it is likely that the true incidence of VF would be much higher. It was previously thought that deflazacort, a derivate of prednisolone, may have less adverse effects on bone metabolism than prednisolone (Loftus *et al.* 1991, Krogsgaard *et al.* 1996) but on further examination of the studies that suggested this, it appears that due to an error in calculating relative potencies, non-equivalent doses were used, and more recent studies have failed to demonstrate a bone-sparing effect of deflazacort (Mayo *et al.* 2012).

1.8 Additional factors affecting bone strength in DMD

It is clear that boys with DMD are more susceptible to fractures than an equivalent healthy population, whether or not they are on steroids; an older retrospective study that was carried out before GC became standard of care found that 44% of steroid-naïve DMD boys had sustained a fracture (Larson *et al.* 2000). This suggests that reduced bone mass in DMD is a result of other factors in addition to chronic GC use. Reduced mobility, and in particular loss of ambulation, is also an established risk factor for bone density and fracture risk (James *et al.* 2015). The prevalence of vitamin D deficiency and insufficiency are also high in DMD and may contribute further (Alshaikh *et al.* 2016). Another study combining both *in-vivo* and clinical data has also suggested that there may be an abnormality of osteoblast function (Rufo *et al.* 2011). These will be discussed in further detail in chapter 4.

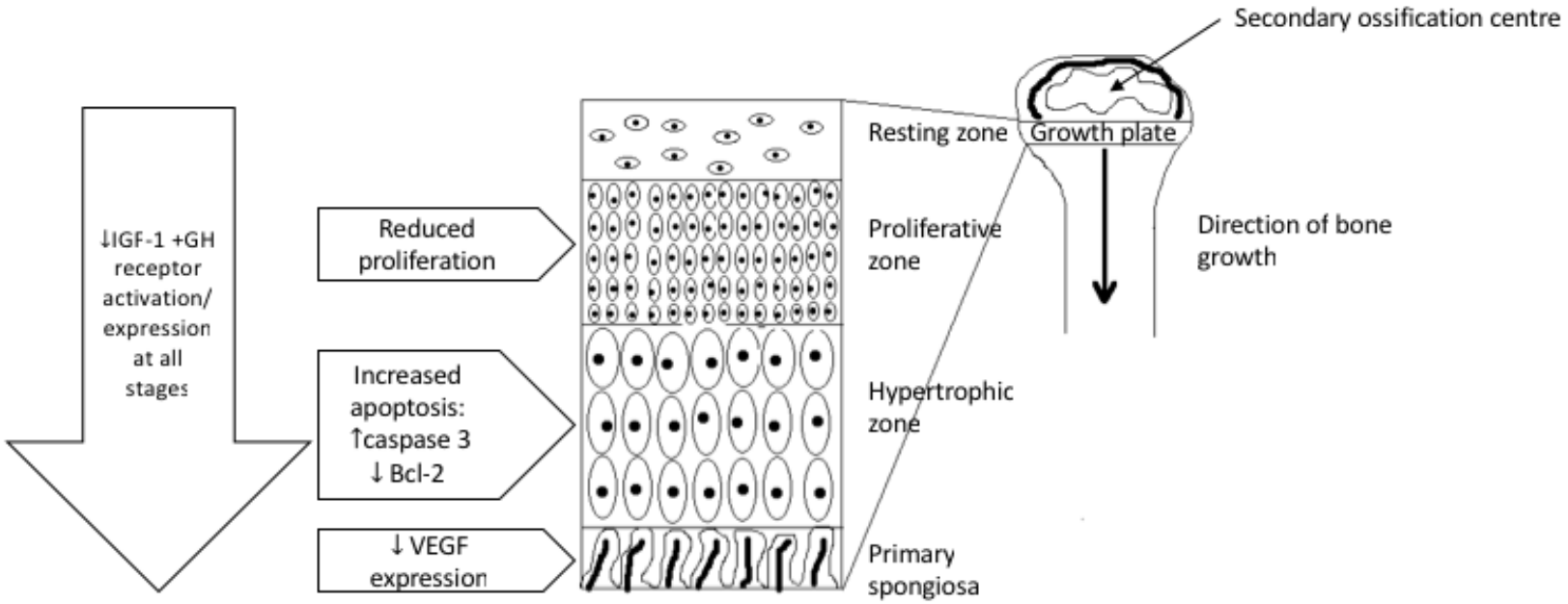

Figure 1-5 Mechanisms of GC- induced growth retardation

1.9 Growth failure in DMD

Short stature is a common feature of boys with DMD even in those who are not treated with GC (Rapaport *et al*. 1991; Matsumoto *et al*. 2017), which further exacerbates the problems caused by reduced growth velocity associated with delayed puberty. In one study of boys with DMD, short stature was seen as a major concern and induced psychological problems including depression in the boys studied (Merlini *et al.* 2012). For many parents the stress caused by psychosocial aspects of the child exceeds the stress caused by the physical aspects of the disease (Nereo *et al.* 2003). Typically, boys with DMD appear to have a slower than expected growth velocity during the first years of life and then continue to grow along their lower centile during childhood and adolescence (Eiholzer *et al.* 1988). By the age of 18 years, most with DMD fall below the 5th centile (McDonald *et al.* 1995). The aetiology of this growth failure is unclear, although several mechanisms have been suggested. Studies in the canine x-linked muscular dystrophy model have suggested that the early poor growth coincides with a period of extreme muscle necrosis and regeneration, which may therefore reflect increased metabolic activity (Rapisarda *et al.* 1995). Low levels of physical activity and associated reduced bone loading and lower bone turnover may also contribute (Nagel *et al.* 1999). Genetic mechanisms including deletions of the SHOX gene, located near to Xp21, or an abnormal response of dystrophic muscle to endogenous GH may also be responsible (Messina *et al.* 2008). Primary GH deficiency is unlikely to be the cause, however, as a study of 34 patients with DMD confirmed that GH secretion was essentially normal (Nagel *et al.* 1999). There also appears to be a variable growth phenotype within DMD, with patients who have a distal deletion within the DMD gene having a higher frequency of short stature (Sarrazin et al. 2014; Matsumoto et al. 2017), suggesting that a dystrophin-specific mechanism may also be involved in the aetiology.

1.9.1 GC-induced growth failure in DMD

Growth retardation is an almost inevitable side effect of GC therapy and height velocity in DMD is slowed considerably after starting GC. In a study looking at the growth suppressive effect of long-term deflazacort treatment in DMD, the treated boys were on average 21cm smaller by 15 years old, compared to those untreated (Biggar *et al.* 2006). The extent of GC-induced growth failure appears to depend on age at initiation, dose and frequency (Allen 1996). Some boys are on daily regimens, whilst

others are on intermittent dosing schedules. Despite it being 30 years since the benefit of GC was first demonstrated, one of the major obstacles to standardisation of care in DMD remains the lack of consensus regarding the risk/benefit ratio of different GC regimens. '*Finding the optimal steroid regimen for Duchenne Muscular Dystrophy'* (www.for-dmd.org) is a double-blinded, placebo-controlled randomised controlled trial that will compare daily versus intermittent (10 days on/10 days off) dosing and prednisolone versus deflazacort regimens. This trial will allow a balanced look at the tolerability, efficacy and long-term side-effects of different steroid protocols (Bushby *et al.* 2011). This will hopefully help to determine the impact of different GC regimens and height on functional outcomes.

It is possible that there is a mechanical advantage to being short (Zatz et al. 1988; Biggar et al. 2006) in DMD and that shorter stature may preserve ambulation through associated biomechanical effects on gait (Ricotti *et al.* 2013). However, growth in children with DMD occurs alongside muscle destruction, and there is a clear interaction between height and GC use, so it is very difficult to tease out the causal relationship. For example, short stature might be an indicator that GC are having a positive effect on disease ameliorating mechanisms (Bodor *et al.* 2013). At the other extreme it is unclear whether very short stature (and often an excessively increased BMI) may have a detrimental effect on motor outcomes. In the meantime, the adolescents themselves clearly express a preference to be taller and we would expect the potential disadvantage of increased height gained during the pubertal growth spurt on motor function to be outweighed by the advantages of increased muscle mass and bone mineralisation.

The timing of onset of GC therapy is also important for both efficacy and side-effect profile. DMD clinical guidelines advise commencing steroid therapy as soon as possible after diagnosis and early data suggests improved outcomes if steroid therapy is commenced between the ages of 4-6 years, when motor skills begin to plateau, as GC do not appear to bring back lost function (Bushby *et al.* 2010, McDonald *et al.* 2012). Data shows that many boys who start GC early are still ambulant beyond16 years of age, by which time they will have been on GC for over 10 years. Studies in other chronic diseases such as cystic fibrosis have found that the younger the onset

of GC therapy, the lower the final height z-score after discontinuation of therapy (Lai *et al.* 2000).

1.10 Current bone treatment strategies in DMD

There are very limited treatment strategies currently available for the treatment of short stature and osteoporosis in DMD. The impaired osteoblast function described in both x-linked muscular dystrophy (*mdx*) mice and patients with DMD (Rufo *et al.* 2011) suggest that an anabolic treatment would be optimal, but there are no current options clinically available. A recent Cochrane review (Bell *et al.* 2017) concluded that, *"We know of no evidence from high-quality randomised controlled trials (RCTs) about the efficacy of interventions to prevent or treat corticosteroid-induced osteoporosis and prevent osteoporotic fragility fractures in DMD in children and adults.."*

The next section focuses on some of the therapies that are currently in use, with examples highlighting their use in DMD:

Bisphosphonates

There is limited evidence for the use of anti-resorptive bisphosphonates (BP) in DMD and their use varies by centre; some advocate prophylactic BP use while in other institutions they are reserved for the treatment of fractures and there is no consensus regarding timing of initiation, drug regimen or cessation of treatment (Wood *et al.* 2016). To the best of knowledge, no study to date has investigated any intervention to prevent the first fracture in DMD. The efficacy of BP therapy on BMD appears to depend on the age at time of treatment and the amount of bone growth remaining (Brumsen *et al.* 1997). Generally, they appear to be a safe and effective therapy in cases of severe bone loss, although the long-term effect of inhibition of bone turnover remains unknown. Osteonecrosis of the jaw and atypical femoral fractures are rare, but potentially serious adverse events that may be related to longer-term exposure to BPs, although there is currently insufficient evidence to suggest a causal relationship and they have never been reported in a child (Kwek et al. 2008; Girgis et al. 2010; Hennedige et al. 2013). Prophylactic BP in DMD in those receiving GC has been reported to be associated with increased survival (Gordon *et al.* 2011) but evidence from this study should be interpreted with caution as it was a retrospective review of

only 16 patients, 12 of whom were on intravenous BP. Although BPs are frequently used to treat osteoporosis in DMD, they do not primarily affect osteoblast function and their use does not prevent the development of new VF (Rauch *et al.* 2002). One study used intravenous BP therapy to treat VF in DMD and found that it was associated with an improvement in back pain and stabilisation or increase in vertebral height ratios of previous VF, but that it did not completely prevent the development of new VF (Sbrocchi *et al.* 2012). However, a retrospective review of patients in the John Walton Muscular Dystrophy Research Centre (JWMDRC) in Newcastle treated with risedronate for a mean of 3.6 years showed significantly less VF in the treated cohort compared to a control group (Srinivasan *et al.* 2016). The lumbar spine (age and size adjusted) BMD Z-scores also remained unchanged in treated patients, and were significantly greater than in the untreated cohort. Recent work utilizing trans-iliac biopsy samples however, suggests that caution needs to be taken before prophylactic BPs are used, particularly in a condition such as DMD, where there are additional risk factors for ongoing bone turnover suppression including myopathy and GC use (Misof *et al.* 2016). They found that bone turnover was already low before the initiation of BPs and then as expected, the anti-resorptive BP treatment decreased bone formation indices further. An unexpected drop in trabecular bone volume, however, was also noted and unlike in osteogenesis imperfecta, no structural improvements were seen.

In view of the risk of fracture in DMD children and the impact of fracture on health and long term mobility, prophylactic use of BPs may therefore be beneficial, but the method of administration and when to start, stop or pause treatment remains unclear. Before deciding about prophylactic BP use, the potential risks must be weighed up against the benefits. It is likely that BPs are effective in the initial period of GC-induced bone loss when there is increased bone remodelling but become less responsive as osteoclast function reduces with prolonged treatment and bone remodelling ceases. After this time, BPs may further dampen bone remodelling and instead compromise skeletal quality, predisposing to fracture.

Parathyroid hormone

High levels of parathyroid hormone (PTH) stimulate osteoclastic bone resorption but intermittent low dose PTH can stimulate osteoblast function by increasing prostaglandin E_2 and TGF-β release from bone (Girotra *et al.* 2007). This could

therefore be a useful anabolic agent to counteract the adverse effects of GCs in osteoblasts and has been shown to be effective in *mdx* mice (Gray *et al.* 2012, Yoon *et al.* 2019). However, recombinant PTH treatment using teriparatide requires daily subcutaneous injections and is currently contraindicated and has a 'black box' warning in those with open epiphyses. Its use is also limited to 2 years duration in adults because of cases of osteosarcoma seen in some strains of rat when high doses were given (Elraiyah *et al.* 2015).

Testosterone

The use of testosterone therapy in DMD has recently been reviewed by our team at the JWMDRC (Wood *et al*. 2015) and there are currently no data available regarding the effects of testosterone on bone density in those on chronic GC treatment. Testosterone appears to be well tolerated in adolescents with DMD but our evaluation of practice found that neither growth nor pubertal developmental were optimal and few subjects had adult endogenous testosterone levels post-treatment. There remains much variability in clinical practice regarding whether oral, topical or intramuscular preparations are used, and the age at initiation and duration of treatment vary greatly by centre. We are currently running a clinical trial to determine the efficacy of a 2-year incremental regimen of intramuscular testosterone in adolescents with DMD and delayed puberty (NCT02571205). The importance of testosterone in the maintenance of muscle mass as well as bone density is critical, and testosterone supplementation should be considered when hypogonadism is present in adults with muscular dystrophies.

Vitamin D and calcium

There are multiple risk factors and evidence for vitamin D deficiency in this population as discussed above and so vitamin D supplementation should routinely be recommended to all patients with a muscular dystrophy. Whilst an adequate dietary calcium is required to satisfy reference intake levels, there is no evidence in the DMD population to indicate that additional calcium will have a beneficial impact on bone health. Patients with DMD are at risk of hypercalciuria and additional calcium may simply increase susceptibility to nephrocalcinosis (Braat *et al.* 2015).

1.11 The role of GH and IGF-1 in DMD

Chronic GC use interferes with the IGF-1/GH axis, both at a systemic level and within the bone and GP itself. GC cause a reduction in pituitary GH secretion via an increase in hypothalamic somatostatin (Barkan *et al.* 2000) tone and increased peripheral IGF-1 and GH resistance. There is only one published case-series describing the use of GH for treatment of short stature in DMD. A retrospective review was carried out on 39 boys who were treated with GH for severe steroid-induced growth failure (Rutter *et al.* 2012). An improvement in growth velocity from a mean of 1.5 cm/year to 5.2 cm/year was observed and an increase in lean body mass. Importantly there was no associated deterioration in muscle or cardiopulmonary function. The effect of GH on bone density, however was not evaluated. GH also has anabolic effects in normal skeletal muscle, but there has been some anecdotal concern that it may speed up disease progression in DMD; one case report showed that a patient with DMD and GH deficiency had a slower than expected disease course and a small case-series showed that low levels of GH can occur in DMD, without an impact on clinical course (Merlini *et al.* 1988). However, the more recent retrospective review of GH therapy did not show a deleterious effect on muscle function and a well-designed, older trial of mazindol, a GH inhibitor, did not show any beneficial effect on muscle function (Griggs *et al.* 1990). Three of the boys in Rutter's study suffered adverse events, one developed benign intracranial hypertension and two, insulin resistance. He concluded that treatment with GH for short stature in DMD could be considered, alongside careful monitoring for the development of side-effects. A randomized controlled trial designed to look at the effects of GH on cardiac function in a series of patients with Duchenne and Becker muscular dystrophy also evaluated skeletal muscle function as a secondary outcome measure (Cittadini *et al.* 2003). Seven out of the sixteen patients showed low initial IGF-1 levels. After treatment with GH, no significant differences were seen in muscle function between the treatment and placebo groups.

IGF-1 is currently approved for use in the treatment of short stature associated with severe IGF-1 deficiency (Bucuvalas *et al.* 2001, Backeljauw *et al.* 2013). Injections of recombinant human (rh)IGF-1 are currently approved for use in the treatment of short stature associated with severe primary IGF-1 deficiency. Although there is very little clinical evidence for the use of rhIGF-1 in DMD, there is currently a pilot, phase 2 clinical study in progress to look at the effect of IGF-1 on muscle function and growth

rate in DMD. Interim analysis suggests that height gain was greater in the IGF-1 group compared to the controls, with doubled height velocity in the treated group compared to controls and only mild adverse events that were felt to be unrelated (Rutter *et al.* 2013). Markers of insulin resistance also improved but there were no difference in functional motor outcomes. IGF may therefore show future promise in the treatment of short stature in DMD. It is likely that the difficulty getting hold of clinical grade recombinant IGF1 has prevented further studies up until now.

In pre-clinical studies, administration of rhIGF-1 to dystrophic mice increased muscle contraction force and enhanced the fatigue resistance of respiratory muscles (Gregorevic *et al.* 2004), while transgenic over expression of IGF-1 in dystrophic mice led to increased muscle fibre size and number (Barton *et al.* 2002) and a reduction in myofiber necrosis during the acute period of muscle necrosis (Shavlakadze *et al.* 2004). Growth and skeletal development were not investigated in these studies.

1.11.1 Rationale for Combined IGF-1 and GH use

There is a complex interplay between the actions of GH and IGF1 and co-administration of GH and IGF-1 may prove synergistic for several reasons. Higher serum IGF-1 levels are achieved with a combination treatment of GH and IGF-1 than with either GH or IGF-1 alone; co-administration influences the half-life, clearance and distribution volume of IGF-1 (Janssen 2009) and the feedback of IGF-1 on pituitary GH secretion. Increased IGFBP concentrations also result, which leads to higher levels of ternary complex formation and a more stable circulating IGF pool and thus higher effective IGF-1 tissue concentrations. Improving tissue IGF1 levels may in fact be more important than increasing serum IGF1 concentrations. IGF-1 may be also be stimulated by other factors (independently from GH) and exert direct actions on tissues. It has also been reported that only GH and IGF1 in combination can bypass the acquired partial GH resistance caused by GC (Janssen 2009). Similarly, a recent study showed that GH treatment did not increase muscle mass in mice that lacked IGF-1 receptor function (Kim *et al.* 2005). Further pre-clinical data suggests that increases in GH can increase the percentage of type1:2 muscle fibre types; skeletal muscle-specific removal of GHR changed fibre type (decreased the proportion of type I fibres and increased the proportion of type II fibres) and resulted in decreased grip strength (Mavalli *et al.* 2010). Kupfer and colleagues showed that GH and IGF-1 together reversed insulin-suppressive effects and had anti-catabolic effects on

muscle mass in calorie-restricted adults (Kupfer *et al.* 1993). A recent study using rhGH in combination with rhIGF-1 for the first time in children with low IGF-1 levels and GH sufficiency also showed that co-administration significantly accelerated linear growth compared with rhGH alone (Backeljauw *et al.* 2015). The combination of GH and IGF-1 probably also counteracts disadvantageous effects on glucose metabolism of either GH alone or IGF-1 alone. Although serum IGF-1 levels in high-normal range have been associated with increased risk of prostate, breast and colorectal cancer, this is unlikely to cause significant clinical concern in DMD.

Given that both rhGH and rhIGF-1 are licensed for use in children with growth disorders and in light of data from children and adults with chronic inflammation (Bucuvalas *et al.* 2001, Mauras *et al.* 2002), there is potential for these anabolic agents to improve growth potential, muscle strength and bone mass, which are fundamental problems in patients with DMD. However, before using these pharmacological agents for this purpose, an improved understanding of (1) their effects on linear growth and bone mass, and (2) the underlying mechanisms through which they exert their effects on bone, is imperative.

1.12 Murine models of Duchenne muscular dystrophy

Animal models of DMD form an integral part of pre-clinical research and are critical for understanding the underlying mechanism of disease. It is essential that an animal model mirrors the underlying genetic defect, disease severity and progression as closely as possible to the clinical scenario and allows a reliable prediction of the response to a given therapeutic intervention in humans (Willmann *et al.* 2009). The model should ideally also be well characterised and easy to obtain and maintain, and have a reproducible disease course. Mice are commonly used as animal models because they are relatively easy and cost-effective (with an accelerated lifespan of 1:30 years) to maintain and share more than 95% of the human genome but can be readily genetically manipulated to simulate specific human diseases. It is also possible to control for the variability found in humans and carry out experiments that would be ethically impossible in humans. In this project, the bone and growth phenotype of three different murine models of muscular dystrophy will be compared.

1.12.1 The muscular dystrophy x-linked (mdx) mouse

The muscular dystrophy x-linked (*mdx)* mouse is the most commonly used and best characterised animal model of DMD. More than 8000 papers have been published since a naturally occurring dystrophin-deficient mouse was first reported in 1984 in a colony of C57BL10 mice (Bulfield *et al.* 1984). The *mdx* mouse carries a point mutation in exon 23 of the mouse dystrophin gene introducing a premature stop codon, which leads to the absence of full-length dystrophin (Figure 1-6). This type of mutation accounts for approximately one third of the mutations found in DMD patients. The lifespan of mdx mice is reduced by approximately 20% compared to their wildtype (WT) controls.

- ***Muscle weakness in the mdx***

Early reports regarding muscle function in the mdx mouse are conflicting. One study suggested that there is an early period, between the end of the second and up to the fifth week of life, when *mdx* mice experience extreme weakness (Muntoni *et al.* 1993). After this critical period, both spontaneous motility and endurance of *mdx* mice, although lower than those of controls, did not show statistically significant differences up to 6 months-of-age. Later on, during development, *mdx* mice were seen to adapt and did not show detectable *in vivo* functional muscle impairment up to 6 months-of-age. By contrast, the earliest reports suggested that at 3 weeks of age, muscle histology shows atrophy with loss of normal muscle fibres but that regeneration occurs by 8 weeks-of-age and that there is no co-existing clinical disease (Bulfield *et al.* 1984). By 12 months-of-age muscular tremors and mild incoordination were described. More recent studies have shown no early signs of clinical deterioration. One report indicated that *mdx* mice have minimal clinical symptoms and their lifespan is only reduced by 19%, to an average of 21.5 months (Chamberlain *et al.* 2007) whilst another found no difference in force contraction compared to C57BL10 control mice at 7 weeks-of-age (Coley *et al.* 2016) but decreased grip strength by 24 weeks-of-age with no signs of cardiomyopathy by 28 weeks-of-age. These latter reports are consistent with many other studies which have not examined the mice during the early period but have found that the severe dystrophic phenotypes, such as muscle wasting, scoliosis and heart failure, do not occur until mice are 15 months-of-age or older (Lefaucheur *et al.* 1995).

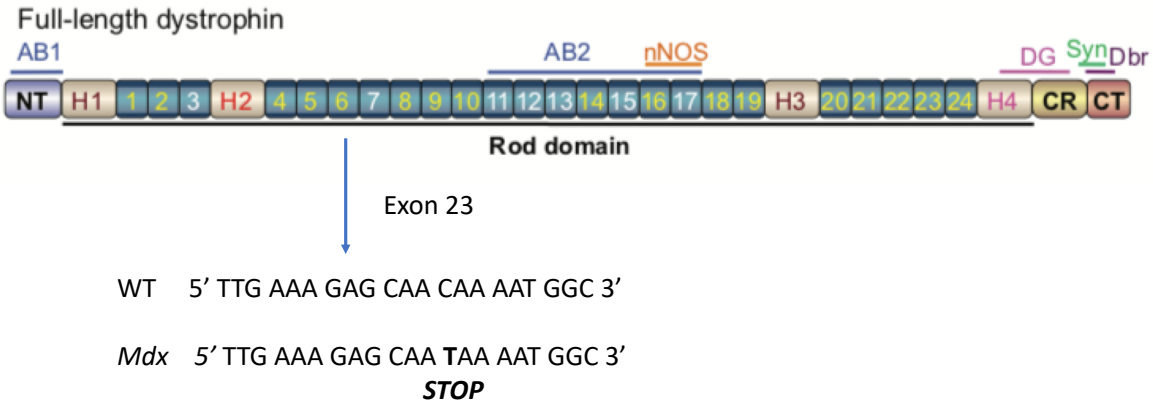

Figure 1-6 shows the DNA sequence position of the main dystrophin domains and the location of the stop mutation at exon 23 in the mdx mouse which results in an absence of functional dystrophin production and leads to the development of DMD (Modified from (McGreevy *et al.*, 2015).

- ***Growth in the mdx***

The growth phenotype of the *mdx* model has not been studied in detail but the phenotype appears to be mild (Connolly *et al.* 2001). A study investigating energy expenditure in *mdx* mice found that overall growth was blunted in juvenile *mdx* mice, with bodyweight and femur and tibia length being significantly shorter at 4-5 weeks old, but by adulthood (14 weeks) no significant difference was demonstrated between *mdx* and WT mice (Radley-Crabb *et al.* 2014). They found that fat free mass was less and whole body protein breakdown was 35% higher in *mdx* juveniles and proposed that their diet did not satisfy their metabolic or protein: energy requirements. The observed gain in overall body size was attributed to muscle hypertrophy and fibrosis. In keeping with this, total 24 hour activity was reduced by 50% in juvenile mice, but there was less difference in activity seen in adult mice. Another study also showed no significant difference in femur length between the *mdx* and WT mice at 3 weeks-of-age suggesting that there is no significant growth retardation in young *mdx* mice (Nakagaki *et al.* 2011).

- ***Bone phenotype in the mdx***

There are conflicting data regarding the bone phenotype in the mdx mouse and unlike in patients with DMD where bone strength decreases with advancing age, the converse appears true in *mdx* mice. In one study, osteopenia and reduced strength were seen in the femur of 3-week old *mdx* mice in the absence of muscle degeneration suggesting primary skeletal fragility (Nakagaki *et al.* 2011). Another showed that at 7 weeks, the *mdx* mouse displays compromised bone structure and function compared to WT mice and giving GC further reduces bone strength and structure (Novotny *et al.* 2011). In keeping with this, Anderson demonstrated lower cortical parameters in *mdx* mice at both 4 and 12 weeks-of-age, with some signs of recovery by 18 weeks-of-age (Anderson *et al.* 1993). This is in keeping with the period of acute muscle necrosis observed in the *mdx* mouse at 3-4 weeks-of-age followed by subsequent regeneration up until approximately 20 months-of-age, after which time the regenerative capacity reduces due to a gradual decline in muscle satellite cell number (Nakagaki *et al.* 2011). However several other studies have shown either no bone phenotype at a young age or results that are limited to a specific bone parameter, (

Table **1-1**), (Isaac *et al.* 2013, Gao *et al.* 2019). One study found that femoral BMD was actually higher in the *mdx* mouse compared to WT, but only female mice were used and their outcome measure was dual xray absorptiometry (DXA) which is less sensitive than micro computed tomography (μCT) (Montgomery *et al.* 2005). Their differences also disappeared after adjusting for body mass.

- ***Limitations of the mdx***

The *mdx* mouse has clear limitations as a model for DMD in humans. Firstly, the phenotype appears to be age-dependent. The *mdx* mouse demonstrates acute muscle necrosis by 3 weeks-of-age, but subsequent muscle regeneration then occurs and the subsequent life span of the *mdx* is nearly normal (reduced by 25% compared to 75% reduction in DMD) (Chamberlain *et al.* 2007). Secondly, the phenotype is much less severe (Bulfield *et al.* 1984, Muntoni *et al.* 1993). In stark contrast to the relentless decline in muscle function seen in children with DMD, the muscle force of adult *mdx* limb muscles are similar to unaffected WT control mice (Lynch *et al.* 2001, Muller *et al.* 2001). It is unclear whether there is a compensatory mechanism (such

as utrophin upregulation) to account for this, or whether the muscle sparing is due to a species-dependent mechanism, such as the replicative potential of murine satellite cells (Helliwell *et al.* 1992). Indeed, few medications that have shown therapeutic benefit in the *mdx* have also shown efficacy in DMD clinical trials (Fairclough *et al.* 2011). Therefore, there is clearly a need for a more appropriate pre-clinical model.

1.12.2 The mdx:utr mouse

Recent studies suggest that *utrophin heterozygous*: *mdx* mice might represent an intermediate model between the extreme double utrophin knockout: *mdx* mouse and the more mildly affected *mdx* mouse (Zhou *et al.* 2008). Utrophin is an autosomal homologue to dystrophin. It is thought that upregulation of utrophin expression in the *mdx* mouse may compensate for the lack of dystrophin and account for the less severe phenotype compared to DMD (Deconinck *et al.* 1997). It is possible that utrophin compensates for the loss of dystrophin more effectively in mice than humans and it is currently being used in a current clinical trial as a potential therapeutic intervention (Ricotti *et al.* 2016). The homozygous double knockout, the *mdx:utr*$^{-/-}$ mouse has severe muscle weakness, significant growth retardation, joint contractures and cardiomyopathy (Isaac *et al.* 2013, Gao *et al.* 2019). However, premature death usually occurs between 6 and 20 weeks and colonies are very difficult to maintain. The heterozygous *mdx:utr* $^{+/-}$ mouse therefore represents a potential compromise with an intermediate phenotype between that of the fatal homozygous *utrn-/-mdx* and the less severe *mdx* mouse (Mcdonald *et al.* 2015).

- ***Muscle weakness in the mdx:utr*$^{+/-}$ *mouse***

There is limited literature regarding the *mdx:utr* $^{+/-}$ mouse. Lifespan seems to be more than 1 year with fibrosis becoming evident at differing time-points from 8 weeks-of-age (Gutpell *et al.* 2015) to 6 months-of-age (Zhou *et al.* 2008). These studies, however, did not conduct any measures of behaviour or grip strength. One study suggested that respiratory function impairment of the *mdx:utr* $^{+/-}$ mouse was worse than the *mdx* mouse but that the mice have a near normal lifespan (Huang *et al.* 2011). By 1 month-of-age, the grip duration of the triceps had decreased and persisted throughout the first year, but otherwise muscle function in the *mdx:utr* $^{+/-}$ was not found to be significantly affected. A further study showed that the mdx:utr$^{+/-}$ mouse

had a shorter latency to fall time in the grip strength test at 3 months-of-age, but that the difference had disappeared by 18 months-of-age (Mcdonald *et al.* 2015).

- ***Growth in the mdx:utr$^{+/-}$ mouse***

There are no published data on bone growth in the *mdx:utr*$^{+/-}$ mouse, only bodyweight, which is inaccurate as can be affected by many other factors rather than just bone growth.

- ***Bone phenotype in the mdx:utr$^{+/-}$ mouse***

There is only one paper investigating the bone phenotype in the *mdx:utr* $^{+/-}$ mouse as part of a larger study. This showed that there was less collagen present in the metaphyseal bone of the *mdx:utr*$^{+/-}$ mouse compared to the *mdx* mouse (Isaac *et al.* 2013).

Study	Age studied (weeks)	Sex	Site	Findings in *mdx* compared to WT
Anderson et al (Anderson *et al.* 1993)	4,12,18	No details	Tibia	Lower cortical parameters at 4 weeks and 12 weeks with some recovery by 18 weeks in mdx
Gao et al (Gao *et al.* 2019)	4, 6	Both	Tibia (Tb) Femur (Ct) Lumbar spine	No significant differences in bone parameters at either age on μCT at any site (some heterotopic bone formation)
Gray et al (Gray *et al.* 2012)	10	Male	Femur	MS/BS of trabeculae and cortex + cortical area increased No difference in femoral length
Montgomery et al (Montgomery *et al.* 2005)	16	Female	Femur Lumbar spine	Higher femoral BMD Lumbar spine BMD similar
Nakagaki et al (Nakagaki *et al.* 2011)	3	Male	Femur	Reduction in Tb.Th & Ct. Th and cross- sectional area
Novotny et al (Novotny *et al.* 2011)	7, 104	Both	Tibia	Reduction in trabecular morphometry and mechanical functional properties
Rufo et al (Rufo *et al.* 2011)	26	Both	Tibia Parietal bone	Reduction in Ct.Ar, Ct.Th and trabecular BV/TV in tibia Increased osteoclast no, reduction in osteoblast number
Yoon et al (Yoon *et al.* 2018)	10	Male	Femur Lumbar spine	No difference in vBMD or cortical phenotype Reduced trabecular BV/TV and reduced SMI
Yoon et al (Yoon *et al.* 2019)	10	Male	Femur Lumbar spine	Minimal effect on cortical bone- reduced periosteal perimeter only Reduced trabecular vBMD and BV/TV, increased Tb.Sp

Table 1-1 Summary of studies of bone properties in *mdx* mice showing no consistent bone phenotype.

BV/TV: bone volume/tissue volume, vBMD: volumetric bone mineral density, Ct.Ar: cortical area, Ct.Th: cortical thickness, MS/BS: mineralising surface/bone surface, SMI: structural model index, Tb.Sp: trabecular spacing

- ***Limitations of the mdx:utr$^{+/-}$ mouse***

Mdx mice with an additional utrophin deletion do not genetically mirror patients with DMD because the muscles of patients with DMD do express utrophin. Despite the additional utrophin deletion the phenotype still seems less severe than the *mdx* mouse.

1.12.3 The mdx:cmah$^{-/-}$ mouse

An alternative model is the double mutant *mdx:cmah*$^{-/-}$ mouse, which carries a human-like mutation in the mouse cytidine monophospho-N-acetylneuraminic acid hydroxylase (*cmah*) gene. During the evolution of humans, approximately 3 million years ago, an inactivating deletion was introduced in the human *Cmah* gene (Hedlund *et al.* 2007). Cytidine monophospho-N-acetylneuraminic acid hydroxylase is an enzyme found in the cytosol, and this mutation prevents synthesis of the common mammalian sialic acid, N-glycolylneuraminic acid in all human cells (Chou *et al.* 1998). It is likely that this stemmed from natural selection. Because infectious agents such as viruses and bacteria often use host cell glycans as receptors, cell surface glycans are prone to alteration during natural selection, therefore creating the difference between mice and humans to prevent disease transmission (Rich *et al.* 2000, Dankwa *et al.* 2016). Sialic acids are expressed on the ends of glycan structures. N-glycolneuraminic acid is not found in humans, but is in mice. Therefore, a human-like deletion introduced into the *cmah* gene in mice prevents hydroxylation of N-acetylneuraminic acid to N-glycolneuraminic acid (Hedlund *et al.* 2007). This is probably partly responsible for less constrained brain growth and makes humans less susceptible to some viruses like malaria, but also appears to cause a weakening of the sarcolemmal membrane and affects the integrity of skeletal muscle fibres (Chou *et al.* 1998, Okerblom *et al.* 2017).

- ***Potential advantages of mdx:cmah$^{-/-}$ mouse***

To the best of knowledge, there is only one paper reporting the phenotype of the *mdx:cmah*$^{-/-}$ mouse (Chandrasekharan *et al.* 2010), referred to in this thesis as the *mdx:cmah mouse*, but it would appear that it is the most similar to DMD at the phenotypic and molecular level. Increased disease severity and reduced lifespan compared to the *mdx* mouse is described. Two mechanisms are postulated for the increased disease severity:

1. Lower levels and function of dystrophin-glycoprotein complex
2. Metabolic accumulation of dietary N-glycolyneuraminic acid (Neu5Gc), generation of Neu5Gc antibodies and deposition/activation of complement on muscle fibres.

Studies carried out in the JWMDRC at Newcastle University have also demonstrated earlier cardiac dysfunction (Blain *et al.* 2018) and less constrained brain growth (unpublished data). This suggests that the *mdx:cmah* mouse may be a more appropriate model for DMD, but this requires further study. The early studies using the *mdx:cmah* may also implicate a direct role for sialic acids in muscle disease and further pre-clinical work is required to elucidate this.

- ***Muscle weakness in the mdx:cmah$^{-/-}$ mouse***

The *mdx:cmah* mice showed a more severe phenotype than *mdx* mice (Chandrasekharan *et al.* 2010), with highly significant decreases in lifespan; almost half of all animals died by 11 months of age. They had increased necrotic foci by 3 months of age in the heart and increased fibrosis by 6 weeks-of-age in the quadriceps. Muscle function tests were only carried out at 8 months-of-age. By this time, the *mdx:cmah* mice had impaired ambulation, showing a 70% reduction in the time they were able to walk on a constant speed rotorod for 5 minutes relative to *mdx* littermates. The mice also had reduced EDL force contractions.

- ***Growth and bone phenotype of mdx:cmah$^{-/-}$ mice***

There are no published data describing either the growth or bone phenotype of the *mdx:cmah* mouse and establishing this knowledge will be essential if future studies of the *mdx:cmah* mice are to yield new insights into DMD. However, unpublished pilot data from the Newcastle University group has shown an adult *mdx:cmah* mouse with a marked scoliosis by 18 months of age when compared with both the *mdx* and WT mice (Figure 1-7).

1.13 Murine models of GC-induced growth retardation and GIO

As part of this PhD project, animal models of both glucocorticoid-induced osteoporosis (GIO) and GC-induced growth retardation were reviewed (Wood *et al.* 2018), with the aim of determining the most appropriate animal model to use when demonstrating the effects of GC on growth and bone structure (see Appendix VI). Data analysed in the review determined that there are currently no established and proven regimens for inducing both GIO and GC-induced growth failure in mice. Results were too heterogeneous to enable one specific model to be advocated over another in all situations. However, there was sufficient evidence to recommend that investigation of GC-induced growth retardation in mice can be performed using dexamethasone 2-5 mg/kg/day by daily SC injection. When investigating GIO, there was insufficient evidence to recommend one specific mode of delivery over another but in most studies a dose of prednisolone 2-5mg/kg/day in mice appeared to be sufficient.

There are specific outcome measures that should be assessed when investigating either GIO or GC-induced growth retardation: growth outcome measures should include serial lengths (using consistent measuring technique) and/or GP height and bone formation rate (BFR); the measurement of body weight for assessing linear growth is too inaccurate. Recommended outcome measures for assessment of GIO include volumetric BMD (by peripheral quantitative CT or μCT rather than by DXA for greater accuracy) and bone biomechanical testing to mimic fracture rate in clinical studies. These recommendations have been taken into consideration when designing the methods for this study.

Mice have been chosen as pre-clinical models of muscular dystrophy throughout this project, because they share more than 95% of the human genome and can be readily genetically manipulated to simulate specific human diseases. It is also possible to control for the variability found in humans and undertake experiments that would otherwise be impossible in humans. They also have the added advantage of being relatively easy and cost-effective to maintain. The adult mammalian skeleton undergoes a continuous remodelling cycle and some of the early pre-clinical studies using different species failed to appreciate this. More recent work has shown that the mouse shows a similar pattern to human GIO, with an early phase of osteoclast

mediated bone resorption, followed by a more indolent phase of decreased osteoblastogenesis and bone formation (Yao *et al.* 2008). Unlike in humans however, bone acquisition and longitudinal bone growth continue in mice and rats after sexual maturity. In mice, whilst the highest growth phase is from weaning until sexual maturation, body weight continues to increase in the mouse up to the end of the 52nd week and long bone growth continues slowly after puberty (Jilka 2013). A gradual decrease in trabecular number is also seen after 2 months of age (Glatt *et al.* 2007). As time constraints prevented the use of two different models in this project, it was decided to use peri-pubertal mice for this project to enable sufficient differences in bone parameters to be induced, without the mice being too young and small to tolerate daily injections.

Prednisolone (or prednisone), methylprednisolone and dexamethasone are the most frequent synthetic GC used in osteoporosis animal models. Many studies implemented regular intramuscular, intraperitoneal or SC injections, but single implantation of slow release SC pellet or oral gavage were also used. In rats of the same strain and age, daily oral gavage of GCs over a 90 day period (Lin *et al.* 2014) led to similar adverse effects on bone (as assessed by histomorphometry and areal BMD) as thrice weekly subcutaneous injections of GC over 56 days (Iwamoto *et al.* 2008). By contrast, a much shorter period of intervention was necessary to induce osteoporosis with daily injections (Ogoshi *et al.* 2008) or continuous infusion through SC implanted osmotic pumps (King *et al.* 1996). Daily injections are stressful for the animals, which may negatively influence the outcome and ethical regulations in some countries may not allow multiple repeated injections over a long time period. For example, the injection of vehicle alone caused a 3-fold increase in serum corticosterone levels in mice, compared to a 5-10 fold increase induced by an intraperitoneal injection of 10 mg corticosterone/kg body weight, 1 hour after injection (Herrmann *et al.* 2009). This technique of administration would also not be acceptable to most patients in the clinical trial setting. Micro-osmotic pumps were found to have a large variation in residual volumes 21 days after implantation. With a filling volume of 250 μl, residual volumes containing active drug ranged from 50 to 180 μl, which indicated major differences in the flow-rate of individual pumps (Herrmann *et al.* 2009). SC insertion of slow release pellets containing corticosterone leads to more consistent drug levels as compared to subcutaneous injections of corticosterone. Oral

gavage seems to be less effective compared to daily injections or slow release subcutaneous pellets, but has the most translational relevance, as this would be the most accepted method of GC administration in the clinical setting. Whilst slow release pellet insertion may reduce unnecessary repetition of periodical injections over the study period their safety and efficacy needs further validation.

1.14 Aims of this project

The main goal of this project is to test the overall hypothesis that:

Mouse models of DMD have an intrinsic abnormality of linear growth and skeletal development that can be rescued by modulation of the GH/IGF-1 axis.

Within this hypothesis, the main aims are to investigate:

1. Growth and GP chondrogenesis in *mdx*, *mdx:utr* and *mdx:cmah* mouse models of DMD and compare them to WT mice.
2. Bone development and mechanical properties in *mdx*, *mdx:utr* and *mdx:cmah* mouse models of DMD and compare them to WT mice.
3. Growth response and bone development of *mdx* and *mdx:cmah* mice following exposure to GCs and VBP-6, a GC-sparing agent.
4. Growth response and bone development of *mdx* mice following treatment with a combination of GH and IGF-1.

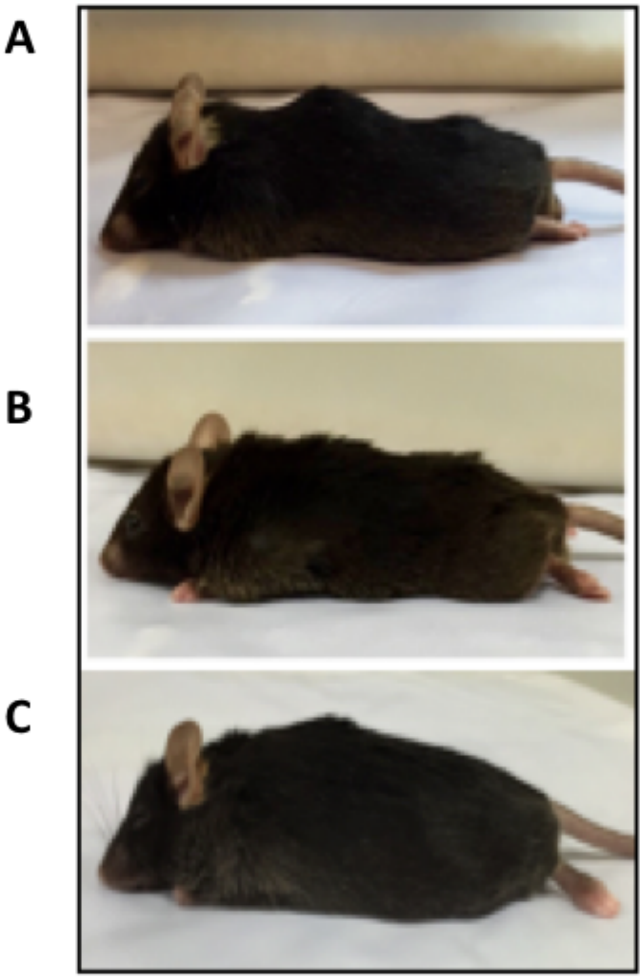

Figure 1-7 Development of scoliosis in the aged *mdx:cmah* mouse:

A) *mdx:cmah*

B) *mdx*

C) WT mouse, all at 18 months of age.

Photos used with kind permission of Dr Emine Bagdatlioglu of Newcastle University.

CHAPTER 2

Materials and methods

2 Materials and Methods

2.1 Reagents and solutions

All chemicals and reagents were provided by Sigma (Poole, UK) and laboratory consumables from Thermo Fisher (Cramlington, UK) unless otherwise stated.

2.2 In vivo studies

2.2.1 Colony establishment

C57BL/10ScSn.*mdx* and C57BL/10ScSn-congenic utrophin/dystrophin double mutant strain (B10ScSn.*utr*/*mdx*) mice strains were obtained from the Jackson laboratory (Bar Harbour, ME, USA, https://www.jax.org/strain/019014 and https://www.jax.org/strain/001801) and quarantined whilst health screening was performed. The *mdx*:*utr* colony was maintained by breeding heterozygote *mdx:utr*$^{+/-}$ females with *mdx* males, to ensure that no double knockout utrophin mice were generated, as these are known to have a more severe phenotype and few survive beyond 18 weeks of age. Mice highlighted in yellow were used to breed next generation, those highlighted in green were used experimentally, where XYUu is a *mdx:utr* heterozygote (X denotes the *mdx* mutation and U the *utr* mutation):

1) XXUu v XYuu

	XU	XU	Xu	Xu
Xu	XXUu	XXUu	XXuu	XXuu
Xu	XXUu	XXUu	XXuu	XXuu
Yu	XYUu	XYUu	XYuu	XYuu
Yu	XYUu	XYUu	XYuu	XYuu

C57BL/10ScSnJ mice were also purchased from Jax to use as wildtype (WT) controls (https://www.jax.org/strain/000476). All mice were bred on the same genetic background to allow valid comparisons between muscular dystrophy models.

Several generations of breeding were required to create the B10.Cg-*CMah*^{tm1Avrk}Dmd*mdx*/PtmJ line (https://www.jax.org/strain/017929), as the only *mdx:cmah* mice that could be supplied by the Jackson laboratory were *cmah* het/*mdx* WT males and *cmah* het/*mdx* het females therefore several crosses were required in

order to obtain the correct mice for use in the study (mdx mutation highlighted in by the red X, *cmah* mutation denoted by c). Mice highlighted in yellow were used to breed next generation, those highlighted in green were used experimentally:

1) XXCc v XYCc

	XC	Xc	XC	Xc
XC	XXCC	XXCc	XXCC	XXCc
Xc	XXCc	XXcc	XXCx	XXcc
YC	XYCC	XYcC	XYCC	XYCc
Yc	XYXc	XYcc	XYCc	XYcc

2) XXcc v XYcc

	Xc	Xc	Xc	Xc
Xc	XXcc	XXcc	XXcc	XXcc
Xc	XXcc	XXcc	XXcc	XXcc
Yc	XYcc	XYcc	XYcc	XYcc
Yc	XYcc	XYcc	XYcc	XYcc

3) XXcc v XYcc

	Xc	Xc	Xc	Xc
Xc	XXcc	XXcc	XXcc	XXcc
Xc	XXcc	XXcc	XXcc	XXcc
Yc	XYcc	XYcc	XYcc	XYcc
Yc	XYcc	XYcc	XYcc	XYcc

For clarity throughout this thesis, the following abbreviations will be used:

Abbreviation	**Full nomenclature**	**Zygosity**
WT (wildtype)	C57BL/10ScSnJ	Homozygous
mdx	C57BL/10ScSn.*mdx*	Hemizygous
mdx:utr	C57BL/10ScSn.*utr*/*mdx*	Heterozygous for *utr*, hemizygous for *mdx*
mdx:cmah	B10.Cg-*CMah*^{tm1Avrk}Dmd*mdx*/PtmJ	Homozygous for *cmah*, hemizygous for *mdx*

Table 2-1 Full nomenclature and abbreviations for mice used within the studies

Where possible animals were bred at the same time and under the same environmental conditions for each group.

2.2.2 Animal welfare

All animals were housed in the Biological Research Facility (BRF) at Roslin Institute, under controlled temperature (approx. 25°C) and light conditions (12:12h light: dark cycle) and offered food and water ad libitum. All experiments were performed in full compliance with Government regulations and guidelines on animal welfare under the terms of the Animals (Scientific Procedures) Act 1986, authorized by the Home Office UK. The projects were carried out under project licence 70/8285, held by Professor Colin Farquharson (updated to include the muscular dystrophy mouse models). All animals were inspected daily to monitor for the development of negative phenotypes and animals exhibiting any harmful abnormal phenotype were humanely killed.

2.2.3 Rationale for choice of time-points

Mice in the cross-sectional characterisation studies of mice were sacrificed at three post-natal developmental ages (3, 5 and 7 weeks) when linear growth is rapid. Three weeks-of-age was chosen to represent pre-pubertal mice; growth is greatest between 2 and 4 weeks of age, thus enabling differences in growth velocity to be determined most effectively. 5 week-of-age mice were chosen as they are peri-pubertal, so allowing any effect of endogenous sex steroid hormone levels on growth and skeletal development to be determined. 7 weeks-of-age mice were chosen as the final timepoint so that the mice are post-pubertal but still have sufficient growth velocity to determine any inter-genotype differences. Muscle cell necrosis usually occurs by 21 days-of-age in *mdx* mice, with the peak of muscle deterioration at around 6-7 weeks-of-age, followed by significant muscle regeneration by 90 days-of-age. (Bulfield *et al.* 1984, Radley-Crabb *et al.* 2014), Therefore assessing mice at multiple time points throughout the juvenile period may enable new onset deterioration in bone and muscle to be assessed. Other studies have shown that the *mdx* is not a good model once muscle regeneration has started to occur, and a recovery in bone parameters has been demonstrated by 18 weeks of age, therefore it is important not to investigate the mice when they are too old (Montgomery *et al.* 2005).

Following a period where several late, peri-weaning, deaths were noted, it was surmised that the *mdx* mice did not respond well to early handling. In the intervention studies it was therefore decided not to start any gavage or injections until at least 28 days. Furthermore, the BRF stipulated that no pump implantation could be carried out in an animal weighing less than 15g. Therefore, guided by weights from the characterisation study, mice in the GH/IGF-1 study (Chapter 6) were weighed at day 32 and provided that their weight exceeded 15g, the pump was implanted and injections/gavages commenced 2 days later, after wound healing. Peak GH activity in mice also occurs between postnatal days 20-40, therefore any divergence in growth velocity by intervention should be most apparent in this age range (Wang *et al.* 2004).

2.2.4 Anthropometric measurements

Animals were measured twice weekly from weaning until cull, by staff in the BRF. Weight, crown to rump and tail lengths were taken using digital weighing scales and a ruler. Where possible, all measurements were taken with the same equipment by the same animal house staff during the study period, in order to minimize inter-observer variability.

2.2.5 Animal sacrifice and collection of blood samples

Mice were culled by exsanguination (non-schedule 1 method), under terminal anaesthesia with confirmation by cervical dislocation. Immediately following sacrifice, blood samples were extracted by cardiac puncture and collected in serum tubes to promote clotting. Samples were left on ice for 30mins and then centrifuged at 1000g for 10mins. A minimum of 75µl of supernatant (serum) was isolated from the whole blood where possible, then aliquoted and stored at -80°C until required.

2.2.6 DNA isolation and genotyping

Ear notches were taken at 2 weeks-of-age for genotyping. DNA was extracted using the HotSHOT method (Truett *et al.* 2000). Briefly a solution of ethylenediaminetetraacetic acid (EDTA), sodium hydroxide and water was added to the ear punch sample and heated at 95°C for 1 hour. The sample was then neutralised using a solution of 1M TRIS and water that had been adjusted to pH 5.5. 5µl of the DNA suspension was added to 20µl of PCR master mix and PCR amplification performed. DNA concentration and quality were assessed using a nanodrop

spectrophotometer (Thermo Scientific, UK). Quality was assessed by the ratio of wavelengths 260nm/280nm, where 1.8-2.0 was considered optimal.

Mdx:utr genotyping

Utrophin primers were purchased from Sigma (for sequences used see Appendix I). The utrophin knockout PCR solution contained: 3µl DNA (10ng/µl); 2.5µl 10x NH_4 buffer; 0.75µl 50mM $MgCl_2$ (Bioline), 2.5µl 2mM dNTPs; 0.5µl 20pmol/µl forward and reverse WT primers; 16µl nuclease free H_2O; 0.25µl 5U/µl BioTaq DNA polymerase. The PCR was performed under the following conditions on a DNA Engine Dyad machine (Peltier Thermal Cycler, Bio-Rad Laboratories, Hertfordshire, UK):

- 2mins at 92°C (denaturing)
- 32 thermocycles consisting of 1min at 92°C (denaturing),1min at 58°C (annealing), 1min at 72°C (extension)
- 10mins at 72°C

PCR products were run on a 1.8% agarose/1x Tris-borate EDTA (TBE) (Ambion, Cambridge, UK) gel containing 0.5ug/ml ethidium bromide. 3µl of 5x blue loading buffer (New England Biolabs, Herts, UK) was added to the PCR product and 13µl of each sample was added to the gel. Electrophoresis was carried out at 160V in a gel tank containing TBE buffer. Hyperladder 1 (Bioline) was used as molecular weight markers for the utrophin knockout PCR. Gels were imaged using a Gel Logic 200 Imaging System and software (Kodak, Hemel Hempstead, Herts, UK).

Mdx genotyping

Mdx genotyping was carried out remotely by sending ear notches to Transnetyx, Inc (Cordova, TN, USA).

Mdx:cmah genotyping

Mdx:cmah mice were originally genotyped at Roslin using primer sequences kindly donated by Prof Straub at the JWMDRC, using the same methodology as for the *mdx:utr* mice above (see Appendix I for primer sequences). A gel was then sent to Transnetyx to enable creation of a probe and subsequently genotyping was carried

out there. The first batches of samples were cross-matched using in-house genotyping to validate the probe (Figure. 2-1).

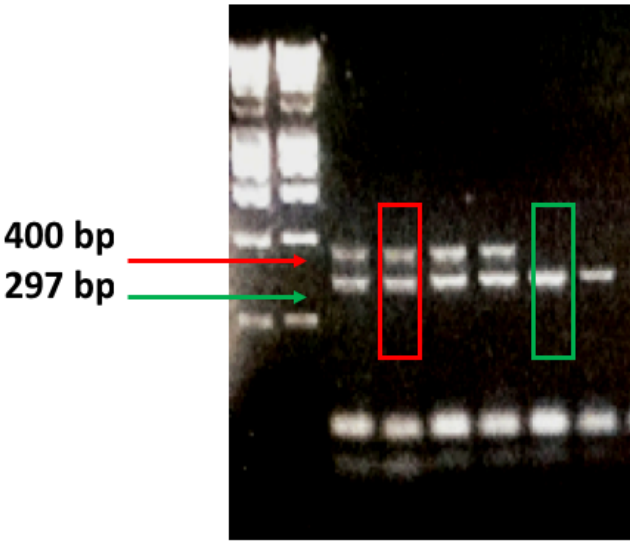

Figure 2-1 An example of a gel from *mdx:cmah* genotyping, showing bands at 297bp (WT) highlighted in green and 400 bp (*cmah*) highlighted in red. See appendix I for full primer sequences.

2.2.7 Fluorochrome labelling

Fluorochrome labelling allows sites of mineralization within bone and GP cartilage to be visualised and enable daily BFR at the chondro-osseous junction to be assessed visually under ultraviolet light, without the need for further staining or decalcification (Owen *et al.* 2009). Calcein fluorescent labels were administered at specific time intervals, dependent on the age of the mouse (van Gaalen *et al.* 2010). A stock solution of 10mg/ml calcein was prepared by adding 0.05g of calcein to 0.07g of 1.4% sodium bicarbonate (NaHCO3) and 5ml of distilled water. It was filter sterilised and stored in the dark at 4°C until required. Aliquots were made (using calcein at a concentration of 10mg/kg bodyweight) up to 200 µl using saline and injections were given intraperitoneally by the BRF staff according to the schedule in Table 2-2. Animals were culled as close to 48 hours after the last injection as possible.

To calculate longitudinal growth rate per day, the distance between the chondro-osseous junction at the distal end of the GP and the fluorescing mineralisation front was measured at 10 different points along the section (see red arrows, Figure 2-2)

and an average taken. Although two calcein injections were administered during the initial experiments, it became clear during preliminary data analysis that the movement of calcein through the mineralising front could be seen with one injection, so ultimately the mean distance was then divided by two, as only the calcein label injected two days prior to cull was used to obtain a growth rate per day. This enabled only one calcein injection to be given in the latter experiments.

2.2.8 Bromodeoxyuridine (BrdU) uptake

5-bromo-2'-deoxyuridine (BrdU) is a synthetic analogue of thymidine. It is incorporated into the DNA of replicating cells during the S phase of the cell cycle as a substitute for thymidine. Proliferation rate can then be assessed using immunohistochemistry (IHC) of tissue sections with antibodies specific for BrdU (Loveridge *et al.* 1990). A stock solution of 20mg/ml BrdU was made by adding 0.2g of BrdU to 10ml of phosphate-buffered saline (PBS) and stored at -20°C until ready for use. It was used at a concentration of 50mg/kg bodyweight and aliquots were made up to 200 µl using saline for intraperitoneal injection by the BRF staff at 24 hours prior to cull.

2.2.9 Glucocorticoids (GC) and GC-sparing agents

Following literature review (Wood *et al.* 2018), it became clear that there was no consensus regarding the optimal regimen to use for giving GC to young mice in order to impair growth and skeletal development, therefore several different types of GC and dosing regimens were trialled as part of the third study aim (Chapter 5), in order to find the most effective before moving to the final study within this project (Chapter 6).

a) Prednisolone by sub-cutaneous (SC) injection

Prednisolone sodium phosphate was dissolved in distilled water and administered by SC injection so that the prednisolone component was given at 5mg/kg bodyweight. Solutions were made up to enable 10µl/g bodyweight to be given daily to each mouse.

b) Prednisolone by oral gavage

Prednisolone was given in a cherry syrup suspension (Humco, Texas, USA) via oral gavage at doses of 10mg/kg and 20mg/kg bodyweight. Suspensions were made up so that 10ul/g bodyweight were given daily to each mouse.

Age at cull	Number of days injection given prior to sacrifice		
	First calcein	Second calcein	BrdU
3 weeks	4 days	2 days	1 day
5 weeks	7 days	2 days	1 day
7 weeks	9 days	2 days	1 day

Table 2-2 Injection timetable for mice

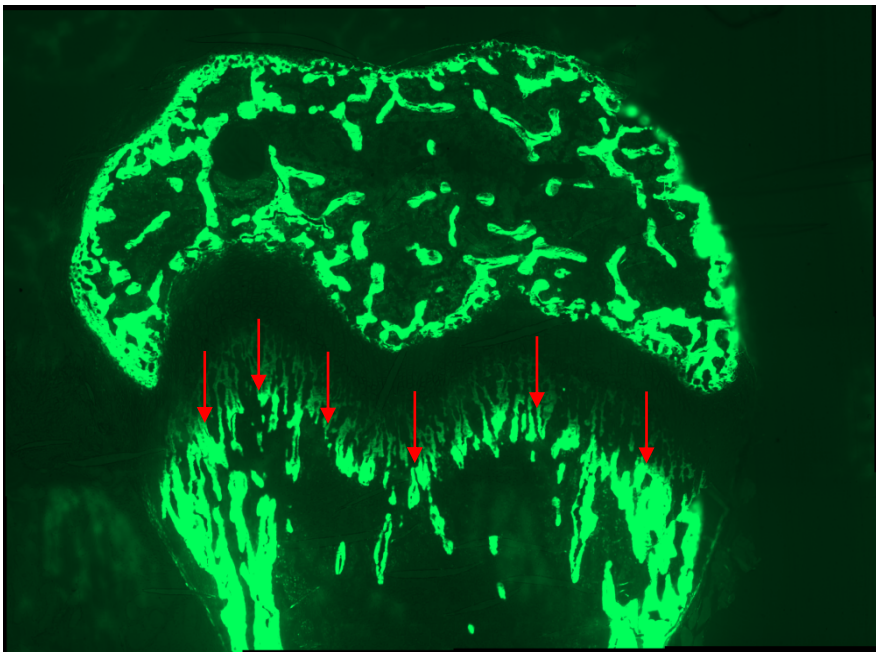

Figure 2-2 An example of a calcein labelled growth plate in a 3 week old mouse. Red arrow shows the distance measured from the chondro-osseus junction to the mineralising front. To calculate longitudinal growth rate per day, the distance was divided by the number of days prior to cull the second calcein was injected (2 days in this study).

c) Dexamethasone by SC injection

Water-soluble dexamethasone (dexamethasone-cyclodextrin) was dissolved in distilled water and given by SC injection so that the dexamethasone component was given at initially at 2.5mg/kg and then at 5mg/kg bodyweight. Solutions were made up to enable 10µl/g bodyweight to be given daily to each mouse.

d) VBP-6 by oral gavage

VBP-6 was kindly supplied as a gift by Jesse Damsker and Eric Hoffman from ReveraGen BioPharma, Rockville, MD, USA. It was also given in a suspension of cherry syrup (Humco, Texas, USA) at 20mg/kg bodyweight. Suspensions were made up to enable 10µl/g bodyweight to be given daily to each mouse.

2.2.10 Continuous delivery of insulin-like growth factor-1 (IGF-1)

Media grade IGF-1 was obtained from Gro-Pep (Adelaide, Australia) as its biological activity at 50% of the effective dose was <30ng/ml, which was greater than other commercially available sources and it has been previously used within the group with success (Dobie *et al.* 2015). In humans, IGF-1 given in bolus doses can cause quite profound hypoglycaemia, so it was decided to administer the IGF-1 in the final study (Chapter 6) via a slow infusion using a pump, rather than as a once daily injection. This also enabled the total number of injections being given to each mouse to be reduced, which was vital because otherwise the study would have exceeded the Home Office recommendation of maximum number of daily injections. The continuous administration of IGF-1 was achieved by implantation of a SC micro-osmotic pump (Alzet model 1004, California, USA). IGF-1 was reconstituted in sterile 0.9% saline prior to use. Micro-osmotic pumps were filled with 100µl of IGF-1 or vehicle and then submerged in sterile 0.9% saline and incubated at 37 °C for 48 hours. This priming step ensures that the pumps begin releasing their contents immediately on implantation. Mice were anaesthetised once they reached 32 days of age and weighed at least 15g. Pumps were implanted SC behind the scapula according to manufacturer's instructions.

A dose of 1mg/kg bodyweight/day via osmotic pump was chosen after an extensive literature review suggested that this was a safe and well tolerated dose (Gregorevic *et al.* 2002, Schertzer *et al.* 2018). The pump rate was 0.11ul/ hour, therefore working

on a mean mouse weight of 23g at 7 weeks (based on the anthropometric data obtained in Chapter 3), 0.87mg was added to 100µl of saline, thus releasing 0.023mg/day in 2.64µl at a rate of 0.11µl//hour in order for 1mg/kg/day to be given.

2.2.11 Growth hormone (GH)

A dose of 3mg/kg twice daily was chosen after an extensive literature review suggested that this was a safe and well tolerated dose with evidence of efficacy both at Roslin and beyond (Masternak *et al.* 2010, Dobie *et al.* 2014, Wong *et al.* 2016). In order to mimic the pulsatile release seen in GH in males, injections would need to be given multiple times a day, but clearly this was not feasible or ethically acceptable in practice. Several studies have emphasised the need for at least twice daily dosing of GH in male mice and also demonstrated an up-regulation of growth using 12-hourly injections (Alba *et al.* 2005, Jarukamjorn *et al.* 2006), therefore twice-daily dosing has been used in this study as a practical compromise, with the two injections spread out as much as possible within the working day. This regime has been used successfully by colleagues at Roslin (Dobie et al. unpublished data). The female mouse has a much more continual pattern of GH release, and so multi-day dosing is less relevant (Norstedt *et al.* 1984).

GH in the form of Norditropin (Novo Nordisk) was kindly supplied by Dr Tim Cheetham and colleagues at the Great North Children's Hospital, Newcastle-upon-Tyne. It was diluted using sterile 0.9% saline to enable 10ul/g bodyweight to be given daily to each mouse.

2.3 Characterisation of muscle phenotype

2.3.1 Forearm grip strength testing

Forelimb grip strength testing was performed using a grip strength meter with a specialised mouse grid (Harvard Biosciences, Massachusetts, USA). A protocol was designed for use in the BRF (Appendix II) which was based on the TREAT-NMD standard operating protocol (Luca 2014). In summary, a grip meter attached to a force transducer was used that measures peak force generated when the mouse is pulled backwards. 3 consecutive measurements were taken and then the mean calculated and divided by the body weight in grams, to obtain a grip strength value normalised

to body weight. Grip strength measurements were always performed within 24 hours prior to cull.

2.3.2 Histological assessment of muscle pathology

The tibialis anterior (TA) muscle of the lower hind limb was used for histological assessment of muscle pathology. The TA is recommended because it is readily accessible, transverse sections are easily obtained and it contains mainly fast myofibres (Grounds 2014). The muscle was firstly dissected and fixed in Neutral-buffered formalin for 48 hours and then transferred to 70% ethanol prior to processing and wax embedding (see Section 2.4.2). Sections were cut at a width of 6µm and collected onto uncoated glass slides and stored in the dark at room temperature until stained. Haematoxylin and eosin (H&E) staining was used for histological assessment of muscle pathology (see Appendix III for protocol). Haematoxylin stains eosinophilic structures (*e.g.* muscle sarcoplasm) pink and eosin stains basophilic structures (*e.g.* nuclei) dark purple, with high RNA producing paler purple staining in the cytoplasm (*e.g.* in young myotubes).

Following H& E staining, images were acquired using a Zeiss AxioImager brightfield microscope and analysed using Fiji, an open source platform for biological image analysis (Schindelin *et al.* 2012). The total cross-sectional area of the muscle was measured first and then areas of infiltrating inflammatory cells were manually measured to determine the proportion of active myfofibre necrosis as a percentage of the total area. The H&E colour deconvolution plugin on Fiji was used to separate the H&E components and the thresholding tool used to select a consistent threshold for each image where nuclei were clearly seen without too much background interference. The 'analyse particles' function was then used to automatically count nuclei. The image was then fully magnified and muscle fibres with central nuclei were manually counted using the plug-in 'cell counter' function. The percentage of regenerating muscle fibres was calculated using: no. fibres with central nuclei/ (total no nuclei x100). From these values, a cumulative measure of skeletal muscle damage was calculated, consisting of the percentage of active necrosis and regenerating cells. This methodology is recommended in the TREAT-NMD protocol (Grounds 2014).

2.3.3 Quantification of creatine kinase activity

Creatine Kinase (CK) is a protein found in cardiac and skeletal muscle. By measuring serum CK levels, it is assumed that an increased level signifies muscle damage and sarcolemma membrane fragility, leading to the release of cytosolic enzymes, including CK, into the bloodstream. Although there is a TREAT-NMD protocol for CK analysis (Luca 2014), the recommended commercial assay was no longer available, therefore an alternative CK assay (Abnova, UK) was used according to the manufacturer's instructions. Absorbance was measured at 340 nm every 30 s for 4 min at 25°C to calculate enzyme activity. All measurements were done in triplicate. However, the results were not as expected; a much smaller variance between WT and mdx was seen compared to previously published data. After discussion with the JWMDRC at Newcastle, who also experienced measurement inconsistencies using the Abnova assay, an alternative assay was utilised (Pointe Scientific, Stroud UK), again according to manufacturer's instructions. Briefly, CK specifically catalyses the transphosphorylation of adenosine diphosphate (ADP) to adenosine triphosphate (ATP). Through a series of coupled enzymatic reactions, NADPH is produced at a rate directly proportional to the CK activity. Therefore, by measuring NADPH absorbance using a plate reader, a quantification of CK activity can be obtained. 10 μl of serum from each mouse sample was loaded into a 96-well plate alongside blanks of distilled water. Each sample was loaded in duplicate. 200μl of working reagent (4 parts buffer:1 part enzyme) was added to each well and the plate loaded into the plate reader. Readings were taken until the absorbance curve reached a plateau. In this experiment, readings for the first minute after 4 minutes of incubation were used. The CK activity was calculated using:

CK (U/L) = Change in absorbance/ minute x3376.

2.4 Ex vivo assessments of bone and growth

2.4.1 Measurement of tibial length

Tibial lengths were obtained using two different techniques. Firstly, using Data viewer software from the whole bone reconstruction of low-resolution μCT images (described in Section 2.8.4), tibial length was measured using the anatomical landmarks shown in Figure 2-4. Tibial length was also measured manually using digital calipers (Mahr,

Gottingen Germany) but as the standard deviation of these measurements was greater than of those obtained using μCT, only the μCT values are presented.

2.4.2 Decalcification and paraffin wax embedding

The right tibiae were fixed in 10% neutral-buffered formalin (NBF) for up to a week and then washed and stored in phosphate buffered saline (PBS) until ready for decalcification. They were then placed in 10% EDTA solution, on rollers, at a pH of 7.0 at 4°C. The solution was changed at least twice weekly for a minimum of 3 weeks, to ensure complete removal of mineral from the bone.

After decalcification, right tibia bones were firstly processed and then embedded in paraffin wax. All tissues were dehydrated using the same processing schedule:

- 70% ethanol- 2 hours
- 90 % ethanol- 2 hours
- Absolute ethanol- 3 hours
- Xylene- 3 hours
- Paraffin wax- 3 hours.

The bones were then sectioned coronally and embedded so that the internal surface was placed face down in paraffin wax at 60°C in metal moulds and left to cool. Excess wax was trimmed on a microtome (Leica Microsystems Ltd, Milton Keynes, UK) until the GP was visible. All tibiae were embedded and cut in the same plane. The samples were then cooled on ice before sections were cut at 6μm, using MX35 Premier+ Microtome Blades (Thermo Scientific, Cheshire, UK). Ribbons of sections were separated in a water bath heated to 40°C and 2-3 sections were mounted onto each poly-l-lysine coated slide (VWR International Ltd, Lutterworth, Leicestershire, UK). 5 slides were prepared in total from each bone. The slides were then placed in a 60°C oven overnight to promote section adherance, and stored at room temperature (RT) in the dark until required.

2.4.3 Methylmethacrylate embedding

Prior to plastic embedding, right femur bones were fixed overnight in 4% paraformaldehyde and then stored in 70% ethanol. Plastic embedding was carried out in Professor Rob van t' Hof's laboratory at Liverpool University. Briefly, bones were dehydrated in incremental ethanol and acetone solutions and then embedded

in methylmethacrylate. Coronal sections were cut at 5 µm using a microtome and left unstained for fluorescent imaging of calcein uptake.

2.4.4 Micro-computed tomography imaging

Micro-computed tomography imaging (µCT) was carried out to assess trabecular architecture, cortical geometry, tibial length and tissue mineral density of bone. µCT involves taking a series of X-rays in different planes and then using computer software to reconstruct a 3-dimensional stack of images which can then be analysed (van 't Hof 2012). µCT imaging was undertaken with guidance from Professor Rob van 't Hof, at Liverpool University. Left tibiae were scanned using a SkyScan 1272 X-ray microtomograph (Bruker Corporation, Kontich, Belgium). After dissection, left tibial bones were stored in water at -20°C and thawed prior to scanning. The bones were wrapped in tissue and enclosed at a consistent vertical height in tightly fitting rigid plastic tubes filled with water, to prevent movement artefact. Two images were averaged at each rotation angle to reduce noise. Settings were changed, dependent on whether cortical or trabecular images were being obtained. For trabecular bone, high resolution images were obtained using a 0.5 mm aluminium filter (to prevent beam hardening where lower energy x-rays are absorbed faster and result in an artefactual non-uniform density), 0.3° rotation step and 4.5µm resolution. For cortical bone image accrual and tibial length measurements, images were obtained using a 0.5 mm aluminium filter, 0.5° rotation step and 9µm resolution.

Scans were reconstructed using NRecon software (Bruker). Initially the whole bone was reconstructed from the low resolution scan, to determine tibial length measurements. For trabecular and cortical analysis, a volume of interest was selected using Data Viewer software (Bruker), see Figure 2-3. 200 slices of the metaphysis were taken for analysis of trabecular bone, using the base of the GP, where the clear bridge of low density cartilage (known as the chondrocyte seam) first becomes visible as the standard reference point and the region of interest (ROI) was started 10 slices below this. It is important when determining the ROI to be used that the offset (*i.e.* the distance below the reference point) needs to be sufficient so that the trabecular ROI begins in a region of trabecular bone, without a significant presence of the fine-structured GP-associated primary spongiosa in the cross-sections. Similarly, it is important that the trabecular ROI does not extend into the diaphysis, otherwise cortical bone will erroneously be included in analysis. For this reason, in the young

mice the analysis was repeated after calculating the size of the ROI dependent on tibial length. For example, the longest tibia at 3 weeks of age was marked as being 100% and 200 slices. The number of slices to include in each ROI was then calculated for each of the shorter tibiae as a percentage of this. After discussion with Rob van t' Hof it was felt unnecessary to adjust the regions of interest for the older mice as these are standardised and well-validated protocols that have been used (Bruker 2017) and there were no significant differences between tibial length measurements of different muscular dystrophy mouse models. 100 slices of the diaphysis were taken for analysis of cortical bone, using the tibia-fibula junction as a standard reference point, with the ROI starting 50 slices above this.

CTAn software (Bruker) was used to analyse appropriate parameters and reduce noise in the reconstructed images by applying a filter. To ensure only bone was analysed, and not surrounding soft tissue, a threshold was set, remaining consistent in all samples. In order to calculate tissue mineral density (TMD) of the cortex, 2 mm calcium hydroxyapatite (CaHA) rod pair phantoms of a known density (0.25g/cm^3 and 0.75g/cm^3) were also scanned using the same settings used for cortical and trabecular image accrual. The primary entity that is measured during μCT is x-ray absorption, defined as the attenuation coefficient in units/mm. Therefore, by linking the mass concentrations of CaHA with the measured x-ray attenuation co-efficient in the μCT image, the tissue density can be calibrated. In this instance, tissue density was calculated rather than BMD, thus the measurement includes only density of the bone rather than also including the bone marrow cavity. The nomenclature used to describe the cortical and trabecular bone parameters is in accordance with the American Society of Bone and Mineral Research (ASBMR) guidelines (Parfitt *et al.* 2009, Bouxsein *et al.* 2010) and presented in Table 2-3 and Figure 2-4.

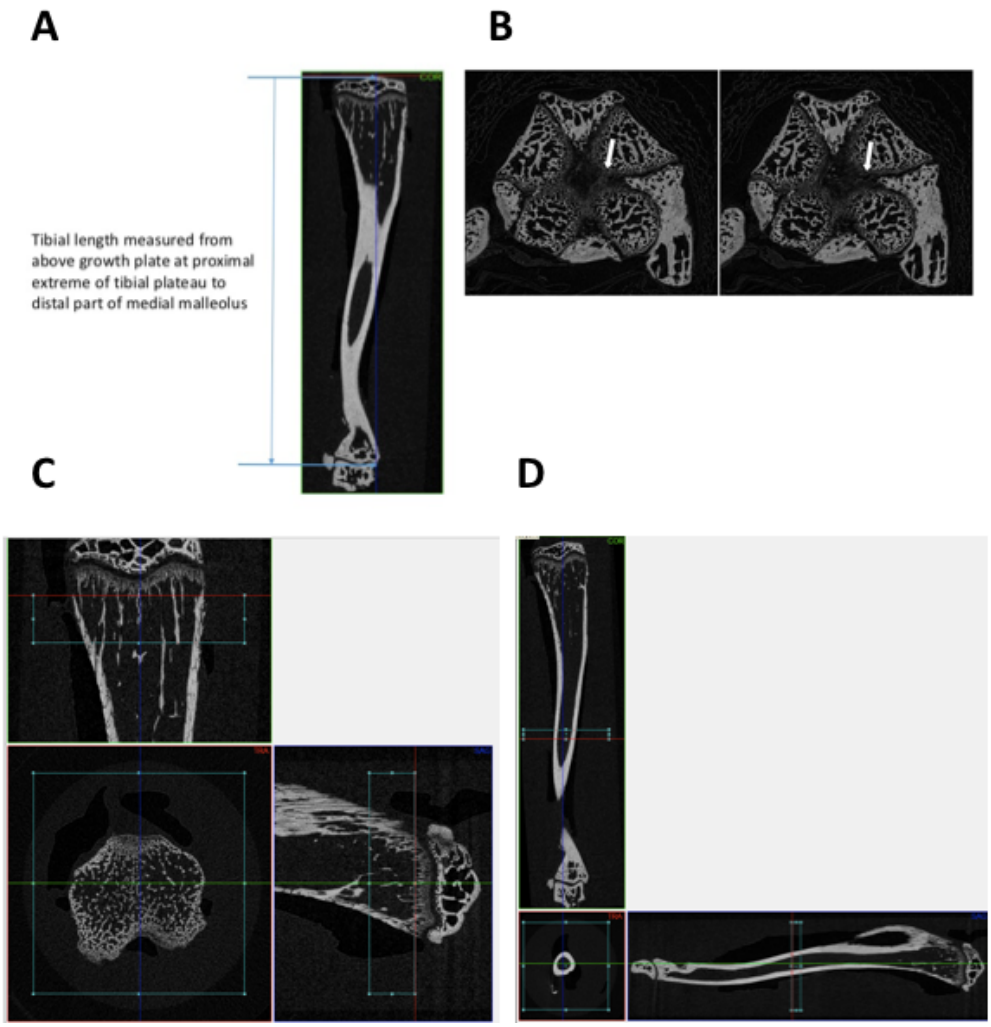

Figure 2-3 Regions of interest and landmarks for μCT analysis

A) Diagram to illustrate the landmarks and technique used for tibial length measurement.

B) A clear bridge of low density cartilage, known as the chondrocyte seam is used as the reference point for the base of the growth plate.

C) ROI for trabecular bone is highlighted by the blue box. 200 slices of the metaphysis were taken for analysis of trabecular bone, using 10 slices below the base of the GP as the reference point.

D) ROI for the cortical bone is highlighted by the blue box. 100 slices of the diaphysis were taken for analysis of cortical bone, using 50 slices above the tibia-fibula junction as a standard reference point.

Trabecular parameter	Units		Description
Trabecular tissue volume	mm^3	Tb.TV	Volume of entire ROI
Trabecular bone volume	mm^3	Tb.BV	Volume of region segmented as bone
Trabecular bone fraction	%	BVTV	Ratio of segmented bone volume to total volume
Trabecular thickness	mm	Tb.Th	Mean thickness of trabeculae
Trabecular separation	mm	Tb.S	Mean distance between trabeculae
Trabecular number	1/mm	Tb.N	Measure of average no of trabeculae per unit length
Structural model index	-	SMI	Relative prevalence of rods and plates, 0 for parallel plates and 3 for cylindrical rods
Connectivity	$1/mm^3$	Conn.D	Measure of degree of connectivity of trabeculae, normalized by TV
Cortical parameter			
Cortical tissue area	mm^2	Ct.TA	Total cross-sectional area inside periosteal envelope
Cortical bone area	mm^2	Ct.BA	Cortical volume/ (no. slices x slice thickness)
Periosteal perimeter	mm	Ps Pm	See Figure 2-4
Endosteal perimeter	mm	Es Pm	See Figure 2-4
Cortical tissue volume	mm^3	Ct.TV	Volume of entire ROI
Cortical bone volume	mm^3	Ct.BV	Volume of region segmented as bone
Cortical bone fraction	%	BVTV	Ratio of segmented bone volume to total volume
Cortical thickness	mm	Ct.Th	See Figure 2-4
Polar moment of Inertia	mm^4	J	Basic strength index (resistance to rotation of a cross-section about a chosen axis)
Mean eccentricity	-	Ecc	An elliptic parameter (higher eccentricity means generally elongated objects)
Tissue mineral density	g/cm^3	TMD	Average attenuation value (density) of bone tissue only

Table 2-3 Trabecular and cortical bone parameters measured by μCT, using ASBMR nomenclature (Parfitt *et al.* 2009)

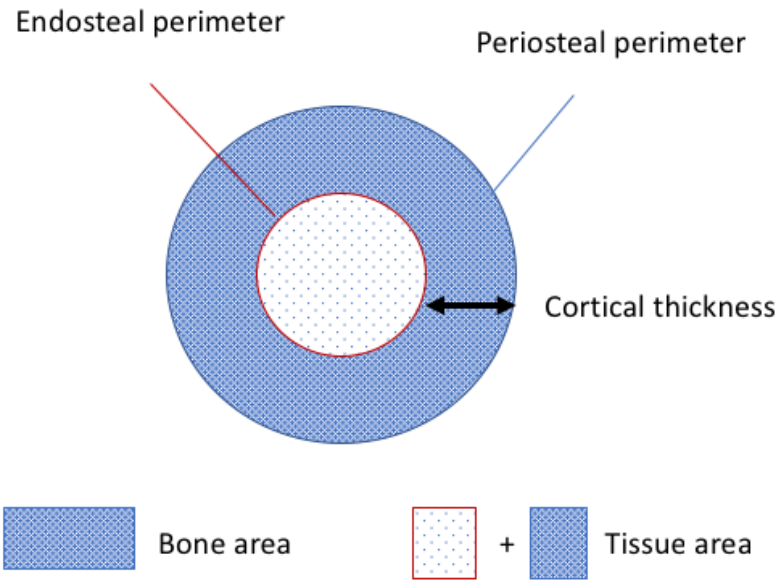

Figure 2-4 Diagram to highlight some of the cortical bone parameters measured by μCT.

A

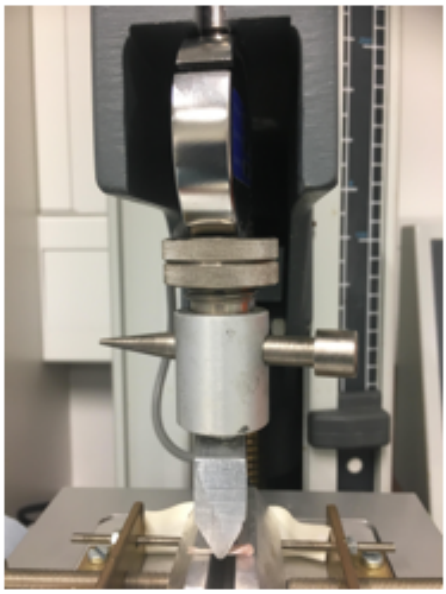

B

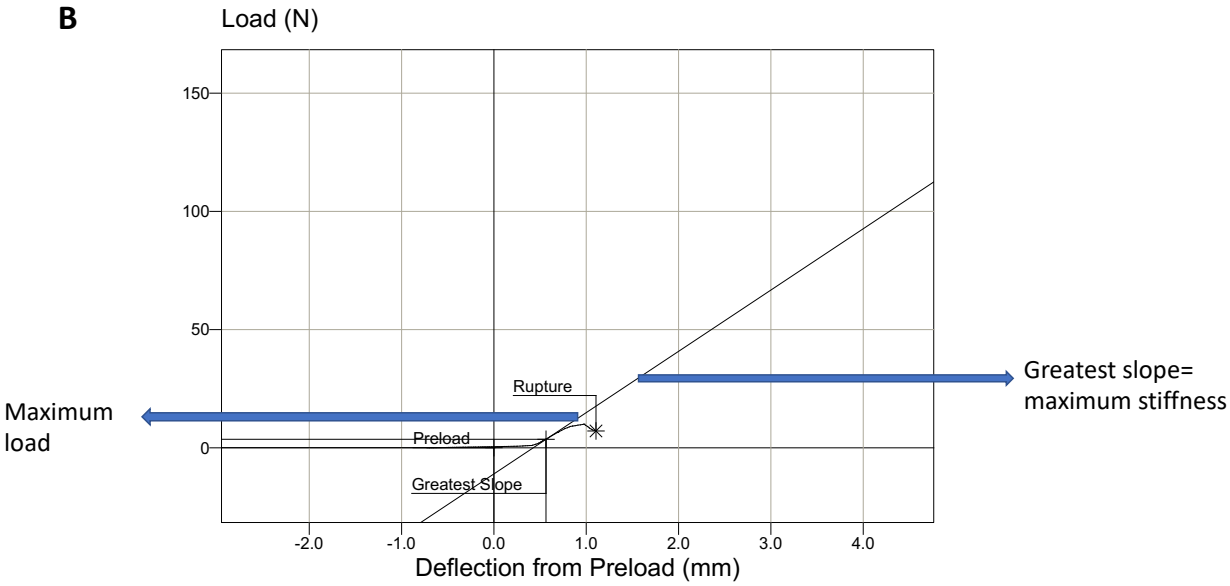

Figure 2-5 Biomechanical testing of tibial bone

A) Photograph to show a tibial bone in situ on the platform of the Lloyd LRX5 materials testing machine, with the cross-head being lowered onto the mid-diaphyseal region.

B) Example of load-deflection graph obtained during biomechanical testing with key parameters of max load and stiffness highlighted by arrows.

2.4.5 Biomechanical testing

Upon completion of μCT testing, bones were subjected to biomechanical testing. A Lloyd LRX5 materials testing machine (Lloyd Instruments, West Sussex, UK) fitted with a 100N load cell was used to determine failure load, work to failure, load to maximum and maximum stiffness of tibiae (Aspden 2003), see Figure 2-5A. The left tibia was used for biomechanical testing as soon as possible after μCT. The span was fixed at 10mm and the cross-head lowered at 1mm/min. Data was recorded after every 0.2mm change in deflection. Each bone was tested to point of failure which was identified from the load-extension curve (Figure 2-5B) as the point of maximum load. The remaining parameters were calculated from a polynomial curve fitted to the rising region of the load-extension curve in Sigmaplot (Systat Software Inc., San Jose, USA). The maximum stiffness was defined as the maximum gradient of the rising portion of the curve. Load at maximum stiffness was calculated as the load at point of maximum stiffness. Work to failure was calculated as the area under the load extension curve up to point of failure. If a maximum load of 5N was not reached, the test was repeated once.

2.4.6 Quantification of bone turnover markers by ELISA

Serum P1NP levels were assessed by ELISA using Fine Test (AMS Biotechnology, Abingdon, UK) Mouse P1NP (N-terminal pro-peptide of collagen alpha-1chain) ELISA kits according to manufacturer's instructions. Serum was diluted 1:10 with sample/standard dilution buffer. Briefly 100μl of diluted sample was added to a 96-well plate in duplicate and incubated at 37°C for 90 minutes. 100μl of biotin-detection antibody working solution was then added for 1 hour. After washing, 100μl of HRP-streptavidin conjugate working solution was then added for 30 minutes, washed and 90μl 3,3' 5,5' tetramethylbenzidine (TMB) chromogenic substrate added, then incubated in the dark for a further 30 minutes. 50μl of stop solution was added and absorbance read at 450nm on the microplate reader. Values were determined by comparison to standard curves which were run simultaneously using standard solutions ranging from 78 ρg/ml to 5000ρg/ml of analyte. Curves were plotted as relative optical density (OD 450) of each standard solution (Y) against respective solution of standard solution (X). P1NP concentration was interpolated from standard curve and multiplied by the dilution factor to obtain the initial concentration. All samples from one experiment were run on the same assay.

Serum Beta-C-terminal telopeptide levels were initially assessed by ELISA using Fine Test (AMS Biotechnolgy, Abingdon, UK) mouse beta CTx ELISA kits according to manufacturer's instructions. Beta CTX was chosen first as this is usually measured clinically (Vasikaran *et al.* 2011). However, concentrations of beta-CTx were consistently lower than the threshold absorbance. It is known that as bone ages, the alpha form of aspartic acid present in CTx converts to the beta form(Wheater *et al.* 2013). Therefore, as bones from juvenile mice are being used, it was decided to instead try and measure serum alpha-CTx levels, using a Fine Test (AMS Biotechnology, Abingdon, UK) Mouse CTx ELISA kit.

Serum was initially diluted 1:10 with sample/standard dilution buffer, and then repeated at 1:5 dilution for optimal results, using the same methodology as for the P1NP ELISA. Values were determined by comparison to standard curves which were run simultaneously using standard solutions ranging from 78 ρg/ml to 5000ρg/ml of analyte. Curves were plotted as relative OD450 of each standard solution (Y) versus respective solution of standard solution (X). CTx concentration was interpolated from standard curve and multiplied by the dilution factor to obtain the initial concentration.

2.4.7 Toluidine blue staining of the growth plate

Toluidine blue is a metachromatic stain whose properties depend on the substance it binds to and the pH of the staining solution used. It is useful to enable the different GP zones to be distinguished. The nucleus will stain dark blue, whilst the cytoplasm usually stains purple, and cartilage blue-purple, leaving the background in green. Once the slides had been prepared as described in Section 2.4.2, they were deparaffinised and rehydrated through a graded series of alcohol solutions using the auto-stainer. They were then stained (see Appendix III for protocol), cleared in 3 changes of xylene, cover-slipped and allowed to dry.

Images were captured using a Zeiss AxioImager brightfield microscope and analysed in Fiji (Schindelin *et al.* 2012). Total GP, proliferative and hypertrophic zone heights were measured at 10 different points along the GP (Figure 2-6) using the measuring ruler and the mean and standard deviation calculated.

2.4.8 Immunohistochemistry using IGF-1, MMP-10 and BMPR1b antibodies

A standard indirect immunohistochemistry technique was used to detect IGF-1, MMP-10 and BMP1bR activity. Antibodies were all sourced from Abcam:

- anti IGF-1 antibody ab9572, (host species rabbit, used at 1:500)
- anti-MMP10 antibody ab 199688 (host species rabbit, used at 1/100)
- anti- BMPR1b antibody ab175385 (host species rabbit, used at 1/100)

Paraffin sections that had been prepared as in Section 2.4.2 were dewaxed in xylene and rehydrated through a graded series of alcohol solutions. Antigen retrieval was achieved by treating sections with 0.1% porcine trypsin for 30 min at 37^{o}C, followed by washing in PBS. Endogenous peroxidases were blocked by incubating the sections with 3% hydrogen peroxide (in methanol), for 30 minutes at room temperature, followed by 3 washes in PBS. Non-specific protein binding was prevented by blocking using 1:5 dilution of normal goat serum for 30 min at RT. Specific primary antibodies were diluted to the optimal concentrations (determined by serial dilution) in PBS/FBS, and sections were covered with diluted antibody solution and incubated in a humidified chamber for 1 hour at RT. Control sections received the same concentration of rabbit IgG. After further washing in PBS, the samples were incubated with secondary goat anti-rabbit horseradish peroxidase (DAKO, Glostrup, Denmark), diluted to 4μg/ml in PBS/FBS for 1 hour at RT in a humidified chamber. 3,3'- diaminobenzidine (DAB) substrate reagent was then added for up to 5 minutes at RT, rinsed in PBS and dehydrated and counterstained with haematoxylin using the auto-stainer. Sections were mounted and images were captured using a Zeiss AxioImager brightfield microscope.

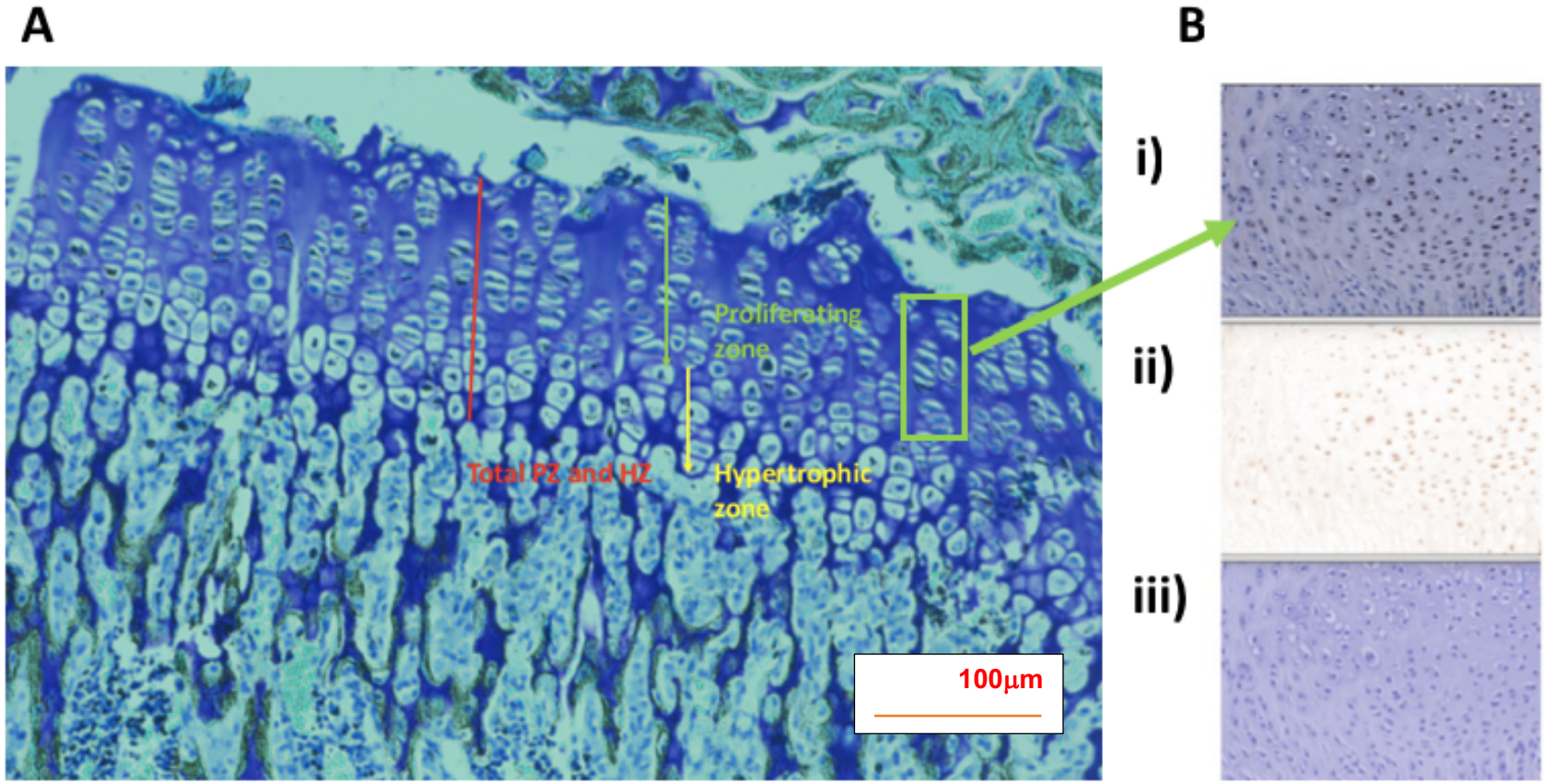

Figure 2-6 Histological assessment of growth rate and proliferation at GP **A)** Toludine blue stained tibial section from a WT mouse showing the GP zones that were measured. **B)** Example image from WT mouse showing the technique used to quantify proliferative activity in the GP using PCNA IHC: i) Immunostaining using PCNA. Only proliferating zone was analysed, highlighted by green arrow. ii) PCNA +ve chondrocytes highlighted using DAB staining (shown after colour deconvolution in Fiji). iii) All chondrocytes stained using haematoxylin (shown after colour deconvolution in Fiji. To calculate the proportion of PCNA +ve chondrocytes the number of DAB stained chondrocytes in ii) was divided by the total number in iii)

2.4.9 BrdU assay

5-bromo-2'-deoxyuridine (BrdU) is a synthetic analogue of thymidine that is incorporated into DNA in place of thymidine during the S-phase of the cell cycle. It can therefore be used to assess cell proliferation rate in any tissue. BrdU injections were given 24 hours prior to cull, as described in Section 2.2.8. Once the slides had been prepared as described in Section 2.4.2, IHC was performed for BrdU, using the BrdU Colometric kit for IHC (Thermo Fisher Scientific, Loughborough, UK) according to the manufacturer's instructions. Briefly, the sections were dewaxed and rehydrated (see Appendix III) and quenched by immersion in 0.3% hydrogen peroxide for 10 minutes. The DNA was denatured to allow antibody access to the incorporated BrdU by immersing the slides in 1X antigen retrieval solution at 97 ^{o}C for 15 minutes. After blocking for 10 minutes at RT, sections were incubated with biotinylated anti-BrdU antibody for 2 hours at RT and then rinsed in PBS. They were then incubated with avidin horseradish peroxidase for 1 hour at RT. DAB substrate was added for 20 minutes to enable detection of the peroxidase activity. After rinsing with distilled water, sections were then counterstained with haematoxylin (see Appendix III), and submerged in PBS. Finally, they were dehydrated and mounted. Sections were viewed using a Zeiss AxioImager brightfield microscope. Control slides (from a previous experiment were used for comparison).

2.4.10 PCNA Immunohistochemistry

The proliferating cell nuclear antigen (PCNA) is synthesised in the early G1 and S phases of the cell cycle, and is particularly prominent in the nucleoli in the late S phase. By performing PCNA IHC and calculating the percentage of PCNA-positive cells in the resulting sections, it can therefore be used as an intrinsic marker to make an estimation of proliferation rate without the need for BrdU injections to evaluate DNA synthesis.

Once the slides had been prepared from mice culled at 3 weeks of age, as described in Section 2.4.2, the Vectastain elite ABC rabbit kit (Vector labs, Peterborough, UK) was used according to manufacturer's instructions, alongside the Abcam anti PCNA (rabbit) antibody (Abcam, Cambridge, UK). Briefly, the sections were dewaxed and rehydrated (see Appendix III) and mounted. Sections were viewed using a Zeiss AxioImager brightfield microscope. The haematoxylin- DAB colour deconvolution

plugin was used on Fiji to separate the haematoxylin and DAB components and the thresholding tool used to select a consistent threshold for each image where positively stained nuclei were clearly seen without too much background interference (Figure 2-6B). The 'analyse particles' function was then used to automatically count nuclei and a % of proliferating nuclei as a function of the total number of chondrocyte nuclei in the proliferating zone was calculated.

2.4.11 Detection of apoptosis

When a cell undergoes apoptosis, a complete change in its morphology occurs. This involves shrinkage, chromatin margination, membrane blebbing, nuclear condensation and then segmentation and division into apoptotic bodies, which may be phagocytosed. The TdT-mediated dUTP nick-end labelling (TUNEL) assay forms the basis of the Apoptag technology. This enables apoptosis to be differentiated from cell necrosis where DNA fragmentation does not occur. DNA strand breaks can be detected by enzymatically labelling the free 3'-OH termini with modified nucleotides. Once the DNA fragments have been labelled with the digoxigenin-nucleotide they can bind to the anti- digoxigenin antibody that is conjugated to fluorescein. The ApopTag Plus Fluorescein In Situ Apoptosis Detection Kit (EMD Millipore, Bedford, MA, USA) was used. Briefly, formalin-fixed, paraffin-embedded sections of the tibial growth plate from the mice culled at 7 weeks of age were pre-treated with proteinase K. After equilibration, terminal deoxynucleotidyl transferase (TdT) enzyme was added, followed by anti-digoxigenin conjugate. Slides were then blocked, washed and stained with fluorescein, counterstained with DAPI, mounted and stored in the dark until they were required. Sections were viewed using a Zeiss AxioImager fluorescent microscope.

2.4.12 Static histomorphometry

Static histomorphometry was performed to quantify osteoblast number using tissue non-specific alkaline phosphatase (TNAP) IHC of H&E stained sections in Chapters 3 and 4 and Goldners trichome stained sections in Chapters 5 and 6. Tartrate-resistant acid phosphatase (TRAP) in conjunction with Fast-red staining was used to determine osteoclast activity.

- **TRAP/Fast-red staining**

Osteoclasts secrete TRAP and can therefore be identified using a combination of TRAP and Fast-red staining to highlight osteoclasts in red. After fixation for up to a week using 10% NBF, right tibial bones were decalcified, wax embedded and cut at 6μm as previously described (see Section 2.4.2). 250μL of N-N dimethyl formanide and 70mg napthol AS-TR phosphate were added to a solution of 0.2M sodium acetate buffer and 115mg of sodium tartrate dihydrate. 70mg of fast red salt TR was dissolved into the solution and warmed to 37^{o}C. The solution was dropped onto the slides and incubated for two hours at 37^{o}C, or until the red staining developed. The sections were then washed in distilled water and counterstained in Mayer's hematoxylin for 5min. After a final wash in PBS, sections were blotted, mounted and imaged immediately using the Nanozoomer slide scanner (Hamamatsu Photonics, Japan).

- **Goldner's trichrome staining**

Goldner's trichrome staining can be used to distinguish mineralised bone (stains blue/green) from osteoid (red) and nuclei (purple). Sections were prepared as described for TRAP staining. They were then dewaxed to water and stained in a solution of Wiegert's haematoxylin for 10 minutes, differentiated in 1% acid alcohol for 15 seconds and washed well for 10 minutes. Sections were then moved through a series of stains, see Appendix III. After rinsing in distilled water and blotting dry, they were then dipped quickly in 99% alcohol and 99% alcohol-xylene before being transferred to xylene and mounted using ClearVue mounting agent (Thermo Fisher). The sections were then imaged as per TRAP-reacted sections.

- **TNAP Immunohistochemistry**

Tissue non-specific alkaline phosphatase plays a key role in bone mineralisation by degrading inorganic pyrophosphate and providing free inorganic phosphate for hydroxyapatite formation. As alkaline phosphatase is an ectoenzyme with activity on the osteoblast cell membrane, IHC can be used to positively identify osteoblasts. Sections were prepared as described for TRAP staining. After washing in PBS, antigen retrieval was performed in a 10mM sodium citrate buffer (made to pH 6) at 70^{o}C for 1 hour. After blocking for 30 minutes at RT in a solution of 3% hydrogen peroxide in methanol, a 10% solution of normal goat serum was added to the slides for 1 hour at RT. A dilute solution of primary TNAP antibody (rat; MAB 2909 R&D

Systems, Minnesota, USA) was prepared at a concentration of 1:1500 in primary antibody buffer and added to slides for 1 hour at RT in a humidified chamber. The sections were then incubated with goat anti-rat HRP secondary antibody (Sigma 9037) diluted 1:1000 in secondary antibody buffer for 1 hour at RT. Diluted DAB substrate (1 drop to 1ml buffer) was added until the colour visibly developed. After rinsing with PBS, sections were then counterstained with Meyer's haematoxylin, for 4 mins, dehydrated (see Appendix III), mounted and scanned as per TRAP-reacted sections.

- **Osteoblast and osteoclast analysis**

Images were compressed and imported into Bioquant Osteo software v 17.2.60 (Bioquant Image Analysis Corp, Nashville, Tennessee, USA). The trabecular area of the proximal tibia was analysed; the ROI included only metaphyseal trabecular bone and extended from 50um below the GP and within the endocortical bone boundary. Osteoclasts were identified as TRAP +ve multinucleated cells lying on the bone surface. Osteoblasts were visualised using TNAP immunostaining and identified by their cuboidal appearance, lying within groups on the bone surface. Osteoblast and osteoclast number were reported normalised to bone surface, in accordance with the ASBMR Guidelines for nomenclature (Dempster *et al.* 2013).

2.4.13 Bone marrow adipose tissue (BMAT) quantification by osmium staining

Osmium staining and μCT for MAT quantification was kindly performed by Dr Rob Wallace, Dr Karla Suchacki and Dr Will Cawthorn at the Queen Margaret Research Institute at Edinburgh University. Bone marrow adipose tissue (BMAT) was assessed by osmium tetroxide staining of intact tibiae. As described previously (Scheller *et al.* 2014), tibiae were fixed in 10% NBF for up to 1 week after dissection and kept in PBS until required. Tibial bones were arranged in parallel and set in 1% agarose gel within a 30ml universal tube. They were scanned prior to de-calcification at a resolution of 6μm, with misalignment of 0.5, ring artefact of 5 and beam hardening set at 40% to determine an accurate marrow volume. Bones were then decalcified in 14% EDTA for 2 weeks and then stained with 1% osmium tetroxide solution for 48 hours. They were then rescanned at a resolution of 12μm, with misalignment of 0.5, ring artefact of 10 and beam hardening set at 40%. Osmium tetroxide is soluble in fats and forms

a black reduction with the carbon-carbon double bonds within unsaturated fatty acids, resulting in covalent incorporation of the osmium atom. Within the bones, unsaturated fatty acids are concentrated within bone marrow adipocytes. Because osmium is radio-dense, its incorporation into bone marrow adipocytes allows direct visualization of BMAT by μCT scanning. Thus, μCT scans of osmium-stained bones allow quantification of MAT volume and spatial distribution *in situ*.

Characteristics of MAT depend on the region and age of the animal examined, and so the tibia-fibula junction was used as an arbitrary cut off when defining the regions containing regulated MAT (rMAT) and constitutive MAT (cMAT), see Figure 2-7. rMAT exists in more proximal skeletal sites, such as the proximal tibia and consists of adipocytes interspersed with haematopoietic bone marrow. It develops with age. cMAT is found in the earliest areas of marrow formation, for example the distal tibia and appears histologically similar to white adipose tissue, with few visible haematopoetic cells.

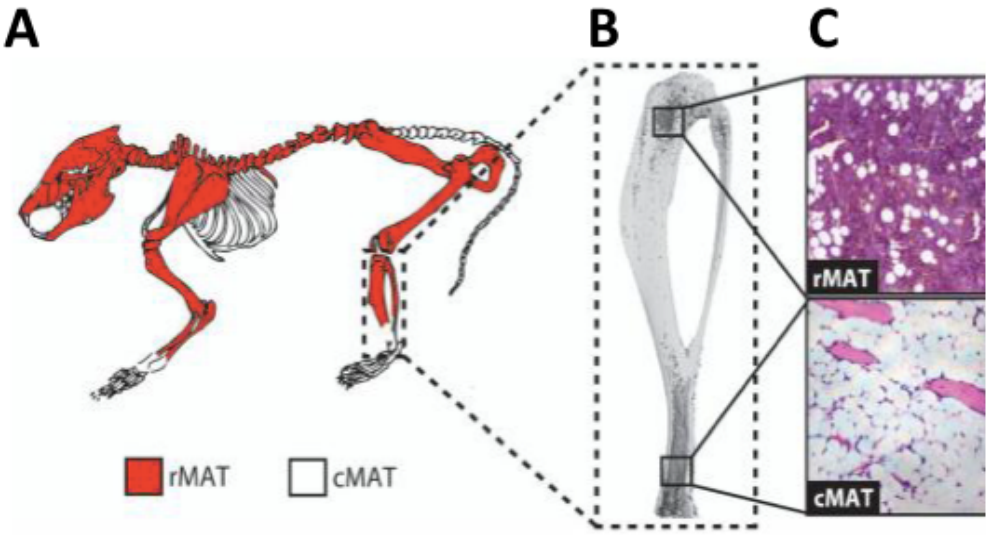

Figure 2-7 Regulated and constitutive bone marrow adipose tissue (BMAT) in the mouse. Reproduced with kind permission from (Scheller *et al.* 2016)

- **A)** Proposed distribution of regulated MAT (rMAT) and constitutive MAT (cMAT) in the mouse skeleton when marrow is present. Regulated MAT is found in the most proximal regions including the mid to proximal tibia. Constitutive MAT is found in the most distal portion of the tibia.
- **B)** Three-dimensional representation of an osmium-stained mouse tibia.
- **C)** Representative histology of rMAT and cMAT adipocytes within the bone marrow.

2.5 RNA and DNA Methods

2.5.1 Isolation of RNA from tissues

RNA was extracted using a modified version of the Qiagen RNeasy kit. Each right humerus sample was snap frozen in liquid nitrogen and stored at -80°C until required. The epiphyses were then removed and the shaft spun down to remove the bone marrow. They were then crushed with a glass rod and then homogenised in QIAzol Lysis Reagent using a hand-held homogeniser (Cole-Parmer Instruments CO. Ltd, London, UK). Chloroform was then added to extract the DNA and run on spin columns. Addition of ethanol provided optimal binding conditions to the silica-based membrane which was then centrifuged in the presence of wash buffers; removing contaminants. The RNA was then eluted in RNase free H_2O, passed through the membrane and stored at -80°C. RNA concentration and quality of all samples were assessed using a nanodrop spectrophotometer (Thermo Scientific, UK). Quality was assessed by the ratio of wavelengths 260nm/280nm, where a ratio of 1.8- 2.0 was considered optimal.

2.5.2 Reverse transcription

RNA was converted into complementary DNA (cDNA) by reverse transcription, using reverse transcriptase, an RNA-dependent DNA polymerase. 10 µl of each RNA sample was incubated with 2µl of random primers (1:60, (Invitrogen) for 10mins at 70°C (DNA Engine Dyad machine) and immediately cooled on ice. A master mix was prepared using 4µl of 5x first strand buffer, 2µl of dithiothreitol (DTT) (0.1M) (Invitrogen), 1µl of dNTP (10mM), and 1µl of Superscript RNAse enzyme (200U/µl). 8µl of the master mix was added to each sample. The reverse transcription was performed using a standard setting on the DNA Engine Dyad machine:

- Annealing for 10min at 25°C
- Elongation for 50mins at 42°C
- Termination for 10min at 70°C.

2.5.3 Quantitative polymerase chain reaction (qPCR)

The cDNA was used on the real-time RT^2 profiler PCR osteogenesis pathway array (Qiagen, Manchester UK), in combination with RT^2 SYBR Green qPCR Mastermix (Qiagen, Manchester UK). For a list of the genes analysed see Appendix IV.

All samples were diluted to the lowest concentration of DNA in nuclease free water, with the aim of starting with 0.5μg total DNA. Briefly, 20 μl of cDNA was mixed with SYBR Green Mastermix and dispensed in the wells containing the osteogenic primers. Each panel contained 86 genes of interest, 6 housekeeping genes, genomic DNA controls, positive PCR controls and RNA controls. Wells were subjected to real-time PCR, using Stratagene Mx3000P (Agilent Technologies, Santa Clara, CA, USA) for 1 cycle of 10 mins at 95°C to activate the HotStart DNA Taq polymerase and then 40 cycles of 15s at 95°C and 1 min at 60°C to perform fluorescence data collection.

A cycle threshold (C_T) >35 was considered a negative cell and marked as N/A. The genomic DNA control wells were checked to ensure that levels of genomic DNA contamination were too low to affect gene expression profiling results. The positive PCR control wells were also checked to ensure sensitivity of the instrument and to exclude the presence of PCR amplification inhibitors.

Mean C_T values for each duplicate were exported to an Excel spreadsheet and uploaded to automated open-source software provided by Qiagen at http://www.qiagen.com/geneglobe. C_T values were normalised based on the *Gapdh* housekeeping gene as this was the gene out of a selection of 5 provided in the panel which showed least variability during the experiments.

The delta-delta C_T ($\Delta\Delta C_T$) method was used to calculate fold change/regulation (Livak *et al.* 2001). ΔC_T was calculated between gene of interest and the housekeeping gene according to:

$$\Delta C_T = C_{T\,(\text{gene of interest})} - C_{T\,(\text{housekeeping gene})}$$

Gene-specific ΔC_T values for samples in the same group (genotype) were then averaged. $\Delta\Delta C_T$ calculations were then performed using:

$$\Delta C_{T\,(\text{test group})} - \Delta C_{T\,(\text{control group}).}$$

When genotypes were being compared, the WT mice were classed as controls. Fold change was calculated by converting the ΔC_T from a $\log^2$ scale to a linear scale using:

$$\text{Fold change} = 2(-\Delta\Delta C_T).$$

A fold change >1 was classed as an upregulation, a fold change <1 was reported as a fold downregulation. Genes were filtered using a significance level of $p<0.05$.

Results where the gene's average threshold cycle could either not be determined or was greater than the defined cut-off (35 cycles) in both samples meaning that its expression was undetected were excluded from results, as the manufacture warned that the resulting fold-change result was liable to be erroneous and un-interpretable.

2.6 Organ/ cell culture

2.6.1 Isolation of osteoblasts from culture of mesenchymal stromal cells.

The femurs of 7-week old mice were dissected under sterile conditions and warmed to 37°C in a bijou containing α-MEM culture medium. Each bone was individually dissected at the proximal and distal ends and using a 5-ml syringe (filled with medium) and 21-gauge needle the marrow was flushed out into a small petriplate. The marrow was flushed several times to ensure a homogenous cell suspension was achieved. It was then transferred to a universal container where it was centrifuged at 1100 rpm for 4 min. After discarding the supernatant, the pellet was re-suspended into 10ml of α-MEM (supplemented with 0.5% gentamycin antibiotic (Gibco) and 10% FBS (Gibco) before use and filtered through a 70 μm sieve into a new sterile universal. The cells were seeded at 2 X 10^6 cells/ well of a 6-well plate, using plain α-MEM (without nucleosides). An osteogenic medium supplemented with 5 μg/ml ascorbic acid and 1 mM dexamethasone was used to promote osteoblast differentiation. Half of the culture medium was changed initially after 6 days and then every 3 days until 3 weeks, when alkaline phosphatase (ALP) activity was determined.

2.6.2 Alkaline phosphatase activity

ALP is a stem cell membrane marker and ALP activity is an early indicator of the differentiation of marrow stem cells towards osteogenic lineage. ALP activity uses sodium α-napthyl phosphate as a substrate for ALP in the presence of fast blue RR (a diazonium salt). When the α-napthyl phosphate is hydrolysed by ALP, the α-napthyl couples with the diazonium site and forms visible dark blue pigment. An ALP staining kit was used according to the manufacturer's instructions. Plates were scanned and the images digitised. The percentage of stained area was then quantified using Fiji and compared between the genotypes.

2.6.3 Isolation of embryonic metatarsals

Metatarsal culture enables the intrinsic bone growth rate of an animal to be determined without any muscle weakness and resulting reduction in bone loading acting as a potential confounding factor. The embryonic mouse metatarsal culture technique provides a more physiological model for studying intrinsic bone growth than a pure in-vitro model and is well established within the group (Houston *et al.* 2016). It maintains cell-cell and cell-matrix interactions and enables quantitative assessment of bone growth.

Culture medium was prepared by adding 0.2% bovine serum albumin, 1.25mg of amphotericin B, 0.05mg/ml gentamicin and 5 μg/ml L-ascorbic acid to α-MEM without nucleosides and filter sterilising through a 0.22 μm filter syringe. Timed matings were performed with WT, *mdx* and *mdx:cmah* mice so that an accurate conception date was known, to within 12 hours. Embryos were decapitated at embryonic day 18 (E18) and the hind-foot removed under sterile conditions. Using a dissecting microscope and keeping the bones moist in culture medium (previously warmed); the middle three metatarsals were removed and stripped of muscle and other soft tissues.

They were cultured, one bone to each well of a 24-well plate, with 300μl of standard culture medium per well in a humidified atmosphere, with 5% CO_2 at 37°C. Culture medium was changed at 3, 5, and 7 days. The total and length of the mineralising zone of the metatarsal and was measured at day 0, 3, 5, 7 and 9 using a Nikon eclipse TE300 microscope with a digital camera attached and Image Tool software (Image Tool Version 3.00, San Antonio, TX).

2.7 Statistical analysis

Mice were identified only by an identity number at the time of culling, in order to be blinded to genotype. Statistical comparisons were made between mice of each genotype and age. One-way ANOVA was used to assess significance of differences between groups and post-test Bonferroni modifications were made to adjust for multiple comparisons. Data are presented as mean (+standard deviation) or median (+inter-quartile range) if the data were non-parametric. $p<0.05$ was accepted as significant. In figures throughout the chapters, * signifies $p<0.05$, ** $p<0.01$ and *** $p<0.001$.

Linear (univariable and multivariable) regression models were used when appropriate to estimate the relationship between the outcome variable under investigation and other independent variables, after adjustment for any potential confounders in the multivariable models. Following model generation, regression diagnostics were performed to check the underlying assumptions of the linear model. Residual normality was checked using a normal probability plot and a residual versus fitted plot drawn to ensure that the variance of errors was constant throughout the range of residuals.

CHAPTER 3

Characterisation of growth in muscular dystrophy mouse models

3 Characterisation of growth in muscular dystrophy mouse models

3.1 Introduction

As discussed in Chapter 1, GC therapy forms part of the Standards of Care for DMD (Birnkrant *et al.* 2018). They improve muscle, cardiac and respiratory function but are associated with many side-effects, including growth retardation and delayed puberty, which in turn further exacerbates the GC-induced reduction in growth velocity (Wood *et al.* 2015). However, short stature is also a common feature of boys with DMD even in those who are not treated with GC (Rapaport *et al.* 1991). Typically, boys with DMD appear to have a slower than expected growth velocity during the first years of life (West *et al.* 2013) and then continue to grow along their lower centile during childhood and adolescence (Eiholzer *et al.* 1988). Figure 3-1 shows a growth chart for ambulant boys, aged 2-12 years (McDonald *et al.* 1995, West *et al.* 2013). A recent study also suggests that there is skeletal disproportion in GC-treated boys with DMD with relatively shorter leg length and more marked reduction of distal long bones (Kao *et al.* 2019). Supra-physiological doses of GC do not appear to cause the same patterns of skeletal disproportion in juvenile arthritis, suggesting that an intrinsic growth disorder may be responsible in DMD (Zak *et al.* 1999).

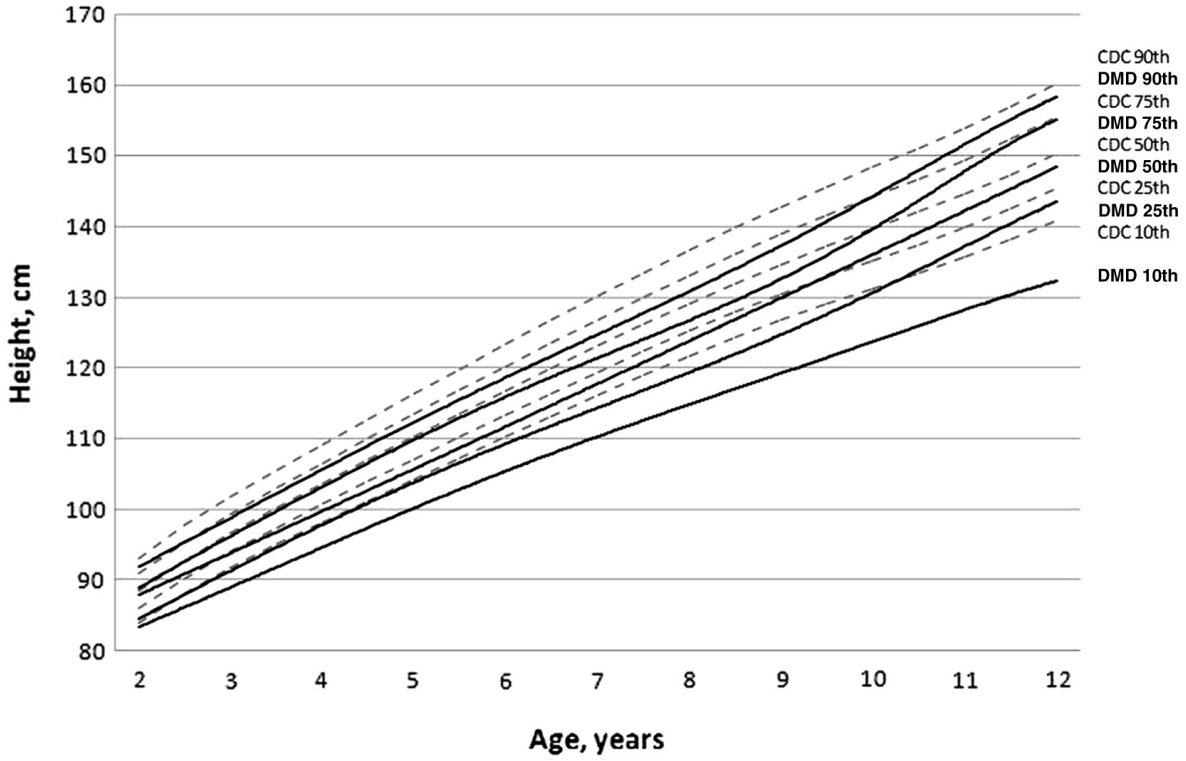

Figure 3-1 Height-for-age percentile curves for ambulant boys ages 2-12 years with DMD compared with the US population CDC 2000 curves, showing the DMD 10th centile falling well below the CDC equivalent. Reproduced from (West *et al.* 2013)

Primary GH deficiency is unlikely to be the primary cause as a study of 34 patients with DMD found GH secretion to be essentially normal. Despite this, abnormal response of dystrophic muscle to endogenous GH or IGF-1 may play a role (Messina *et al.* 2008). Studies in the x-linked muscular dystrophy dog have suggested that the early poor growth coincides with a period of extreme muscle necrosis and regeneration, which may therefore reflect increased metabolic activity (Rapisarda *et al.* 1995). Low levels of physical activity and associated reduced bone loading and lower bone turnover probably also contribute (Nagel *et al.* 1999) although there must be other contributory factors as ambulant boys are short prior to onset of marked muscle weakness.

3.1.1 Rationale for studying growth in mouse models of DMD

Despite some clinical evidence to suggest intrinsic growth failure in boys with DMD, there are little published data regarding the growth in muscular dystrophy mouse models. Prior to investigating the role of anabolic agents such as GH and IGF-1 on bone and growth, it is essential to determine the normal growth trajectory in these models.

3.2 Hypothesis

Growth and GP chondrogenesis are impaired in all muscular dystrophy mouse models when compared to WT mice and more severely in the *mdx*:*cmah* mouse model.

3.3 Aims

1. Compare parameters of muscle function.
2. Compare gross growth rates.
3. Assess rates of growth within the growth plate.
4. Compare metatarsal growth rate.

   All studies will compare male WT and muscular dystrophy mouse models (*mdx*, *mdx*:*utr* and *mdx*:*cmah*) that are culled at 3,5 and 7 weeks of age.

3.4 Material and Methods

For all experiments in this chapter, n=6 mice or more in each group were studied (except for *mdx*:*utr* at 5 weeks, where n=5 as one mouse had to be culled just prior to the study end point because of hydrocephalus and poor weight gain).

3.4.1 Grip strength

Forelimb grip strength testing was performed using a grip strength meter with a specialised mouse grid (Harvard Biosciences, Massachusetts, USA), see also Chapter 2.3.1.

3.4.2 Creatine kinase assay

Quantification of serum creatine kinase activity was carried out using a Pointe Scientific kit (Chapter 2.3.3). The change in NADPH absorbance was measured every 30s at 340nm for 4 min at 25°C and a mean value calculated.

3.4.3 Muscle histology

The TA muscle of the lower hind limb was used to determine muscle necrosis and inflammation. Sections were cut at a width of 6µm and H&E staining was used for histological assessment of muscle pathology, as outlined in Chapter 2.3.2.

3.4.4 Gross body growth parameters

Animals were measured twice weekly from weaning until cull, by staff in the BRF. Weight, crown to rump and tail lengths were taken using the same digital weighing scales and a ruler. Crown-rump and tail length data throughout the study periods has not been reported in this thesis, however, as there was found to be great inter-observer variability in these measurements. In order to maximise validity only the data at time of cull is shown, because the same technician performed the anthropometric measures at cull during the study; this was unfortunately not possible for the entire study period due to shift patterns.

3.4.5 Testes weight

Testes were dissected immediately post cull and weighed on the same digital scales for every mouse. A combined weight is presented, alongside a weight normalised to the overall bodyweight.

3.4.6 Analysis of growth plate height

Right tibiae were removed at dissection and fixed in 10% NBF for 1 week then stored in PBS until required. They were decalcified and embedded in paraffin wax (Section 2.4.2). All tibiae were embedded and cut in the same plane. Sections were cut at 6µm and stained with toluidine blue, further details are given in Section 2.4.8. Images were captured using a Zeiss AxioImager brightfield microscope and GP zone heights measured using Fiji (Schindelin *et al.* 2012). Ten measurements were taken per section and the mean height calculated for each zone.

3.4.7 Dynamic histomorphometry

Calcein is taken up by mineralising bone surfaces and can therefore be used to determine longitudinal bone growth rate. Mice were injected with calcein 2 days prior to cull, as described in Section 2.2.7. At dissection, right femurs were fixed overnight in PFA and then stored in 70% ethanol. Plastic embedding was carried out in Rob van t'Hof's laboratory at Liverpool University. Images were captured using a Zeiss AxioImager fluorescence microscope. The distance between the chondro-ossesous junction and calcein labelling front was measured using Fiji and divided by the time between injection and sacrifice (2 days) to give the BFR per day (Figure 2.2). Multiple measurements were taken per section and the mean growth rate calculated.

3.4.8 Tibial length measurement

Tibial length was measured using images obtained by µCT and viewed in Dataviewer, as outlined in Section 2.4.4.

3.4.9 Assessment of chondrocyte proliferation rate

IHC for BrdU and PCNA detection were performed as described in Sections 2.4.10 and 2.4.11. Sections were taken from the right tibiae of 3-week-old mice of each

genotype. This age of mouse was used as growth rate and therefore proliferation rate was likely to be maximal.

BrdU IHC was performed using a range of BrdU antibody concentrations, but it was felt that the staining obtained was very variable amongst samples studied and overall too poor to allow accurate differentiation between positive and negatively stained cells in the growth plate. It is possible that there was a discrepancy in the administration protocol for the BrdU injections. Due to these inconsistencies in BrdU detection, dividing nuclei were identified and counted using the PCNA IHC protocol (see Section 2.4.11)

3.4.10 Assessment of apoptosis rate

Rates of apoptosis were investigated using the Apoptag kit, as described in Section 2.4.12. Right tibiae from 7-week-old mice were used.

3.4.11 Embryonic metatarsal culture

Metatarsal culture was performed as described in Section 2.6.3. Twelve metatarsals were isolated from each genotype and cultured. The *mdx:utr* model was not used for metatarsal culture as this phase of the study was commenced after the decision had been made not to take the *mdx:utr* mouse forward for the later phases of the project. Because of the considerable financial costs of breeding and maintenance of mice, the cohort was therefore not maintained specifically to achieve timed pregnancies. All embryos were taken from one pregnant mouse of each genotype at day E18. Metatarsal growth in culture was noted to slow down after day 7, (mean difference in length between days 5 and 7of 0.44mm, compared to 0.17mm between days 7 and 9) see Figure 3-2C, so only length data up to and including day 7 was included in the analysis. Total metatarsal length and mineralising zone length were measured (see Section 2.6.3 and Figures 3-2A and B).

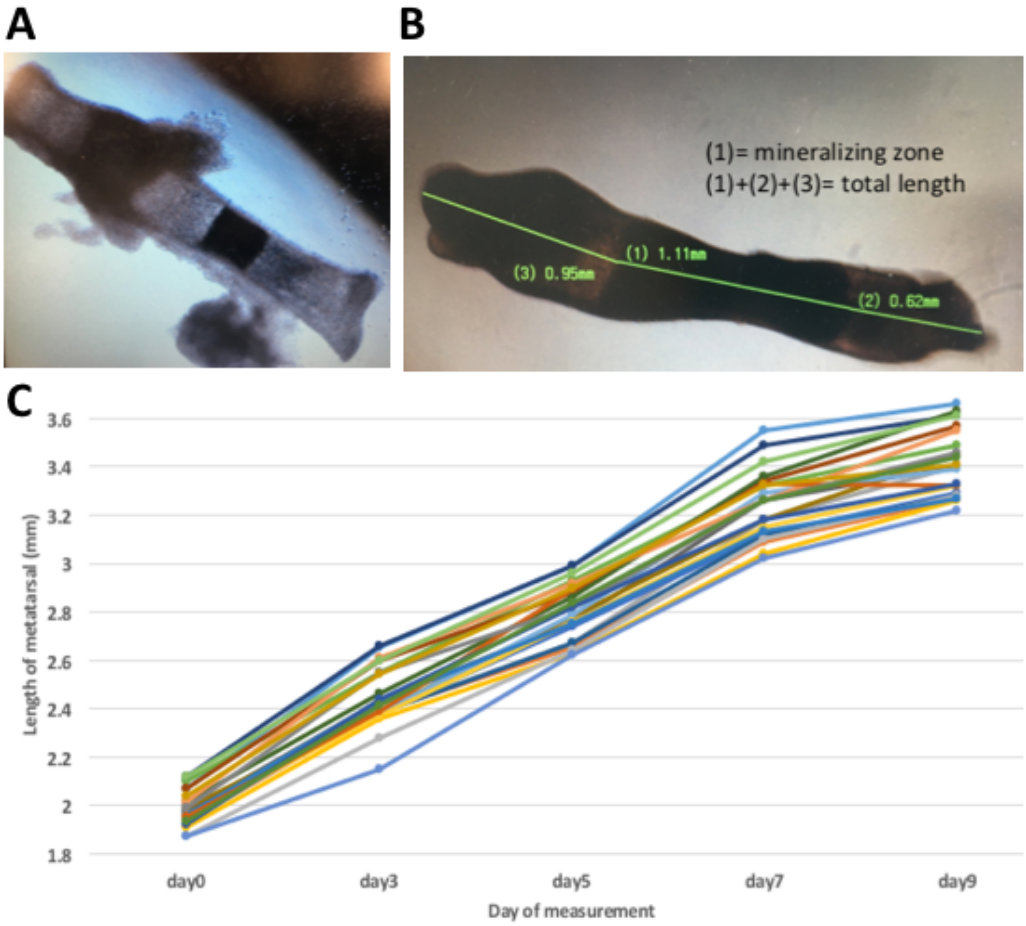

Figure 3-2 Metatarsal culture

A) shows a metatarsal from E18 WT mouse under magnification at day 0, midway through stripping the skin and the removal of the tarsus.

B) Metatarsal of WT mouse at day 7 showing the measurements taken for mineralising zone and total length.

C) Graph showing the slowing of metatarsal growth in culture of a WT mouse after day 7 (n=24).

3.5 Results

3.5.1 Grip strength

In the youngest mice (3 weeks-of-age at cull), grip strength normalised to bodyweight was significantly less in all muscular dystrophy models compared with WT mice ($p<0.01$) (Figure 3-3, Table 3-1). At 5 weeks-of-age, only the normalised grip strength of *mdx*:*utr* mice was significantly less than WT mice ($p=0.03$), and at 7 weeks-of-age, only the *mdx*:*cmah* mice was significantly lower ($p=0.04$); at this age the normalised grip strength was 38% lower in the *mdx*:*cmah* than WT mice.

3.5.2 Creatine kinase assay

Whilst there was considerable variability in serum CK levels by age as well as genotype, there was significantly (in the order of 10-fold) higher CK activity in all muscular dystrophy models and at all ages compared to WT mice (Table 3-2 and Figure 3-4). CK was significantly higher in *mdx* mice at 5 weeks-of-age and in the *mdx:cmah* mice at both 5 and 7 weeks-of-age compared to the mice of their respective genotype that were 3 weeks-of-age at cull (Table 3-2). Although it did not reach statistical significance, as the SD in the CK measurements of the *mdx*:*utr* mice were much greater, the same trend for higher CK at the older ages was also seen in these mice.

The relationship between CK and genotype/age was investigated in further detail using a multivariable linear regression model to estimate the relationship between CK and genotype after adjusting for age (Tables 3-3 and 3-4). Age and genotype together explained 71% of the variance in CK values ($R^2= 0.71$). Using WT and 3 weeks-of-age as comparators, age at cull and genotype were both significantly associated with CK levels (Table 3-4). The interaction between age and genotype was also assessed to determine whether the effect of genotype was age dependent. As expected, there was a significant interaction between age and genotype in both the *mdx* and *mdx*:*cmah* mice. On its own, age only accounted for 5% of overall variance in CK levels but when combined with genotype, the contribution of the combined model to CK levels increases from 0.62 to 0.71.

Mouse type	**Absolute grip strength, g (SD)**		
	3 weeks at cull	5 weeks at cull	7 weeks at cull
WT	62.36 (14.3)	74.86 (10.54)	96.75 (29.33)
mdx	63.25 (30.63)	58.30 (18.82)	49.48 (9.29)
mdx:u*tr*	31.37 (11.60)	50.27 (20.75)	79.42 (22.80)
mdx:c*mah*	32.15 (10.93)	55.08 (10.20)	74.63 (18.19)
Mouse type	**Grip strength normalised to bodyweight, g/g(SD)**		
	3 weeks at cull	5 weeks at cull	7 weeks at cull
WT	5.78 (0.86)	4.54 (0.82)	4.74 (0.82)
mdx	3.87 (0.78) **	3.38 (0.99)	3.54 (1.50)
mdx:u*tr*	3.40 (1.11) **	2.89 (1.19) *	3.82 (1.07)
mdx:c*mah*	3.94 (1.20) **	3.27 (0.69)	2.96 (0.62) *

Table 3-1 Absolute and normalised grip strength data from mice culled at 3, 5 and 7 weeks-of-age. Data are presented as mean (+/- standard deviation). * denotes $p<0.05$, ** $p<0.01$ when compared to WT mice.

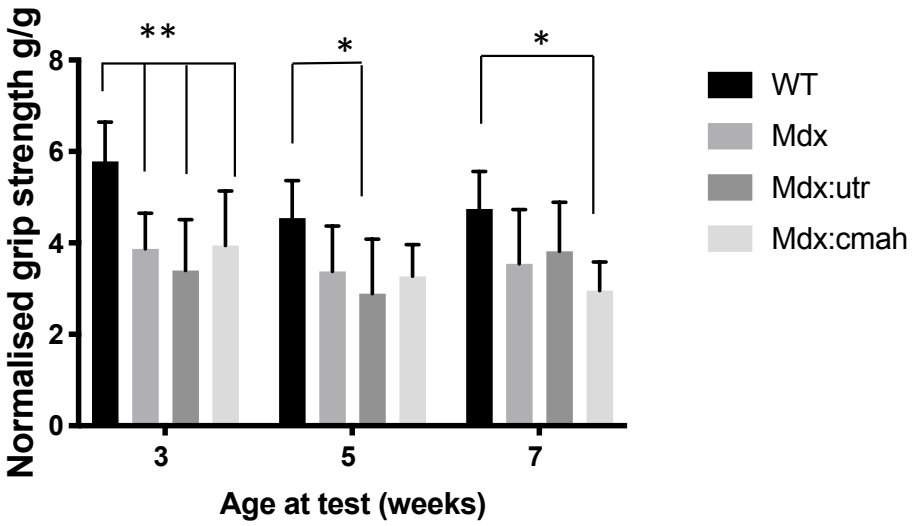

Figure 3-3 Normalised mean grip strength (g/g) by age (3, 5 and 7 weeks) and phenotype (WT compared to *mdx*, *mdx:utr* and *mdx:cmah*) showing the reduction in normalised grip strength in muscular dystrophy mice. n=6 in each group except for *mdx:utr* at 5 weeks where n=5. ** denotes $p<0.01$ when compared to WT mice at 3 weeks-of-age, * denotes $p<0.05$ in *mdx:utr* mice at 5 weeks-of-age and *mdx:cmah* mice at 7 weeks-of-age compared to WT.

3.5.3 Muscle Histology

Histological analysis of the TA muscle revealed a clear necrosis with inflammatory infiltration by 3 weeks-of-age in all the muscular dystrophy mouse models. The corresponding WT mice showed normal, regular myofibres with peripheral nuclei and intact sarcoplasm at all ages with minimal evidence of inflammation or regeneration (Figure 3-5A). This was confirmed by the significant increase in % of inflammatory cells seen in the muscular dystrophy models compared to the WT mice at 3 weeks-of-age (Table 3-5). There was evidence of regeneration with larger, irregular myofibres containing central nuclei seen by 5 weeks-of-age in all the muscular dystrophy mouse models, (Figure 3-5C and D) but more so in the *mdx* and *mdx*:*utr* models. The amount of muscle regeneration was significantly lower in the *mdx:cmah* mice compared to *mdx* and *mdx:utr* mice at both 5 and 7 weeks-of-age (Table 3-5).

3.5.4 Gross body growth parameters

Length measurements were only started at 3 weeks-of-age once the mice were weaned (to minimise handling), therefore changes in growth parameters are not available in the 3 week-old mice. As expected, values for bodyweight, crown-rump length and tail length increased with the age of the mouse at cull. The *mdx*:*cmah* mice were 1.96g lighter than WT mice at 3 weeks-of-age (8.07g v 10.03g, p=0.02), but were 3.0g heavier by 7 weeks-of-age (21.97g v 24.97g, p=0.02), see Table 3-6. Consistent with this, when analysing the mice that were culled at either 5 or 7 weeks-of-age and hence had longitudinal growth data available, the *mdx:cmah* mice gained significantly more weight than WT mice between 3 and 5 weeks-of-age (8.77g, v 10.61g, p=0.01) suggesting catch-up growth. Weight gain slowed between 5 and 7 weeks-of-age in all models and there were no differences in weight gain during this period by genotype (Figure 3-6). No differences in bodyweight were observed in the *mdx* or *mdx:utr* mice compared to WT mice at any time-point studied.

Crown-rump length was greater in *mdx:cmah* mice compared to WT mice at 5 weeks-of-age (8.01 v 7.09 cm, p=0.04), (Table 3-6), but otherwise there were no significant differences in crown-rump or tail length between groups at any age.

Mouse type	Mean CK value, in U/L (SD)		
	3 weeks at cull	**5 weeks at cull**	**7 weeks at cull**
WT	151.1 (134.2)	230.1 (121.8)	234.4 (167.0)
mdx	1365.3 (589.0) *	2424.0 (506.9) *** $^{\Delta\Delta}$	1483.0 (153.70) ***
mdx:u*tr*	1594.6 (754.1) *	2468.0 (1170.3) ***	2281.3 (277.5) ***
mdx:*cmah*	1483.2 (749.0) *	2602.2 (671.7) *** $^{\Delta}$	2530.3 (562.6) *** $^{\Delta}$

Table 3-2 Increased serum CK levels in muscular dystrophy mice at 3, 5 and 7 weeks-of-age. Data are presented as mean (+/- standard deviation). * denotes p<0.05, *** p<0.001 compared to WT mice. $^{\Delta}$ denotes p<0.05, $^{\Delta\Delta}$ p<0.01 compared to mice of the same genotype at 3 weeks-of-age. n=6 in each group except for mdx:utr at 5 weeks where n=5.

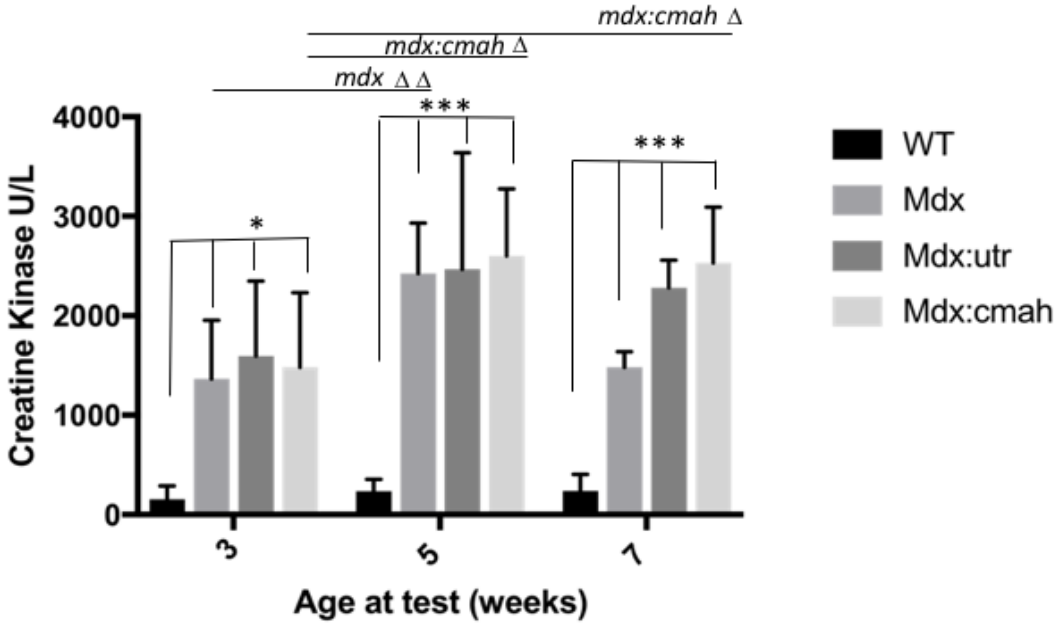

Figure 3-4 Higher CK levels in muscular dystrophy mice at 3,5 and 7 weeks-of-age. Data are presented as mean (+/- standard deviation). * denotes p<0.05 *** p<0.001 compared to WT mice. $^{\Delta}$ denotes p<0.05, $^{\Delta\Delta}$ p<0.01 compared to mice of the same genotype at 3 weeks-of-age. n=6 in each group except for mdx:utr at 5 weeks where n=5.

Independent variable	Co-efficient	95% CI	p-value	R^2
Genotype (WT as comparator)				0.62
mdx	1463.08	1057.76, 1868.39	0.000	
mdx:*utr*	1947.72	1454.81, 2440.63	0.000	
mdx:*cmah*	1967.68	1532.10, 2403.27	0.000	
Age at cull (3 wks as comparator)				0.05
5 weeks	559.67	-38.92, 1158.25	0.066	
7 weeks	298.94	-286.76, 884.64	0.312	

Table 3-3 Univariable linear regression model showing the individual effects of age and genotype on CK level.

Independent variable	Co-efficient	95% CI	p-value	R^2
Genotype (WT as comparator)				0.71
mdx	1604.36	1243.12, 1956.6	0.000	
mdx:*utr*	1979.70	1546.88, 2412.52	0.000	
mdx:*cmah*	2059.51	1675.17, 2443.84	0.000	
Age at cull (3 wks as comparator)				0.05
5 weeks	787.13	444.99, 1129.27	0.000	
7 weeks	479.21	145.85, 812.58	0.006	

Table 3-4 Multivariable linear regression model showing the adjusted effects of age and genotype on CK level.

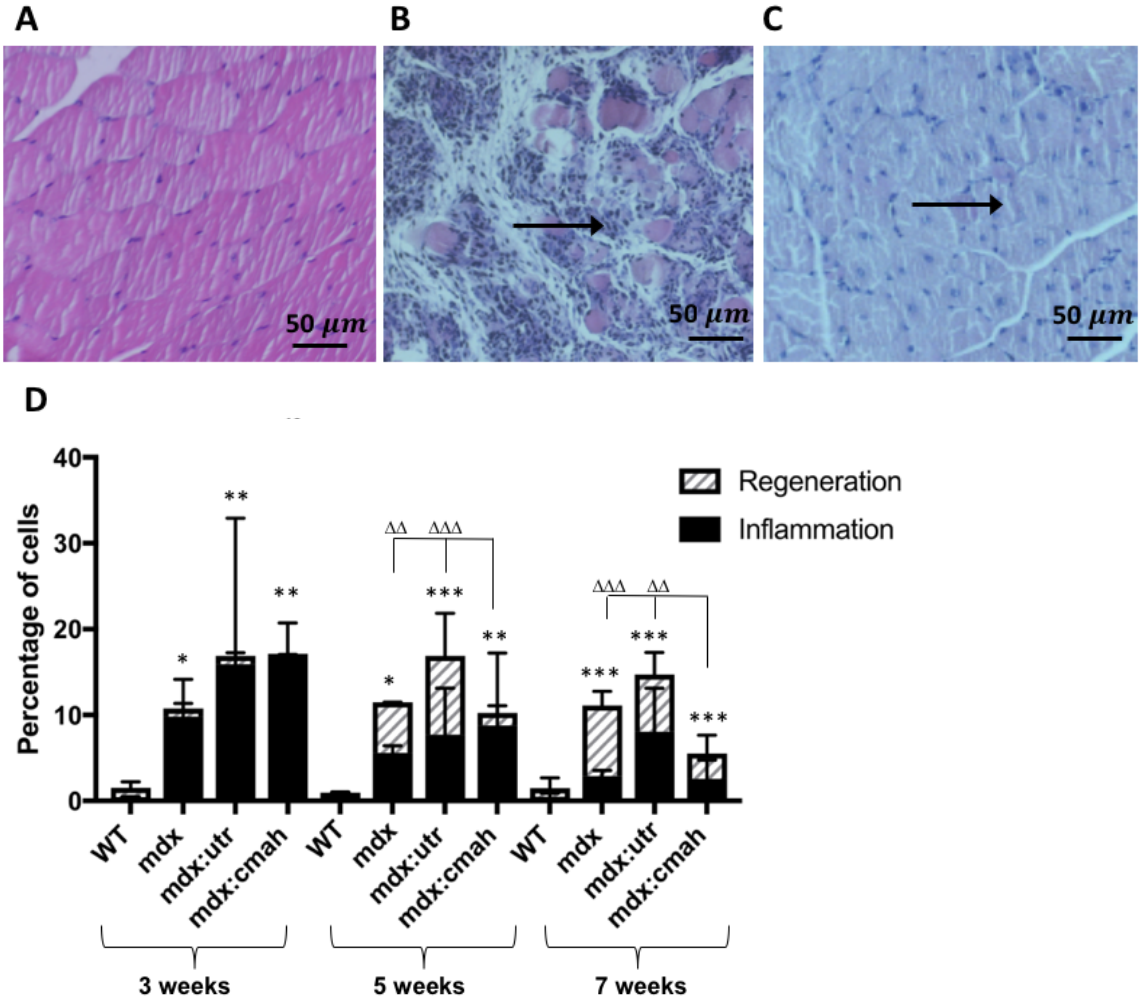

Figure 3-5 Histology of TA muscle showing pathology in muscular dystrophy models. H&E stained section of TA from a:

A) 3-week-old WT with normal, regular myofibres, peripheral nuclei, intact sarcoplasm**.**

B) 3- week-old *mdx:utr* mouse showing many inflammatory cells (arrow) and barely visible sarcoplasm.

C) 7-week-old *mdx* mouse showing regeneration with larger myofibres and central nuclei (arrow).

D) Muscle cell inflammation seen in all muscular dystrophy models by 3 weeks-of-age followed by subsequent regeneration at 5 and 7 weeks-of-age. Data are presented as mean+/- SD. * denotes $p<0.05$, ** $p<0.01$, *** $p<0.001$ for cumulative percentage values compared to WT mice at the same age. $^{\Delta\Delta}$ denotes $p<0.01$, $^{\Delta\Delta\Delta}$ $p<0.001$ for % regeneration compared to *mdx:cmah* mice at the same age. n=6 in each group except for mdx:utr at 5 weeks where n=5.

Mouse type	3 weeks at cull	5 weeks at cull	7 weeks at cull
	% of inflammatory cells, signifying active cell damage (SD)		
WT	0.27 (0.22)	0.45 (0.54)	0.35 (0.54)
mdx	9.83 (4.32)*	5.59 (0.83)**	2.88 (0.67)*
mdx:u*tr*	15.92 (16.98)**	7.73 (5.39)**	8.04 (5.07)***
mdx:c*mah*	16.74 (3.96) **	8.77 (8.45)**	2.57 (2.18)
	% of central nuclei, signifying regeneration (SD)		
WT	1.23 (0.72)	0.42 (0.18)	1.14 (1.20)
mdx	0.92 (0.59)	5.88 (0.01)** $^{\Delta\Delta}$	8.23 (1.64)*** $^{\Delta\Delta\Delta}$
mdx:u*tr*	1.01 (0.37)	9.14 (4.97) *** $^{\Delta\Delta\Delta}$	6.68 (2.58)*** $^{\Delta\Delta}$
mdx:c*mah*	0.17 (0.14)	1.47 (0.85)	2.96 (2.12)*
	Cumulative percentage (SD)		
WT	1.50 (0.50)	0.87 (0.59)	1.48 (1.21)
mdx	10.75 (4.55)	11.47 (0.82)*	11.11 (1.30)*** $^{\Delta\Delta\Delta}$
mdx:u*tr*	16.93 (17.20)**	16.87 (6.22)*** $^{\Delta\Delta}$	14.72 (3.41)*** $^{\Delta\Delta\Delta}$
mdx:c*mah*	16.91 (3.92)**	10.06 (7.84)**	5.53 (1.61)***

Table 3-5 Histology of TA muscle showing pathology in muscular dystrophy models at 3,5 and 7 weeks-of-age. Data are presented as mean (+/- standard deviation). * denotes $p<0.05$, ** denotes $p<0.01$ *** $p<0.001$ compared to WT mice at the same age. $^{\Delta}$denotes $p<0.05$, $^{\Delta\Delta}$ denotes $p<0.01$, $^{\Delta\Delta\Delta}$ denotes $p<0.001$ compared to *mdx:cmah* mice at the same age.

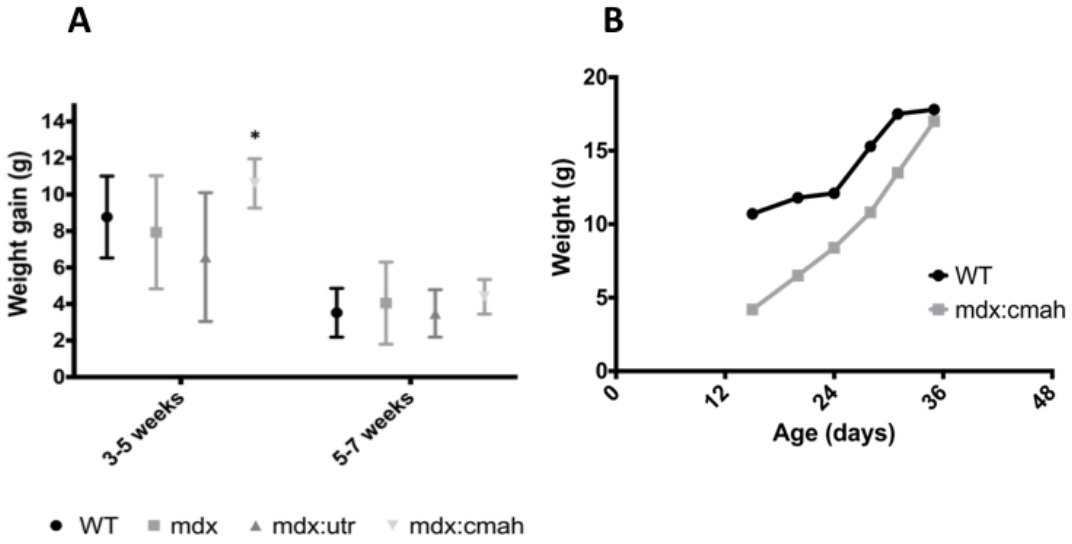

Figure 3-6 Increased weight gain is seen in the young *mdx:cmah* mice

A) Increased rate of weight gain in the *mdx:cmah* occurred between 3 and 5 weeks-of-age but not between 5 and 7 weeks-of-age. Data presented are mean (symbol) and standard deviation (whiskers). * denotes $p<0.05$ compared to WT mice.

B) Example of a growth chart for a WT mouse compared to a *mdx:cmah* mouse showing the lower initial weight and the rapid growth velocity seen in the early weeks in the *mdx:cmah* mouse.

Mouse type	3 weeks at cull	5 weeks at cull	7 weeks at cull
		Bodyweight at cull, in g (SD)	
WT	10.03 (1.62)	17.33 (0.98)	21.97 (1.42)
mdx	9.43 (1.23)	19.07 (2.13)	23.09 (2.90)
mdx:u*tr*	8.84 (0.55)	17.36 (1.59)	24.65 (1.62)
mdx:*cmah*	8.07 (0.90)*	17.17 (3.13)	24.97 (1.58)*
		Gain in BW, in g (SD)	
		From 3-5 weeks	From 5-7 weeks
WT	-	8.77 (2.24)	3.52 (1.34)
mdx	-	7.93 (3.10)	4.05 (2.25)
mdx:u*tr*	-	6.57 (3.53)	3.48 (1.30)
mdx:*cmah*	-	10.61 (1.35) *	4.40 (0.95)
		Crown-rump length, in cm (SD)	
WT	-	7.49 (0.84)	8.84 (0.39)
mdx	-	8.09 (0.23)	8.93 (0.37)
mdx:u*tr*	-	8.13 (0.38)	8.92 (0.22)
mdx:*cmah*	-	8.01 (0.30)*	8.55 (0.36)
		Tail length, in cm (SD)	
WT	-	6.86 (0.55)	7.56 (0.26)
mdx	-	6.86 (0.20)	7.42 (0.18)
mdx:u*tr*	-	6.98 (0.30)	7.74 (0.21)
mdx:*cmah*	-	6.87 (0.33)	7.25 (0.51)

Table 3-6 Change in growth parameters during the study period. Data are presented as mean (+/- standard deviation), * denotes $p<0.05$ compared to WT mice at the same age.

3.5.5 Testes weight

Testes weight increased by more than 200% between 3 and 5 weeks-of-age and were greatest at 7 weeks-of-age in all genotypes. This is consistent with most male mice reaching puberty by 30-38 days of age or approximately 5 weeks-of-age. Even when normalised for bodyweight, normalised testes weight still increased by between 117 and 166% between 3 and 7 weeks-of-age. Combined testes weight was, in comparison to WT mice, significantly less in *mdx* mice (p=0.001) and when normalised to BW, the testes weight was significantly less in both *mdx* and *mdx*:*utr* mice at 7 weeks-of-age compared to WT mice (p=0.001(Table 3-7)).

3.5.6 Analysis of growth plate heights

There was no significant difference in either total GP height or of the individual maturation zones by genotype (Table 3-9; Figure 3-7C+D). Total GP height was however significantly greater at 3 and 5 weeks-of-age compared to 7 weeks-of-age after adjustment for genotype in a multivariable linear regression model (Table 3-8, Figure 3-7A+B). This is consistent with the theory that the volume of hypertrophic chondrocytes is proportional to growth rate (Breur *et al.* 1991).

3.5.7 Dynamic histomorphometry

Dynamic histomorphometry of the GP using fluorescent calcein labelling revealed a lower longitudinal BFR with increasing age, and in particular a reduction in growth velocity after 5 weeks-of-age, shown in the multivariable model in Table 3-11 (p=0.000). The longitudinal BFR of *mdx*:*cmah* mice at 5 weeks-of-age was significantly greater than *mdx*, *mdx*:*utr* and WT mice (p=0.01) (Table 3-10). When genotype and age at cull were incorporated into a multivariable linear regression model, the *mdx*:*cmah* mice was associated with an increased overall growth rate (p=0.007) and increasing age was associated with a reduction in growth rate (Table 3-11).

Mouse type	**Combined testes weight, in g (SD)**		
	3 weeks at cull	5 weeks at cull	7 weeks at cull
WT	0.05 (0.02)	0.12 (0.01)	0.17 (0.003)
mdx	0.04 (0.01)	0.12 (0.01)	0.13 (0.03) **
mdx:u*tr*	0.03 (0.01)	0.12 (0.01)	0.15 (0.01)
mdx: c*mah*	0.04 (0.01)	0.12 (0.01)	0.17 (0.02)
Mouse type	**Combined testes weight, normalised to body weight in g/g (SD)**		
	3 weeks at cull	5 weeks at cull	7 weeks at cull
WT	0.0048 (0.001)	0.0071 (0.001)	0.0080 ((0.001)
mdx	0.0047 (0.001)	0.0062 (0.001)	0.0056 (0.002) ***
mdx:u*tr*	0.0039 (0.001)	0.0068 (0.001)	0.0062 (0.001) *
mdx: c*mah*	0.0054 (0.002)	0.0073 (0.001)	0.0068 (0.001)

Table 3-7 Combined testes weight in muscular dystrophy models at 3,5 and 7 weeks-of-age. Data are presented as mean (+/- standard deviation). * denotes $p<0.05$, ** $p<0.01$, *** $p<0.001$ compared to WT mice.

Independent variable	**Co-efficient**	**95% CI**	**p-value**	**R^2**
				0.42
Genotype (WT as comparator)				
mdx	26.23	-23.62,76.07	0.295	
mdx:*utr*	-13.12	-65.97,39.74	0.620	
mdx:*cmah*	13.19	-41.08, 67.45	0.627	
Age at cull (3 wks as comparator)				
5 weeks	-61.73	-112.30, -11.16	0.018	
7 weeks	-122.96	-165.57, -80.35	0.000	

Table 3-8 Multivariable linear regression model showing the adjusted effects of age and genotype on total GP height.

Mouse type	**Total GP height, in μm (SD)**		
	3 weeks at cull	5 weeks at cull	7 weeks at cull
WT	330.82 (46.90)	261.42 (9.17)	196.20 (19.93)
mdx	373.85 (104.63)	223.93 (52.15)	218.33 (26.47)
mdx:u*tr*	248.53 (77.34)	279.42 (80.04)	221.42 (25.98)
mdx:c*mah*	344.48 (80.12)	302.54 (14.50)	157.28 (25.70)
	Height of hypertrophic zone in μm (SD)		
WT	129.53 (24.17)	113.24 (2.16)	88.89 (11.15)
mdx	151.05 (32.78)	98.37 (13.35)	90.52 (4.62)
mdx:u*tr*	100.17 (45.23)	131.37 (49.54)	95.44 (11.56)
mdx:c*mah*	150.24 (30.78)	110.64 (11.79)	81.54 (6.59)
	Height of hypertrophic zone as % of total height (SD)		
WT	39.03 (3.89)	43.33 (0.89)	45.68 (6.94)
mdx	42.48 (11.75)	43.37 (1.88)	42.09 (6.77)
mdx:u*tr*	39.88 (8.89)	46.38 (4.44)	43.14 (2.65)
mdx:c*mah*	42.59 (8.30)	37.95 (1.44)	52.20 (4.34)
	Height of proliferative zone in μm (SD)		
WT	188.96 (60.23)	115.78 (9.12)	109.30 (15.30)
mdx	183.89 (83.98)	117.77 (26.69)	123.19 (13.34)
mdx:u*tr*	129.89 (43.85)	107.62 (17.49)	112.98 (22.89)
mdx:c*mah*	139.33 (33.00)	140.64 (17.26)	111.16 (39.51)
	Height of proliferative zone as % of total height (SD)		
WT	56.47 (12.56)	44.40 (4.97)	55.71 (5.22)
mdx	48.97 (15.52)	52.63 (0.33)	56.68 (4.74)
mdx:u*tr*	53.66 (13.92)	41.25 (20.65)	51.78 (12.91)
mdx:c*mah*	40.93 (5.70)	46.41 (3.91)	69.55 (13.76)

Table 3-9 Analysis of overall height and individual GP zone heights in muscular dystrophy models compared to WT mice at 3, 5 and 7 weeks-of-age.
Data are presented as mean (+/- standard deviation).

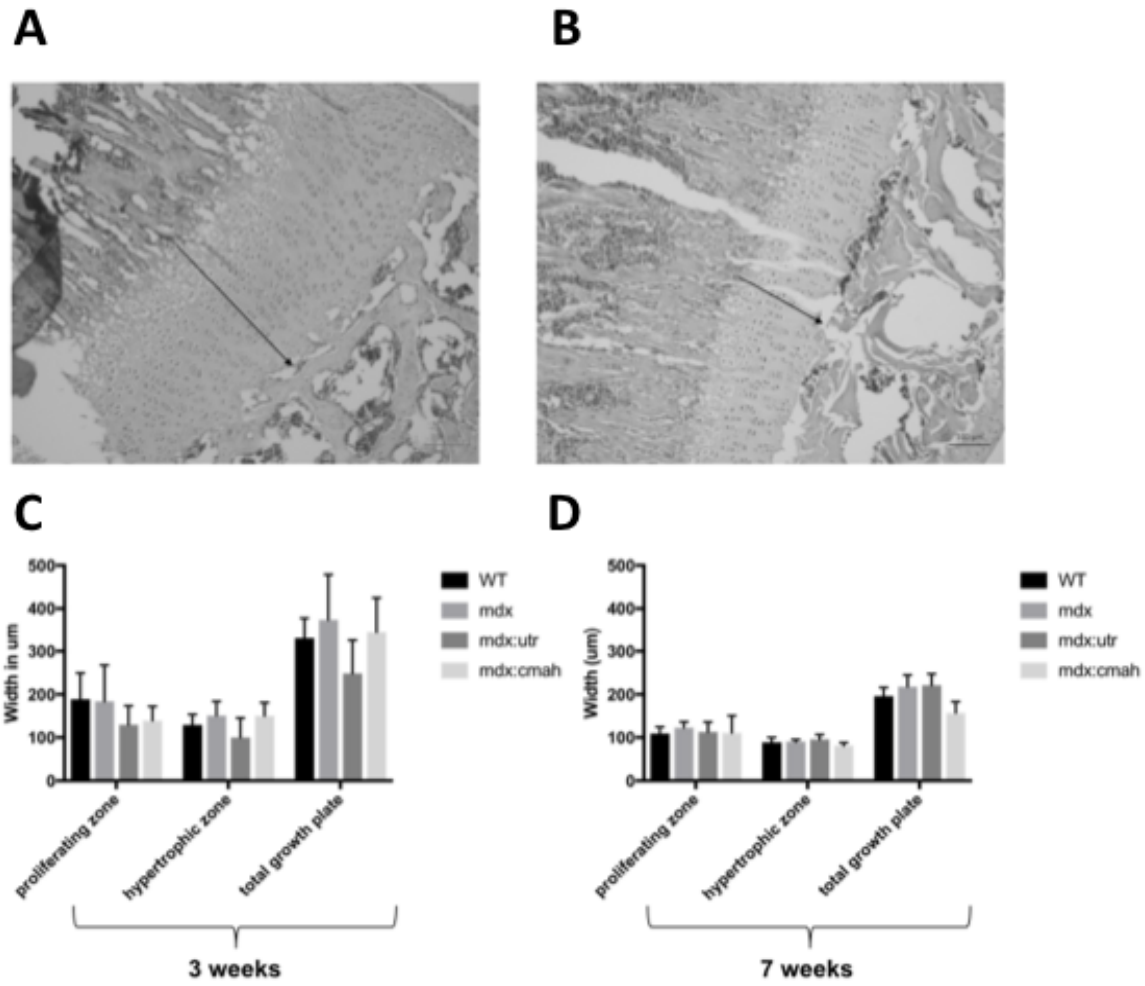

Figure 3-7 Representative GP images from WT mice at **(A)** 3 and **(B)** 7 weeks-of-age, highlighting the reduction in total GP height at 3 weeks (p=0.000) compared to 7 weeks-of-age. There was no significant difference in total GP height or of individual zones by genotype at either **(C)** 3 or **(D)** 7 weeks-of-age. n=6 in each group except for *mdx:utr* at 5 weeks where n=5.

Mouse type	Longitudinal growth rate, in μm/day (SD)		
	3 weeks at cull	**5 weeks at cull**	**7 weeks at cull**
WT	124.38 (18.73)	76.54 (15.39)	36.61 (15.44)
mdx	97.33 (22.31)	73.73 (15.67)	46.21 (18.10)
mdx:u*tr*	89.65 (15.77)	82.35 (27.27)	29.24 (6.77)
mdx:c*mah*	126.29 (26.09)	116.65 (25.64)*	49.07 (10.66)

Table 3-10 The effect of genotype and age at cull on longitudinal growth rate using calcein labelling. Data are presented as mean (+/- standard deviation). * denotes $p<0.05$ compared to WT mice at the same age.

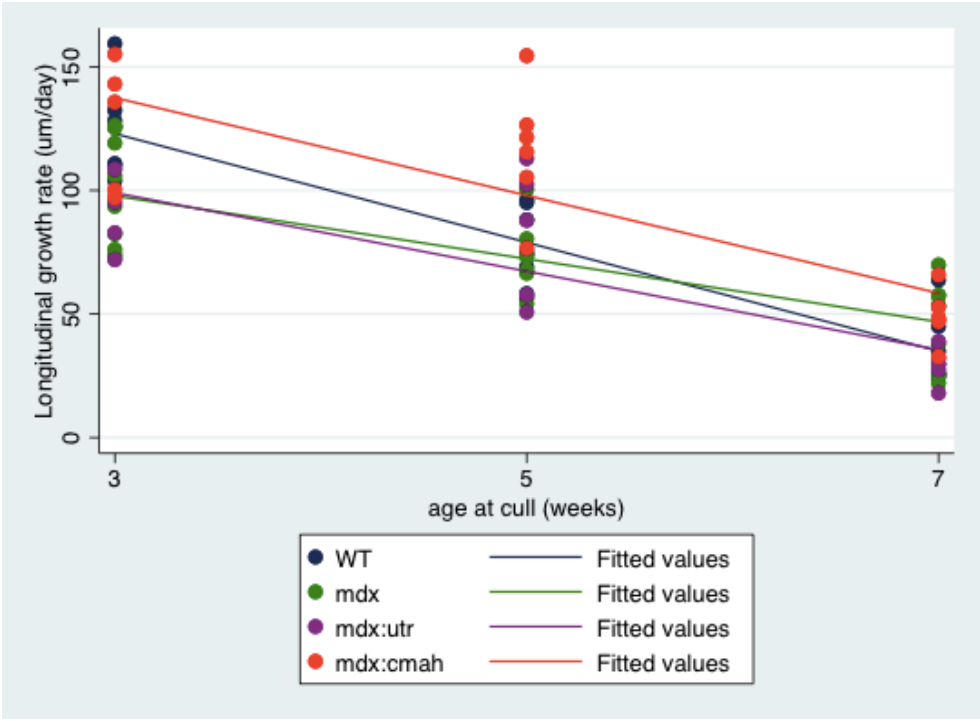

Figure 3-8 Longitudinal BFR, as assessed by calcein labelling (μm/day) by genotype and age at cull. The longitudinal BFR of the *mdx:cmah* at 5 weeks-of-age was significantly greater than the *mdx*, *mdx:utr* and WT mice ($p=0.01$). n=6 per group, except for *mdx:utr* at 5 weeks, where n=5.

Independent variable	Co-efficient	95% CI	p-value	R^2
				0.69
Genotype (WT as comparator)				
mdx	-6.79	-19.23, 5.66	0.280	
mdx:*utr*	-11.24	-25.02, 2.54	0.108	
mdx:*cmah*	18.54	5.27, 31.82	0.007	
Age at cull (3 wks as comparator)				
5 weeks	-23.92	-35.48, -12.36	0.000	
7 weeks	-69.34	-80.89, -57.78	0.000	

Table 3-11 Multivariable linear regression model showing the adjusted effects of age and genotype on longitudinal growth rate per day.

Mouse type	Tibial length on CT, in mm (SD)		
	3 weeks at cull	5 weeks at cull	7 weeks at cull
WT	13.02 (0.96)	14.93 (0.18)	16.07 (0.17)
mdx	12.07(0.49)	14.82 (0.59)	16.10 (0.35)
mdx:u*tr*	12.42 (0.12)	14.84 (0.84)	16.27(0.30)
mdx:c*mah*	12.45 (0.39)	14.99 (0.53)	16.60 (0.42)
	Tibial length/bodyweight, in mm/g (SD)		
	3 weeks at cull	5 weeks at cull	7 weeks at cull
WT	1.30 (0.22)	0.88 (0.07)	0.74 (0.05)
mdx	1.33 (0.14)	0.76 (0.09)	0.68 (0.08)
mdx:u*tr*	1.43 (0.11)	0.94 (0.12)	0.66 (0.40)
mdx:c*mah*	1.52 (0.44)	0.91 (0.25)	0.67 (0.05)

Table 3-12 μCT analysis of tibial length in muscular dystrophy models at 3, 5 and 7 weeks-of-age. Data are presented as mean (+/- standard deviation).

3.5.8 Tibial length measurement

When tibial length was measured by μCT, bone length was similar in the muscular dystrophy and WT mice at 3, 5 and 7 weeks-of-age (Table 3-12). In order to determine whether the bone growth was in proportion to weight gain, the tibial length was also standardised to bodyweight (mm/g) but again there were no significant difference in the length of tibia from muscular dystrophy and WT mice groups at all ages studied (Table 3-12).

3.5.9 Assessment of proliferation rate

There was no significant difference in the % of PCNA positive nuclei in proliferating chondrocytes of 3-week-old muscular dystrophy and WT mice (Figure 3-9).

3.5.10 Assessment of chondrocyte apoptosis

After analysis of the first 12 sections processed using the Apoptag detection kit, (3 from each genotype) it was felt that the number of chondrocytes dying via apoptosis was too low to enable accurate quantification. As Figure 3-10 demonstrates, there were only scattered apoptotic cells, mainly within the hypertrophic zone of the growth plate, the secondary ossification zone and in the upper metaphysis. As expected, apoptosis was not observed in the less mature proliferating chondrocytes.

3.5.11 Metatarsal culture

There was a 175% increase in the length change of the mineralising zone from day 0 to 7 in the *mdx*:*cmah* mice ($p<0.001$) compared to both WT and *mdx mice.* However, the overall growth rate of metatarsals from WT, *mdx* and *mdx:cmah* mice was similar after 7 days of culture. (Table 3-13 and Figure 3-11).

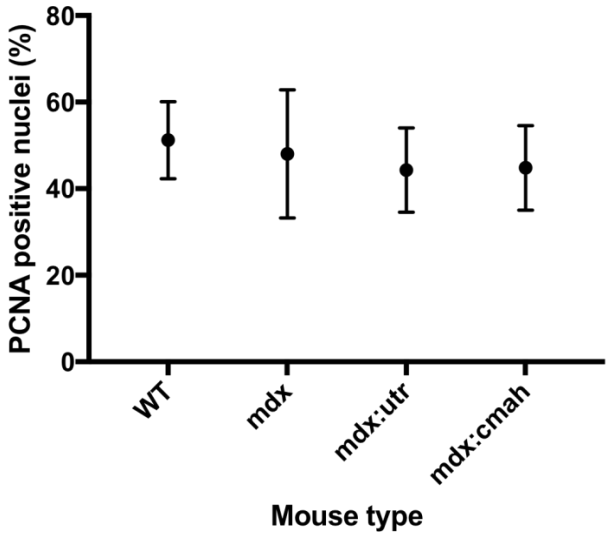

Figure 3-9 The percentage of PCNA positive nuclei in the proliferating zone did not vary significantly between 3-week-old muscular dystrophy and WT mice. Data presented are mean (symbol) and standard deviation (whiskers).

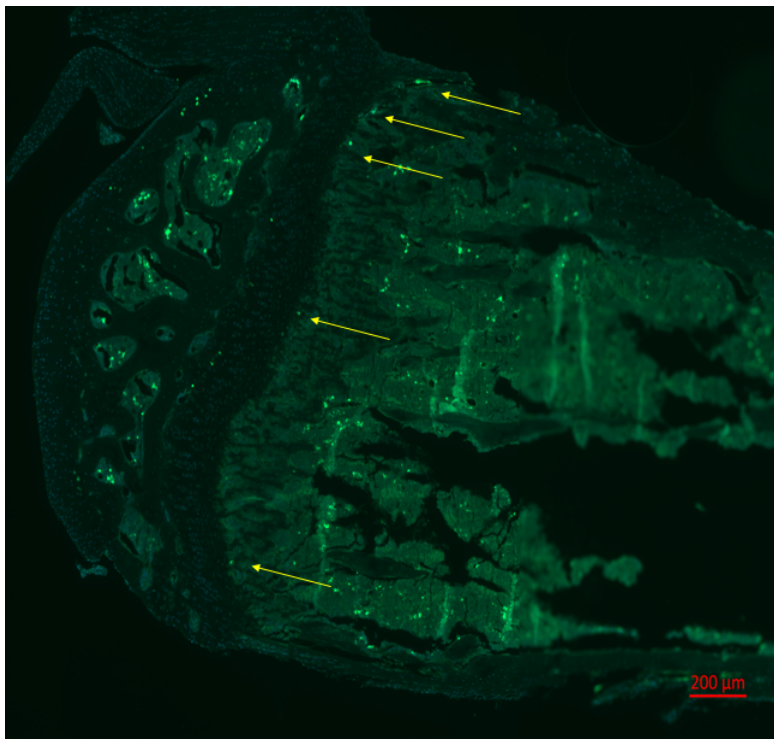

Figure 3-10 Example of a formalin-fixed, paraffin-embedded tibial GP in an *mdx:utr* mouse culled at 7 weeks-of-age. Positively-stained apoptotic cells have been stained by fluorescein and counterstained using DAPI (arrows).

Metatarsal parameter	**WT**	***mdx***	***mdx:cmah***
Day 0 total length, mm	1.97 (0.07)	2.01 (0.07)	1.92 (0.37)
Day 0 mineralising zone, mm	0.62 (0.02)	0.64 (0.03)	0.33 (0.05)
Day 7 total length, mm	3.23 (0.11)	3.25 (0.16)	3.15 (0.53)
Day 7 mineralising zone, mm	0.76 (0.10)	0.73 (0.09)	0.89 (0.16)
Total length increase, mm	1.26 (0.07)	1.25 (0.11)	1.22 (0.51)
Mineralising zone increase, mm	0.15 (0.10)	0.09 (0.09)	0.57 (0.16)
Total length % change	64.2 (3.54)	62.3 (4.30)	66.8 (29.8)
Mineralising zone % change	23.6 (16.8)	13.7 (14.1)	175.3 (56.9)***

Table 3-13 Metatarsal parameters after 7 days in culture. Data are presented as mean (+/- standard deviation). *** denotes $p<0.001$ compared to WT mice.

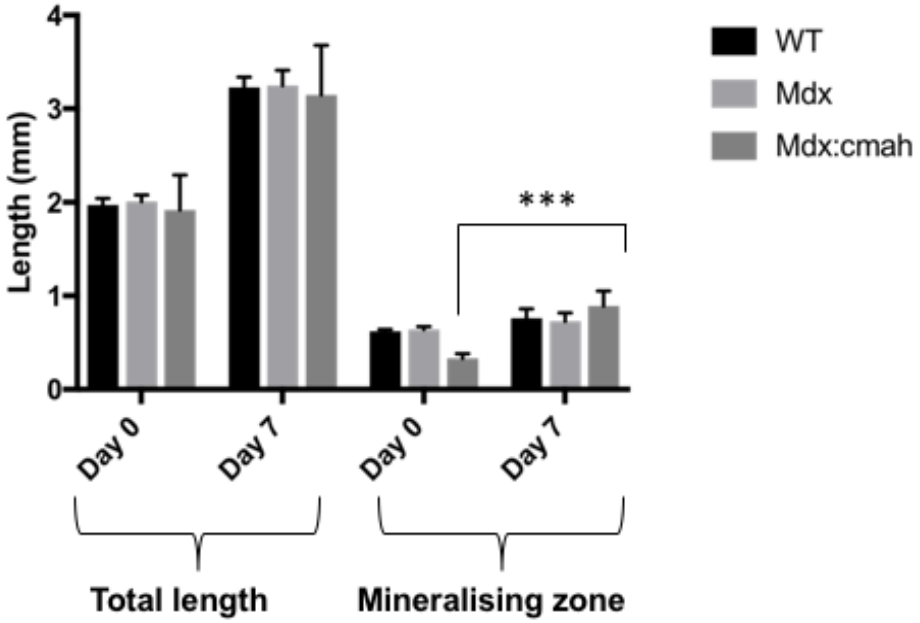

Figure 3-11 Change in total length and mineralising zone of E19 metatarsals by genotype. There was a 175% increase in length of the mineralising zone from day 0 to 7 in the *mdx:cmah mice*. *** denotes p<0.001 for length at day 0 compared to day 7. N=12 metatarsals from 1 mouse of each genotype.

3.6 Discussion

Results presented in this chapter confirm the presence of a muscle phenotype in all the muscular dystrophy mouse models. Genotype and age-dependent differences were observed. The muscle phenotype in the *mdx* mice was most marked in the youngest mice; normalised grip strength was significantly lower in the *mdx mice* compared to *WT* mice at 3 weeks-of-age but not beyond this. CK levels in the mice culled at 7 weeks-of-age were lower in the *mdx* compared to the *mdx:utr* and *mdx:cmah* mice*,* although still raised 10-fold compared to WT mice*.* Muscle regeneration was evident on histology by 5 weeks-of-age with larger, irregular myofibres with central nuclei in all the muscular dystrophy models, but significantly less in the *mdx:cmah* mice compared to *mdx* and *mdx:utr* mice. This is consistent with published data on the *mdx* mouse which suggests that there is an early period, between the end of the second and up to the fifth week of life, when the mice experience histological necrosis and functional weakness. After this critical period, regeneration occurs and there are no co-existing clinical features of DMD such as scoliosis and heart failure until mice are at least 15 months or older (Bulfield *et al.* 1984, Muntoni *et al.* 1993, Lefaucheur *et al.* 1995, Chamberlain *et al.* 2007, Coley *et al.* 2016).

There is limited literature regarding the heterozygous *mdx:utr* mouse. Like all the muscular dystrophy models that were tested in this study, CK levels were significantly higher in *mdx:utr* mice compared with WT mice and histology also demonstrated ongoing inflammation and regeneration from 5 weeks-of-age onwards. However, the normalised grip strength of the *mdx:utr* mice was only lower than WT mice at 3 weeks-of-age. Other studies have also reported a variable muscle phenotype. In one study, grip duration of the triceps decreased in the *mdx:utr* mice by 1 month of age compared to *mdx mice*, and persisted throughout the first year, but otherwise muscle function was not significantly affected (Huang *et al.* 2011). Another recent study found the *mdx:utr* to have a shorter latency to fall time in the grip strength test at 3 months-of-age, but noted no difference by 18 months (Mcdonald *et al.* 2015).

The muscle data demonstrated in this chapter are consistent with published data suggesting that *mdx:cmah* mice have a more severe muscle phenotype than either

mdx or *mdx:utr mice* with less muscle regeneration seen in this study at both 5 and 7 weeks-of-age (Chandrasekharan *et al.* 2010). The only reduction in normalised grip strength compared to *WT* mice at 7 weeks-of-age was seen in the *mdx:cmah* and linear regression demonstrated an association of both age and *mdx:cmah* genotype with increased serum CK level. It is thought that lower levels and reduced functionality of the DGC and metabolic accumulation of dietary N-glycolyneuraminic acid (Neu5Gc) as a consequence of the *cmah* mutation contribute to a more severe muscle phenotype than in the *mdx* mouse (Chandrasekharan *et al.* 2010).

The results in this chapter do not support the chapter hypothesis that *'growth and GP chondrogenesis are impaired in all muscular dystrophy mouse models when compared to WT mice and more severely in the mdx:cmah mouse model'*. Despite the obvious muscle phenotype there was no evidence of growth retardation in any of the models. No differences in growth were seen between *mdx* and WT mice, either using crude measures of change in bodyweight, crown-rump and tail length, or at the GP using static or dynamic histomorphometric techniques. The growth phenotype of the *mdx* model has not previously been studied in detail but available data are mixed. One study found that *mdx* mice became obese as they aged (Connolly *et al.* 2001) whilst another (Radley-Crabb *et al.* 2014) found that overall growth was blunted in juvenile *mdx mice*, with bodyweight and femur and tibia length being significantly reduced in 4-5 week-old *mdx* mice, but not when assessed in adulthood (14 weeks-of-age) compared to WT mice. In contrast, but consistent with the data presented in this chapter are data from a study which analysed the growth of young *mdx* mice (Nakagaki *et al.* 2011). In this study the authors reported no significant difference in femur length between *mdx* and WT 3-week-old mice. Similarly, the results in this chapter show no suggestion of a growth phenotype in *mdx:utr* mice, with no differences seen in growth rates at the GP, on anthropometry or in tibial length. There are currently no published growth data for the heterozygous *mdx:utr mice* with which to compare the data of this chapter.

This is the first time that the growth phenotype of the *mdx:cmah* mouse have been described. Rather than displaying the most marked growth retardation in accordance with the hypothesis, this discussion will instead focus on the possible mechanisms for

the observed catch-up growth in the *mdx:cmah* mice. Despite being bred in exactly the same conditions and during the same season, the *mdx:cmah* mice were unexpectedly 2.0g lighter than the *WT* mice at 3 weeks-of-age (p=0.02) but demonstrated an increased growth velocity or 'catch-up' growth, such that by 7 weeks-of-age, they were 3.0g heavier than *WT* (p=0.02). The catch-up growth was demonstrated using several different techniques. There was a larger increase in both BW and crown-rump length between 3 and 5 weeks-of-age and a significantly higher longitudinal BFR at 5 weeks-of-age (using calcein labelling) in the *mdx:cmah* mice compared to WT mice. There was also a 175% increase in length of the mineralising zone of *mdx:cmah* E19 metatarsals after 7-days of culture, although there was no change in overall metatarsal length. Further evidence for this catch-up growth from the PCR osteogenesis array data will also be discussed in Chapter 4.

Although GP height was not significantly different between the *mdx:cmah* and WT mice despite other parameters being suggestive of an increased growth velocity, it has been suggested that GP height may be misleading when used as the sole parameter to quantitate effects on skeletal growth, as it does not necessarily change in proportion to growth rate (Hunziker *et al.* 1994). Similarly, although tibial length was unchanged by genotype, the single, cross-sectional measurement cannot be used to demonstrate growth velocity which would likely be higher in *mdx:cmah mice*. Ideally, length of the tibia would be recorded longitudinally *in-vivo* at several time points during the study, for example by x-ray or DXA, to enable change in length to be calculated (Iida-Klein *et al.* 2003). This facility was not available during this study, however, and also has associated limitations as the associated radiation exposure may also impact on growth (Mustafy *et al.* 2018).

The precise aetiology of the catch-up growth in the *mdx:cmah* mouse is unclear, but it appears to be initiated prior to 5 weeks-of-age. It does appear to be a consequence of the additional *cmah* mutation as the *mdx* mice do not show the same trait. The smaller absolute bodyweight in the youngest *mdx:cmah* mice may be a reflection of several factors, including poorer general health in the mothers prior to or during pregnancy or a problem pre- or peri-weaning in the offspring. Consistent with this, the *mdx:cmah* mice were much harder to breed than expected with a lower frequency of

litters and a higher than expected number of pre-wean deaths. According to the Barker hypothesis and the developmental origins of health and disease, predisposition to the development of the metabolic syndrome begins in utero with changes occurring during critical periods of foetal development that promote survival of the foetus in an adverse intrauterine environment which can have a lasting impact on health in later life and the development of the metabolic syndrome (Hales *et al.* 2001, Barker 2004). The *mdx:cmah* mice in this study were smaller than expected for the C57BL10 background genetic strain and displayed catch-up growth in keeping with the 'thrifty phenotype' Although the exact aetiology and role of the additional *cmah* mutation remains unclear, *cmah*-null mouse models have been proposed as one of the best to mimic the human metabolic disorder phenotype (Kwon *et al.* 2015). A recent study reported that *cmah*-null mice fed a high fat diet exhibit fasting hyperglycaemia and glucose intolerance and postulated that the *cmah* mutation contributes to pancreatic β-cell dysfunction in mice (Kavaler *et al.* 2011). Similarly, several genes responsible for glycolysis and gluconeogenesis were significantly upregulated in *cmah*-null mouse livers (Kwon *et al.* 2014). It is possible that mitochondrial dysfunction caused by oxidative stress may be either a cause or consequence of insulin resistance (Kwon *et al.* 2015). It was unfortunately not possible within the time constraints of this study to investigate the metabolic function or cause of the catch-up growth of the *cmah:mdx* mice in greater detail. This study demonstrated glucose levels that are consistent with other published data from the *mdx* mice (Strakova *et al.* 2018) but no significant difference in non-fasted serum glucose level by genotype. However, as the mice were very young, not fasted prior to cull and had not been stressed (for example by glucose tolerance test), it was not possible to speculate further regarding their insulin sensitivity or underlying metabolic function.

Financial and time restrictions prevented the use of a WT:*cmah*$^{-/-}$ control group of mice and therefore the role and significance of the *cmah* mutation independently of the *mdx* is unclear. However, the purpose of this chapter was to characterise the growth of mouse models of muscular dystrophy with the aim of determining the most appropriate model to use during the latter stages of the project.

In summary, the data have indicated that none of the muscular dystrophy mouse models studied demonstrated growth retardation when assessed at 3, 5 or 7 weeks-of-age. In particular, the *mdx:cmah* mouse is not an appropriate model to mimic the intrinsic growth failure seen in patients with DMD, as it appears to demonstrate catch up growth. The next chapter seeks to determine whether any of the muscular dystrophy mouse models have impaired skeletal development.

CHAPTER 4

Characterisation of bone in muscular dystrophy mouse models

4 Characterisation of bone in muscular dystrophy mouse models

4.1 Introduction

It is recognised that boys with DMD are more susceptible to fractures than an equivalent healthy population, whether or not they are on GC (Buckner *et al.* 2015). An older retrospective study performed before GC therapy became included in the Standards of Care found that 44% of steroid-naïve DMD boys had sustained a fracture (Larson *et al.* 2000). BMD in adulthood depends predominantly on growth and mineralisation of the skeleton and crucially on the bone mass achieved during childhood and puberty. In healthy individuals, 80% of bone mass is accrued by 18 years of age (Bachrach 2001) and a reduced peak BMD in childhood has been proposed as one of the strongest predictors of later life fractures (Wood *et al.* 2015).

There are several factors that may contribute to impaired skeletal development in DMD, in addition to GC use. Bone and muscle are intrinsically linked and the mechanostat model (Frost 2003) is a widely accepted theory; normal bone mineral accrual depends on a regulatory circuit sensing the bone deformations that are produced by muscle contractions to regulate osteocyte activity and modulate bone strength. The muscle weakness and reduced mobility that occurs in DMD causes reduced loading forces on the bone, diminished bone growth and mineral accrual and results in the formation of low density bone and low-trauma fractures, *i.e.* fractures that result from mechanical forces that would not ordinarily result in fracture (Feber *et al.* 2012, Matthews *et al.* 2016). A concise review has recently been published describing the muscle-bone interaction (Veilleux *et al.* 2017). It is of great significance to the DMD population that up to half are estimated to lose ambulation after their first fracture, as this is associated with loss of independence and a considerable reduction in quality of life. In addition, loss of ambulation can lead to a further reduction in bone mass (Larson *et al.* 2000). Once a patient becomes non-ambulatory and no dynamic or gravitational bone loading occurs, the fine balance between bone resorption and formation is shifted and resorption exceeds formation; a phenomenon often termed disuse osteoporosis (Takata *et al.* 2001). In support of this, retrospective data from the Muscular Dystrophy Surveillance, Tracking and Research network combining

DMD and Becker muscular dystrophy patients shows that full-time wheelchair use increased the risk of first fracture by 75% for every 3 months of use (James *et al.* 2015).

Vitamin D is essential for skeletal health through its regulation of calcium and phosphate absorption and may also have an additional role in muscle strength (Tomlinson *et al.* 2015). Despite most boys with DMD receiving vitamin D supplementation as per guidelines, insufficient levels are often detected (Alshaikh *et al.* 2016). Vitamin D absorption is further impaired by GC use (Patschan *et al.* 2001).

Testosterone acts via its conversion to 5-α dihydrotestosterone or oestradiol to enhance osteoblast differentiation and action and reduce osteoclast activity (Sinnesael *et al.* 2011). Puberty is a crucial time for bone mineral accrual and pubertal timing is an important determinant of peak bone mass. It is often delayed in many childhood chronic conditions and is almost universally delayed or absent in GC-treated DMD (Bianchi *et al.* 2011; Wood *et al.* 2015; Wood *et al.* 2015). Over half of patients were found to have low testosterone levels when measured in 59 men with different dystrophinopathies (Al-Harbi *et al.* 2008).

The inflammatory process and cytokine release associated with muscular dystrophies may also contribute further to low BMD, as described in other chronic diseases (Joseph *et al.* 2016). In particular in DMD, the activation of the NF-Kβ pathway may also cause altered muscle metabolism and activation of osteoclastogenesis (Morgenroth *et al.* 2012).

There are some data to suggest that there is abnormal osteoblast function in DMD. Bone healing was investigated after making an incision over the tibia in three different strains of muscular dystrophy mice (*mdx; mdx:utr*$^{+/-}$*; mdx:utr*$^{-/-}$*).* μCT was performed on anaesthetised mice at 5 weeks-of-age and delayed bone healing was demonstrated in the *mdx:utr*$^{-/-}$ mice (Isaac *et al.* 2013). This delay in bone healing suggests that a deficiency in osteoblast function may exist. A reduction in all bone formation markers as well as bone resorption markers has also been shown in DMD patients (Söderpalm *et al.* 2007). Furthermore, a recent study in which human primary

osteoblasts were incubated with either 10% of DMD or normal human sera showed that mRNA expression levels of osterix, an early osteoblast transcription factor and osteocalcin, a mature osteoblast secreted matrix protein, were significantly decreased in DMD sera supplemented cultures (Rufo *et al.* 2011). These authors also reported a decrease in expression of other osteogenic factors including various BMPs (Rufo *et al.* 2011). Using μCT in the same study, a lower osteoblast surface per bone surface and lower mineral apposition rate (MAR) were found in *mdx* mice compared to WT mice, further suggesting impaired osteoblast formation and/or function.

4.1.1 Bone marrow adipose tissue (BMAT) in DMD

Since osteoblasts and adipocytes derive from the same population of mesenchymal stem cells (MSC), a shift away from the osteoblast lineage possibly via less osterix expression, would send more cells down the adipocyte lineage (Hong *et al.* 2005). In keeping with this, increases in BMAT are seen in ageing-associated osteoporosis and after GC treatment (Vande Berg *et al.* 1999). Unpublished data from the Glasgow Developmental Endocrinology Research Group has also shown an increase in vertebral bone marrow adiposity in GC-treated patients with DMD. (https://slideplayer.com/slide/12570222/)

4.1.2 Rationale for studying skeletal development in mouse models of DMD

The data regarding skeletal development in mouse models of DMD remain conflicting, as discussed in Chapter 1. Some studies have shown a bone phenotype in the *mdx* and *mdx:utr* mice, while others haven't, and the skeletal phenotype of *mdx:cmah* mice has never been reported. Results appear to depend on the age of the mice and the locations and techniques used to assess bone structure and function. It is important to characterise skeletal development in GC-naïve muscular dystrophy mouse models in order to elucidate the mechanism behind any potentially disordered bone development and to generate more information before the trial of potentially suitable therapies in patients with DMD.

4.2 Hypothesis

Bone development is impaired in all DMD models when compared to WT mice, and more severely in the *mdx*:*cmah* mouse model.

4.3 Aims

1. Assess bone structure and density.
2. Assess biomechanical properties of bone.
3. Quantify bone marrow adipose tissue.

All studies will compare male WT and muscular dystrophy mouse models (*mdx*, *mdx*:*utr* and *mdx*:*cmah*).

4.4 Material and Methods

4.4.1 Micro computed tomography (μCT)

μCT was carried out according to the protocol described in Section 2.4.4. One of the potential limitations when using very young and small mice is that the type of bone within the ROI may vary dependent on bone length if a constant number of slices is analysed from a fixed landmark. For this reason the analysis was repeated after adjusting for length in the youngest mice.

Tissue mineral density (TMD) is the density measurement restricted to within the volume of calcified bone tissue, and is most appropriate when estimating the density of cortical bone, whereas the combined density of a well-defined volume which contains a mixture of both bone and soft tissue, such as a selected volume of trabecular bone in a tibia, is usually referred to as BMD (Bouxsein *et al.* 2010). During this chapter, TMD calculations were made using the cortical ROI defined in Section 2.4.4.

4.4.2 Biomechanical properties assessed by 3-point bending

3-point bending was performed on all tibiae as soon as possible after μCT analysis, as described in Section 2.4.5.

4.4.3 Assessment of bone turnover markers by ELISA

Serum αCTx and P1NP levels were measured as described in Section 2.4.6. All samples for the characterisation study were taken from mice at either 3 or 5 weeks-of-age. Samples from *mdx* and *mdx:cmah* mice at 8 weeks-of-age were also taken for use as controls in the GC study (Chapter 5). Results have also been shown in this chapter to demonstrate the age-related changes seen. As the *mdx:utr* mouse was not used in the GC study, there are no results available for older mice (8 weeks-of-age) of this strain..

4.4.4 Static histomorphometry

Static histomorphometry was performed on paraffin-embedded, decalcified sections of tibiae from mice culled at 5 weeks-of-age. A combination of TRAP activity and fast-

red staining was used to enable osteoclast number to be determined. TNAP IHC was used to identify osteoblasts, see Section 2.4.13 for further details. The ROI included only metaphyseal trabecular bone which extended from 50μm below the GP and within the endocortical bone boundary. Osteoblast and osteoclast number per bone surface were determined using BioqantOsteo v 17.2.6 (Bioquant Image Analysis Corp, Nashville, Tennessee, USA).

4.4.5 Bone marrow adipose tissue (BMAT) quantification

All bones were taken from mice that were 7 weeks-of-age at the time of cull. This age was chosen as there is more normative data available in older mice and also to ensure that there was sufficient BMAT present to enable any genotype-specific differences to be determined. In order to analyse BMAT within tibiae, for which there is the most normative data available, additional mice (*mdx*, *mdx:cmah*, and WT) were bred to allow BMAT quantification, as both tibiae from the initial study had been used (one for μCT and 3-point bending, the other for paraffin embedding). *Mdx:utr* mice were not used for BMAT quantification as this colony of mice had been closed down after the decision had been made not to use them for the later interventional studies within this project. Bones were decalcified and scanned for marrow volume, then stained with osmium and rescanned to assess BMAT volume, as described in Section 2.4.14. Layers of 5 tibiae were arranged in parallel in 1% agarose in a 30ml universal and scanned together to minimise the scan time required. Any bones which ruptured during embedding or scanning were excluded from analysis due to possible loss of BMAT. This left 5 bones from WT and *mdx* mice and 6 from *mdx:cmah* mice that were suitable for analysis.

4.4.6 PCR Osteogenesis pathway array – transcriptomic analysis

RNA was extracted from the right humerus of mice culled at 7 weeks-of-age, as described in Section 2.5.1 and then reverse transcribed (Section 2.5.2). The cDNA was used for the real-time RT^2 profiler PCR osteogenesis pathway array and mean threshold cycle values (C_T) were calculated. The fold changes in gene expression were commuted relative to a housekeeping gene (*Gapdh*) using the ΔΔCT method (section 2.5.3). A cut off for fold regulation of 2 and p-value of 0.05 were used throughout.

4.4.7 Immunohistochemistry

Selected findings from the transcriptomic analysis (Section 4.4.6) were validated using a standard indirect IHC procedure to detect IGF-1 and MMP-10 protein expression in the GP and metaphyseal bone of tibiae from 7-week-old mice as described in Section 2.4.9. After the images were captured using Fiji, the haematoxylin-DAB colour deconvolution plugin was used to separate the haematoxylin and DAB components and the 'analyse-measure' tool used to determine the absorbance in a consistent region of each sample, containing both GP and metaphyseal bone. Optical density (OD) was then calculated using the equation:

OD= negative (base10)log of mean intensity of transmitted image/illumination (max intensity of image)

Maximum intensity was taken to be 255 for 8-bit images in Fiji (Ruifrok *et al.* 2001).

4.4.8 Assessment of alkaline phosphatase activity in MSC-derived culture

Both femurs were dissected from an *mdx:cmah* and corresponding WT mouse at 7 weeks-of-age. The oldest mice were chosen in order for the femurs to contain sufficient bone marrow for extraction. From experience during RNA extraction, the younger mice had very limited volumes of bone marrow and it was felt likely that this would be insufficient to enable isolation of bone marrow stromal cells (MSC). MSCs were isolated as described in Section 2.6.1 and cultured. After 3 weeks culture in osteogenic differentiation, measurement of alkaline phosphatase (ALP) activity was performed. The plates were scanned and the images digitised. Using Fiji, the % of ALP +ve area and number of ALP +ve particles was calculated for each well of every plate and then a mean calculated for the *mdx:cmah* mice and compared to WT mice.

4.5 Results

4.5.1 Trabecular bone parameters assessed by μCT

Overall there were no consistent trends seen by genotype during the μCT analysis of trabecular bone. A small reduction in trabecular tissue volume was seen in the *mdx*:*cmah* mice compared to WT mice at both 3 ($p<0.001$) and 7 weeks-of-age ($p<0.001$), see Table 4-1. However, as bone volume did not vary significantly between groups at any age examined, the overall % bone volume/tissue volume remained similar between groups at all ages (Table 4-1 and Figure 4-1). There were no consistent changes in trabecular number, thickness or separation by genotype.

Connectivity is a 3-dimensional measure of the number of inter-trabecular connections, normalised by tissue volume (Odgaard *et al.* 1993). It was significantly lower in *mdx*:*utr* mice at 5 weeks and *mdx*:*cmah* mice at both 5 and 7 weeks-of-age when compared to WT mice (Table 4-1).

Structural model index (SMI) is an estimation of the plates and rod characteristic of trabecular bone and a suggestion of the shape of the trabeculae and therefore of its ability to provide mechanical support. An SMI of zero would represent a plate whereas one of 3 would show a perfect cylinder. SMI was broadly similar by genotype, it was only lower in the *mdx*:*utr* mice at 3 weeks-of-age compared to WT ($p<0.05$).

There were no signficiant differences between the length-adjusted and unadjusted values (see Appendix V for adjusted data).

4.5.2 Cortical bone parameters assessed by μCT

Few structural changes were observed in the cortical bone of the muscular dystrophy mice compared to WT mice (Figure 4-2 and Table 4-3). TMD was higher in *mdx*:*cmah* mice at 3 and 7 weeks-of-age ($p<0.05$ and <0.01, respectively) and in *mdx*:*utr* mice at 5 weeks-of-age ($p<0.01$) when compared to WT mice (Table 4-2).

Cortical bone area and cortical bone fraction were significantly lower in 3-week-old *mdx:cmah* mice compared to WT mice; this is shown in the representative images in

Figure 4-3(i). This trend was reversed, however, by 5 and 7 weeks-of-age, where cortical bone fraction was significantly greater in all of the muscular dystrophy models ($p<0.05$ for all) compared to WT mice, see Figure 4-2(C) and (D), although the actual difference was small (62.0% WT vs 64-65.0% in muscular dystrophy models).

There was no significant difference between cortical bone parameters that were adjusted for tibia length at 3 weeks-of-age and the unadjusted data, (see Appendix V for adjusted data).

Figure 4-3 shows that the cortices in all groups looked immature at 3 weeks-of-age and were less uniform than at 5 and 7 weeks-of-age. This is consistent with the marked increase in cortical bone fraction seen in older mice (Figure 4-2 (D)).

4.5.3 Biomechanical properties assessed by 3-point bending

After μCT, bones were subjected to the 3-point bending test to assess the biomechanical properties of the bone. As expected, the overall trend was that maximum load, deflection at maximum load and stiffness increased with age (Table 4-4). Consistent with the small structural changes observed in the trabecular and cortical compartments, there were no significant differences in the biomechanical properties of WT and muscular dystrophy model bones, except for a small reduction in deflection at maximum load at 5 weeks seen in *mdx:cmah* mice compared to *WT* mice. This trend was also seen at 3 and 7 weeks-of-age but did not reach statistical significance.

Results for work to maximum load, load at rupture and deflection at rupture are not shown but also display the same trend by age and genotype.

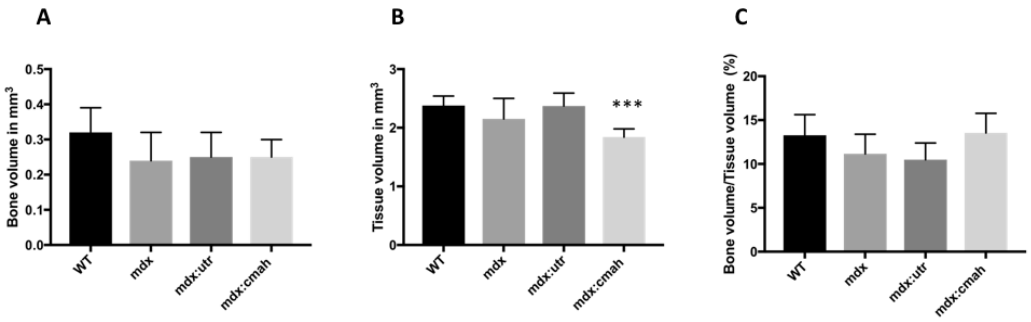

Figure 4-1. Trabecular bone parameters assessed by μCT in mice culled at 7 weeks-of-age. n=6 in each group except for *mdx:utr* at 5 weeks where n=5.

A and C) show that bone volume and % bone volume/ tissue volume were similar between groups despite

B) show that *mdx:cmah* mice have a smaller trabecular tissue volume.

Data are presented as mean (+/- standard deviation), *** denotes $p<0.001$ when compared to WT mice.

Mouse type	3 weeks at cull	5 weeks at cull	7 weeks at cull
Tissue volume, in mm^3 (SD)			
WT	1.48 (0.27)	1.91 (0.36)	2.38 (0.16)
mdx	1.24 (0.09)	1.90 (0.15)	2.15 (0.35)
mdx:u*tr*	1.17 (0.09)	1.79 (0.27)	2.37 (0.22)
mdx:c*mah*	1.03 (0.22) ***	1.54 (0.19)	1.84 (0.14) ***
Bone volume, in mm^3 (SD)			
WT	0.11 (0.03)	0.19 (0.05)	0.32 (0.07)
mdx	0.08 (0.02)	0.16 (0.04)	0.24 (0.08)
mdx:u*tr*	0.08 (0.01)	0.14 (0.04)	0.25 (0.07)
mdx: c*mah*	0.08 (0.02)	0.16 (0.03)	0.25 (0.05)
BV/TV % (SD)			
WT	6.78 (0.79)	9.71 (1.61)	13.28 (2.34)
mdx	6.55 (1.17)	8.36 (1.55)	11.16 (2.23)
mdx:u*tr*	6.82 (1.10)	7.83 (1.32)	10.49 (1.90)
mdx: c*mah*	8.30 (1.15)	10.36 (1.88)	13.54 (2.24)
Trabecular thickness, in mm (SD)			
WT	0.03 (0.003)	0.04 (0.003)	0.04 (0.001)
mdx	0.03 (0.002)	0.04 (0.001)	0.04 (0.002)
mdx:u*tr*	0.03 (0.002)	0.04 (0.002)	0.04 (0.001)
mdx: c*mah*	0.03 (0.001)	0.04 (0.002)	0.05 (0.003) *
Trabecular separation, in mm (SD)			
WT	0.30 (0.05)	0.24 (0.05)	0.18 (0.02)
mdx	0.37 (0.07)	0.26 (0.04)	0.21 (0.02)
mdx:u*tr*	0.36 (0.03)	0.30 (0.06)	0.20 (0.02)
mdx: c*mah*	0.29 (0.46)	0.23 (0.02)	0.19 (0.01)
Trabecular number, in 1/mm (SD)			
WT	2.04 (0.15)	2.64 (0.43)	3.10 (0.43)
mdx	2.08 (0.42)	2.17 (0.39)	2.67 (0.44)
mdx:u*tr*	2.06 (0.38)	1.96 (0.29) *	2.62 (0.45)
mdx: c*mah*	2.66 (0.45) *	2.54 (0.35)	2.96 (0.41)
Structural Model Index (SD)			
WT	2.32 (0.08)	2.19 (0.10)	2.14 (0.10)
mdx	2.20 (0.10)	2.31 (0.11)	2.18 (0.07)
mdx:u*tr*	2.15 (0.10) *	2.31 (0.06)	2.21 (0.14)
mdx: c*mah*	2.19 (0.09)	2.15 (0.13)	2.07 (0.19)
Connectivity (SD)			
WT	618.9 (121.4)	867.3 (221.4)	1042.6 (195.2)
mdx	516.5 (147.2)	702.6 (136.8)	818.1 (207.2)
mdx:u*tr*	429.6 (108.8)	554.4 (78.1) *	897.5 (177.2)
mdx: *mah*	561.8 (72.5)	527.5 (107.8) **	723.3 (85.0)***

Table 4-1 Trabecular parameters assessed by µCT. Data are presented as mean (+/- standard deviation), * denotes $p<0.05$, ** $p<0.01$, *** $p<0.001$ when compared to WT mice. n=6 in each group except for *mdx:utr* at 5 weeks where n=5.

Mouse type	Tissue mineral density in g/cm^3 (SD)		
	3 weeks at cull	**5 weeks at cull**	**7 weeks at cull**
WT	1.04 (0.04)	1.14 (0.12)	1.19 (0.08)
Mdx	1.02 (0.09)	1.16 (0.10)	1.25 (0.18)
Mdx:*Utr*	1.13 (0.18)	1.38 (0.02) **	1.15 (0.03)
Mdx: *Cmah*	1.19 (0.04) *	1.24 (0.03)	1.32 (0.05) **

Table 4-2 Tissue mineral density assessed by µCT. Data are presented as mean (+/- standard deviation), * denotes $p<0.05$, ** $p<0.01$ compared to WT mice. n=6 in each group except for *mdx:utr* at 5 weeks where n=5.

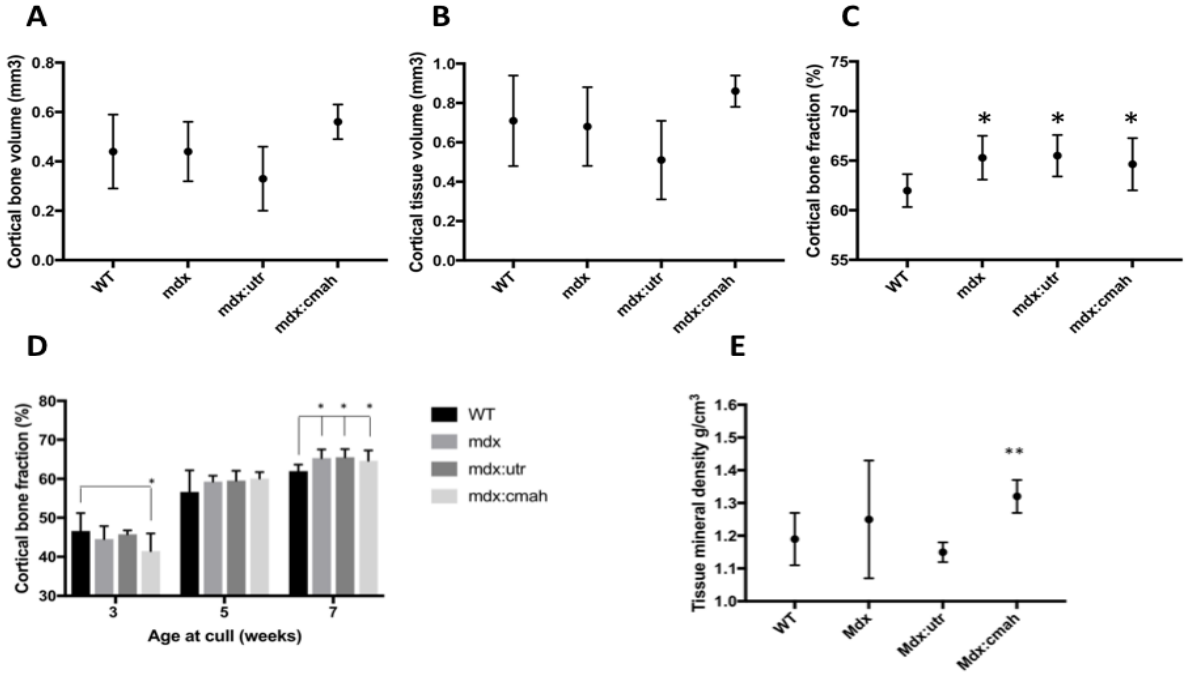

Figure 4-2 Cortical parameters assessed by μCT. n=6 in each group except for *mdx:utr* at 5 weeks where n=5. **A, B and C)** show cortical bone and tissue volume at 7 weeks-of-age. There was no significant change in **(A)** cortical bone or **(B)** cortical tissue volume, but in combination, there was a significantly higher cortical bone fraction **(C)** in all muscular dystrophy models. **D)** shows an increase in cortical bone fraction with age in all mouse models. **E)** Tissue mineral density was higher in *mdx*:*cmah* mice at 7 weeks-of-age ($p<0.01$) when compared to WT mice. Data are presented as mean (+/- standard deviation), * denotes $p<0.05$, ** $p<0.01$ compared to WT mice.

Mouse type	3 weeks at cull	5 weeks at cull	7 weeks at cull
Cortical tissue area, mm^2 (SD)			
WT	0.62 (0.09)	0.71 (0.08)	0.94 (0.06)
mdx	0.56 (0.05)	0.81 (0.07)	0.92 (0.10)
mdx:u*tr*	0.54 (0.06)	0.81 (0.05)	0.97 (0.08)
mdx:c*mah*	0.54 (0.07)	0.76 (0.06)	0.96 (0.08)
Cortical bone area, mm^2 (SD)			
WT	0.29 (0.07)	0.41 (0.07)	0.58 (0.07)
mdx	0.25 (0.03)	0.48 (0.05)	0.60 (0.07)
mdx:u*tr*	0.25 (0.03)	0.49 (0.02)	0.63 (0.05)
mdx:c*mah*	0.22 (0.03) *	0.46 (0.05)	0.62 (0.07)
Periosteal perimeter, in mm (SD)			
WT	3.01 (0.22)	3.16 (0.21)	3.74 (0.11)
mdx	2.85 (0.13)	3.42 (0.16)	3.69 (0.22)
mdx:u*tr*	2.81 (0.18)	3.45 (0.10)	3.80 (0.16)
mdx:c*mah*	2.78 (0.20)	3.38 (0.19)	3.78 (0.17)
Endosteal perimeter, in mm (SD)			
WT	2.20 (0.11)	2.09 (0.09)	2.33 (0.09)
mdx	2.19 (0.11)	2.21 (0.09)	2.21 (0.17)
mdx:u*tr*	2.08 (0.09)	2.19 (0.12)	2.23 (0.12)
mdx:c*mah*	2.15 (0.19)	2.09 (0.09)	2.22 (0.07)
Cortical tissue volume, in mm^3 (SD)			
WT	0.45 (0.20)	0.59 (0.14)	0.71 (0.23)
mdx	0.34 (0.16)	0.72 (0.06)	0.68 (0.20)
mdx:u*tr*	0.45 (0.14)	0.73 (0.05)	0.51 (0.20)
mdx:c*mah*	0.48 (0.06)	0.69 (0.06)	0.86 (0.08)
Cortical bone volume, in mm^3 (SD)			
WT	0.22 (0.11)	0.34 (0.09)	0.44 (0.15)
mdx	0.15 (0.07)	0.43 (0.04)	0.44 (0.12)
mdx:u*tr*	0.20 (0.06)	0.44 (0.02)	0.33 (0.13)
mdx:c*mah*	0.20 (0.03)	0.41 (0.04)	0.56 (0.07)
Cortical bone fraction (%) (SD)			
WT	46.62 (4.55)	56.63 (5.57)	61.98 (1.66)
mdx	44.56 (3.30)	59.31 (1.51)	65.30 (2.20) *
mdx:u*tr*	45.76 (1.02))	59.56 (2.50)	65.50 (2.09) *
mdx:c*mah*	41.46 (4.50) *	60.10 (1.61)	64.64 (2.64) *
Cortical thickness, in mm (SD)			
WT	0.50 (0.08)	0.52 (0.06)	0.51 (0.08)
mdx	0.46 (0.08)	0.55 (0.02)	0.49 (0.07)
mdx:u*tr*	0.48 (0.07)	0.55 (0.03)	0.43 (0.06)
mdx:c*mah*	0.54 (0.04)	0.54 (0.02)	0.55 (0.02)
Mean polar moment of inertia, in mm^4 (SD)			
WT	0.05 (0.02)	0.06 (0.02)	0.12 (0.02)
mdx	0.04 (0.01)	0.09 (0.01)	0.12 (0.03)
mdx:u*tr*	0.03 (0.01)	0.09 (0.01)	0.14 (0.02)
mdx:c*mah*	0.03 (0.01)	0.08 (0.01)	0.13 (0.03)
Mean eccentricity (SD)			
WT	0.57 (0.10)	0.55 (0.15)	0.52 (0.09)
mdx	0.47 (0.11)	0.60 (0.07)	0.59 (0.11)
mdx:u*tr*	0.61 (0.10)	0.63 (0.03)	0.56 (0.07)
mdx:c*mah*	0.58 (0.10)	0.53 (0.06)	0.57 (0.11)

Table 4-3 μCT of cortical bone parameters. * denotes $p<0.05$ compared to WT mice. n=6 in each group except for *mdx:utr* at 5 weeks where n=5.

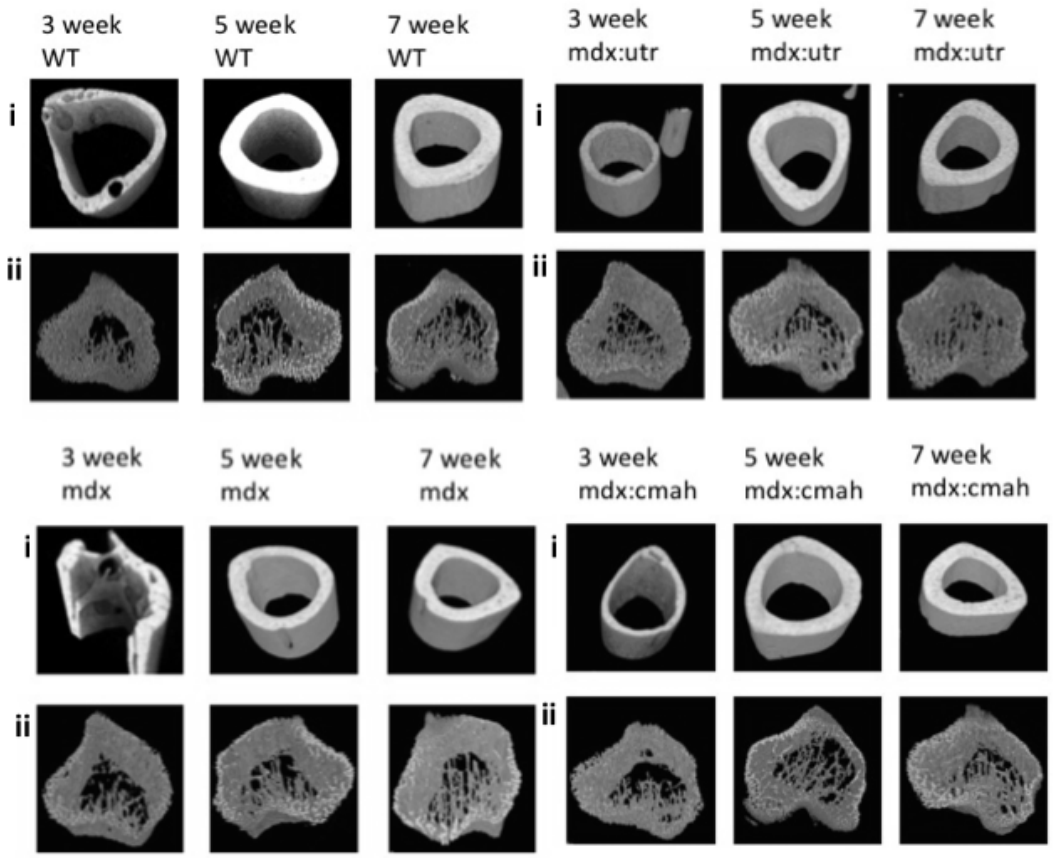

Figure 4-3 Representative μCT images of tibiae from all genotypes at 3, 5 and 7 weeks-of-age to show bone development and increased homogeneity and bone fraction with age (n=6 in each group except for *mdx:utr* at 5 weeks where n=5):

(i) upper rows show mid diaphysial cortical bone

(ii) lower rows show metaphyseal trabecular bone

4.5.4 Assessment of bone turnover markers by ELISA

In all genotypes, serum levels of both P1NP (bone formation marker) and αCTX (bone resorption marker) were lower in the older mice (co-eff -6.29, p=0.009 and co-eff -2.55, p=0.000 respectively in a linear regression model, using age as the dependent variable). This is consistent with the marked reduction in bone modelling seen after puberty, which was demonstrated in Figure 3-7. There was no significant difference in P1NP values by genotype at either age (Table 4-5). However, αCTX levels were significantly higher in serum from 3-5 week-old *mdx:cmah* mice (p=0.002), whereas serum samples from mice taken at 8 weeks-of-age were similar in all genotypes.

4.5.5 Static histomorphometry

There were no significant differences in either osteoclast or osteoblast number/ bone surface by genotype (Figure 4-4).

4.5.6 Bone marrow adipose tissue (BMAT) quantification by μCT

Individual images of bones from mice scanned at 7 weeks-of age show the distribution of BMAT within the marrow cavity of WT**,** *mdx* and *mdx:cmah* mice (Figure 4-5, A-C). There was no overall difference in the proportion of total MAT within the marrow cavity by genotype (Figure 4-5, E). There was, however, a significant increase in rMAT in both muscular dystrophy models assessed (*mdx* and *mdx:cmah*) compared to WT mice, (Figure 4-5, F), and a reduction in the proportion of cMAT compared to that in WT mice (Figure 4-5, G). The data are summarised in Table 4-6.

4.5.7 PCR Osteogenesis pathway array – transcriptomic analysis

In diaphyseal bone from 7 week-old-mice, PCR array revealed between 2 and 3.75 fold upregulation in the expression of *Mmp-10* and *BMP receptor type 1b* (*Bmpr1b*) genes in all muscular dystrophy models compared to WT mice (Table 4-7). In addition, in the *mdx:cmah* mice, there was increased expression of many growth factors compared to WT mice. In particular, there was increased expression of *Igf-1* (30-fold), *Igf1R* (10-fold) and vascular endothelial growth factor A (*Vegfα;* 32-fold), see Table 4-7.

Mouse type	3 weeks at cull	5 weeks at cull	7 weeks at cull
	Maximum load, in N (SD)		
WT	3.16 (1.68)	7.42 (3.11)	6.87 (4.57)
mdx	5.33 (8.12)	5.16 (0.80)	9.30 (2.94)
mdx:utr	3.69 (3.76)	4.49 (0.55)	10.62 (3.01)
mdx:cmah	1.77 (0.37)	4.47 (1.17)	7.10 (0.92)
	Deflection at max load, in mm (SD)		
WT	1.21 (0.15)	1.58 (0.66)	1.07 (0.58)
mdx	1.92 (1.36)	1.07 (0.51)	1.31 (0.58)
mdx:utr	1.14 (0.37)	1.19 (0.06)	1.61 (0.70)
mdx:cmah	0.69 (0.31)	0.72 (0.26) *	0.74 (0.28)
	Stiffness, in Nmm (SD)		
WT	19.24 (16.6)	33.41 (28.41)	37.27 (3.44)
mdx	11.27 (12.6)	17.11 (5.21)	25.69 (14.18)
mdx:utr	14.84 (14.3)	11.39 (3.21)	25.59 (15.25)
mdx:cmah	9.09 (5.92)	17.20 (6.87)	19.46 (4.65)

Table 4-4 Biomechanical properties assessed by 3-point bending.
Data are presented as mean (+/- standard deviation), * denotes $p<0.05$ compared to WT mice. n=6 in each group except for *mdx:utr* at 5 weeks where n=5.

Mouse type	P1NP (pg/ml) 3-5 weeks	P1NP (pg/ml) 8 weeks	αCTx (pg/ml) 3-5 weeks	αCTx (pg/ml) 8 weeks
WT	394.84 (151.22)	209.87 (60.03)	181.70 (78.51)	102.52 (86.56)
mdx	642.85 (92.10)	316.67 (134.48)	178.42 (69.30)	132.38 (52.38)
mdx:utr	487.58 (241.93)	Not done	181.60 (55.74)	Not done
mdx:cmah	384.21 (57.76)	169.12 (89.58)	406.36 (46.51)**	145.41 (96.95)

Table 4-5 Bone turnover markers by genotype. Data are presented as mean (+/- standard deviation), ** denotes $p<0.01$ compared to WT mice. n=6 in each group except for *mdx:utr* at 5 weeks where n=5.

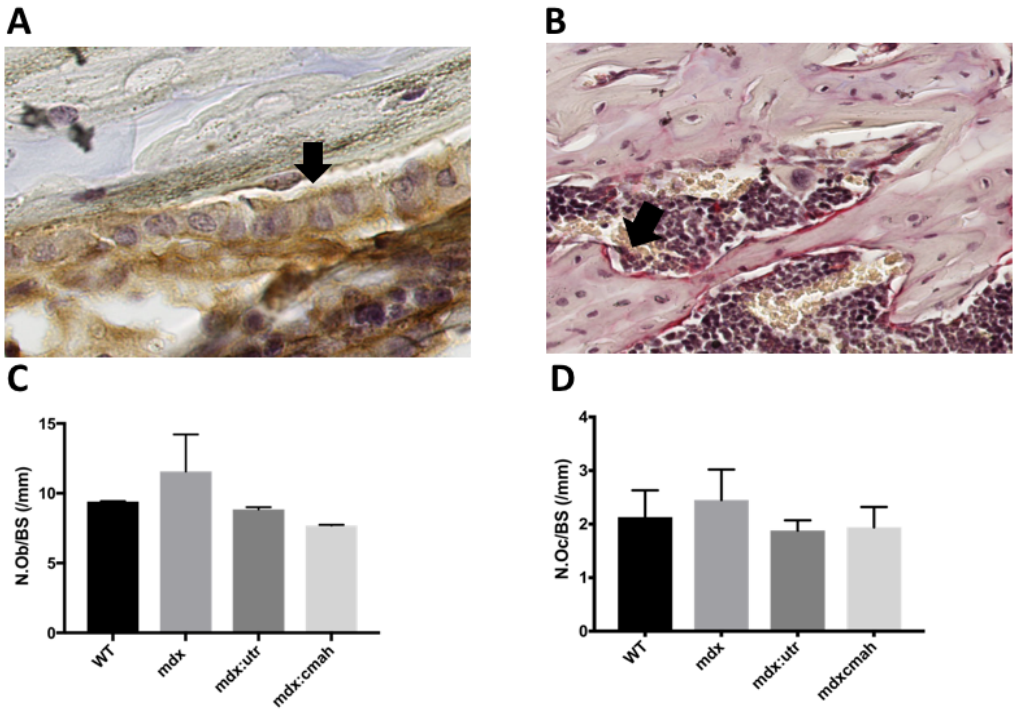

Figure 4-4 Histomorphometric analysis of osteoclast and osteoblast number in muscular dystrophy mouse models culled at 5 weeks-of-age. n=6 in each group except for *mdx:utr* at 5 weeks where n=5.

- **A)** Representative TNAP activity within cuboidal shaped osteoblasts (arrow) on trabecular bone surface of the proximal tibia metaphysis of 5-week-old *mdx* mouse.
- **B)** Representative TRAP activity (arrow) and fast-red stained image of trabecular bone from proximal tibia metaphysis of 5-week-old *mdx* mouse.
- **C)** Quantification of osteoblast number/bone surface by genotype at 5 weeks-of-age
- **D)** Quantification of osteoclast number/bone surface by genotype at 5 weeks-of-age

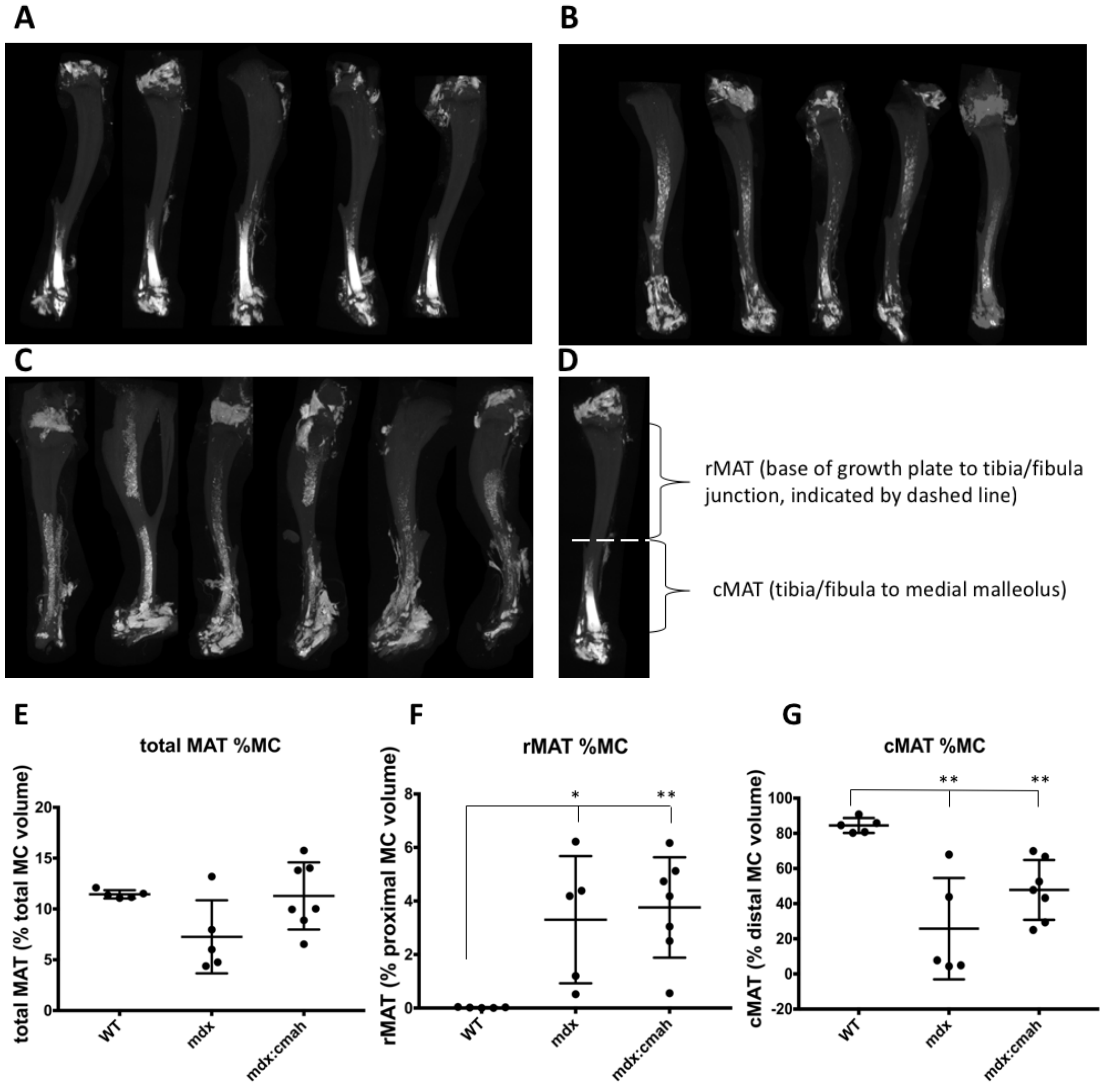

Figure 4-5 Three-dimensional μCT reconstructions of 7-week-old osmium-stained tibiae from: **A)** WT (n=5) **B)** *mdx (n=5)*, **C)** *mdx:cmah* (n=6) mice. Bone appears grey, MAT is white. **D)** highlights the MAT regions; regulated marrow adipose tissue (rMAT) which lies proximal to tibia/fibula junction and constitutive MAT (cMAT) which lies distal to tib-fib junction (dashed line). Marrow cavity volume was determined by μCT prior to osmium staining and then rMAT, cMAT and total MAT were calculated as a % of marrow cavity (MC) volume of corresponding region. Figures E-G show individual data and mean (+/- standard deviation) **E)** There were no overall differences in the % total MAT by genotype. **F)** shows an increase in % rMAT in *mdx* and *mdx:cmah* mice compared to WT mice **G)** shows a reduction in % cMAT in *mdx* and *mdx:cmah* mice compared to WT mice. * denotes $p<0.05$, **$p<0.01$ compared to WT mice.

Genotype	rMAT % (SD)	cMAT % (SD)	Total MAT % (SD)
WT	0.02 (0.015)	84.47 (4.25)	11.44 (0.41)
mdx	3.30* (2.34)	25.74** (28.82)	7.26 (3.60)
mdx:cmah	3.76** (1.88)	47.80** (17.06)	11.28 (3.30)

Table 4-6 Proportion of MAT occupying marrow cavity (%), by genotype and region of bone studied. Data are presented as mean (+/- standard deviation), * denotes $p<0.05$, ** $p<0.01$ compared to WT mice. n=5 in WT and *mdx* groups and n=6 in *mdx:cmah*.
rMAT: regulated marrow adipose tissue, cMAT: constitutive marrow adipose tissue.

4.5.8 Immunohistochemistry

Selected findings from the transcriptomic gene profiling were validated using IHC to confirm the presence of IGF-1, BMPR1b and MMP-10 protein in paraffin-embedded tibiae sections. MMP-10 and BMPR1b were chosen as they were found to be upregulated in all muscular dystrophy mouse models. IGF-1 was chosen because it is an essential factor in the regulation of post-natal growth, was planned for use as an interventional agent in Chapter 6 and showed a marked upregulation of expression in the bone of *mdx:cmah* mice compared to WT mice.

Despite using serial dilutions of primary antibody it was not possible to generate robust positive staining compared to control sections (no primary antibody) using the BMPR1b antibody (data not shown). MMP-10 was localised to the GP chondrocytes and cells of the metaphysis in all sections examined and no genotype-specific differences in staining distribution or intensity were noted (Figure 4-6).

IGF-1 was localised throughout all maturation zones of the GP and cells of the metaphysis. In the GP of *mdx:cmah* mice more chondrocytes were positively stained for IGF-1 (Figure 4-7, A) compared to the WT GP where some individual chondrocytes and columns of chondrocytes did not stain at all (Figure 4-7, B). Also the intensity of the staining was much stronger in chondrocytes of the *mdx:cmah* GP compared to the control GP. These findings are in keeping with the results in section 4.5.7. Quantification of staining intensity confirmed this greater IGF-1 expression; optical density was significantly greater in both the GP and metaphysis in the sections from *mdx:cmah* mice compared to WT mice (Table 4-8). The intensity of stain in sections from *mdx* and *mdx:utr* mice was not significantly different from sections from WT mice (Table 4-8).

4.5.9 Assessment of alkaline phosphatase activity in MSC-derived culture

After 3 weeks (in culture conditions favouring osteogenic differentiation) there were no differences in the overall proportion of ALP +ve areas or number of ALP +ve particles in the MSCs isolated from *mdx:cmah* mice compared to WT mice (see Figure 4-8 and Table 4-9).

***mdx* compared to WT**	**Fold regulation**	**p-value**
Bone morphogenetic protein receptor (Bmpr1b)	2.69	0.041712
Matrix metallopeptidase 10 (Mmp10)	2.03	0.000014
***mdx:utr* compared to WT**	**Fold regulation**	**p-value**
Bone morphogenetic protein 6 (Bmp6)	3.6	0.007723
Bone morphogenetic protein receptor (Bmpr1b)	2.29	0.000014
Fibroblast growth factor 2 (Fgf2)	3.16	0.040671
Integrin alpha M (Itgam)	11.04	0.041707
Matrix metallopeptidase 10 (Mmp10)	2.39	0.000000
Noggin (Nog)	3.56	0.005635
Tumour necrosis factor (Tnf)	2.38	0.000923
***mdx:cmah* compared to WT**	**Fold regulation**	**p-value**
Alpha-2-HS-glycoprotein (Ahsg)	3.51	0.038127
Bone morphogenetic protein 2 (Bmp2)	3.24	0.024496
Bone morphogenetic protein receptor (Bmpr1b)	3.63	0.000001
Colony stimulating factor 3, granulocyte (Csf3)	4.05	0.000000
Epidermal growth factor (Egf)	4.68	0.045871
Intercellular adhesion molecule 1 (Icam1)	6.18	0.011895
Insulin-like growth factor 1 (Igf1)	30.58 (A)	0.012304
Insulin-like growth factor 1 receptor (Igf1r)	9.98	0.047431
Indian hedgehog (Ihh)	4.08	0.000000
Integrin alpha 2b (Itga2b)	4.19	0.024383
Integrin alpha 3 (Itga3)	4.85	0.003215
Matrix metallopeptidase 10 (Mmp10)	3.75	0.000000
Matrix metallopeptidase 8 (Mmp8)	7.64	0.005422
Noggin (Nog)	5.69	0.000823
SRY-box containing gene 9 (Sox9)	6.18	0.015479
Tumour necrosis factor (Tnf)	4.11	0.011907
Vascular cell adhesion molecule 1 (Vcam1)	4.03	0.023302
Vascular endothelial growth factor A (Vegfa)	32.39 (A)	0.001731
Vascular endothelial growth factor B Vegfb	7.82	0.037848
Common to all muscular dystrophy models	**Fold regulation**	
Bone morphogenetic protein receptor (Bmpr1b)	2.29-3.63	
Matrix metallopeptidase 10 (Mmp10)	2.03-3.75	

Table 4-7 Transcriptomic results from the osteogenesis gene array.
(A) Denotes that the gene's average threshold cycle is relatively high (>30) in either the control or the test sample and is reasonably low in the other sample (<30), suggesting that the actual fold-change value is at least as large as the calculated and reported fold-change result. n=6 in each group except for *mdx:utr* at 5 weeks where n=5.

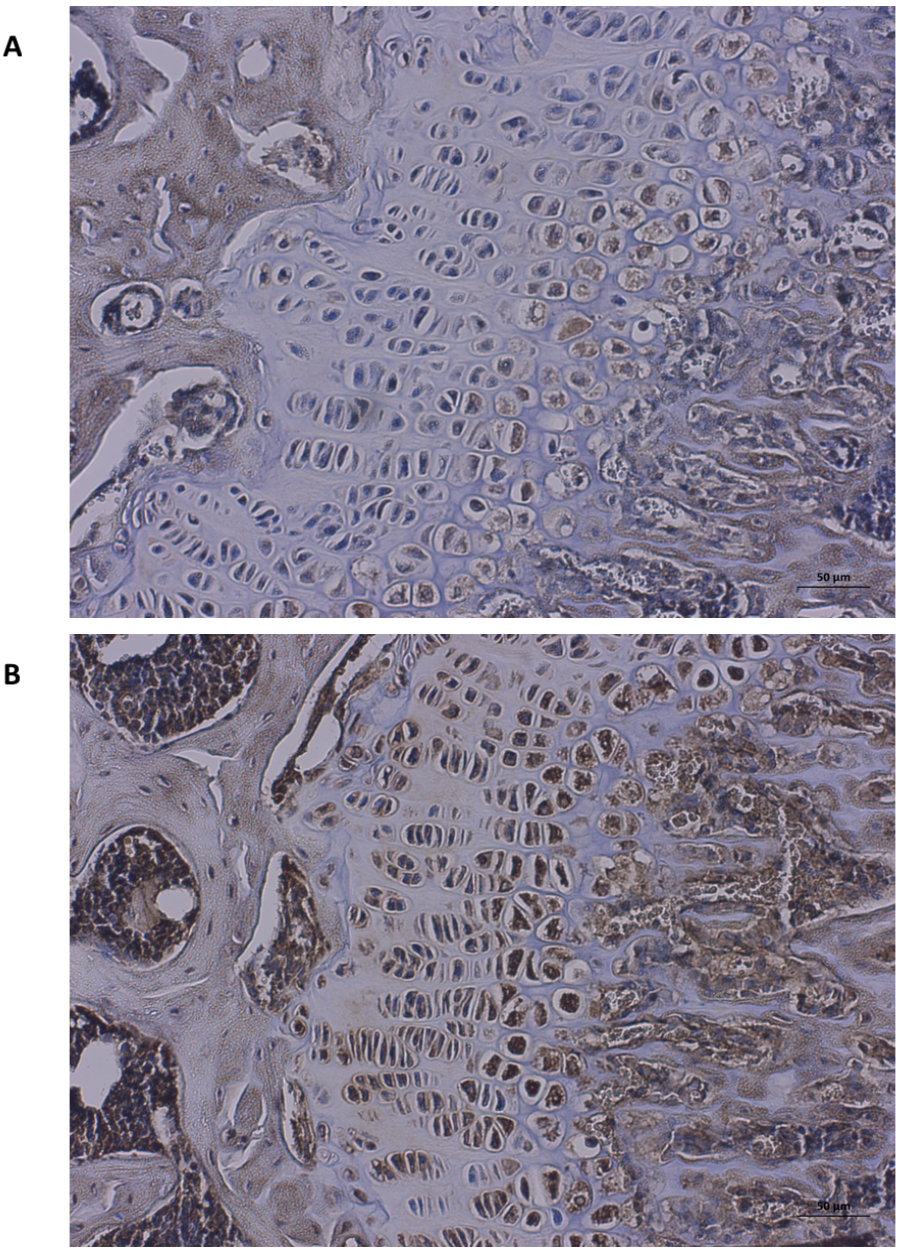

Figure 4-6 (A) Non-specific staining was minimal in control sections in which the primary antibody was omitted. **(B)** MMP-10 (1:100 dilution of primary antibody) was localised to the chondrocytes in the GP and to metaphyseal bone of a 7-week-old *mdx* mouse.

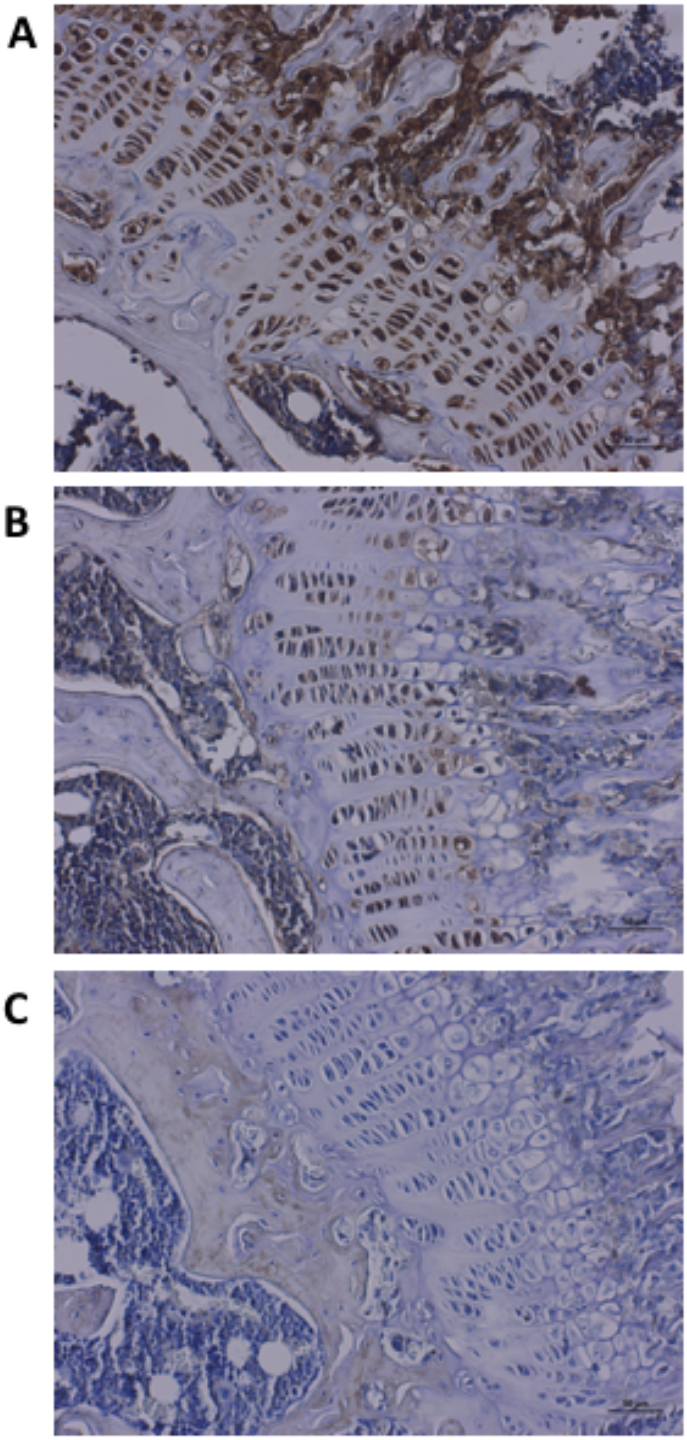

Figure 4-7 IGF-1 (1:500 dilution of primary antibody) was localised to the chondrocytes in the GP and to metaphyseal bone of a 7-week-old **(A)** *mdx:cmah* and **(B)** WT mouse. **(C)** Non-specific staining was minimal in control sections in which the primary antibody was omitted.

Mouse type	Optical density GP (SD)	Optical density metaphysis (SD)
WT	0.100 (0.086)	0.084 (0.090)
mdx	0.104 (0.037)	0.042 (0.035)
mdx*:*utr	0.186 (0.025)	0.092 (0.040)
mdx*:*cmah	0.241 (0.035)*	0.224 (0.022)**

Table 4-8 Comparison of optical density of IGF-I staining in the GP and metaphysis of the tibiae between WT mice and muscular dystrophy mouse models.
Data are presented as mean (+/- standard deviation), * denotes $p<0.05$, ** denotes $p<0.001$ compared to WT mice.

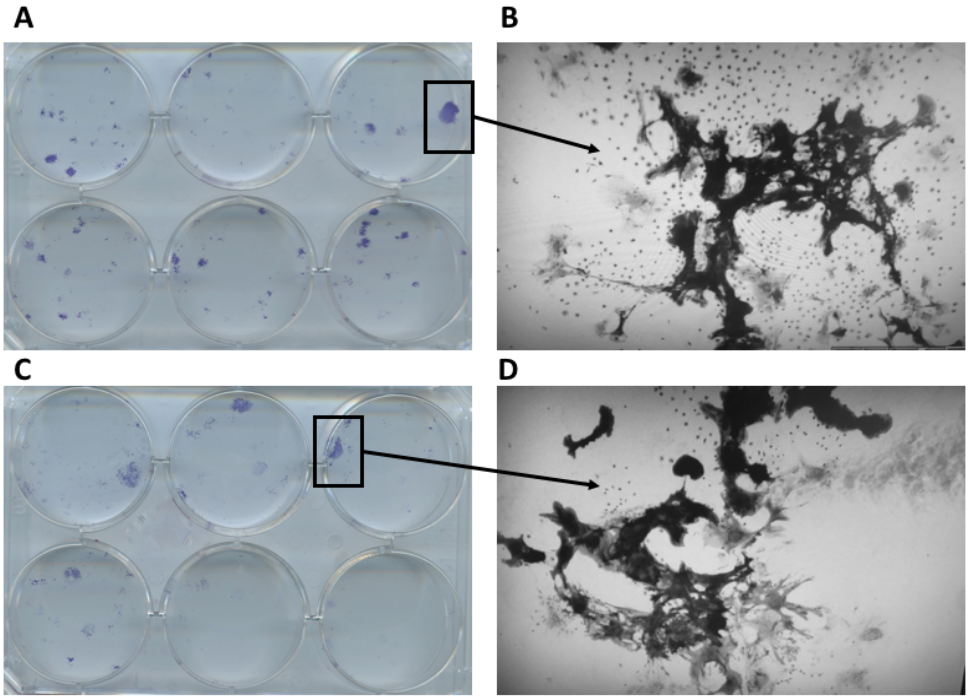

Figure 4-8 MSC colonies that were ALP+ve after culture for 3 weeks in osteogenic medium. Examples of:

- **A)** 6-well plate from MSC colony cultured from femur of WT mouse.
- **B)** Inset-magnified and thresholded image to show area analysed for % of ALP+ve area and number of ALP+ve particles in MSC colony cultured from femur of WT mouse.
- **C)** 6-well plate from MSC colony cultured from femur of *mdx:cmah* mouse.
- **D)** Inset- magnified and thresholded image to show area analysed for % of ALP+ve area and number of ALP+ve particles in MSC colony cultured from femur of *mdx:cmah* mouse.

Mouse type	Number of ALP+ve particles	Percentage of ALP+ve area
WT	2680 (607)	1.34 (0.59)
mdx:*cmah*	2567 (742)	1.45 (1.19)

Table 4-9 Quantification of ALP+ve area and particles in WT and *mdx:cmah* cultures. Data are presented as mean (+/- standard deviation).

4.6 Discussion

The results in this chapter do not support the hypothesis that *'bone development is impaired in all DMD models when compared to WT mice, and most severely in the mdx:cmah mouse model'.* Conversely, some evidence of increased bone turnover and bone formation were found in the muscular dystrophy mouse models, although these changes were not consistent and age and genotype-specific differences were noted. These will be discussed further below.

When considering the bone phenotype in *mdx* mice, a higher cortical bone fraction was demonstrated when compared to WT mice, but only at 7 weeks-of-age and no differences were disclosed in any other parameters obtained from μCT, biomechanical testing or in assessments of bone turnover markers. The increased cortical bone fraction may reflect the muscle-bone crosstalk and the potential for an adaptive bone response alongside the muscle regeneration in the *mdx mouse,* as discussed in Section 3.6. Published data regarding the bone phenotype in the *mdx* mouse are conflicting and unlike in patients with DMD where bone strength decreases with advancing age, the converse appears true in some studies of *mdx* mice. For example a longitudinal study demonstrated lower cortical parameters in *mdx* mice at both 4 and 12 weeks-of-age, with some evidence of recovery by 18 weeks (Anderson *et al.* 1993). This is in keeping with the period of acute muscle necrosis observed in *mdx* mice at 3-4 weeks-of-age followed by subsequent regeneration up until approximately 20 months of age, after which time the regenerative capacity reduces due to a gradual decline in muscle satellite cell number. One study demonstrated osteopenia and reduced strength in the femur of 3 week old *mdx* mice in the absence of muscle degeneration, thus suggesting primary skeletal fragility, whilst another attributed the reduced cortical thickness and lower mechanical resistance in the tibia of 4 week-old mice to muscle weakness resulting from intense muscle fibre necrosis (Anderson *et al.* 1993, Nakagaki *et al.* 2011). At 7 weeks-of-age, a further study found that *mdx* mice displayed compromised bone structure and function compared to WT mice (Novotny *et al.* 2011). By contrast, other studies have either shown no significant differences in any bone structural parameters (as assessed by μCT) between male *mdx* and *WT* mice at 6 weeks-of-age (Isaac *et al.* 2013) or a paradoxical increase in

femoral BMD (as assessed by DXA) in 16-week-old female *mdx* mice compared to WT mice (Montgomery *et al.* 2005).

During this study, no differences in trabecular or cortical bone architecture, bone turnover markers or biomechanical properties were observed in the *mdx:utr* mouse when compared to WT mice. Bone structural data was inconsistent and showed paradoxically that the TMD was higher in *mdx:utr* mice compared to WT mice, but only at 5 weeks-of-age, while the cortical bone fraction was also greater than that of WT mice, but only in those culled at 7 weeks-of-age. There appears to be only one publication reporting the bone phenotype in the *mdx:utr* mouse. This was part of a larger study, where it was noted that there was less collagen present in the metaphyseal bone of the *mdx:utr* mouse compared to *mdx* and WT mice, but this study did not extend to the analysis of trabecular and/or cortical bone in the *mdx:utr* or *mdx* mice under investigation (Isaac *et al.* 2013). It is therefore difficult to draw comparisons between this present study and that of Isaac and colleagues (Isaac *et al.* 2013).

Despite the hypothesis that the *mdx:cmah* mouse would have the most impaired skeletal development of all the muscular dystrophy models examined, results showed that the TMD of cortical bone was increased compared to WT mice at both 3 and 7 weeks-of-age and cortical bone fraction was also higher at 7 weeks-of-age. This may partly be due to muscle regeneration as described above in the *mdx* mouse, but as lower levels of regeneration were seen in the *mdx:cmah* mouse than in *mdx* and *mdx:utr* mice, it is likely that there are other factors responsible. For example, one study demonstrated that the *cmah* gene is upregulated in adult human stem cells, of both haematopoietic and mesenchymal origin. Overexpression of *cmah* causes accumulation of nuclear β-catenin (Nystedt *et al.* 2009) and associated restriction of Wnt signalling. Therefore it is possible that the absence of the *cmah* gene in the *mdx:cmah* mouse model may cause a reduction in nuclear β-catenin expression and unregulated Wnt signalling and thereby promote the osteoblast lineage and bone formation (Westendorf *et al.* 2004).

Further evidence of increased bone turnover in the young 3-5-week-old *mdx:cmah* mice was inferred by the significantly higher α-CTX levels compared to WT mice. Although the bone formation marker P1NP was not raised at this age, bone formation and bone resorption are intrinsically linked and therefore it is likely that the finding of increased bone resorption may be a suggestion of a higher bone turnover state but other indices of bone formation would be required before such an assertion could be made. This possible increased bone turnover rate in the young *mdx:cmah* mice mirrors the catch-up growth described in Chapter 3.

Additional evidence for the catch-up growth was found in the transcriptomic results from the osteogenesis PCR array panel. Upregulation of many growth factors was demonstrated in diaphyseal bone from the *mdx:cmah* mouse, including a 30-fold increase in *Igf-1* and *Vegf-*α gene expression compared to WT mice. The increase in *Igf-1* gene expression was also confirmed by IHC which revealed increased IGF-1 protein expression in the GP and metaphyseal bone of the *mdx:cmah* mouse compared to WT mice.

It was not possible to confirm the presence of BMPR1b in the GP and metaphyseal bone using IHC. There are many possible reasons for this. Firstly, the RNA was obtained from the diaphysis of the humerus, whilst the protein expression was carried out on sections from the proximal tibia therefore they are from different bone compartments and so not directly comparable. Secondly, the upregulation of gene expression does not necessarily infer an increase in protein production that could be detectable by IHC. There are many factors downstream of gene expression that could influence the ultimate levels of protein production. IHC was chosen over Western blotting as it would enable localisation of different protein levels within specific regions of the bone and GP which may have helped to elucidate the aetiology behind the catch up growth demonstrated in Chapter 3, or may have helped identify a cause of growth retardation had it been demonstrated. Nevertheless, the use of IHC to quantify antigen presence has limitations. For example IHC is not a stoichiometric technique and therefore the intensity of the resultant stain does not necessarily directly equate to the quantity of antigen present. It is also not possible to determine how much of the analyte was present prior to fixing and embedding. Therefore conditions were

standardised as much as possible in order to achieve the greatest level of reliability possible during quantitative scoring. Fixation and antigen retrieval were carried out using the same methodology throughout and all IHC for each antibody was performed on the same day under identical conditions, with control specimens also tested for each genotype. It is generally accepted that if these pre-requisites are followed that semi-quantitative analysis can be carried out (Taylor *et al.* 2006).

All of the muscular dystrophy mouse models that were analysed demonstrated an up-regulation in *Mmp-10* and *Bmpr1b* gene expression in cortical bone of the diaphysis when compared to the expression in WT mice. IHC validated the presence of MMP-10 protein in the GP and metaphyseal bone, but did not reveal any obvious increase in MMP-10 protein expression between genotypes. It may be that the 2-3 fold increase in gene expression was insufficient for a difference to be detected at the protein level. Matrix metalloproteases (MMPs) are members of a family of calcium-dependent proteinases which can cleave a wide range of extracellular proteins including components of the extracellular matrix. MMP10 is known to be involved in bone growth but has also been shown to be involved in tissue repair processes and specifically in muscular dystrophy mouse models (Ortega *et al.* 2004). Increased skeletal muscle MMP-10 protein expression occurs in response to the damaged, dystrophic muscle seen in the *mdx* mouse and is also likely to explain the upregulation of *Mmp-10* in bone seen in this study, as the bone-muscle unit is intrinsically interlinked (Veilleux *et al.* 2017). Growth factors of the transforming growth factor (TGFβ) family include bone morphogenetic proteins (BMPs) and they are recognised to have an important role in skeletal development (Chen *et al.* 2012). BMP signalling in particular has been shown to induce the expression and activity of genes necessary for osteoblast differentiation (Song *et al.* 2009). Overactive BMP signalling has also been implicated in the pathogenesis of DMD and recent studies have suggested an essential role of BMPs and also the type 1 receptor in regeneration after muscle damage, which is consistent with the upregulation of *Bmpr1b* expression seen in this study (Shi *et al.* 2013). Unfortunately it was not possible to confirm this increased expression at the protein level due to the inability to achieve robust and convincing immunolocalisation.

Assessment of BMAT revealed a significant increase in regulated BMAT (rMAT) in both *mdx* and *mdx:cmah* mice and a reduction in the constitutive BMAT (cMAT). The reason for this is unclear but several potential mechanisms are possible. Studies have shown that MAT is increased during caloric restriction (Devlin 2011, Cawthorn *et al.* 2014). This is probably a survival mechanism; BMAT secretes adipokines, which promote appetite and increase insulin sensitivity (Cawthorn *et al.* 2016). BMAT in mice develops from distal to proximal and highly defined cMAT occurs early in vertebrate development (Scheller *et al.* 2015). It is possible therefore that the increase in rMAT has occurred as a response to the increased metabolic demands on the muscular dystrophy mice. The role of dystrophin in the regulation of metabolism is poorly understood and is difficult to evaluate clinically as body composition in DMD is confounded by the long term use of high-dose GC. However, a recent study demonstrated that dystrophin deficiency in the *mdx* mouse resulted in reduced body fat (confirmed by DEXA body composition studies) and a consistently lower core body temperature, despite no overall bodyweight difference between *mdx* and WT mice (Strakova *et al.* 2018). Similar studies have shown increases in energy expenditure and muscle protein synthesis in *mdx* mice and an altered response to high fat diet compared to WT controls (Radley-Crabb *et al.* 2011, 2014). Studies examining serum lipid levels have shown no difference between *mdx* and WT mice (Milad *et al.* 2017) but there appears to be primary adipose progenitor cell expansion defects *in vitro* (Joseph *et al.* 2018). The increase in rMAT warrants further investigation and studies of MAT in older *mdx* mice would be useful, as rMAT accumulation from 12-56 weeks-of-age in mice has been shown to correlate negatively with trabecular number and positively with trabecular thickness in C57BL6 mice (Scheller *et al.* 2015). Logic dictates that accumulation of rMAT in the proximal tibia must occur at expense of either haematopoiesis or osteoblastogenesis and bone formation, since the size of the space within the skeleton is finite. Osteoporosis has been associated with a decrease in MAT unsaturation (Yeung *et al.* 2005) and bone marrow fat composition has been suggested as a useful biomarker in post- menopausal women with fragility fractures (Patsch *et al.* 2013). This may have a role in the evaluation of skeletal fragility in DMD.

Several of the bones that were analysed for MAT were found to have ruptured. The ruptures were unlikely to have occurred during life as all mice had their grip strength assessed within 24 hours of cull and a tibiae fracture would have been noticed at this time. Instead, the ruptures most likely occurred ex-vivo during decalcification, staining or scanning and have been previously reported as a potential confounder during MAT analysis (Wallace *et al.* 2016). Cortical bone ruptures can confound osmium based MAT detection as the rupture allows potential escape of the bone marrow and may result in decreased osmium staining compared to intact tibiae. Although the results showed that MAT volumes were not significantly lower in the ruptured bones, their data was excluded from analysis.

Figure 4-3 highlights the potential limitation of analysing bones of young mice. It is clear from the representative images that the cortices remain immature at 3 weeks-of age and it is possible that the ROI chosen may not represent the entirety of the diaphysis, for example if the bone is not fully mineralised in one of the ROIs scanned the overall TMD may appear erroneously lower. Similarly, the proximal tibia of young mice comprise only a limited proportion of trabecular bone (8-9% for the WT mice in this study, as reported in Chapter 4) which may consist of only a few trabecular profiles and therefore effectively result in inadequate power or sensitivity by which to determine any changes by genotype. Also, mice bred on the C57 genetic background strain are known to have lower cortical bone densities than other strains of mice (Beamer *et al.* 1996). If this study was to be repeated, a recommendation would be that mice are not scanned until they reach 5-weeks-of age, by which time the bone morphology becomes more homogenous.

In summary, none of the muscular dystrophy mouse models demonstrated consistent evidence of an intrinsic defect in skeletal development. In the next chapter, GC regimens were tested to find an appropriate regimen to best mimic the marked growth retardation and osteoporotic changes that are seen in patients with DMD.

CHAPTER 5

Finding the appropriate glucocorticoid regimen

5 Finding the appropriate GC regimen

5.1 Introduction

Glucocorticoids (GC) are the only intervention in DMD that are proven to stabilise muscle strength, including both cardiac and respiratory function. Their use is integral to the treatment of patients with DMD and form part of the Standards of Care; patients usually start high dose GC from about 5 years of age (Birnkrant *et al.* 2018). As discussed in Chapter 1, the long-term use of high dose GC are associated with many side-effects. Two of the most clinically significant and challenging to manage are GIO and growth retardation and an efficacious anabolic agent would greatly benefit this population. When trialling bone protective therapies in animal models, it is important that the agents are tested in muscular dystrophy animal models that are also being co-treated with GC, in order to make the results translationally relevant.

5.1.1 Mouse models of GC-induced growth retardation and GIO

Despite the extensive literature review (Wood *et al.* 2018), see appendix VI, it was still unclear which GC regimen would be most effective to simultaneously induce both GIO and growth retardation in juvenile mice. It was, therefore, necessary to test the most promising regimens for evidence of both GC-induced growth retardation and GIO, in order to find the most appropriate regimen to take forward into the later phases of the project. For the purpose of this project it was decided to trial both oral gavage (to mimic the delivery route in patients) and daily SC injections; the animal house staff had no prior experience of SC pellet administration (although the literature review suggested some success with these) and as IGF-1 was to be given via osmotic pump in the later study (Chapter 6) this option, which would involve the implantation of a second osmotic pump, was also not possible on animal welfare grounds. Starting doses of prednisolone and dexamethasone were chosen based on the literature review and then increased according to response.

5.1.2 VBP-6: a GC-sparing agent

Finding an alternative compound to traditional GC that has equivalent anti-inflammatory effects but a reduced side-effect profile could have huge clinical impact in DMD. Traditional GC have an 11-beta-hydroxy or an 11-keto group whereas a new class of compounds have been designed with a key conversion from the hydroxyl

group to a double bond between carbons 9 and 11, leading to a Δ9,11 C ring as the backbone (see Figure 5-1).

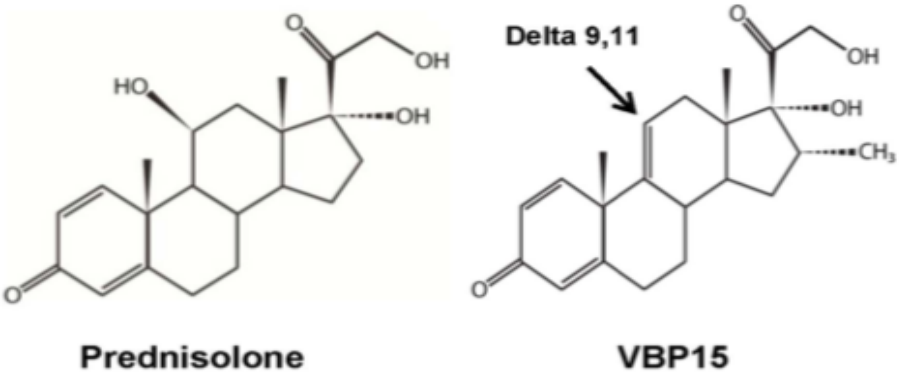

Figure 5-1 Comparison of the chemical structures of prednisolone and VBP-15. VBP compounds include a delta- 9,11 double bond and tail group modifications. Reproduced from (Damsker *et al.* 2013)**.** The exact structure of VBP6 has not been published.

This modification still enables the compound to effectively inhibit NF-κB activity and thus have an anti-inflammatory role, but it appears to do so without inducing GRE-mediated transcription and thus avoiding many of the classical GC side-effects (Reeves *et al.* 2013). As described in Chapter 1, by dissociating the gene transcriptional (classic GC) properties from the anti-inflammatory (NF-κB) properties, it is envisaged that these compounds should still improve muscle function in DMD without inducing growth failure or GIO. However, some studies have now suggested that some side-effects of GC can be attributed to both transactivation and transrepression, therefore it is possible that even the steroid analogues which do not cause transactivation may still result in skeletal abnormalities (Newton *et al.* 2007). Some basic bone and growth data have previously been reported in a study comparing one of these Δ9,11 steroids (VPB-15) to prednisolone in *mdx* mice (Heier *et al.* 2013). In this study, X-rays of tibiae were used to show that VBP-15 does not cause growth retardation at doses of up to 45mg/kg body weight, whilst the equivalent dose of prednisolone administered to *mdx* mice caused significant stunting of growth compared to the controls. Similarly, μCT analysis of trabecular bone demonstrated that oral prednisolone caused a significant decrease in trabecular thickness unlike the equivalent dose of VPB-15. This suggests that VBP-6, a metabolic precursor for VBP-

15 (VBP-15 is not available for use in pre-clinical work as it is currently being used in an early phase clinical trial, (Conklin *et al.* 2018)) should have a similar effect (Reeves *et al.* 2013). This work has not been carried out in other murine models of DMD and not at the level of detail required to gain a full understanding of its effects (or lack of) in the skeleton (Reeves *et al.* 2013). The data gained in this proposed study would therefore expand the current field of knowledge for VBP-6/VBP-15. This additional pre-clinical work may provide crucial extra data to support the clinical trial outcomes, where growth and bone are very difficult to accurately quantify given the short time frames involved. If successful, the work could also be extended to other childhood diseases where inflammation affects growth, or where GC are required, including for example in the treatment of inflammatory bowel diseases and juvenile arthritis. Since this project began, VBP-15, also known as vamorolone, has shown promising results in phase 1 studies (Hoffman *et al.* 2018) and has now moved into early phase 2 clinical trials (Conklin *et al.* 2018).

5.2 Hypothesis

Growth and GP chondrogenesis and bone development are impaired by GC but not by VBP-6 in WT mice and muscular dystrophy mouse models.

5.3 Aims

To assess:

1. Muscle pathology and function after exposure to varying GC regimens and VBP-6, expecting the muscle phenotype to be improved by both treatments.
2. Growth and GP chondrogenesis and bone fragility after exposure to varying GC regimens, expecting the growth response and bone health to be impaired.
3. Growth and growth plate chondrogenesis and bone fragility after exposure to VBP-6, expecting the growth response and bone health to remain unaffected.

All studies will compare the effects of GC and VBP-6 on male WT and muscular dystrophy (*mdx* and *mdx*:*cmah*) mouse models.

5.4 Material and Methods

5.4.1 Administration of GC or vehicle

All mice were given either GC or vehicle for 28 days, starting from between 27 and 29 days-of-age (approximately 4 weeks) and culled between 55 and 57 days-of-age (at approximately 8 weeks).

The study was initially designed to test the efficacy of prednisolone versus dexamethasone, and so the plan was to find the optimal dosage for each and then determine which regimen to move forward with into the final study. An initial pilot study was performed to determine whether 2.5mg/kg/day or 5mg/kg/day of dexamethasone would be the most appropriate dose to give SC for 28 days. Daily dexamethasone injections, at a dose of 5mg/kg/day SC for 7 days, were used by a previous student during her PhD at Roslin (Owen *et al.* 2009). During the 7-day period, the dexamethasone caused a reduction in bodyweight gain, reduced tibial length and reduction in longitudinal bone growth rate. However, it is not clear whether the mice would tolerate a 5mg/kg/day regimen for 28 days as the weight loss was marked in previous studies and would have likely exceeded the Home Office permitted weight loss (20%) if the regimen had been continued. Once it became clear that the 3 mice in the pilot study tolerated 2.5mg/kg/day of dexamethasone without significant adverse effects, 6 mice were moved onto the main study and given 5mg/kg/day. For this reason, there is only basic anthropometric data for the 2.5mg group.

Guided by the evidence from the literature review, the studies were carried out initially using prednisolone at a dose of 5mg/kg, but as there was minimal response, the dose was increased incrementally up to 20mg/kg/day to maximise efficacy, subject to tolerance of GC-associated side-effects.

All controls were administered vehicle by the same means as the GC. For example both dexamethasone 2.5mg and 5mg regimens were administered by SC injection, so the respective controls were given physiological saline by SC injection. Prednisolone was initially administered at a dose of 5mg/kg/day by SC injection. However oral gavage of prednisolone suspension in cherry syrup was used for the 10mg/kg/day and 20mg/kg/day regimens (Humco, TX, USA), with the respective controls receiving cherry syrup alone by gavage (without anaesthesia). Cherry syrup

was used as the vehicle for oral gavage, as prednisone is given in this way to DMD patients in the USA and also VBP-6 is insoluble and needs to be given in suspension. It was not known when the study was designed that VBP-6 was insoluble and hence the initial regimens were planned with SC injections. In order to make the regimens comparable, the later dosing was all carried out by oral gavage. In previous work, VBP compounds were administered using cherry syrup so the same vehicle was used in this study (Heier *et al.* 2013). For further details regarding regimens used, see section 2.2.1.

A minimum of 6 male mice were used in each group, except for the dexamethasone 2.5mg pilot group where n=3, as explained above. Additional mice were added to the prednisolone 10mg/kg group in order to match starting body weights, as marked variation was noted between the initial bodyweights in this group. The total number of mice used was 11. The results shown include all 11 mice as the data were not significantly affected if only the 6 closest in initial weight were retained.

Dexamethasone was trialled in WT and *mdx* mice but when it became clear that the regimens were not as effective in causing growth retardation as the prednisolone regimens, it was not used in the *mdx:cmah* mice. Prednisolone at a dose of 20mg/kg/day was given to *mdx:cmah* mice in addition to WT and *mdx* mice to see if the effects of GC were different in the *mdx:cmah* mice which had demonstrated catch up growth (as discussed in Section 3.6.)

5.4.2 Gross body growth parameters

Bodyweights of mice were measured twice weekly throughout the study period by staff in the animal house, from the start of the intervention/control regimen at 4 weeks-of-age, until cull. Body weight, crown to rump and tail lengths were taken using the same digital weighing scales and a ruler. Longitudinal crown-rump and tail length data throughout the study periods have not been shown as there was found to be great inter-observer variability in these measurements. In order to maximise validity only the data from time of cull are shown, because the same technician performed the anthropometric measures at cull during the study; this unfortunately was not possible for the entire study period due to shift patterns within the animal house.

5.4.3 Testes weight

Testes were dissected immediately post cull and weighed on the same digital scales for every mouse. A combined weight is presented, alongside a weight normalised to the overall bodyweight.

5.4.4 Grip strength

Forelimb grip strength testing was performed within 24 hours prior to cull, using a grip strength meter with a specialised mouse grid (Harvard Biosciences, Massachusetts, USA). See Chapter 2.3.1 for further details.

5.4.5 Muscle histology

The TA muscle of the lower hind limb was used to determine muscle necrosis and inflammation. Sections were cut at a width of 6 µm and H&E staining was used for histological assessment of muscle pathology, as outlined in Chapter 2.3.2.

5.4.6 Creatine kinase assay

Quantification of serum CK activity was carried out using a Pointe Scientific kit (Chapter 2.3.3). The change in NADPH absorbance was measured every 30s at 340nm for 4 min at 25°C.

5.4.7 Analysis of growth plate height

Right tibiae were removed at dissection and fixed in 10% NBF for up to one week, and then decalcified and embedded in paraffin wax (Chapter 2.4.2). Sections were cut at 6 µm and stained with H &E, further details are given in Chapter 2.4.8. Images were captured using a Zeiss AxioImager brightfield microscope. Heights of the GP zones were measured using Fiji (Schindelin *et al.* 2012). Ten measurements were taken per section and the mean height calculated for each zone.

5.4.8 Micro Computed tomography (µCT)

µCT was carried out according to the protocol described in Chapter 2.4.4.

5.4.9 Tibial length measurement

Tibial length was measured using images obtained by µCT and viewed in Dataviewer, as outlined in Section 2.4.4.

5.4.10 Biomechanical properties assessed by 3-point bending

As soon as possible after μCT, bones were subjected to the 3-point bending test to assess the biomechanical properties of the bone, as described in Section 2.4.5.

5.4.11 Assessment of bone turnover markers by ELISA

Serum αCTx and P1NP levels were measured as described in Section 2.4.6. All samples were taken from mice that were culled at the end of the study period, when they were 8 weeks-of-age.

5.4.12 Assessment of chondrocyte proliferation rate

IHC for PCNA detection was performed as described in Section 2.4.11.

5.4.13 Static histomorphometry

Static histomorphometry was performed on paraffin-embedded, decalcified sections of tibiae, as described in Chapter 2.4.2. A combination of TRAP activity and fast-red staining was used to enable osteoclast number to be determined. Osteoblasts were identified using Goldners trichome staining (see Section 2.4.13 for further details). The ROI included only metaphyseal trabecular bone and extended from 50 μm below the GP. Osteoblast and osteoclast number per bone surface were determined using BioqantOsteo v 17.2.6 (Bioquant Image Analysis Corp, Nashville, Tennessee, USA).

5.5 Results

5.5.1 Gross body growth parameters

a) Prednisolone regimens

There were no significant differences in % weight gain between WT mice given prednisolone at a dose of 5 mg/kg/day (SC) or 10mg/kg/day (via oral gavage) and their respective controls. Mean % weight gain of the WT mice treated with 20mg/kg/day of prednisolone was significantly lower during the study period compared to their controls (12.9% in prednisolone-treated mice v 59.2% gain in control mice, $p<0.001$), see Table 5-1. The same trend was observed in both the *mdx* and *mdx:cmah* mice, but did not reach statistical significance (Figure 5-2 and Table 5-2). The WT and *mdx:cmah* mice given VBP-6 gained significantly more weight (%) than their respective controls given cherry syrup (mean 94.0% gain v 59.2% in WT mice ($p<0.01$) and mean 115.1% gain v 72.7% in *mdx:cmah* mice ($p<0.001$)). There was no significant difference in the % weight gain of the *mdx* mice given VBP-6 compared to their controls.

There was no significant effect of any prednisolone regimen on change in crown-rump or tail length during the study period in any of the treatment groups (Tables 5-3 and 5-4).

b) Dexamethasone regimens

There was no significant change in anthropometric measures in either the WT or *mdx* mice given dexamethasone at either 2.5mg/kg/day or 5mg/kg/day compared to their controls (Tables 5-5). As explained in Section 5.4.1, three mice were initially given dexamethasone at 2.5mg/kg/day as a pilot group to ensure tolerability. Once it became clear that the mice tolerated it well and there were no real changes in bodyweight, the dose was increased to 5mg/kg/day and the data from the mice that received 2.5mg/kg of dexamethasone were not analysed further.

5.5.1 Testes weight

Although both the unadjusted and normalised testes weights were lower in the *mdx* mice compared to WT (consistent with results in Chapter 3), there was no significant difference between treatment regimens within each genotype, see Tables 5-6 and 5-7.

Parameter (SD)	WT Controls (PBS)	WT Pred 5mg/kg (PBS	WT Controls (syrup)	WT Pred 10mg/kg (syrup)	WT Pred 20mg/kg (syrup)	WT VBP6 20mg/kg (syrup)
Initial weight,g	19.2 (1.54)	18.2 (2.08)	14.7 (1.83)	17.1 (2.71)	17.8 (1.37)	15.5 (2.28)
Weight at cull, g	24.4 (1.75)	22.3 (1.86)	23.1 (1.14)	21.2 (2.51)	20.1 (1.89)	22.6 (1.8)
Weight change (%)	27.4 (9.65)	23.0 (7.68)	59.2 (16.4)	25.3 (11.51)	12.9 (5.44)***	45.8 (6.60)**

Table 5-1 Bodyweight data for WT mice given prednisolone or VBP6 for 28 days from 4 weeks-of-age. Data are presented as mean (+/- standard deviation), ** denotes p<0.01, *** p<0.001 compared to their respective controls. n=6, except pred 10mg/kg where n=11.

Parameter (SD)	*mdx* Controls (syrup)	*mdx* Pred 20mg/kg (syrup)	*mdx* VBP6 20mg/kg (syrup)	*mdx:cmah* Controls (syrup)	*mdx:cmah* Pred 20mg/kg (syrup)	*mdx:cmah* VBP6 20mg/kg (syrup)
Initial weight, g	20.5 (1.52)	16.5 (1.49)	14.7 (3.48)	15.1 (2.2)	11.6 (1.63)	11.1 (1.48)
Weight at cull, g	27.3 (2.6)	21.1 (1.3)	25.1 (0.79)	25.7 (1.93)	19.3 (1.83)	23.4 (0.95)
Weight change (%)	34.0 (17.7)	28.0 (10.2)	56.3 (31.7)	72.7 (20.12)	67.5 (11.51)	115.1 (28.83) ***

Table 5-2 Bodyweight data for *mdx* and *mdx:cmah* mice given prednisolone or VBP-6 for 28 days from 4 weeks-of-age. Data = mean (+/- standard deviation), *** denotes p<0.001 compared to their respective controls. n=6 in each group.

Parameter (SD)	WT Controls (PBS)	WT Pred 5mg/kg (PBS)	WT Controls (syrup)	WT Pred 10mg/kg (syrup)	WT Pred 20mg/kg (syrup)	WT VBP6 20mg/kg (syrup)
Change in CR length /day, cm	0.03 (0.01)	0.02 (0.01)	0.03 (0.01)	0.04 (0.03)	0.02 (0.01)	0.04 (0.01)
Change in tail length /day, cm	0.02 (0.01)	0.02 (0.01)	0.03 (0.01)	0.02 (0.02)	0.03 (0.01)	0.04 (0.01)

Table 5-3 Crown-rump and tail length data for WT mice given prednisolone or VBP-6 for 28 days from 4 weeks-of-age. Data are presented as mean (+/- standard deviation). n=6, except pred 10mg/kg where n=11.

Parameter (SD)	*mdx* Controls (syrup)	*mdx* Pred 20mg/kg (syrup)	*mdx* VBP6 20mg/kg (syrup)	*mdx:cmah* Controls (syrup)	*mdx:cmah* Pred 20mg/kg (syrup)	*mdx:cmah* VBP6 20mg/kg (syrup)
Change in CR length /day, cm	0.04 (0.02)	0.02 (0.01)	0.06 (0.02)	0.03 (0.01)	0.04 (0.01)	0.04 (0.01)
Change in tail length /day, cm	0.02 (0.01)	0.01 (0.00)	0.05 (0.01)	0.03 (0.01)	0.03 (0.01)	0.05 (0.01)

Table 5-4 Crown-rump and tail length data for *mdx* and *mdx:cmah* mice given prednisolone or VBP-6 for 28 days from 4 weeks-of-age. Data are presented as mean (+/- standard deviation). n=6 in each group.

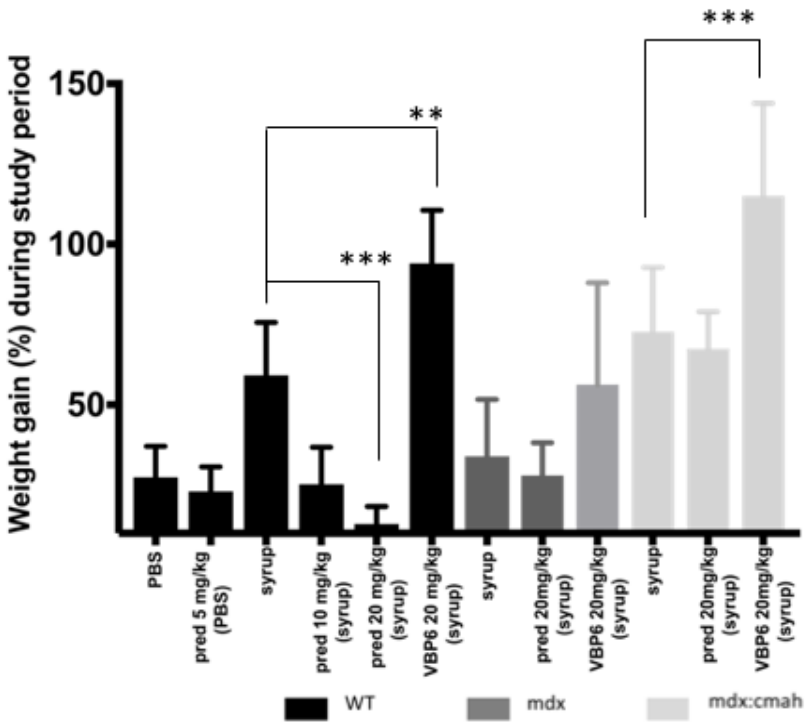

Figure 5-2 A bar chart to highlight the lower % weight gain seen in the WT mice given prednisolone at 20mg/kg/day compared to their controls and higher % weight gain in the WT and *mdx:cmah* mice given VBP-6 at 20mg/kg/day compared to their controls. Data are presented as mean (+/- standard deviation). ** signifies $p<0.01$, *** signifies $p<0.001$ compared to their respective controls. n=6, except pred 10mg/kg where n=11.

Mouse group	WT Control (injection)	WT dex 2.5mg/kg (injection)	WT dex 5mg/kg (injection)	*mdx* control (injection)	*mdx* dex 5mg/kg (injection)
Initial weight, g	18.1 (0.91)	20.5 (0.99)	18.1 (1.65)	20.2 (1.75)	20.1 (0.91)
Weight at cull, g	21.0 (1.56)	22.1 (0.36)	19.6 (2.78)	27.5 (3.55)	22.1 (1.42)
Weight change (%)	16.16 (7.09)	8.14 (5.19)	7.73 (6.89)	37.4 (23.9)	9.89 (5.31)
Change in CR length/ day, cm	0.02 (0.01)	0.02 (0.02)	0.02 (0.01)	0.05 (0.01)	0.03 (0.01)
Change in tail length/ day, cm	0.02 (0.01)	0.01 (0.01)	0.01 (0.00)	0.02 (0.01)	0.01 (0.01)

Table 5-5 Bodyweight, crown-rump and tail length data data for WT and *mdx* mice given dexamethasone for 28 days from 4 weeks-of-age. Data are presented as mean (+/- standard deviation). n=6, except dex 2.5mg/kg where n=3.

Parameter (SD)	WT Controls (PBS)	WT Pred 5mg/kg (PBS)	WT Controls (syrup)	WT Pred 10mg/kg (syrup)	WT Pred 20mg/kg (syrup)	WT VBP6 20mg/kg (syrup)
Combined testes weight, in g	0.20 (0.02)	0.19 (0.01)	0.20 (0.05)	0.17 (0.01)	0.18 (0.004)	0.17 (0.02)
Combined testes weight, normalised to BW	0.008 (0.001)	0.006 (0.001)	0.009 (0.02)	0.008 (0.001)	0.009 (0.001)	0.007 (0.0004)

Table 5-6 Unadjusted testes weight and testes weight normalized to BW for WT mice given prednisolone or VBP-6 for 28 days from 4 weeks-of-age. Data are presented as mean (+/- standard deviation). $^{\Delta\Delta}$ denotes p<0.01, $^{\Delta\Delta\Delta}$ denotes p<0.001 compared to equivalent. n=6, except pred 10mg/kg where n=11. WT group. BW: bodyweight

Parameter (SD)	*mdx* Controls (syrup)	*mdx* Pred 20mg/kg (syrup)	*mdx* VBP6 20mg/kg (syrup)	*mdx:cmah* Controls (syrup)	*mdx:cmah* Pred 20mg/kg (syrup)	*mdx:cmah* VBP6 20mg/kg (syrup)
Combined testes weight, in g	0.11 (0.05) $^{\Delta\Delta\Delta}$	0.11 (0.04) $^{\Delta\Delta}$	0.15 (0.01)	0.16 (0.02)	0.16 (0.01)	0.18 (0.01)
Combined testes weight, normalised to BW	0.004 (0.002) $^{\Delta\Delta\Delta}$	0.005 (0.002) $^{\Delta\Delta\Delta}$	0.006 (0.003)	0.006 (0.0003)	0.008 (0.0005)	0.008 (0.0006)

Table 5-7 Unadjusted testes weight and testes weight normalized to BW for *mdx* and *mdx:cmah* mice given prednisolone or VBP-6 for 28 days from 4 weeks-of-age. Data are presented as mean (+/- standard deviation). $^{\Delta\Delta}$ denotes p<0.01, $^{\Delta\Delta\Delta}$ denotes p<0.001 compared to equivalent WT group. n=6 in each group. BW: bodyweight

5.5.2 Grip strength

a) Prednisolone/ VBP-6 regimens

There were no significant differences in either the absolute or BW-normalised grip strength values between any of the WT animals that were treated with varying prednisolone regimens and their controls (Table 5-8). However, the normalised grip strength was significantly higher in the *mdx* mice who were given prednisolone at a dose of 20mg/kg/day compared to their controls (Table 5-9). The administration of 4 weeks of VBP-6 at the equivalent dose (20mg/kg/day) did not significantly change grip strength compared to their controls in either the WT or *mdx* mice.

b) Dexamethasone regimens

There were no significant differences in either the absolute or BW-normalised grip strength values between any of the WT or *mdx* animals who were treated with dexamethasone via SC injection at dose of 5mg/kg/day for 4 weeks and their respective controls (Table 5-10).

5.5.3 Muscle histology

As the previous results in this chapter have shown no conclusive evidence for the efficacy of the trialled dexamethasone regimens or prednisolone at doses of 5 or 10mg/kg/day to induce growth retardation, histological analysis of the TA muscle was only carried out in sections from the mice who were treated with either prednisolone at 20mg/kg/day or VBP-6 at 20mg/kg/day and their respective controls.

Histology of the muscular dystrophy models was consistent with Chapter 3 and revealed higher levels of inflammation and muscle cell regeneration seen in samples from both the *mdx* and *mdx:cmah* mice culled at 8 weeks of age, compared to WT mice (Figures 5-3 B,C and 5-4 and Table 5-11). Prednisolone given for 4 weeks at 20mg/kg/day caused a 70% reduction in cumulative TA muscle damage in the *mdx:cmah* mice. The same trend was also seen in the *mdx* mice but did not reach statistical significance. 4 weeks of VBP-6 given at 20mg/kg/day significantly reduced the cumulative muscle damage in the TA of *mdx* mice.

As previously noted in Chapter 3, histological sections from WT mice revealed regular myofibres with peripheral nuclei and intact sarcoplasm (Figure 5-3A). This was unaffected by the administration of either prednisolone or VBP-6 (Figures 5-3 and 5-4 and Table 5-11).

5.5.1 Creatine kinase assay

There were no significant difference in serum CK values after 4 weeks of either prednisolone or VBP-6, when given at 20mg/kg/day, compared to their respective controls (Table 5-12). CK values were higher in the untreated *mdx* mice compared to WT, as previously shown in Section 3.5.2.

5.5.2 Analysis of growth plate height

a) Prednisolone/ VBP-6 regimens

The total height of the GP was significantly less in the WT mice given prednisolone at a dose of 20mg/kg/day than those given syrup alone (mean 122.1 μm in prednisolone-treated mice v 167.5μm in syrup control mice, $p<0.01$, Table 5-13, Figure 5-5). The height of the proliferative zone was also significantly less in the mice given prednisolone at 20mg/kg/day compared to their syrup controls (mean 67.4μm in prednisolone-treated mice v 100.1μm in syrup control mice, $p<0.05$). Four weeks of VBP-6 did not significantly change the total height of the GP or its individual zones (Table 5-11).

There were no significant changes to GP height or height of its individual maturational zones in the *mdx* mice given either prednisolone or VBP-6 compared to their respective controls (Table 5-14).

b) Dexamethasone regimens

There were no significant differences in either total GP height or of the individual maturation zones between the WT and *mdx* mice given dexamethasone 5mg/kg/day and their respective controls (Table 5-15).

Parameter (SD)	Controls (PBS)	Controls (syrup)	Pred 5mg/kg (PBS)	Pred 10mg/kg (syrup)	Pred 20mg/kg (syrup)	VBP6 20mg/kg (syrup)
Grip strength,g	107.7 (16.4)	94.3 (14.0)	90.2 (23.0)	101.7 (17.1)	96.3 (18.6)	95.9 (15.1)
Grip strength normalised to BW	4.4 (0.8)	4.3 (0.6)	4.05 (1.02)	4.8 (0.7)	4.8 (0.8)	4.1 (0.6)

Table 5-8 Absolute and normalised grip strength from WT mice culled at 9 weeks-of-age after 4 weeks of either daily vehicle, prednisolone, or VBP-6. Data are presented as mean (+/- standard deviation). n=6, except pred 10mg/kg where n=11.

Parameter (SD)	*mdx* Controls (syrup)	*mdx:cmah* Controls (syrup)	*mdx* Pred 20mg/kg (syrup)	*mdx:cmah* Pred 20mg/kg (syrup)	*mdx* 20mg/kg (syrup)	VBP6
Grip strength,g	94.6 (5.4)	104.8 (27.1)	98.5 (17.1)	74.8 (5.7)	91.9 (14.3)	
Grip strength normalised to BW	3.5 (0.6)	4.1 (0.9)	4.7 (0.7)*	3.9 (0.2)	3.7 (0.6)	

Table 5-9 Absolute and normalised grip strength from *mdx* and *mdx:cmah* mice culled at 9 weeks-of-age after 4 weeks of either daily vehicle, prednisolone, or VBP-6. Data are presented as mean (+/- standard deviation).* denotes $p<0.05$ compared to their control. n=6 in each group.

Parameter (SD)	WT Controls	WT Dex 5mg/kg	*mdx* Controls	*mdx* Dex 5mg/kg
Grip strength	103.1 (10.5)	81.3 (15.9)	94.6 (5.4)	82.5 (13.7)
Grip strength normalised to BW	5.0 (0.8)	4.3 (1.3)	3.5 (0.6)	3.8 (0.8)

Table 5-10 Absolute and normalised grip strength from *mdx* and WT mice culled at 9 weeks-of-age after 4 weeks of either daily vehicle or dexamethasone. Data are presented as mean (+/- standard deviation). n=6 in each group.

Parameter (SD)	WT Controls (syrup)	WT Pred 20mg/kg (syrup)	WT VBP6 20mg/kg (syrup)	*mdx* Controls (syrup)	*mdx* Pred 20mg/kg (syrup)	*mdx* VBP6 20mg/kg (syrup)	*mdx:cmah* Controls (syrup)	*mdx:cmah* Pred 20mg/kg (syrup)
% of inflamm cells-cell damage (SD)	0.33 (0.65)	0.73 (0.75)	0.38 (0.54)	5.62 (1.02)	3.05 (1.52)	1.60 (0.56)	2.57 (2.28)	0.67 (0.46)
% of central nuclei-regeneration (SD)	1.19 (1.60)	0.18 (0.08)	1.02 (0.39)	2.87 (1.02)	2.80 (1.13)	2.43 (0.93)	2.96 (2.22)	0.99 (0.23)
Cumulative percentage (SD)	1.52 (1.55)	0.91 (0.83)	1.40 (0.93)	8.48 (3.57)	5.85 (2.49)	4.03 (1.06)*	5.53 (1.69)	1.66 (0.69)***

Table 5-11 Histology of TA muscle showing effect of 4 weeks of either prednisolone, VBP6 or vehicle on muscle cell inflammation and regeneration. Data are presented as mean (+/- standard deviation). * denotes $p<0.05$, *** denotes $p<0.001$ compared to respective control. n=6, except pred 10mg/kg where n=11.

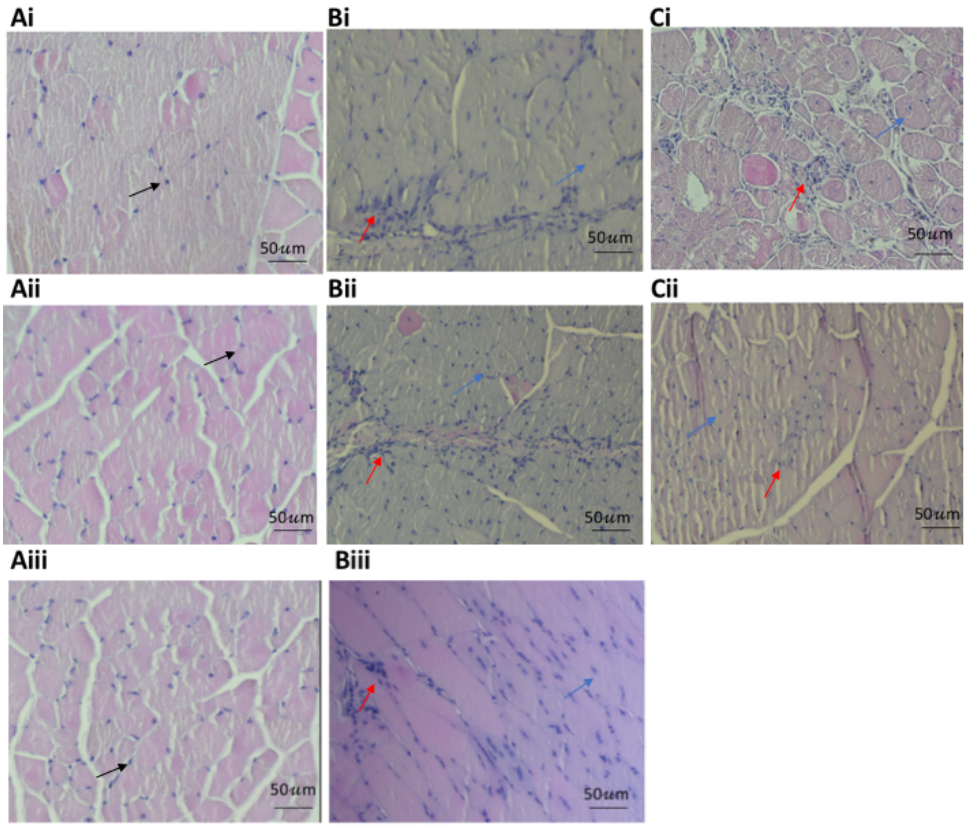

Figure 5-3 Ai) H&E stained section of TA from 8-week-old WT mouse showing normal, regular myofibres with peripheral nuclei (black arrow) and intact sarcoplasm.
Aii) H&E stained section of TA from 8-week-old WT mouse after 4 weeks of prednisolone 20mg/kg/day: regular myofibres, peripheral nuclei (black arrow) and intact sarcoplasm.
Aiii) H&E stained section of TA from 8-week-old WT mouse after 4 weeks of VBP-6 at 20mg/kg/day: normal, regular myofibres, peripheral nuclei (black arrow), intact sarcoplasm.
Bi) H&E stained section of TA from 8-week-old *mdx* mouse: many inflammatory cells (red arrow) and evidence of regeneration with larger myofibres and central nuclei (blue arrow).
Bii) H&E stained section of TA from 8-week-old *mdx* mouse after 4 weeks of pred 20mg/kg/day: some normal, regular myofibres with peripheral nuclei and intact sarcoplasm, less inflammatory cells than in Bi) (red arrow), some evidence of regeneration (blue arrow).
Biii) H&E stained section of TA from 8-week-old *mdx* mouse after 4 weeks of VBP-6 at 20mg/kg/day: some normal, regular myofibres with peripheral nuclei and intact sarcoplasm, less inflammatory cells than in Bi) (red arrow) and some regeneration (blue arrow).
Ci) H&E stained section of TA from 8-week-old *mdx:cmah* mouse: many inflammatory cells (red arrow), evidence of regeneration (larger myofibres,central nuclei (blue arrow)).
Cii) H&E stained section of TA from 8-week-old *mdx:cmah* mouse after 4 weeks of prednisolone at 20mg/kg/day showing some normal, regular myofibres with peripheral nuclei and intact sarcoplasm, less inflammatory cells than in Ci) (red arrow) and also less evidence of regeneration than in Ci) (blue arrow).

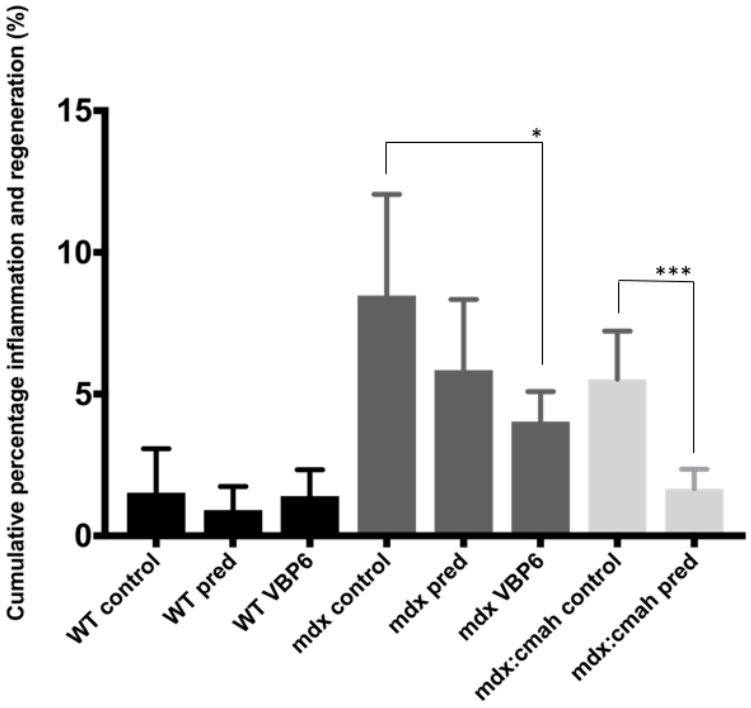

Figure 5-4 Histology of TA muscle showing pathology in *mdx* and *mdx:cmah* mice compared to WT mice showing a cumulative reduction in muscle damage after 4 weeks of VBP-6 in the *mdx* mice and 4 weeks of prednisolone at 20mg/kg/day in *mdx:cmah* mice. Data are presented as mean (+/- standard deviation). * denotes $p<0.05$, *** denotes $p<0.001$ compared to respective control. n=6 in each group.

Group	Mean CK value in U/L (SD)
WT control	43.9 (28.8)
WT pred 20	108.0 (66.8)
WT VBP-6	168.0 (61.9)
mdx control	290.3 (57.3) $^{\Delta}$
mdx pred 20	679.7 (519.4)
mdx VBP-6	281.9 (161.5)

Table 5-12 No differences were noted in CK levels at 9 weeks-of-age by GC regimen. Data are presented as mean (+/- standard deviation), $^{\Delta}$ denotes $p<0.001$ compared to WT mice. n=6 in each group.

5.5.3 Trabecular bone parameters, assessed by μCT

Micro CT was not carried out on the mice treated with dexamethasone due to the lack of any observed anthropometric changes. No differences that were observed in trabecular parameters between treated and control groups were consistent across both the WT and muscular dystrophy models (Tables 5-16 and 5-17). A small but significant decrease in trabecular separation was observed in the WT and *mdx* mice treated with prednisolone at 20mg/kg/day when compared with their cherry syrup controls. This difference was not observed in the 20mg/kg/day prednisolone-treated *mdx:cmah* mice. In contrast to this, there was a small decrease in trabecular thickness observed in the *mdx*:*cmah* mice treated with prednisolone at 20mg/kg/day when compared with their cherry syrup controls, but this was not observed in the WT or *mdx* mice.

Structural model index was reduced in the WT mice treated with prednisolone at 10mg and 20mg/kg/day but not in the *mdx*:*cmah* or *mdx* mice treated with the equivalent regimens. Connectivity was also increased in the WT and *mdx* mice treated with prednisolone at 20mg/kg/day compared to their controls, but again this finding was not replicated in the *mdx*:*cmah* group. There were no further differences observed between the mice given prednisolone at 5 or 10mg/kg/day and their respective controls (Table 5-16).

There were no significant differences in trabecular bone parameters measured in either the WT or *mdx* mice that were given 4 weeks of VBP-6 compared to their controls (Figure 5-7, Tables 5-16 and 5-17).

5.5.4 Cortical bone parameters, assessed by μCT

Cortical tissue area, bone area, tissue volume and bone volume were all significantly less in both the WT and muscular dystrophy mouse models that were treated with prednisolone at 20mg/kg/day (Tables 5-18, 5-19, Figures 5-6 and 5-7). In keeping with this, mean cortical bone fraction was also significantly less, at 57% in prednisolone-treated WT mice v 63% in WT syrup controls; 59% in prednisolone-treated *mdx* mice v 66% in the *mdx* syrup controls and 55% in prednisolone-treated *mdx*:*cmah* mice v 66% in the *mdx*:*cmah* syrup controls (Figure 5-6). Cortical bone fraction was also lower in the WT mice treated with 10mg/kg/day of prednisolone

compared to their controls (60% in prednisolone-treated mice v 63% in syrup controls), Table 5-18. Cortical tissue area and periosteal perimeter were also significantly lower in the *mdx*:*cmah* group treated with prednisolone at 20mg/kg; this was consistent with the same trends in the WT group (Table 5-19).

Mean polar moment of inertia (J) was also significantly lower in all mice that there were given prednisolone at 20mg/kg/day compared to their controls (Tables 5-18 and 5-19).

There were no significant differences in cortical bone parameters measured in either the WT or mdx mice that were given 4 weeks of VBP-6 compared to their controls (Tables 5-18 and 5-19 and Figure 5-6).

There were no differences in TMD by group, except in WT mice where the TMD was actually greater after 4 weeks of daily VBP-6 by oral gavage (Tables 5-18 and 5-19).

5.5.5 Tibial length, assessed by μ-CT

Tibial length at 8 weeks was significantly less (0.57 mm difference in WT, 0.88 mm in *mdx* and 1.39mm difference in *mdx:cmah*) in all the mice given prednisolone 20mg /kg daily (Table 5-20). No differences in tibial length were seen after 4 weeks of daily VBP-6 treatment in either the WT, *mdx* or *mdx:cmah* mice.

Parameter	Controls (PBS)	Controls (syrup)	Pred 5mg/kg (PBS)	Pred 10mg/kg (syrup)	Pred 20mg/kg (syrup)	VBP6 20mg/kg (syrup)
Total growth plate height, μm	153.71 (17.81)	167.54 (28.32)	152.10 (21.44)	166.15 (21.78)	122.1 (17.02)**	157.8 (15.96)
Height of hypertrophic zone, μm	87.99 (17.52)	54.87 (5.90)	80.49 (10.33)	70.13 (13.19)	59.54 (2.19)	59.33 (2.67)
Height of proliferative zone, μm	82.87 (8.47)	100.14 (23.71)	75.00 (11.66)	88.11 (17.31)	67.33 (10.66)*	89.54 (14.11)

Table 5-13 Analysis of GP heights in WT mice given either prednisolone or VBP-6 for 28 days from 4 weeks-of-age. Data presented as mean (+/- standard deviation), * denotes $p<0.05$, ** $p<0.01$ compared to their respective controls. n=6, except pred 10mg/kg where n=11.

Parameter	*mdx* Controls (syrup)	*mdx* Pred 20mg/kg (syrup)	*mdx* VBP6 20mg/kg (syrup)
Total growth plate height, μm	139.39 (9.34)	139.72 (1.72)	145.76 (19.94)
Height of hypertrophic zone, μm	52.00 (6.71)	55.3 (2.34)	61.84 (5.71)
Height of proliferative zone, μm	75.03 (12.08)	68.55 (7.57)	97.98 (1.16)

Table 5-14 Analysis of GP heights in *mdx* mice given either prednisolone or VBP-6 for 28 days from 4 weeks-of age. Data are presented as mean (+/- standard deviation). n=6 in each group.

Parameter	WT Controls (injection)	WT Dex 5mg/kg (injection)	Mdx controls (injection)	Mdx Dex 5mg/kg (Injection)
Total growth plate height, μm	128.16 (7.99)	139.56 (8.30)	144.71 (2.25)	143.85 (10.40)
Height of hypertrophic zone, μm	52.81 (6.73)	60.48 (4.59)	49.22 (6.62)	59.25 (10.67)
Height of proliferative zone, μm	68.78 (7.69)	70.89 (11.80)	70.77 (13.53)	86.80 (6.75)

Table 5-15 Analysis of GP heights in *mdx* and WT mice on dexamethasone regimens. Data are presented as mean (+/- standard deviation). n=6 in each group.

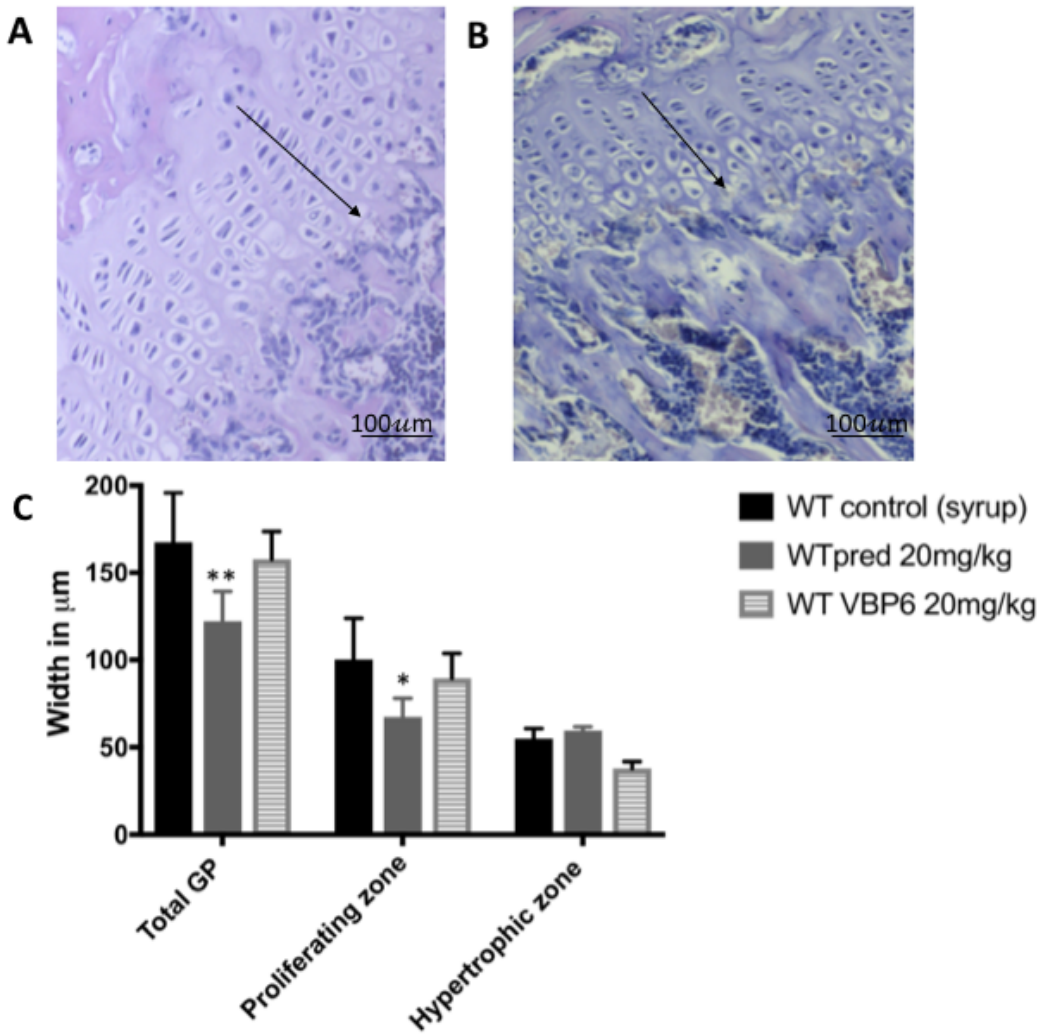

Figure 5-5 Representative GP images from WT mice given (A) cherry syrup control for 28 days from 4 weeks-of age and (B) prednisolone 20mg/kg/day for 28 days from 4 weeks-of age, highlighting the reduction in total GP height in (A), shown by arrows. (C) Bar chart showing the significant reduction in total GP and proliferating zone in WT mice given prednisolone 20mg/kg/day for 28 days from 4 weeks of age compared to their controls. There were no differences seen after giving VBP-6 20mg/kg to WT mice. Data are presented as mean (+/- standard deviation), * denotes $p<0.05$, ** denotes $p<0.01$ compared to their respective controls.

Parameter	Controls (PBS)	Controls (syrup)	Pred 5mg/kg (PBS)	Pred 10mg/kg (syrup)	Pred 20mg/kg (syrup)	VBP6 20mg/kg (syrup)
TV, mm^3	2.54 (0.22)	2.33 (0.07)	2.65 (0.27)	2.57 (0.42)	2.45 (0.28)	2.34 (0.30)
BV, mm^3	0.54 (0.12)	0.40 (0.05)	0.60 (0.11)	0.55 (0.19)	0.54 (0.12)	0.45 (0.13)
TVBV, %	20.92(3.19)	17.0 (1.72)	22.32 (3.08)	21.00 (4.35)	22.37 (5.48)	18.89 (3.44)
Tb.N, 1/mm	4.11 (0.50)	3.56 (0.24)	4.57 (0.53)	4.50 (0.80)	4.34 (0.80)***	3.78 (0.41)
Tb.Th, mm	0.05 (0.05)	0.05 (0.003)	0.05 (0.003)	0.05 (0.002)	0.04 (0.02)	0.05 (0.005)
Tb.S, mm	0.15 (0.01)	0.16 (0.09)	0.14 (0.01)	0.14 (0.02)	0.13 (0.03)***	0.16 (0.01)
SMI	1.73 (0.18)	1.98 (0.08)	1.65 (0.17)	1.70 (0.21)*	1.63 (0.20)*	1.89 (0.18)
Conn	1289 (254)	1120 (107.2)	1685 (363.3)	1872 (643.2)	2259 (1130)***	1254 (257)

Table 5-16 Trabecular bone parameters from μCT in 8 week-old WT mice using different prednisolone and VBP-6 regimens. Data are presented as mean (+/- standard deviation).* signifies $p<0.05$, *** signifies $p<0.001$ compared to their respective controls. n=6, except pred 10mg/kg where n=11.

Parameter (SD)	*mdx:cmah* controls	*mdx:cmah* pred 20mg/kg syrup	*mdx* controls	*mdx* pred 20mg/kg syrup	*mdx* VBP6 20mg/kg syrup
TV, mm^3	1.97 (0.15)	1.84 (0.06)	2.51 (0.21)	2.52 (0.18)	2.25 (0.08)
BV, mm^3	0.33 (0.05)	0.32 (0.05)	0.44 (0.08)	0.54 (0.06)	0.34 (0.08)
TVBV, %	16.88 (2.42)	17.21 (2.77)	17.41 (2.28)	21.55 (1.30)	15.34 (0.58)
Tb.N, 1/mm	3.35 (0.55)	4.05 (0.53)	3.59 (0.45)	5.27 (0.52)***	3.33 (0.19)
Tb.Th, mm	0.05 (0.001)	0.04 (0.00)***	0.05 (0.003)	0.04 (0.002)	0.05 (0.02)
Tb.S, mm	0.17 (0.16	0.15 (0.01)	0.17 (0.01)	0.12 (0.01)*	0.17 (0.01)
SMI	1.96 (0.21)	1.85 (0.16)	1.87 (0.12)	1.80 (0.13)	2.06 (0.04)
Conn	824.5 (159.0)	1362 (284)	1174 (319)	2460 (545)***	1022 (74)

Table 5-17 Trabecular bone parameters from μCT in 8 week-old *mdx* and *mdx:cmah* mice given prednisolone or VBP-6. Data are presented as mean (+/- standard deviation).* signifies $p<0.05$, *** signifies $p<0.001$ compared to their respective controls. n=6 in each group.

Parameter	Controls (PBS)	Controls (syrup)	Pred 5mg/kg (PBS)	Pred 10mg/kg (syrup)	Pred 20mg/kg (syrup)	VBP6 20mg/kg (syrup)
TMD g/cm^3	1.40 (0.07)	1.30 (0.06)	1.36 (0.06)	1.39 (0.04)	1.33 (0.03)	1.43 (0.01)**
Ct.TAr , mm^2	1.02 (0.10)	1.00 (0.07)	1.03 (0.08)	0.91 (0.11)	0.93 (0.06)**	0.97 (0.08)
Ps Pm, mm	3.88 (0.20)	3.86 (0.13)	3.91 (0.17)	3.66 (0.24)	3.70 (0.12)	3.64 (0.12)
Ct Bar, mm^2	0.66 (0.06)	0.64 (0.04)	0.64 (0.06)	0.55 (0.08)	0.52 (0.04)***	0.62 (0.05)
Es Pm, mm	2.31 (0.14)	2.31 (0.10)	2.39 (0.10)	2.29 (0.13)	2.40 (0.10)	2.26 (0.12)
Ct.TV, mm^3	0.91 (0.09)	0.92 (0.05)	0.92 (0.07)	0.82 (0.10)	0.80 (0.05)**	0.87 (0.07)
Ct.BV, mm^3	0.59 (0.06)	0.58 (0.03)	0.58 (0.05)	0.49 (0.07)	0.46 (0.03)***	0.56 (0.05)
TVBV, %	64.22 (1.76)	63.53 (1.49)	62.44 (2.02)	60.30 (1.99)***	57.17 (2.23)***	64.17 (1.49)
J, mm^4	0.15 (0.03)	0.15 (0.02)	0.15 (0.02)	0.11 (0.03)	0.11 (0.02)***	0.13 (0.02)
Ct.Th, mm	0.58 (0.03)	0.58 (0.02)	0.59 (0.02)	0.57 (0.01)	0.60 (0.03)	0.56 (0.03)
Ecc	0.50 (0.07)	0.50 (0.08)	0.55 (0.07)	0.51 (0.06)	0.54 (0.03)	0.52 (0.13)

Table 5-18. Cortical bone parameters from μCT in 8 week-old WT mice who were given daily vehicle, prednisolone or VBP-6. Data are presented as mean (+/- standard deviation). ** signifies p<0.01, *** signifies p<0.001 compared to their respective controls. n=6, except pred 10mg/kg where n=11.

Parameter (SD)	*mdx:cmah* controls	*mdx:cmah* pred 20mg/kg syrup	*mdx* controls	*mdx* pred 20mg/kg syrup	*mdx* VBP6 20mg/kg syrup
TMD g/cm^3	1.27 (0.03)	1.26 (0.01)	1.29 (0.12)	1.33 (0.10)	1.25 (0.03)
Ct.TAr , mm^2	0.99 (0.001)	0.81 (0.09)***	1.06 (0.04)	0.87 (0.05)***	1.04 (0.01)
Ps Pm, mm	3.86 (0.18)	3.47 (0.20)*	3.97 (0.08)	3.58 (0.14)	3.94 (0.04)
Ct Bar, mm^2	0.66 (0.05)	0.45 (0.05)***	0.70 (0.03)	0.51 (0.03)***	0.67 (0.008)
Es Pm, mm	2.21 (0.11)	2.29 (0.13)	2.29 (0.07)	2.28 (0.08)	2.33 (0.02)
Ct.TV, mm^3	0.89 (0.07)	0.73 (0.07)***	0.96 (0.04)	0.78 (0.05)***	0.93 (0.01)
Ct.BV, mm^3	0.59 (0.05)	0.41 (0.05)***	0.63 (0.03)	0.56 (0.03)***	0.60 (0.007)
TVBV, %	66.1 (0.88)	55.46 (1.49)***	65.57 (1.49)	58.82 (1.17)***	64.38 (0.82)
J, mm^4	0.15 (0.03)	0.09 (0.02)***	0.16 (0.01)	0.10 (0.01)***	0.156 (0.004)
Ct.Th, mm	0.55 (0.02)	0.58 (0.02)	0.58 (0.02)	0.57 (0.02)	0.57 (0.02)
Ecc	0.50 (0.07)	0.57(0.09)	0.64 (0.05)	0.49 (0.11)	0.53 (0.14)

Table 5-19 Cortical bone parameters from μCT in 8 week-old *mdx* and *mdx:cmah* mice who were given daily vehicle, prednisolone or VBP-6 from 4 weeks-of-age. Data are presented as mean (+/- standard deviation).* signifies $p<0.05$, *** signifies $p<0.001$ compared to respective control. n=6 in each group.

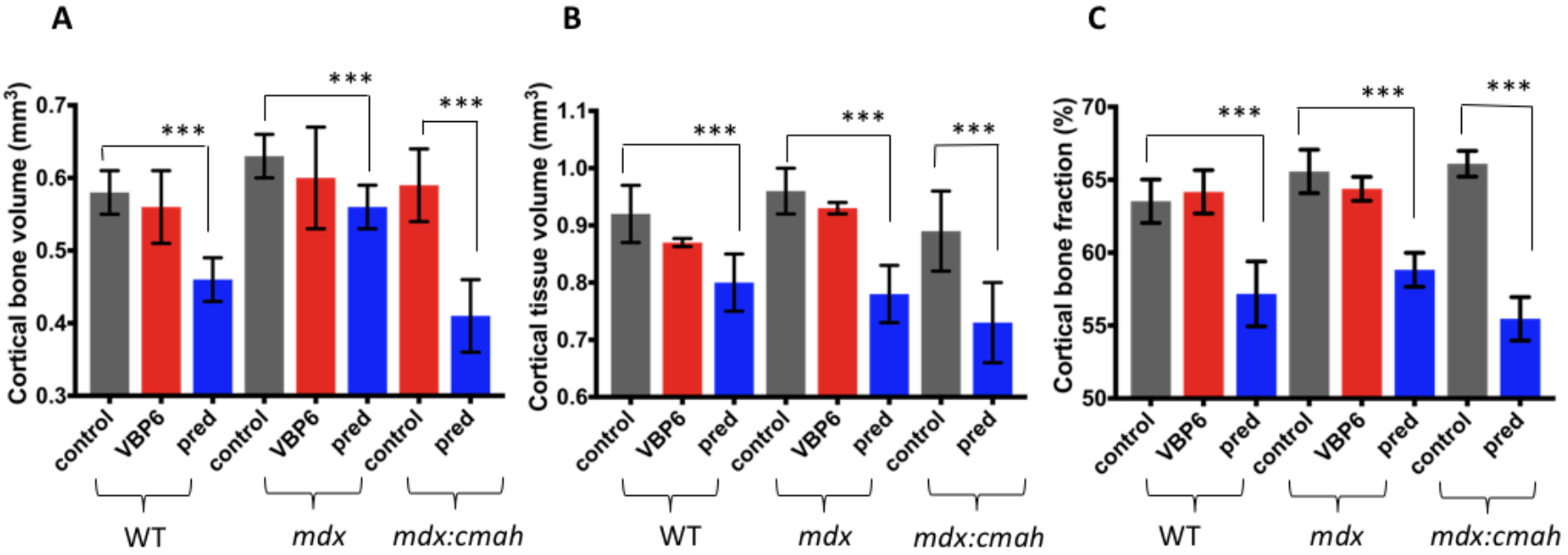

Figure 5-6 Cortical bone parameters assessed by μCT in 8 week-old WT *mdx* and *mdx:cmah* mice who were given daily vehicle, prednisolone or VBP-6 from 4 weeks-of-age, showing a significant reduction in **A)** cortical bone volume, **B)** cortical tissue volume and **C)** cortical tissue volume in all mice models who were given prednisolone compared to their respective controls. Data are presented as mean (+/- standard deviation).* signifies $p<0.05$, ** signifies $p<0.01$ compared to respective control. n=6 in each group.

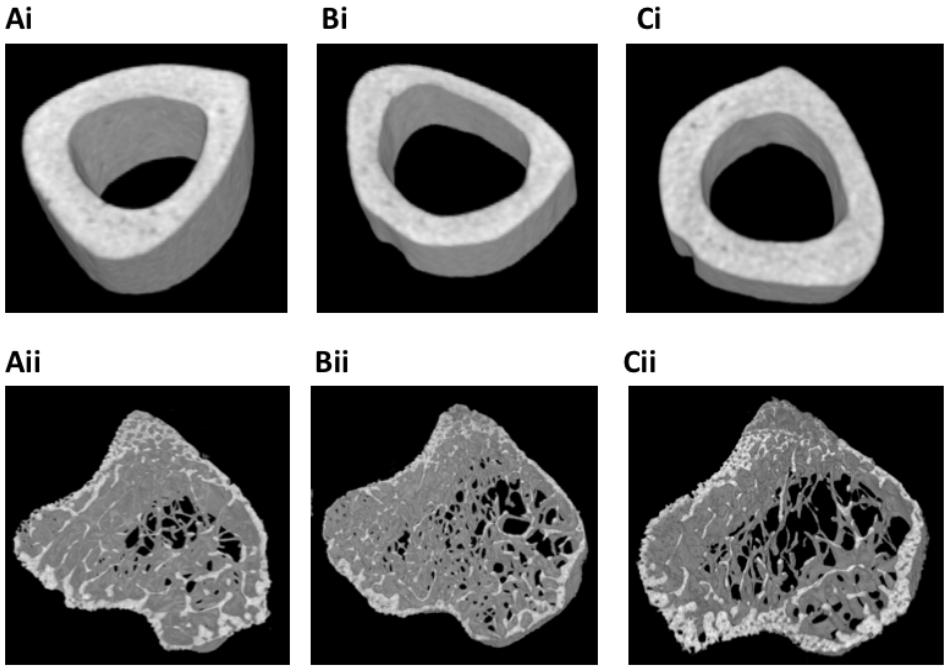

Figure 5-7 Representative μCT images of tibiae from WT mice culled at 8 weeks-of age after:

A) 4 weeks of cherry syrup by oral gavage

B) 4 weeks of prednisolone at 20mg/kg/day by oral gavage

C) 4 weeks of VBP-6 at 20mg/kg/day by oral gavage

(i) upper row shows mid-diaphyseal cortical bone and the reduction in cortical bone fraction after administration of prednisolone in (Bi)

(ii) lower row shows metaphyseal trabecular bone with no significant changes seen by intervention group.

Parameter	WT controls (PBS)	WT controls (syrup)	WT pred 5mg/kg (PBS)	WT pred 10mg/kg (syrup)	WT pred 20mg/kg (syrup)	WT VBP6 20mg/kg (syrup)
Tibial length, mm	16.81 (0.38)	16.68 (0.35)	16.52 (0.38)	16.29 (0.46)	16.11 (0.14)**	16.39 (0.57)

	mdx:cmah controls (syrup)	*mdx:cmah* pred 20mg/kg (syrup)	*mdx* controls (syrup)	*mdx* pred 20mg/kg (syrup)	*mdx* VBP6 20mg/kg (syrup)
Tibial length, mm	17.07 (0.04)	15.68 (0.21)**	16.86 (0.48)	15.98 (0.36)*	16.64 (0.10)

Table 5-20 μCT analysis of tibial length in WT, *mdx* and *mdx:cmah* mice at 8 weeks-of-age after 4 weeks of either daily vehicle, prednisolone or VBP-6. Data are presented as mean (+/- standard deviation). * denotes p<0.05, ** denotes p<0.01 compared to respective control group. n=6, except pred 10mg/kg where n=11.

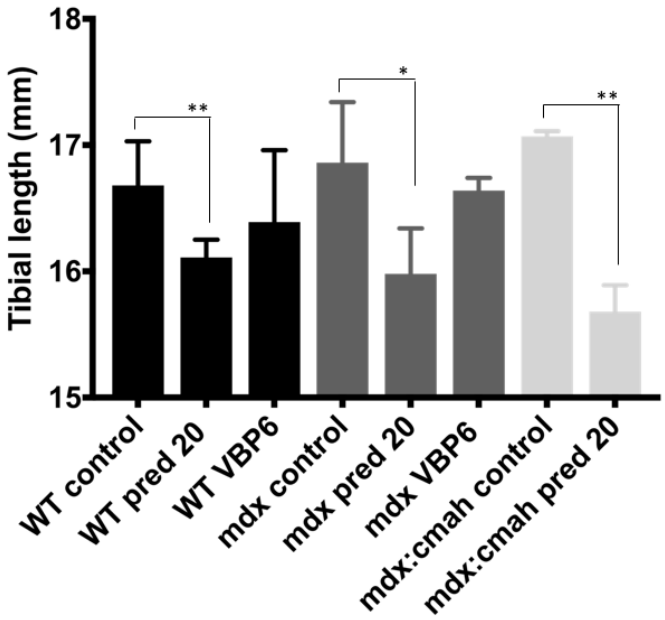

Figure 5-8 μCT analysis of tibial length in WT, *mdx* and *mdx:cmah* mice at 8 weeks-of-age after 4 weeks of either daily vehicle, prednisolone or VBP-6. Data are presented as mean (+/- standard deviation). * denotes p<0.05, ** denotes p<0.01 compared to respective control group. n=6 in each group.

5.5.6 Biomechanical properties, assessed by 3-point bending

Table 5-21 shows that there were no significant differences in biomechanical properties between either the WT, *mdx*, or *mdx:cmah* mice given prednisolone or VBP-6 regimens and their respective controls.

5.5.7 Bone turnover markers assessed by ELISA

Table 5-22 and Figure 5.9 show that both P1NP and αCTX concentrations were significantly lower in the WT mice that were given 4 weeks of prednisolone at 20mg/kg/day. P1NP concentrations were not tested in the WT mice given prednisolone at 10mg/kg/day because there were insufficient volumes of serum obtained from cardiac puncture, but the same trend for a reduction in CTX concentration after 4 weeks of treatment was seen, although this did not reach statistical significance.

Four weeks of VBP-6 treatment at 20mg/kg/day in the WT mice caused a significant reduction in P1NP levels, but there was no associated change in αCTX levels (Table 5-22).

There were no significant differences seen in the *mdx* mice who were treated with either prednisolone at 20mg/kg/day or VBP-6 at the same dose, compared to their respective controls.

5.5.8 Assessment of chondrocyte proliferation rate

Figure 5-10 shows that chondrocyte proliferation rates, as assessed by PCNA IHC, were similar after 4 weeks of either prednisolone or VBP6 in both WT and *mdx* mice, compared to their respective controls.

5.5.9 Static histomorphometry

There were no significant differences in either osteoblast (Figure 5-11A) or osteoclast number/bone surface (Figure 5-11AB) by intervention group, in either the WT or *mdx* mice, when measured at 8 weeks of age.

Table 5-23 shows a summary of the changes observed when mice were either given prednisolone at 20mg/kg/day or VBP6 at 20mg/kg/day.

Parameter	WT controls (PBS)	WT controls (syrup)	WT pred 5mg/kg (PBS)	WT pred 10mg/kg (syrup)	WT pred 20mg/kg (syrup)	WT VBP6 20mg/kg (syrup)
Maximum load (N)	8.36 (1.11)	6.05 (2.70)	8.70(2.71)	5.82 (2.02)	6.35 (1.59)	7.70 (1.41)
Deflection at max load (mm)	0.60 (0.11)	0.80 (0.52)	0.84 (0.54)	0.96 (0.56)	0.85 (0.47)	1.16 (0.48)
Stiffness (Nm)	25401 (4908)	20594 (4852))	29514 (15759)	23239 (18903)	17952 (4788)	20190 (4196)

Parameter	*mdx:cmah* controls (syrup)	*mdx:cmah* pred 20mg/kg (syrup)	*mdx* controls (syrup)	mdx pred 20mg/kg (syrup)	mdx VBP6 20mg/kg (syrup)
Maximum load (N)	8.70 (2.44)	5.14 (1.80)	8.87 (2.50)	6.35 (3.00)	8.63 (1.72)
Deflection at max load (mm)	0.82 (0.89)	0.75 (0.26)	0.67 (0.15)	0.67 (0.32)	1.03 (0.43)
Stiffness (Nm)	37791 (31153)	17352 (10669)	26475 (7448)	17576 (1788)	21067 (5462)

Table 5-21 Biomechanical properties of WT mice given prednisolone and VBP-6 regimens, assessed by 3-point bending. Data are presented as mean (+/- standard deviation). n=6, except pred 10mg/kg where n=11.

	WT controls (syrup)	WT Pred 10mg/kg	WT Pred 20mg/kg	WT VBP6 20mg/kg (syrup)	*mdx* controls (syrup)	mdx pred 20mg/kg (syrup)	mdx VBP6 20mg/kg (syrup)
P1NP (pg/ml)	367.6 (184.2)	Not done	159.9 (84.4)*	62.5 (30.4)**	58.3 (27.6)	107.8 (93.6)	55.9 (25.2)
αCTX (pg/ml)	180.4 (86.9)	105.1 (45.5)	75.7 (23.1)*	112.2 (62.3)	158.3 (99.3)	206.6 (55)	66.4 (25.6)

Table 5-22 Comparison of bone turnover markers with different GC regimens. Data are presented as mean (+/- standard deviation).* signifies $p<0.05$, ** signifies $p<0.01$ compared to respective control. n=6 in each group.

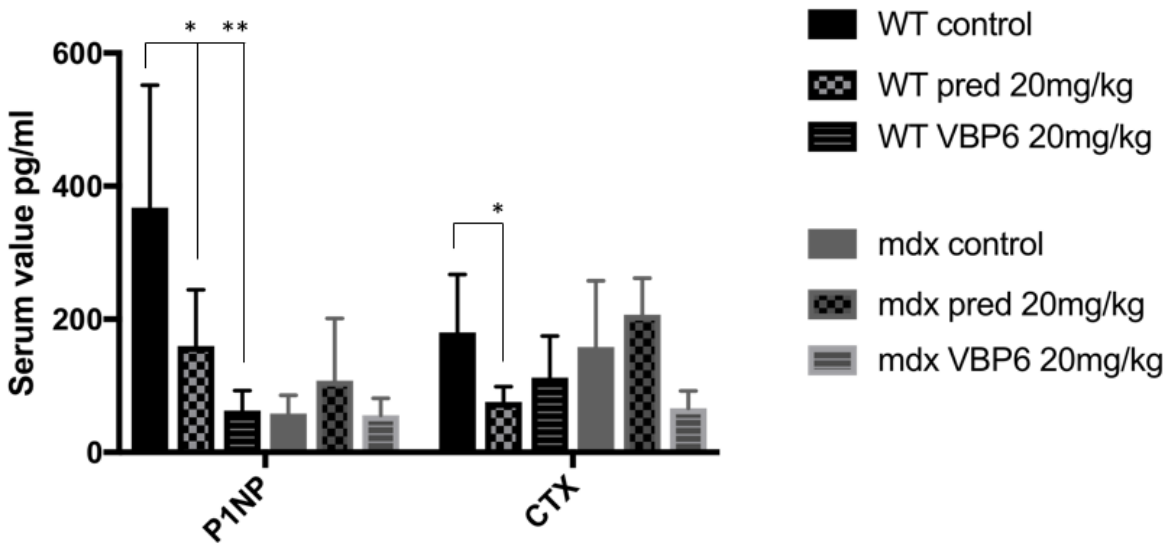

Figure 5-9 Comparison of bone turnover markers in WT and *mdx* mice at 8 weeks-of-age, after 4 weeks of either vehicle, prednisolone 20mg/kg/day or VBP-6 20mg/kg/day, showing the reduction in both P1NP and αCTX in WT mice treated with prednisolone and in αCTX in WT mice treated with VBP-6. Data are presented as mean (+/- standard deviation). * signifies $p<0.05$, ** signifies $p<0.01$ compared to their respective controls. n=6 in each group.

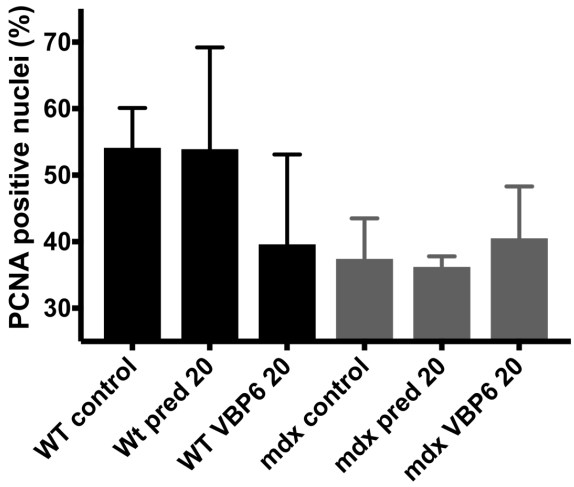

Figure 5-10 The % of PCNA positive nuclei in the proliferating zone of the GP did not vary significantly between the WT or *mdx* mice given syrup and those given either prednisolone (20mg/kg/day) or VBP-6 (20mg/kg/day) for 4 weeks. Data presented are mean +/- standard deviation. n=6 in each group.

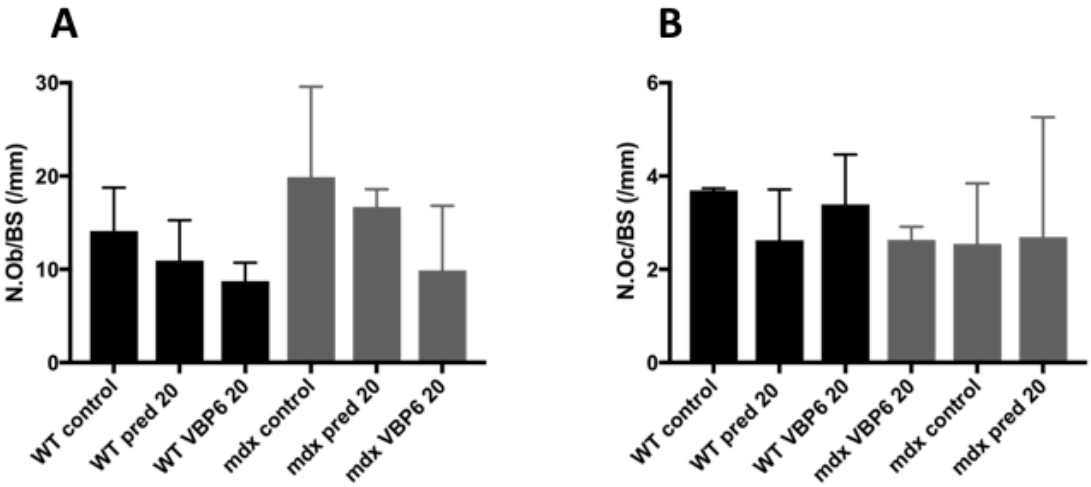

Figure 5-11 Histomorphometric analysis of osteoclast number and osteoblast number in **A)** WT and **B)** *mdx* mice. Data presented are mean +/- standard deviation. n=6 in each group.

A) There was no significant difference in osteoblast number/bone surface by intervention group at 8 weeks-of-age.

B) There was no significant difference in osteoclast number/bone surface by intervention group at 8 weeks-of-age

Parameter	Prednisolone (20mg/kg/day)	VBP6 (20mg/kg/day)
Anthropometry	↓ weight WT (same trend in *mdx:cmah* and *mdx)* CR and tail length unchanged	↑ weight trend in WT and *mdx:cmah* CR and tail length unchanged
Cumulative muscle damage in TA	↓in *mdx:cmah* and same trend in *mdx*	↓in *mdx:cmah* and *mdx*
Grip strength	↑ normalised grip strength in *mdx*	unchanged
Height of growth plate zones	↓total height and PZ in WT	unchanged
Tibial length	↓	unchanged
Trabecular parameters on μCT	↓ trabecular separation in WT and *mdx* ↓ trabecular thickness *mdx:cmah* ↓ SMI in WT ↓ SMI in WT	unchanged
Cortical parameters on μCT	↓ cortical tissue area ↓ cortical bone area ↓ cortical tissue vol ↓ cortical bone vol	unchanged
Tissue mineral density	unchanged	↑ in WT
Biomechanical properties	unchanged	unchanged
Chondrocyte proliferation rate	unchanged	unchanged
Creatine kinase assay	unchanged	unchanged
Bone turnover markers	↓ P1NP and αCTX in WT	
Osteoclast/osteoblast number	Unchanged	unchanged

Table 5-23 Summary of changes after 4 weeks of prednisolone (20mg/kg/day) or 4 weeks of VBP 6 (20mg/kg/day)

5.6 Discussion

Low doses of prednisolone and dexamethasone were initially trialled in this study, based on results of the studies identified by literature review (Wood *et al.* 2018). However, it became clear after the initial pilot studies that juvenile C57BL10 were fairly resistant to GC challenge. Dexamethasone also seemed to be less effective than prednisolone in inducing growth retardation so in the latter stages of the study, dexamethasone regimens were omitted and only higher doses of prednisolone were trialled. Whilst trends for a reduction in longitudinal bone growth, bone resorption and cortical bone fraction were seen at a prednisolone dose of 10mg/kg/day, the mice appeared to tolerate higher doses comfortably and only prednisolone at a dose of 20mg/kg bodyweight daily was sufficient to induce growth retardation and changes in cortical bone in both the C57BL10 WT mice and DMD models over a 28-day period.

Consistent with the improvement in muscle function seen in boys with DMD who take long-term high dose GC (Biggar *et al.* 2006, Manzur *et al.* 2008), and in other studies of GC in animal models of muscular dystrophy (Yoon *et al.* 2016, 2018), this study has demonstrated an improvement in grip strength in juvenile *mdx* mice given 4 weeks of prednisolone at 20mg/kg/day by oral gavage. A reduction in cumulative muscle damage by histological analysis of the TA was also seen in the muscular dystrophy models, which is in keeping with other studies (Yoon *et al.* 2016, 2018). Although no reduction in CK was demonstrated in GC-treated mice during this study, CK is often regarded as a very useful diagnostic biomarker, but not such a reliable pharmacodynamic biomarker, due to intra-individual variability, and exercise-related fluctuation (Szigyarto *et al.* 2018). As the mice in this experiment all had grip strength performed just prior to cull, this may have affected the results to some extent.

Growth retardation was evident in mice given prednisolone at 20mg/kg/day. A significant reduction (46.3%) in the amount of weight gained during the intervention period was seen in the WT mice and the same trend observed in the muscular dystrophy models. This is consistent with other studies, were BW was 4% less in *mdx* mice treated with a prednisolone implant (0.8-1.3mg/kg/day) after 60 days (Novotny *et al.* 2012) and 20% less after 8 weeks of prednisolone treatment (Yoon *et al.* 2016) In addition, tibial length was significantly less in all muscular dystrophy models after

4 weeks of 20mg/kg/day prednisolone and GP height was also significantly less in the WT mice treated with 20mg/kg/day prednisolone .

By contrast, and in accordance with the hypothesis, VBP-6 seemed to protect against the GC-induced growth retardation as no changes were seen in the anthropometric or histological parameters of growth that were assessed during the study. VBP-6 at a dose of 20mg/kg/day was able to improve muscle strength and reduce cumulative muscle damage in the TA of *mdx* and *mdx:cmah* mice, without causing detectable skeletal side-effects. In fact, the mice treated with VBP-6 gained significantly more weight than their syrup fed controls. The absence of growth retardation is in keeping with results from other pre-clinical studies of VBP-15 and further supports the theory that VBP-6 and VBP-15 are able to dissociate the GC-associated side-effects from their efficacy (Baudy *et al.* 2012, Damsker *et al.* 2013, Reeves *et al.* 2013).

The negative effects of GC on bone growth and strength are well described in patients with DMD (Larson *et al.* 2000, Bianchi *et al.* 2003, Joseph *et al.* 2019). In this study, the administration of 4 weeks of prednisolone at 20mg/kg/day to both WT and muscular dystrophy mice has consistently demonstrated a reduction in cortical bone volume, tissue volume and cortical bone fraction. In addition, a change in bone modelling/remodelling was suggested in the WT mice by a reduction in both bone resorption (CTX) and formation (P1NP) markers. This pattern is common in the later stages of GC treatment in humans; typically an increase in bone resorption is seen initially, follow by a later stage of suppressed bone turnover where markers of bone formation and resorption are often both reduced (LoCascio *et al.* 1990). In keeping with the reduction in cortical bone volume, further evidence for a reduction in longitudinal bone growth was demonstration by the reduction in tibial length seen in the mice given prednisolone. Another study in *mdx* mice also showed a similar effect on cortical bone geometry and tibial length after prednisolone administration. They did not assess trabecular bone parameters so a comparison with this study cannot be made (Novotny *et al.* 2012). In addition, a reduction in the polar moment of inertia was demonstrated in all the mice given prednisolone at 20mg/kg/day in this study, which suggests that the smaller bones are less resistant to torsion. These findings have also been replicated in a recent study investigating the use of bisphosphonates in GC-treated *mdx* mice (Yoon *et al.* 2016).

Despite the reduction in cortical bone parameters, no significant changes were noted in biomechanical properties of GC-treated mice as assessed by 3-point bending. It is possible that the reduction in cortical bone geometry was insufficient to cause a reduction in bone strength as assessed by 3-point bending. The study period was short (4 weeks) in comparison to a study where prednisolone was given at a dose of 4.15mg/kg/day by slow release pellet for 8 weeks and changes in both cortical bone geometry and mechanical bone strength were detected (Yoon *et al.* 2016). However, in another study where prednisolone administration for 60 days at a dose of 0.8-1.3mg/kg/day via slow release pellet resulted in an 8% reduction in cortical bone area, only ultimate load was affected and no other changes in biomechanical properties or bone density were seen (Novotny *et al.* 2012). It is therefore possible that μCT is more sensitive to identifying changes than biomechanical testing by 3-point bending.

The effects of GC on trabecular bone parameters were not consistent with the observed cortical changes. In fact trabecular number and connectivity were increased and trabecular separation decreased in both the WT and *mdx* mice after 4 weeks of prednisolone 20mg/kg/day therapy. In keeping with this, there was no reduction seen in either osteoclast or osteoblast number in the metaphyseal bone, which would have been expected as GC are known to affect both bone modelling/remodelling in humans.

Similar to the results of this study, when prednisolone was given alone to *mdx* mice as a control in an interventional study of vitamin D and pamidronate administration, one study group also found an improvement in trabecular bone parameters with a large increase in number of trabeculae that were more closely spaced (Yoon *et al.* 2018). The same study group found that osteoclast number per bone surface increased after 8 weeks of GC treatment in mdx mice but that there was no change in osteoblast number (Yoon *et al.* 2016). It is possible that osteoblast activity may be affected without an actual decrease in osteoblast number in metaphyseal bone, which may explain why CTX and P1NP concentrations were reduced after GC treatment without observed changes in osteoclast or osteoblast number in this study. Alternatively, if the cortical bone had been assessed instead, then the findings may have been different. Furthermore, the static histomorphometry was only carried out

at the time of cull (8 weeks of age), when growth rate had slowed anyway and mice were post-pubertal. Therefore it is possible that if the same data were collected earlier during the intervention period, changes may have been seen.

Unlike in human studies of GIO where there is a plethora of data to show that GCs predominantly affect trabecular bone (Van Staa *et al.* 2002), especially in the short term after exposure, there is less evidence for this phenomenon in mice. In fact, consistent with the data shown in this chapter, several studies have only demonstrated changes to cortical bone after GC exposure in mice. A recent study where prednisolone was given via an osmotic pump at an equivalent dose of 11mg/kg/day to 12-week old female C57BL6 mice reported a small but significant effect of prednisolone on tibial cortical bone (decreased cortical area, cortical thickness, cortical bone volume and polar moment of inertia), but no effect on trabecular tibial volumetric bone density (Bergström *et al.* 2018). A similar study investigating the effects of prednisolone on femoral bone also found that there was no effect on trabecular bone (Abe *et al.* 2016). There are studies using older C57BL6 mice that have demonstrated trabecular changes in vertebrae (Rauch *et al.* 2010) suggesting that GC effects on trabecular bone may be site as well as age-specific. The subtle increase in trabecular bone in combination with a reduction in cortical content and thickness has also been observed in a study where female C57BL6 mice were treated with dexamethasone for 2.5 weeks (Grahnemo *et al.* 2015). Here, the increase in trabecular bone density was attributed to alterations in the lymphocyte populations and suggested that GC administration resulted in a redistribution of bone from the cortical to trabecular compartments. Within the time constraints of this project it was not possible to investigate this in greater detail which would have required the use of a bone tracer to determine the redistribution of bone.

There are also marked strain differences between mouse models in their susceptibility to GIO. The muscular dystrophy mouse models used in this project were all bred on a C57BL10 genetic background. It is known that the C57BL6 mice represent a challenging strain in in which to try and induce osteopaenia and therefore it is likely that similar problems will also be encountered in the C57BL10 mice. Several studies have found that the frequently measured parameters consistent with GIO do not change in C57BL6 mice but do in other strains, for example CD1 and Swiss-Webster

mice (Lane *et al.* 2006). C57BL6 mice are already known to have a low skeletal mass and trabecular bone content at the metaphysis compared to other strains (Judex *et al.* 2004), therefore it is likely that the C57BL10 mice also exhibit a similar phenotype. This will likely make it harder to elicit a phenotype. As already discussed in Chapter 4, this is a particular limitation in the proximal tibia of young mice. If the metaphyseal tissue volume comprises only 6-8% of trabecular bone, this will contain only a few trabecular profiles and it is possible that there will be insufficient power to detect a difference. There may also be mechanisms that prevent GIO in younger mice that only become more apparent with age, for example the shift from osteoblastogenesis towards adipogenesis in the bone marrow of the older mice may make them more susceptible to GC-effects (Bethel *et al.* 2013).

Since this project began, preliminary data assessing the impact of vamorolone (renamed from VBP15) on bone health in 48 children with DMD treated for 2 weeks as part of an open-label phase IIa multiple ascending dose study has been released. These have shown a significant decrease in CTX, P1NP and osteocalcin (at highest dose only) after vamorolone use, but with a reduced potency in decreasing bone formation markers relative to prednisolone, coupled with a dose-related reduction in bone resorption (in contrast to prednisolone). The exploratory biomarker study also showed an increase in IGFBP3 at all doses, but a decrease in IGFBP2 (Conklin *et al.* 2018). These data suggest the potential for improvement in bone safety with vamorolone compared to traditional GC This present study has demonstrated that VBP-6 at a dose of 20mg/kg/day by oral gavage is capable of rescuing cumulative muscle damage in the TA of *mdx* mice without the negative effects on cortical bone geometry that were seen when using prednisolone at an equivalent dose. No change in CTX (bone resorption) was seen, but there was a reduction in P1NP levels after 4 weeks of treatment, suggesting a reduction in bone formation. This is consistent with the human studies, where a reduction in bone formation markers were also seen (Conklin *et al.* 2018). The pre-clinical findings provide additional and supportive data to suggest the efficacy of VBP-6/15 as a GC-sparing agent.

As the *mdx:cmah* mouse demonstrated a paradoxical increase in growth rate during weeks 3-5, which equate to human ‘childhood’ (Chapter 3) and did not show any defect in skeletal development (Chapter 4), this model was not felt to be an

appropriate one to take forward to the interventional studies. It did however, as the results in this chapter demonstrate, behave in a similar way to the *mdx* mouse when GC were administered. As the *mdx* is the best characterised mouse model of DMD it was therefore decided to use this model to proceed to the final phase of the study, where GH and IGF-1 will be used in combination to try and rescue the GC-mediated bone and growth phenotype. Based on the results of this chapter, prednisolone will be co-administered by oral gavage at a dose of 20mg/kg/day.

CHAPTER 6

The role of exogenous growth hormone and insulin-like growth factor 1 on the bone and growth of muscular dystrophy mice

6 The role of exogenous GH and IGF-1 on the bone and growth of muscular dystrophy mice

6.1 Introduction

Results from Chapter 5 show that prednisolone given by oral gavage at a dose of 20mg/kg/day to young *mdx* mice mimics the side-effect profile seen when boys with DMD use daily GC therapy as advised in the Standards of Care for DMD. Growth retardation and GIO were demonstrated in juvenile WT and muscular dystrophy mouse models. Although GC-treated DMD does not appear to be associated with an overt GH or IGF-1 deficiency, it is likely that the combination of chronic disease and long-term, high dose GC treatment induce functional GHR resistance or insensitivity (Barkan *et al.* 2000). Despite IGF-1 and GH being clinically available for treatment in children, their combined use in DMD has not been investigated before. Having tested the most appropriate GC regimen to induce growth retardation and GIO, the final study of this project therefore seeks to investigate the efficacy of administering GH and IGF-1 in combination to rescue the GC-induced growth and bone phenotype.

GH is the main regulator of IGF-1 action and together they have many interdependent and synergistic effects, as described in Section 1.4, as well as independent effects. For example, GH stimulates pre-chondrocyte differentiation whilst chondrocytes may be more responsive to IGF-1 (Lindahl *et al.* 1987). Given that they also have contrasting effects on glucose metabolism, combined administration may therefore result in a more effective strategy to improve growth and skeletal development than giving either alone, whilst also limiting the hyperglycaemia/insulin resistance or hypoglycaemia that are associated with individual administration of GH or IGF-1, respectively (Janssen 2009) Co-administration has been shown to have an additive effect in studies of rats with chronic renal failure and GH deficiency as well as in humans with caloric restriction and children with idiopathic short stature (Kupfer *et al.* 1993, Clark *et al.* 1995, Fielder *et al.* 1996, Backeljauw *et al.* 2015). If the *in vivo* studies described in this chapter are successful, this work could be carried forward to clinical trials in patients with DMD.

6.2 Hypothesis

Exogenous GH and IGF-1 given in combination for 4 weeks is able to rescue the GC-induced skeletal impairment and growth retardation in *mdx* mice.

6.3 Aims

1. Compare parameters of muscle function
2. Compare gross growth rates
3. Assess rates of growth within the growth plate
4. Assess bone structure and density
5. Assess biomechanical properties of bone.

The studies will compare 6-8 male *mdx* mice in three different groups:

1) Mice given cherry syrup vehicle by oral gavage, SC injection of vehicle and vehicle (via osmotic pump) from 5 to 9 weeks-of-age.
2) Mice given GC by oral gavage, SC injection of vehicle and vehicle (via osmotic pump) from 5 to 9 weeks-of-age.
3) Mice given a combination of GC by oral gavage, rhGH (via twice daily SC injection) and rhIGF-1 (via osmotic pump) from 5 to 9 weeks-of-age.

6.4 Material and Methods

6.4.1 Administration of GC or vehicle

Pilot studies were performed (see Chapter 5) to investigate the tolerability and efficacy of different regimens of GC in the muscular dystrophy mouse models and their WT controls. Following the pilot studies it was decided to proceed with prednisolone in cherry syrup suspension at 20mg/kg/day, given via oral gavage (or the equivalent volume of cherry syrup as vehicle). Suspensions were made up so that 10ul/g bodyweight were given daily to each mouse. GC was given daily from day 35 (5 weeks-of-age) to cull at day 62-64 (9 weeks-of-age).

6.4.2 Administration of GH and IGF-1 or vehicle

rhGH was given by SC injection at a dose of 3mg/kg twice daily, from day 35 (5 weeks) to cull at day 62-64 (9 weeks-of-age), except for at weekends when only one dose was given daily due to staffing within the BRF. In the animals receiving vehicle the equivalent volume of physiological saline was injected (see Section 2.2.10).

Either rhIGF-1 or the equivalent volume of physiological saline was given by micro-osmotic pump at a dose of 1mg/kg/day, as described in Chapter 2.2.11. The pump was implanted at day 32 and 48 hours was given for wound healing before the SC injections and oral gavages were commenced.

6.4.3 Grip strength

Forelimb grip strength testing was performed using a grip strength meter with a specialized mouse grid (Harvard Biosciences, Massachusetts, USA), either on the day of, or within 24 hours prior to cull. See Chapter 2.3.1 for more details.

6.4.4 Creatine kinase assay

Quantification of serum creatine kinase activity was carried out using a Pointe Scientific kit (Chapter 2.3.3). The change in NADPH absorbance was measured every 30s at 340nm for 4 mins at 25°C and the mean value calculated.

6.4.5 Muscle histology

The tibialis anterior (TA) muscle of the lower hind limb was used to determine muscle necrosis and inflammation and response to intervention. Sections were cut at a width of 6µm and H&E staining was used for histological assessment of muscle pathology, as outlined in Chapter 2.3.2.

6.4.6 Gross body growth parameters

Animals were measured twice weekly from day 32 until cull, by staff in the BRF. Body weight, crown to rump and tail lengths were taken using the same digital weighing scales and a ruler.

6.4.7 Testes weight

Testes were dissected immediately post cull and weighed on the same digital scales for every mouse. A combined weight is presented, alongside a weight normalised to BW.

6.4.8 Analysis of growth plate height

Right tibiae were removed at dissection and fixed in 10% NBF for up to one week. They were then decalcified and embedded in paraffin wax (Chapter 2.4.2). Sections were cut at 6 µm and stained with H&E; further details are given in Chapter 2.4.8. Images were captured using a Zeiss AxioImager brightfield microscope. The growth plate zone heights were measured using Fiji (Schindelin *et al.* 2012). Ten measurements were taken per section and the mean height calculated for each zone.

6.4.9 Micro Computed tomography (µCT)

Left tibiae were dissected and stored at -20°C in water until required. µCT was carried out according to the protocol described in Chapter 2.4.4.

6.4.10 Tibial length measurement

Tibial length was measured using images of the left tibia, obtained by µCT and viewed in Dataviewer, as outlined in Section 2.4.4.

6.4.11 Biomechanical properties assessed by 3-point bending

3-point bending was performed on all left tibiae as soon as possible after μCT analyses, as described in Section 2.4.5.

6.4.12 Assessment of bone turnover markers by ELISA

Blood samples were obtained by cardiac puncture at the time of cull. Serum was extracted and stored at -80°C until required. Serum αCTx and P1NP levels were measured as described in Section 2.4.6.

6.4.13 Static histomorphometry

Static histomorphometry was performed on paraffin-embedded, decalcified sections of proximal right tibiae (Section 2.4.2). A combination of TRAP and fast-red staining was used to enable osteoclasts to be identified . Osteoblasts were identified using Goldners trichome staining, see Section 2.4.8 for further details. The ROI included only metaphyseal trabecular bone and extended from 50um below the GP. Osteoblast and osteoclast number per bone surface were determined using BioqantOsteo v 17.2.6 (Bioquant Image Analysis Corp, Nashville, Tennessee, USA).

6.4.14 Assessment of chondrocyte proliferation rate

IHC for PCNA detection was performed on sections from right proximal tibiae, as described in Section 2.4.11.

6.5 Results

Throughout this chapter, the intervention groups will be referred to as groups 1,2, and 3. These correspond to:

Group 1) 8 *mdx* mice given cherry syrup vehicle by oral gavage, SC injection of saline vehicle and saline vehicle (via osmotic pump) from 5 to 9 weeks-of-age.

Group 2) 6 *mdx* mice given prednisolone (20mg/kg/day by oral gavage), SC injection of saline vehicle and saline vehicle (via osmotic pump) from 5 to 9 weeks-of-age.

Group 3) 6 *mdx* mice given a combination of prednisolone (20mg/kg/day by oral gavage), rhGH (3mg/kg via twice daily SC injection) and rhIGF-1 (1mg/kg/day via osmotic pump) from 5 to 9 weeks-of-age.

6.5.1 Grip strength

Absolute grip strength was higher in the mice in group 3 (prednisolone and rhGH/IGF-1) then in either groups 2 (pred+vehicle) or 1 (vehicle only), $p<0.01$ and $p<0.05$ respectively. When grip strength was normalised to bodyweight, it was significantly greater in both the mice in group 2 ($p<0.01$) and group 3 (16.9% increase, $p<0.05$) compared to those in group 1 who were given vehicle only, see Table 6-1 and Figure 6.1.

6.5.2 Creatine kinase assay

There was no significant change in serum CK levels by intervention group in *mdx* mice at 9 weeks-of-age (Table 6-2). Levels were consistently 3-5 times higher than the serum CK levels seen in the WT mice when measured at 7 weeks-of-age in Chapter 3.

6.5.3 Muscle Histology

Histological analysis of the TA muscle in all 3 groups of mice revealed clear evidence of muscle necrosis with inflammatory infiltration alongside evidence of regeneration with larger, irregular muscle fibres containing central nuclei (Figure 6-2 A, B, C). There were no significant differences in the amount of inflammation or muscle regeneration in group 3 compared to either the *mdx* control mice (group 1) or the *mdx* mice treated with prednisolone in group 2 (Figure 6-2D).

6.5.1 Gross body growth parameters

As also shown in Chapter 5, bodyweight at cull was significantly lower in mice given 4 weeks of prednisolone by oral gavage at a dose of 20mg/kg/day compared to control mice. The same trend was also seen for a reduction in % bodyweight gain in the GC-treated mice, but this did not reach statistical significance. (Table 6-4 and Figure 6-3). The administration of rhGH and rhIGF-1 in group 3 were unable to rescue the GC-induced weight deficit in group 2. Gain in crown-rump length and tail length during the course of the study were also lower in the GC-treated mice in group 2 compared to those given cherry syrup in group 1. In contrast to the BW data, the administration of both rhGH and rhIGF-1 in group 3 was sufficient to rescue the linear growth retardation caused by GC alone in group 2 and cause an overall significant difference in both crown-rump gain and tail length gain growth parameters during the 4 week study period, compared to those given prednisolone alone (CR length gain of 1.35cm in group 3 v 0.64cm in group 2 and tail length gain of 0.95cm in group 3 v 0.32cm in group 2, see Table 6-4 and Figures 6-3 and 6-4.) The gains in tail length and crown-rump in the *mdx* mice from group 3 were not significantly greater than those in group 1, although there was a trend for increased growth rate compared to the controls (Table 6-4 and Figures 6-3 and 6-4.).

6.5.2 Testes weight

There was no significant difference in either testes weight, or testes weight, normalised to BW in *mdx* mice at 9 weeks of age, after 4 weeks of intervention (Table 6.5).

Parameter	Vehicle (1)	Pred+ vehicle (2)	Pred+GH+IGF-1 (3)
Absolute grip strength, g (SD)	103.13 (12.66)	98.46 (17.09)	125.41 (11.60)$^{**, \Delta}$
Grip strength normalised to bodyweight (SD)	3.80 (0.61)	4.66 (0.67)*	5.61 (0.83)**

Table 6-1 Absolute and normalised grip strength data. Data are presented as mean (+/- standard deviation). * denotes $p<0.05$, ** denotes $p<0.01$ when compared to vehicle group, $^{\Delta}$ denotes $p<0.05$ when compared to group 2 (pred + vehicle). n= 8 in group 1, and 6 each in groups 2 and 3.

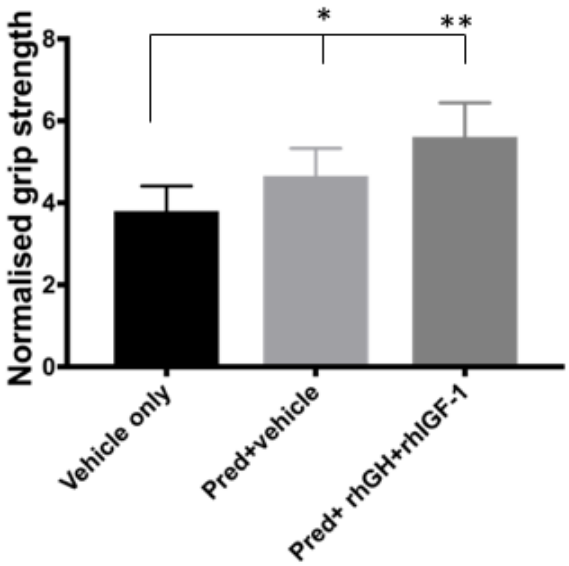

Figure 6-1 Normalised mean grip strength by interventional group, showing the significant increase in grip strength in groups 2 and 3, * denotes $p<0.05$, ** denotes $p<0.01$, compared to group 1(vehicle only). n= 8 in group 1, and 6 each in groups 2 and 3.

Parameter	Vehicle (1)	Pred+ vehicle (2)	Pred+GH+IGF-1 (3)
CK	697.7 (546.9)	916.9 (420.2)	1100.6 (243.5)

Table 6-2 Serum CK levels were similar in all groups of mice at 9 weeks-of-age. Data are presented as mean (+/- standard deviation). n= 8 in group 1, and 6 each in groups 2 and 3.

Parameter	Vehicle (1)	Pred+ vehicle (2)	Pred+GH+IGF-1 (3)
% of inflammatory cells, signifying active cell damage (SD)	2.85 (1.78)	4.35 (2.88)	2.40 (1.88)
% of central nuclei, signifying regeneration (SD)	2.51 (1.65)	2.51 (1.09)	2.73 (1.50)
Cumulative percentage (SD)	5.37 (2.85)	6.86 (2.86)	5.13 (3.16)

Table 6-3 TA muscle pathology in *mdx* mice at 9 weeks-of-age was unchanged in the intervention groups. Data are presented as mean (+/- standard deviation). n= 8 in group 1, and 6 each in groups 2 and 3.

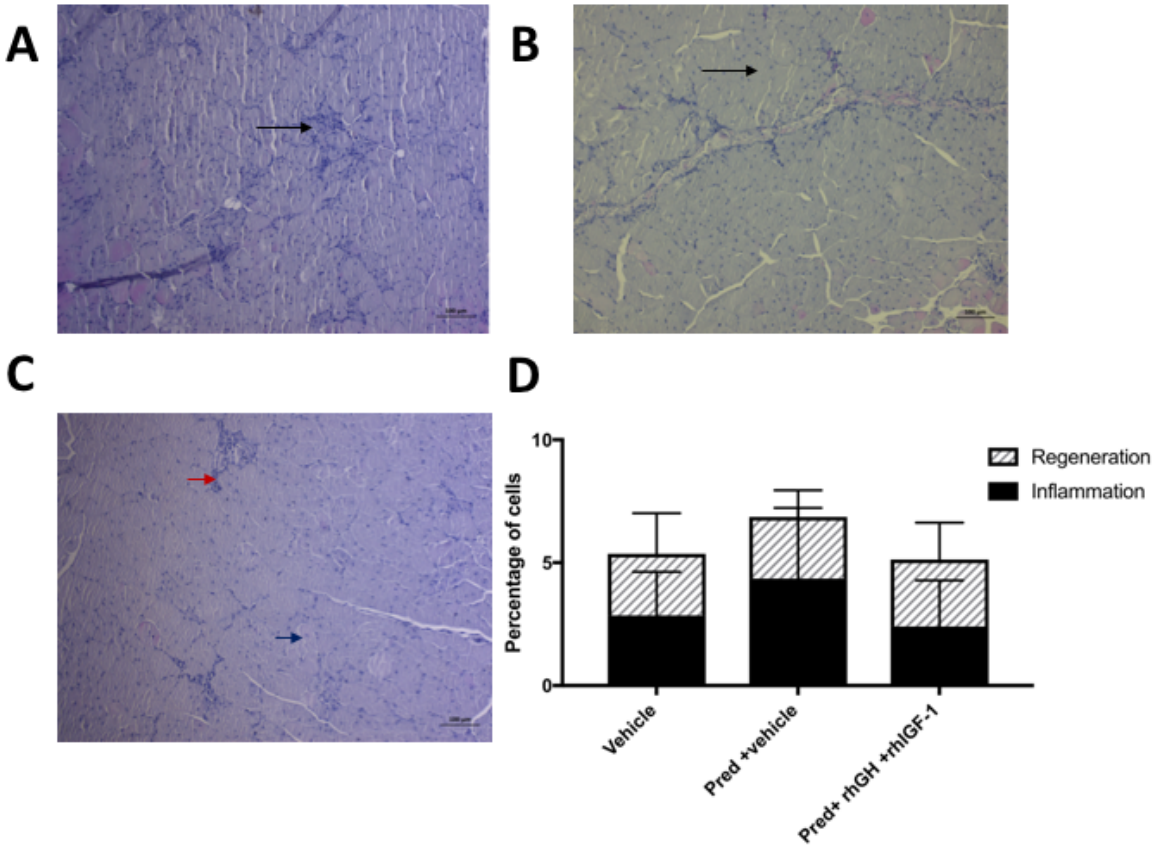

Figure 6-2 TA muscle pathology in *mdx* mice at 9 weeks-of-age in:

A) H&E stained section of TA treated with vehicle only. Black arrow highlighting presence of inflammatory cells.

B) H&E stained section of TA treated with prednisolone and vehicle. Black arrow showing area of regeneration with larger myofibres and central nuclei.

C) H&E stained section of TA treated with daily prednisolone, GH and IGF-1 for 4 weeks showing muscle cell inflammation (red arrow) and regeneration (blue arrow).

D) The number of cells showing muscle cell inflammation and regeneration were similar in all three groups Data are presented as mean (+/-standard deviation).

Parameter	Vehicle (1)	Pred+ vehicle (2)	Pred+GH+IGF-1 (3)
Bodyweight at cull, in g	27.35 (2.42)	21.07 (1.27)***	22.56 (1.71)**
Gain in BW , in %	32.12 (17.20)	27.98 (10.21)	31.90 (13.75)
Gain in crown-rump length, in cm	1.00 (0.65)	0.64 (0.30)	1.35 (0.45) $^{\Delta\Delta}$
Gain in tail length, in cm	0.60 (0.27)	0.32 (0.14)	0.95 (0.40) $^{\Delta\Delta}$

Table 6-4 Change in *mdx* growth parameters during the study period, by intervention group. Data are presented as mean (+/- standard deviation), ** denotes p<0.01, *** denotes p<0.001 compared to group 1, $^{\Delta\Delta}$denotes p<0.01 compared to group 2. n= 8 in group 1, and 6 each in groups 2 and 3.

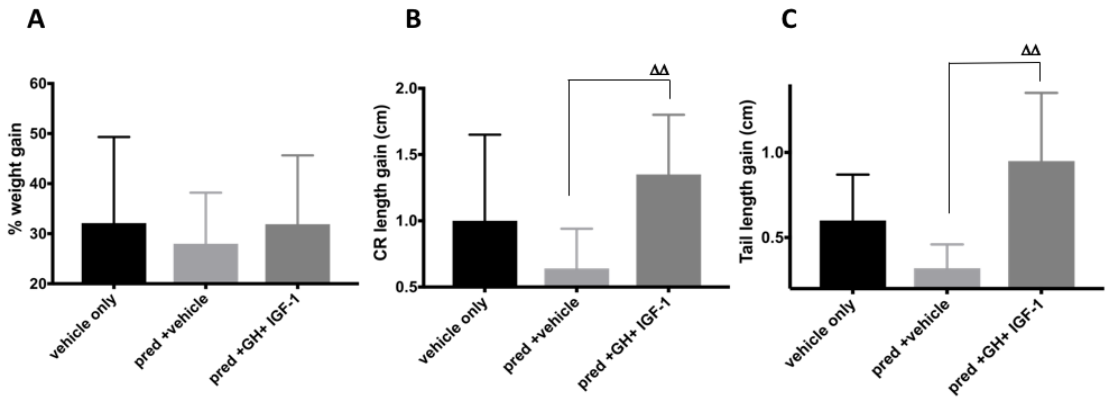

Figure 6-3 Change in *mdx* growth parameters during the study period, by intervention group. Data are presented as mean (+/- standard deviation), $^{\Delta\Delta}$denotes p<0.01 compared to group 2 (pred + vehicle). n= 8 in group 1, and 6 each in groups 2 and 3.

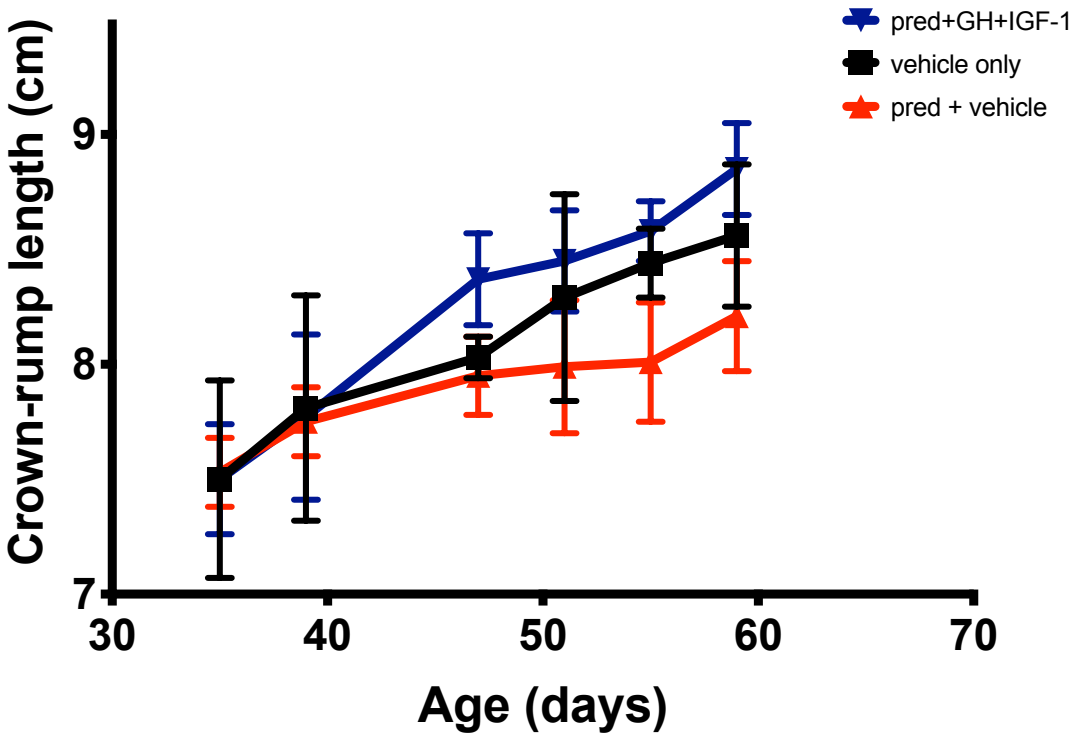

Figure 6-4 Mean crown-rump length at each timepoint during the intervention period showing the growth retardation in the *mdx* mice given prednisolone and the increased growth velocity in the *mdx* mice given rhGH and rhIGF-1 in addition to prednisolone. n= 8 in group 1, and 6 each in groups 2 and 3.

Parameter	Vehicle (1)	Pred+ vehicle (2)	Pred+GH+IGF-1 (3)
Combined testes weight, in g (SD)	0.121 (0.27)	0.112 (0.14)	0.138 (0.40)
Combined testes weight, normalised to BW (SD)	0.0044 (0.002)	0.0054 (0.002)	0.0061 (0.001)

Table 6-5 Combined testes weight in *mdx* mice at 9 weeks-of-age, showing no significant difference by intervention group. Data are presented as mean (+/- standard deviation). n= 8 in group 1, and 6 each in groups 2 and 3.

6.5.3 Analysis of growth plate height

Although there was a trend for greater total GP height and hypertrophic zone height in the mice treated with rhGH and rhIGF-1 (group 3) compared to both groups 1 and 2, as highlighted in the representative images in Figure 6-5, this did not reach statistical significance, see Table 6-6.

6.5.4 Trabecular bone parameters assessed by μCT

Consistent with the data presented in Chapter 5, GC treatment of *mdx* mice caused a reduction in both trabecular thickness and separation, which was unchanged by the addition of GH and IGF-1 in group 3 (Table 6-7). In addition, trabecular number, bone fraction and connectivity were also increased in groups 2 and 3 compared to the GC-naïve group 1, but again the addition of GH and IGF-1 did not materially alter these findings.

6.5.5 Cortical bone parameters assessed by μCT

There were no significant differences in TMD by intervention group; in keeping with the results in Chapter 5, giving prednisolone did not significantly affect TMD (Table 6-8). As also shown in Chapter 5, cortical bone area and bone volume were significantly less in the mice in groups 2 and 3 that were treated with prednisolone at 20mg/kg/day. In keeping with this, cortical bone fraction was also significantly less in these groups (58.8 and 59.4% in groups 2 and 3 respectively compared to 66.2% in group 1, see also Figure 6-8). Cortical tissue area and volume were also smaller in groups 2 and 3. The addition of rhGH and rhIGF-1 in combination to *mdx* mice who were treated with prednisolone did not appear to be able to rescue the cortical bone deficit caused by GC as the cortical bone values in group 3 were very similar to those found in group 2 (Table 6-8 and Figure 6-7).

6.5.6 Tibia length measurement

When tibia length was measured by μCT, bone length was reduced in the mice that received 4 weeks of prednisolone at 20mg/kg/day (groups 2 and 3). The addition of rhGH and rhIGF-1 did not appear to be able to rescue the GC-induced reduction in bone growth (Table 6-9).

Parameter	Vehicle (1)	Pred+ vehicle (2)	Pred+GH+IGF-1 (3)
Height of total growth plate, μm	139.39 (9.34)	139.7 (1.72)	155.96 (16.78)
Height of hypertrophic zone, μm	52.00 (6.71)	55.3 (2.34)	60.52 (7.03)
Height of proliferative zone, μm	75.03 (12.08)	68.55 (7.57)	60.52 (7.05)

Table 6-6 Analysis of overall height and individual growth plate zone heights in *mdx* mice at 9 weeks-of age, showing no significant difference by intervention group. Data are presented as mean (+/- standard deviation). n= 8 in group 1, and 6 each in groups 2 and 3.

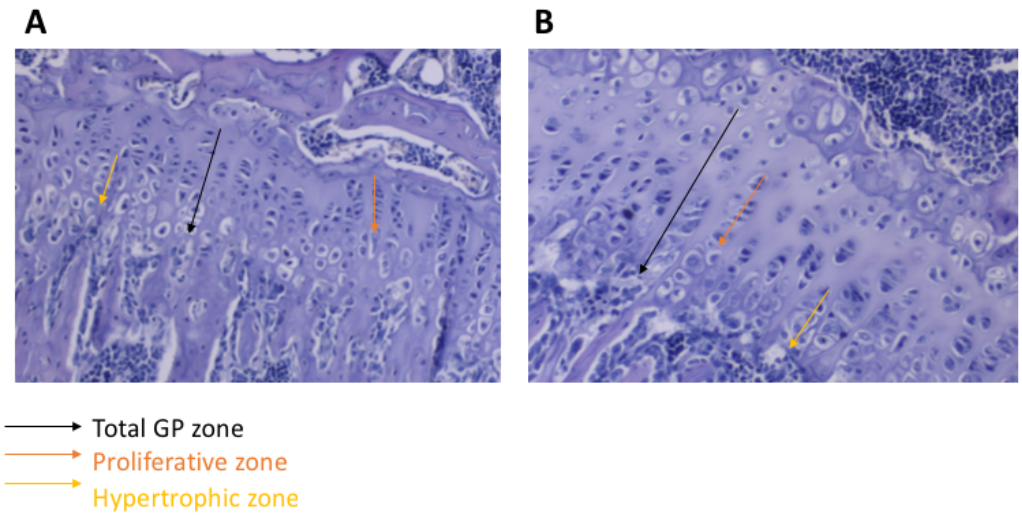

Figure 6-5 Representative H&E stained GP images from:
A) *mdx* mouse from group 2
B) *mdx* mouse from group 3, showing the trend for increase in total GP height and of individual proliferative and hypertrophic zones.

Parameter	Vehicle (1)	Pred+ vehicle (2)	Pred+GH+IGF-1 (3)
TV, mm^3	2.54 (0.21)	2.52 (0.18)	2.69 (0.31)
BV, mm^3	0.45 (0.08)	0.54 (0.05)	0.55 (0.09)
TVBV, %	17.60 (2.18)	21.55 (1.30)**	20.38 (2.37)**
Tb.N, 1/mm	3.63 (0.43)	5.27 (0.52)***	5.15 (0.62)***
Tb.Th, mm	0.05 (0.002)	0.04 (0.002)***	0.04 (0.002)***
Tb.S, mm	0.16 (0.01)	0.12 (0.01)***	0.13 (0.01)***
SMI	1.87 (0.11)	1.80 (0.13)	1.89 (0.14)
Conn	1202 (305)	2460 (545)***	2703 9372)***

Table 6-7 Trabecular bone parameters from μCT in *mdx* mice at 9 weeks-of-age, after either 4 weeks of (1) vehicle only,(2) pred + vehicle or (3) pred+rhGH+rhIGF-1. Data are presented as mean (+/- standard deviation). ** signifies p<0.01, *** signifies p<0.001 compared to control group (1). n= 8 in group 1, and 6 each in groups 2 and 3.

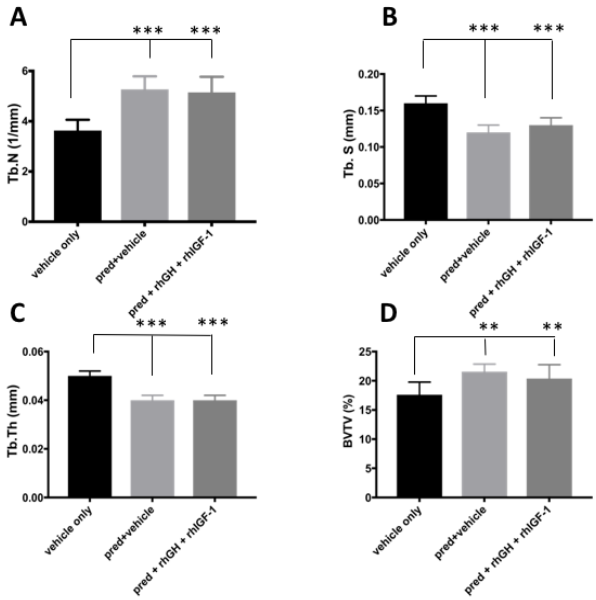

Figure 6-6 Trabecular bone parameters assessed by μCT in *mdx* mice culled at 9 weeks-of-age. A) and B) show an increase in trabecular number and corresponding reduction in trabecular separation in groups 2 and 3 compared to group 1.
C) shows a reduction in trabecular thickness and an overall increase in trabecular bone fraction in groups 2 and 3 compared to control (group 1). Data are presented as mean (+/- standard deviation), ** denotes p<0.01, *** denotes p<0.001 compared to group 1. n= 8 in group 1, and 6 each in groups 2 and 3.

Parameter	Vehicle (1)	Pred+ vehicle (2)	Pred+GH+IGF-1 (3)
TMD g/cm^3	1.28 (0.12)	1.33 (0.10)	1.30 (0.04)
Ct.TAr , mm^2	1.08 (0.05)	0.87 (0.05)***	0.88 (0.09)***
Ps Pm, mm	4.12 (0.44)	3.58 (0.14)**	3.60 (0.19)**
Ct Bar, mm^2	0.71 (0.05)	0.51 (0.03)***	0.53 (0.06)***
Es Pm, mm	2.29 (0.07)	2.28 (0.08)	2.28 (0.12)
Ct.TV, mm^3	0.97 (0.04)	0.78 (0.05)***	0.79 (0.08)***
Ct.BV, mm^3	0.64 (0.04)	0.46 (0.03)***	0.47 (0.06)***
TVBV, %	66.18 (2.20)	58.82 (1.17)***	59.42 (2.68)*
J, mm^4	0.19 (0.06)	0.10 (0.01)	0.11 (0.02)
Ct.Th, mm	0.58 (0.02)	0.57 (0.02)	0.57 (0.03)
Ecc	0.67 (0.08)	0.49 (0.11)*	0.54 (0.12)

Table 6-8 Cortical bone parameters from μCT in *mdx* mice at 9 weeks of age, after either 4 weeks of (1) vehicle only, (2) prednisolone or (3) pred+ rhGH+ rhIGF-1. Data are presented as mean (+/- standard deviation). * signifies p<0.05, *** signifies p<0.001 compared to control group (1). n= 8 in group 1, 6 each in groups 2 and 3.

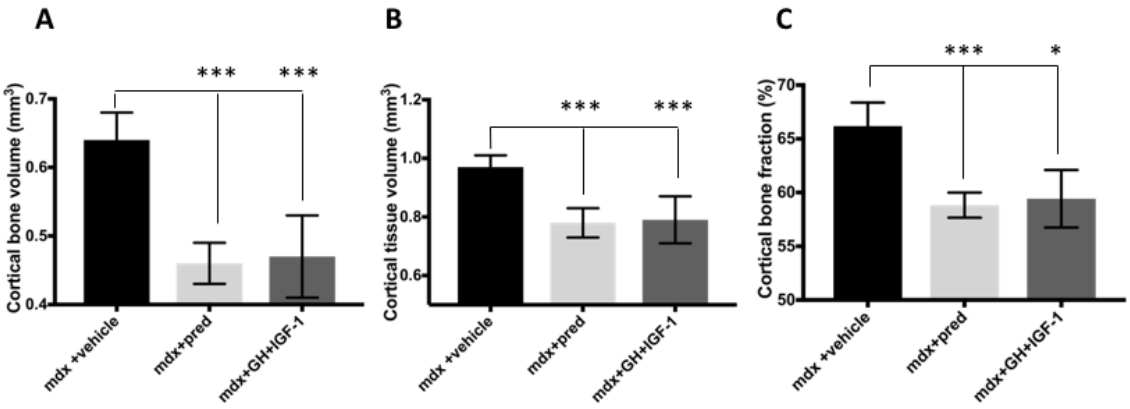

Figure 6-7 Cortical bone parameters assessed by μCT. Data are presented as mean (+/- standard deviation). * denotes p<0.05, *** denotes p<0.001 when compared to group 1. Bar graphs show reduced **A)** cortical bone volume, **B)** cortical tissue volume and **C)** cortical bone fraction in the mdx mice in group 2 who were given 4 weeks of prednisolone compared to group 1. The addition of rhGH and rhIGF-1 in group 3 did not rescue the cortical bone deficit. n= 8 in group 1, and 6 each in groups 2 and 3.

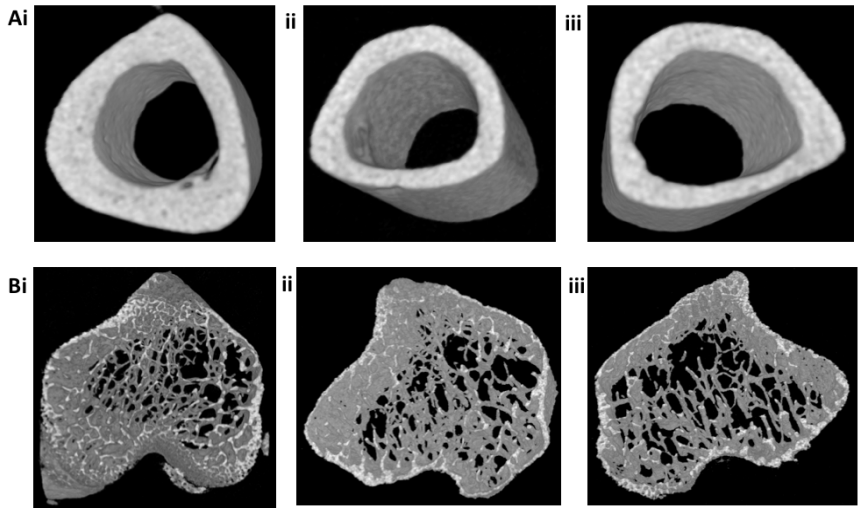

Figure 6-8 Representative μCT images of tibiae from mdx mice at 9 weeks-of-age after 4 weeks of intervention

A) Show mid diaphyseal cortical bone in i) group 1(vehicle only), ii) group 2 (pred and vehicle) and group 3 (pred, rhGH and rhIGF-1)

B) Show metaphyseal trabecular bone in i) group 1(vehicle only), ii) group 2 (pred and vehicle) and group 3 (pred, rhGH and rhIGF-1)

Parameter (SD)	**vehicle (1)**	**pred +vehicle(2)**	**pred+GH+IGF-1 (3)**
Tibial length on μCT, mm	16.91 (0.44)	15.98 (0.36)**	15.87 (0.49)**

Table 6-9 μCT analysis of tibial length in mdx mice at 9 weeks-of-age, by intervention group. Data are presented as mean (+/- standard deviation) ** denotes $p<0.01$ when compared to group 1. n= 8 in group 1, and 6 each in groups 2 and 3.

6.5.7 Biomechanical properties assessed by 3-point bending

There were no significant differences in the biomechanical properties of the *mdx* tibiae by intervention group (Table 6.10). Results for work to maximum load, load at rupture and deflection at rupture are not shown but also displayed the same trends.

6.5.1 Assessment of bone turnover markers by ELISA

There was no significant difference between serum bone turnover markers after the addition of rhGH and rhIGF-1 to GC-treated mice in group 3 (Table 6-11).

6.5.2 Static histomorphometry

There were no significant differences in either osteoclast or osteoblast number/ bone surface by intervention group (Figure 6-10).

6.5.1 Assessment of chondrocyte proliferation rate

There was no significant difference in the percentage of PCNA positive nuclei seen in chondrocytes of the proximal tibial GP of 9-week-old *mdx* mice, irrespective of intervention group (Figure 6-11).

Parameter	vehicle (1)	pred +vehicle(2)	pred+GH+IGF-1 (3)
Maximum load, N	9.06 (2.38)	7.16 (1.84)	6.15 (1.16)
Deflection at max load,	0.65 (0.14)	0.64 (0.17)	0.62 (0.11)
Stiffness, Nm	27423 (7399)	31407 (20054)	17724 (5373)

Table 6-10 Biomechanical properties assessed by 3-point bending in *mdx* mice at 9 weeks of age, by intervention group. Data are presented as mean (+/- standard deviation). n= 8 in group 1, and 6 each in groups 2 and 3.

Parameter	mdx +vehicle (1)	mdx+pred (2)	mdx+pred+GH+IGF-1 (3)
P1NP	59.4 (25.8)	32.5 (21.9)	47.7 (23.4)
αCTX	159.2 (92.0)	224.5 (61.9)	212.9 (81.4)

Table 6-11 Bone turnover markers in *mdx* mice at 9 weeks of age, by intervention group. Data are presented as mean (+/- standard deviation). n= 8 in group 1, and 6 each in groups 2 and 3.

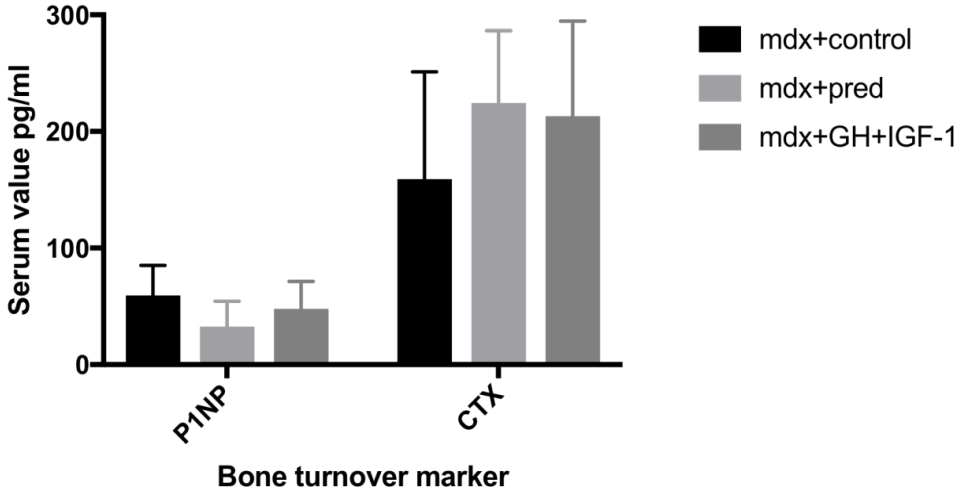

Figure 6-9 Serum bone turnover markers in *mdx* mice at 9 weeks-of-age after 4 weeks of intervention. n= 8 in group 1, and 6 each in groups 2 and 3.

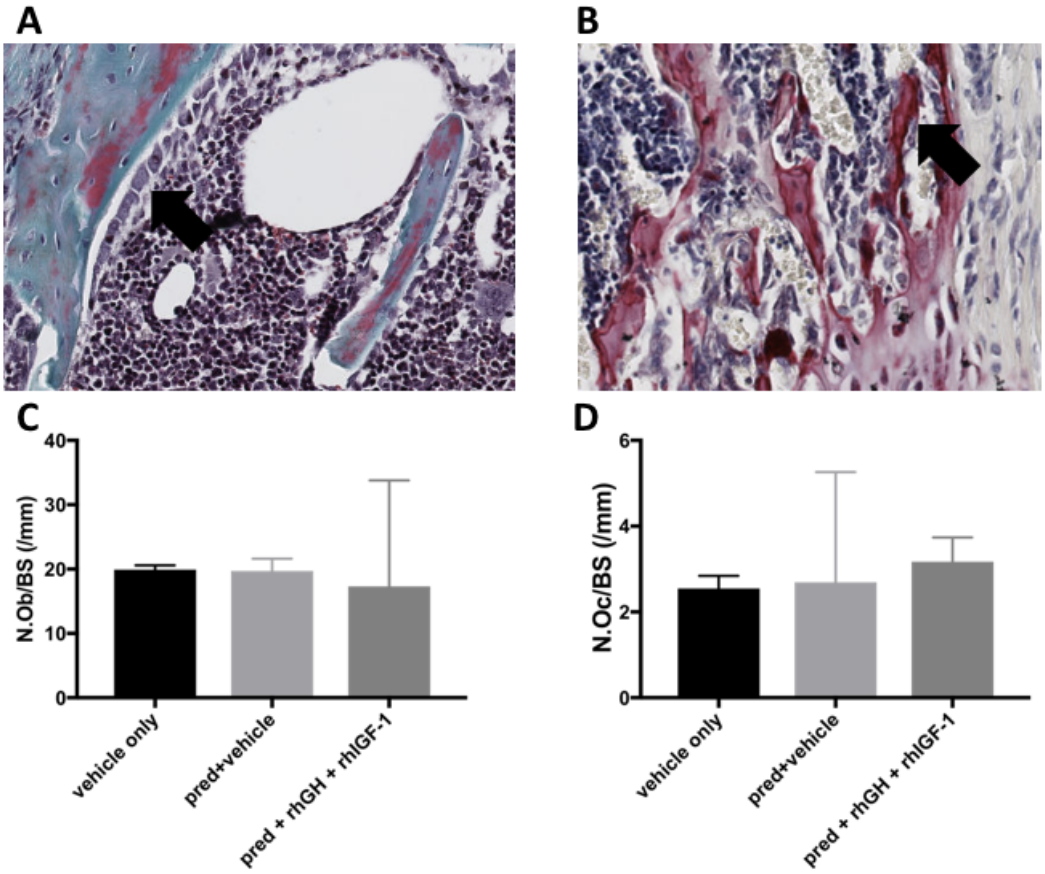

Figure 6-10 Histomorphometric analysis of osteoclast and osteoblast number in *mdx* mice culled at 9 weeks-of-age.

- **A)** Example of Goldners trichome stained section from proximal tibia metaphysis of a 9-week-old *mdx* mouse from group 1 (after 4 weeks of cherry syrup vehicle) showing cuboidal shaped osteoblasts (arrow) on trabecular bone surface.
- **B)** Representative TRAP activity (arrow) and fast-red stained image of trabecular bone from proximal tibia metaphysis of 9-week-old *mdx* mouse from group 1 (after 4 weeks of cherry syrup vehicle).
- **C)** Quantification of osteoblast number/bone surface by intervention group in *mdx* mice culled at 9 weeks-of-age
- **D)** Quantification of osteoclast number/bone surface by intervention group in *mdx* mice culled at 9 weeks-of-age.

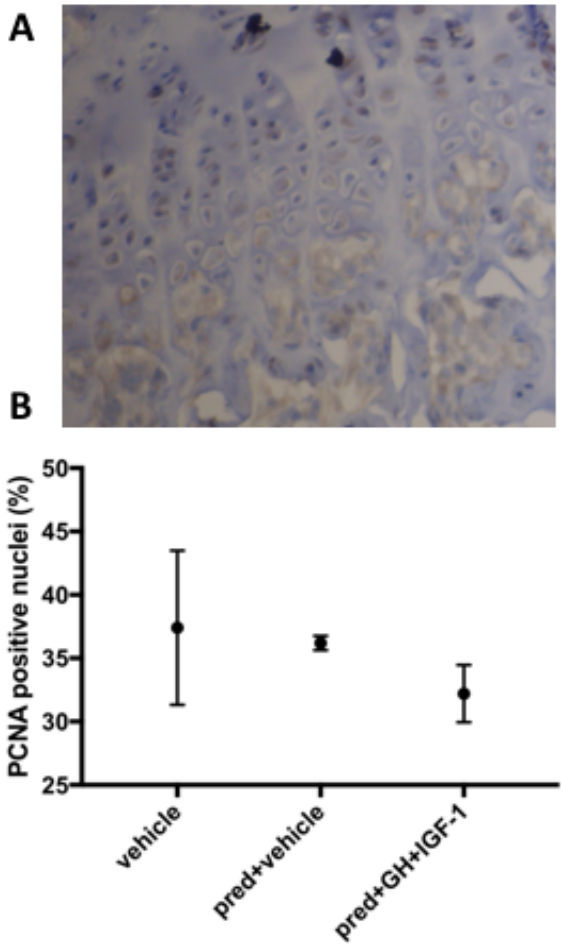

Figure 6-11

A) Representative image from haematoxylin-DAB stained proximal tibial sections of 9 week-old mdx mice after 4 weeks of cherry syrup vehicle only (group 1)

B) a box (mean) and whisker (standard deviation) plot, highlighting the lack of significant difference in the percentage of PCNA positive nuclei by intervention type.

6.6 Discussion

The results of this study suggest that both prednisolone given alone and alongside a combination of rhGH and rhIGF-1 for 4 weeks improves both absolute and BW-normalised grip strength in young adult *mdx* mice. Absolute grip strength data also suggested that there was an additional strength increase in the mice given rhGH and rhIGF-1, compared to those mice given GC alone. Whilst the same trend was also observed in the normalised grip strength data, the difference did not reach statistical significance. This is consistent with a study where rhIGF-1 was given to adult *mdx* mice (aged 5-6 weeks-of-age), for 8 weeks at the same dose as in the current study, which resulted in a 49% increase muscle contraction force (Gregorevic *et al.* 2004).

This study has not demonstrated a change in the muscle necrosis or regeneration parameters measured by histology of the TA. This is in contrast to data from other studies using the *mdx* mouse which have suggested that transgenic over expression of IGF-1 in dystrophic mice led to increased muscle fibre size and number and a reduction in myofibre necrosis (Barton *et al.* 2002, Shavlakadze *et al.* 2004). The results are however in keeping with the study by Gregorevic and colleagues who did not report an increase in myofibre size. In their study they found a 4-fold increase in serum IGF-1 but no change in muscle IGF-1 concentration. This suggests that a muscle-specific targeted over-expression may be required to directly affect myofibre necrosis and subsequent regeneration (Gregorevic *et al.* 2004)

The results in this chapter show an increase in somatic growth rate during 4 weeks of combination rhGH and rhIGF-1 therapy, as demonstrated by increases in both crown-rump length and tail length. Bodyweight gain also showed the same trends, but did not show a statistically significant difference. It is not a surprise that BW gain was not as useful a marker of increased somatic growth compared to crown-rump length and tail length. Bodyweight does not necessarily reflect linear growth (Lupu *et al.* 2001) and has already been described in Chapter 3 as a crude marker of growth at best. GH changes body composition and has been shown to reduce the percentage of fat tissue which may confound any apparent changes in BW gain (Kasukawa *et al.* 2003). The effects of GH on bodyweight also appear to be sexually dimorphic. For example, GH overexpression in transgenic mice had little or no effect on BW at 3 weeks of age

in mice of either sex, and after this point, BW gain was only more marked in the female mice (Eckstein *et al.* 2004). In the current study, there was also a trend towards increased testes weight in group 3 (Table 6-5). The anabolic effects of GH and IGF-1 may have promoted somatic growth of other organs, such as the liver, kidney, thymus and spleen. As this was not the focus of this study, however, organs, apart from the testes were not weighed therefore it is unknown whether the combination therapy had an anabolic effect on organ size.

Despite demonstrating an improvement in somatic growth when juvenile *mdx* mice were treated with 4 weeks of rhGH and rhIGF-1 alongside prednisolone, there was no evidence of an anabolic effect on bone, and GH and IGF-1 given alongside prednisolone were unable to rescue the GC-induced cortical bone phenotype that was clearly demonstrated in Chapter 5 and has been replicated here (Table 6-8 and Figure 6-7). There is robust evidence for the anabolic effects of IGF-1 on skeletal development *in vitro* (Zhang *et al.* 2002, Oh *et al.* 2003). However, the relative importance of local versus systemic IGF-1 in bone turnover and formation is less clear *in vivo*, and in particular, the evidence of an anabolic bone effect in rodents is conflicting. For example, systemic IGF-1 administration partially rescued the bone phenotype in the GH receptor deficient mouse by improving cortical bone thickness without an impact on trabecular bone (Yakar *et al.* 2002). Another study showed that IGF-1 infusion into ovariectomised rats increased trabecular bone turnover and cortical porosity, resulting in reduced BMC (Ibbotson *et al.* 2009). Others have demonstrated an increased bone formation rate (Ammann *et al.* 1993, Mueller *et al.* 1994). Interestingly, in a further study the increased bone formation rate in osteocalcin/IGF-1 transgenic mice was not associated with an increased number of osteoblasts, osteoclasts or osteocytes. The authors therefore concluded that individual osteoblast activity must be increased (Zhao *et al.* 2000).

The absence of an increase in bone turnover markers in this study is also consistent with other studies where a reduction in bone turnover markers was reported in GH over-expressing transgenic mice (Eckstein *et al.* 2004). In humans, IGF-1 at high doses has been shown to increase biochemical markers of bone turnover, but at low doses, the effect seems to be limited to osteoblast function, without a corresponding

effect on bone resorption (Grinspoon *et al.* 1996). Serum markers also only provide indirect evidence of bone formation and resorption rates.

No significant differences were seen in either osteoclast or osteoblast number per bone surface by intervention type, and chondrocyte proliferation rate within the GP remained unchanged between any of the intervention groups. There were also no differences in biomechanical properties assessed by 3-point bending. It is unclear why there were no changes in osteoblast or osteoclast number or chondrocyte proliferation rate within the GP in the mice treated with a combination of GH and IGF-1 as both hormones are known to influence osteoblast growth and differentiation (Zhao *et al.* 2000). IGF-1 acts as a systemic and local regulator of osteoblast function (Gazzerro *et al.* 2006). IGF-1 dimerizes on ligand binding and undergoes autophosphorylation, leading to the activation of insulin receptor substrates IRS1 and 2. IGF-1 stabilises the β-catenin enhancing Wnt dependent activity by inducing PI3K and activating Wnt (Playford *et al.* 2000). Systemic IGF-1 appears to contribute more to cortical bone integrity while local IGF-1 seems to have a greater role in trabecular bone development (Wu *et al.* 2009).

It may be that higher doses of either hormone or both would be required to induce an anabolic bone effect. The dose response effect of combined GH and IGF-1 intervention may also be more complex due to the concomitant administration of GCs. GC cause osteoporosis by inhibiting Wnt signaling (Canalis *et al.* 2007). GC also decrease IGF-1 transcription in osteoblasts (Delany *et al.* 2001). The GR also binds STAT5 and therefore interferes with downstream GH signaling and acts as a functional GH antagonist (Herrington *et al.* 2001). It may be that the circulating levels of GC in this study were such that the addition of GH and IGF-1 at the levels used within this study was insufficient to provide an anabolic stimulus to bone. Although it was outside the remit of this project, it would have been interesting to have an additional intervention group to investigate the role of combined GH and IGF-1 administration without GC. Prolactin and GH also have similar tertiary structures and human GH also binds to the prolactin receptor in mice. It is not possible from the experiments carried out in this study to differentiate between the actions of GH and prolactin.

It is also possible that the 4-week intervention period was sufficient to demonstrate somatic growth promoting effects, but insufficient to enhance longitudinal bone growth; sensitivity to GH in target tissues is known to be time and tissue-dependent (Kasukawa *et al.* 2003). There is a critical post-weaning growth spurt in mice, with initiation of GH action at approximately 2 weeks of age. This phase of growth peaks at 25 days and then subsequently declines. Studies have shown that growth retardation in mouse mutants lacking the GH/IGF-1 receptor were most marked during this period (Lupu *et al.* 2001). It is possible, therefore, that if the intervention had started earlier, than larger changes and also anabolic skeletal development may have been observed as well. This was not possible as the animal house stipulated that the mice had to weigh a minimum of 15g prior to pump implantation and therefore, based on the body weights recorded in Chapter 3, the intervention period could not begin until approximately day 35. It is difficult to balance the most appropriate intervention period to identify changes in somatic growth compared to changes in skeletal development (Wood *et al.* 2018). Steady increases in bone parameters of mice are seen until 6 months of age, therefore if the intervention period was extended, then changes in bone may have become apparent (Eckstein *et al.* 2004). Sexually dimorphic patterns in pulsatility in GH secretion also commence at approximately postnatal day 20 (Davey *et al.* 1999). Due to animal house staffing and ethical constraints, the current study was limited to twice daily GH dosing and once at the weekend. This may not mimic normal male mice GH secretion sufficiently to promote growth. In addition, studies of GH transgenic mice have also shown that bone responds to GH excess in a gender-specific manner. For example, total body (weight-adjusted) BMC was increased by 25% in female transgenic mice compared to only 10% in males (Eckstein *et al.* 2004) and effects were marked pubertally. This difference is likely to be a result of the interaction between oestrogens, androgens and GH.

Studies suggest that the long-term growth promoting effects of IGF-1 and GH are related to changes in regulation of IGFBPs but the relationship between IGF-1 concentration and growth rate remains poorly understood. The ALS is thought to be primarily under GH control whilst circulating IGFBP3 levels are probably related to IGF-1 concentrations (Fielder *et al.* 1996). It was not possible within the time and

financial constraints of this study to tease out the differential effects of local and systemic GH and IGF-1 action and GC may further affect GH and IGF-1 bioavailability. Further work to determine the contribution of local and systemic influences would aid mechanistic understanding. For example it would be useful to measure serum levels of IGF-1 as well as IGFBP3 in addition to quantifying levels of IGF-1 and GH within the GP.

After review of the literature (as discussed in Section 6.1), it was felt that the combination of exogenous GH and IGF-1 would be more likely to be effective than giving either agent alone. Furthermore previous studies from the Farquharson group had not demonstrated an effect of exogenous GH on growth in male mice (Dobie *et al.* 2015). Given the time and financial constraints on the project it was decided to initially trial the agents in combination. If they did not show an effect then it would not have been ethically appropriate to test them individually. Given that the combination therapy was able to rescue the longitudinal bone growth caused by GC, but not the cortical bone defect, it is unlikely that the agents acting alone could induce an effect of the same magnitude. If the combination therapy had shown a marked improvement, then the logical next step would have been to try the agents individually.

In conclusion, this study has partly fulfilled the hypothesis of Chapter 6, as rhGH and rhIGF-1 given in combination for 4 weeks is able to rescue the growth retardation in *mdx* mice, but not the GC-induced skeletal impairment.

CHAPTER 7

General discussion and future work

7 General discussion and future work

Duchenne muscular dystrophy is a severe and ultimately fatal X-linked recessive disease. Although progression of DMD can be slowed with the administration of GC, therapy is often associated with growth retardation and skeletal fragility (Biggar *et al.* 2006, Joseph *et al.* 2019). However, it is also clear that growth impairment and fractures are also prevalent in steroid-naïve boys with DMD (Rapaport *et al.* 1991, Larson *et al.* 2000, Matsumoto *et al.* 2017) suggesting that there may be an intrinsic abnormality of growth and skeletal development in DMD (Eiholzer *et al.* 1988, Larson *et al.* 2000). Another study combining both *in-vivo* and clinical data has also suggested that there may be an abnormality of osteoblast function (Rufo *et al.* 2011). To improve understanding of the underlying defect in growth and skeletal development in DMD, there is a critical need for an animal model that closely mimics the clinical features of DMD.

The original and most frequently used animal model of DMD is the *mdx* mouse, but it has significant limitations as its phenotype is much less severe than DMD and it appears to show an increase in muscle strength with age and growth. As described in Chapter 1, there are conflicting data regarding the bone and growth phenotype of the *mdx* and *mdx:utr* mice and the skeletal development of the newer *mdx:cmah* mouse has not been previously characterised. The aim of the first part of this project was therefore to characterise the muscle, growth and bone phenotype of these muscular dystrophy mouse models with the aim of determining whether there is an intrinsic abnormality of skeletal development, and also to determine which model would be the most appropriate to carry forward to the later phases of the project.

As expected, the results presented in Chapter 3 confirmed that all three of the muscular dystrophy mouse models under investigation show a marked muscle phenotype. As well as clear differences seen in the percentage of inflammatory cells seen on TA muscle histology between the muscular dystrophy models and WT mice, serum CK levels, a marker of muscle cell catabolism, were 10-fold higher in the muscular dystrophy models at all time points. In addition there were also age-dependent differences. These were probably a result of the muscle regeneration that was demonstrated histologically to occur to a greater extent in the *mdx* and *mdx*:*utr*

models than in the *mdx*:*cmah* mice, and is consistent with the literature (Turk *et al.* 2005). No evidence of growth retardation was seen in any of the muscular dystrophy mouse models and in fact the *mdx:cmah* displayed an increase in growth velocity consistent with catch-up growth. Additional evidence for catch-up growth in the *mdx:cmah* mouse was found in the transcriptomic results from the osteogenesis PCR array panel, which showed upregulation of several growth factors, including *Igf-1* and *Vegf*α gene expression. This pattern of increased growth during childhood does not mimic the typical DMD growth trajectory and therefore makes the *mdx:cmah* an unsuitable model to take forward for the interventional studies in this project (Eiholzer *et al.* 1988, West *et al.* 2013). However, further studies using the *mdx:cmah* model may shed light on the phenomenon of catch-up growth and have further implications for understanding the putative role of *cmah* in other diseases..

Results from Chapter 4 of this project showed that there was also no consistent evidence of an intrinsic defect in skeletal development which refuted the hypothesis that bone development was impaired in all the DMD models. In fact the *mdx:cmah* mouse showed increased bone turnover with a resultant increase in TMD and cortical bone fraction. This is consistent with the catch up growth and increase in longitudinal growth rate that was seen in Chapter 3 and underscored the need for a suitable GC regimen to induce both growth retardation and osteoporosis prior to testing anabolic agents.

The aim of the second part of the project was therefore to identify a suitable GC regimen which would induce both growth retardation and osteoporosis in juvenile *mdx and mdx:cmah* mice and their wildtype C57BL10 controls. Chapter 5 confirmed that mice on a C57BL10 background were resistant to GC challenge. After trialling several regimens with escalating GC doses, prednisolone given for 4 weeks at a dose of 20mg/kg/day by oral gavage was shown to improve grip strength and reduce cumulative muscle damage whilst replicating the adverse effects of short stature and osteoporosis that are common side-effects in GC-treated patients with DMD. Prednisolone given by oral gavage at a dose of 20mg/kg/day caused a reduction in longitudinal bone growth and cortical bone development with an associated reduction in both bone resorption and bone formation when assessed by serum bone turnover markers. Despite the high doses, however, this regimen was not able to induce a

reduction in trabecular bone and in fact trabecular number and connectivity were increased and trabecular separation decreased in both the WT and *mdx* mice after 4 weeks of GC therapy. The potential reasons for this have been discussed in Chapter 5 and the results are in keeping with other similar studies of GC-treated *mdx* mice (Yoon *et al.* 2016, 2018, 2019). This highlights the challenge of finding an appropriate pre-clinical model that is able to simultaneously induce both GIO and growth retardation. In addition, mice usually respond to GC by losing weight, whereas long-term high dose GC in boys usually cause changes in body composition and an increase in adiposity and body mass index which lead to changes in bone loading that cannot be similarly replicated in mice (Weber *et al.* 2018). Whilst pre-clinical models can provide a very useful means to test new agents and underlying mechanisms, it is important to recognise the translation limitations of this mouse model when investigating the efficacy of exogeneous GH and IGF-1 in the later phase of this project.

In addition to finding a tolerable GC regimen that was able to induce skeletal changes, the role of VBP-6 as a GC-sparing agent was also evaluated. Data from this study confirm that VBP-6 was able to improve muscle strength and reduce cumulative muscle damage in *mdx* and *mdx:cmah* mice, without causing detectable skeletal side-effects. An analogue of VBP-6 (VBP-15 or vamorolone) is currently being investigated in a phase 2 clinical trial, and in keeping with the data reported here, early results have suggested an improvement in bone safety with vamorolone compared to traditional GC (Conklin *et al.* 2018). If vamorolone continues to cause stabilisation of muscle strength in combination with an acceptable safety profile in the current phase 2b studies, then it could potentially offer a life-changing alternative to the current GC regimens that are used in DMD.

However, until a GC-sparing agent, such as vamorolone, is shown to be as effective as the traditional GCs in DMD, then the long-term use of prednisolone or deflazacort will remain part of the Standards of Care and bring with them the adverse effects on the skeleton. The final interventional study in this project was designed to evaluate the effect of exogenous GH and IGF-1 on bone and growth, when given in combination to GC-treated juvenile *mdx* mice. This study showed that a combination of exogenous GH and IGF-1, when given concomitantly with 4 weeks of prednisolone,

was able to rescue the growth defect but did not improve the GC- induced cortical bone defects.

7.1 Areas for future research

The assessment of BMAT in Chapter 4 provided some very interesting and unexpected findings. Analysis of BMAT by μCT showed a significant increase in rBMAT in both the *mdx* and *mdx:cmah* mice but a marked decrease in cBMAT. The causes and consequences of this alteration in BMAT in the muscular dystrophy mouse models, as well as its clinical relevance, warrant further investigation. It would be interesting to look at the marrow compartment in patients with DMD and see if there are similar differences. Altered BMAT may also have a useful prognostic role in DMD and future studies should explore these possibilities.

The results in Chapter 6 suggested that a combination of rhGH and rhIGF-1 at the doses used were able to rescue the growth retardation caused by GC, but not the cortical bone defect. It remains unclear whether an increased dose or length of study may have unmasked anabolic effects to the skeleton. Future studies could be carried out with incremental regimens of GH and IGF-1 and the duration could also be increased. It is also possible that individual use of the agents may have produced similar results but given the time and financial constraints of this project it was not possible to investigate this further. However, there are always inherent limitations regarding the generalisability of pre-clinical work with mouse models. Given that rhIGF-1 and rhGH are available clinically, under specific conditions, for the treatment of short stature in children, it may now be appropriate to consider designing a small pilot clinical study to evaluate the safety and tolerability of combination GH and IGF-1 therapy in a small group of patients with DMD.

The introduction to this project highlighted the importance of identifying a suitable anabolic agent to treat the GIO and GC-induced growth retardation in DMD. There are other compounds that could be tested in the GC-treated *mdx* mouse model, which may be effective in addition to exogenous GH and IGF-1. These include compounds such as sclerostin antibody therapies, which reverse the Wnt pathway antagonism effects of sclerostin (McClung 2017) or selective oestrogen receptor modulators (Gennari *et al.* 2007). Tamoxifen has already been shown to improve the muscle

pathology in the *mdx* but the effects on the skeleton have not been determined (Dorchies *et al.* 2013).

In summary, for as long as GC remain part of the Standards of Care, finding an appropriate anabolic agent for the treatment of GIO and GC-induced growth retardation will remain a clinical priority in the management of DMD.

CHAPTER 8

References

8 References

van ‘t Hof, RJ, 2012. Analysis of Bone Architecture in Rodents Using Microcomputed Tomography. *Methods Mol Biol*, 816, 461–476.

Abe, T, Sato, T, Kokabu, S, Hori, N, Shimamura, Y, Sato, T, and Yoda, T, 2016. Zoledronic acid increases the circulating soluble RANKL level in mice, with a further increase in lymphocyte-derived soluble RANKL in zoledronic acid- and glucocorticoid-treated mice stimulated with bacterial lipopolysaccharide. *Cytokine*, 83, 1–7.

Al-Harbi, TM, Bainbridge, LJ, McQueen, MJ, and Tarnopolsky, MA, 2008. Hypogonadism is common in men with myopathies. *J Clin Neuromuscul Dis*, 9 (4), 397–401.

Alba, M, Fintini, D, and Salvatori, R, 2005. Effects of recombinant mouse growth hormone treatment on growth and body composition in GHRH knock out mice. *Growth Horm IGF Res*, 15 (4), 275–282.

Allen, DB, Mullen, M, and Mullen, B, 1994. A meta-analysis of the effect of oral and inhaled corticosteroids on growth. *J Allergy Clin Immunol*, 93 (6), 967–976.

Allen, DB, 1996. Growth suppression by glucocorticoid therapy. *Endocrinol Metab Clin NA*, 25 (3), 699–717.

Alshaikh, N, Brunklaus, A, Davis, T, Robb, SA, Quinlivan, R, Munot, P, Sarkozy, A, Muntoni, F, Manzur, AY, and Dubowitz Neuromuscular Team, 2016. Vitamin D in corticosteroid-naïve and corticosteroid-treated Duchenne muscular dystrophy: what dose achieves optimal 25(OH) vitamin D levels? *Arch Dis Child*, 101 (10), 957–961.

Ammann, P, Rizzoli, R, Müller, K, Slosman, D, and Bonjour, JP, 1993. IGF-I and pamidronate increase bone mineral density in ovariectomized adult rats. *Am J Physiol*, 265 (5 Pt 1), E770-6.

Anderson, JE, Lentz, DL, and Johnson, RB, 1993. Recovery from disuse osteopenia coincident to restoration of muscle strength in mdx mice. *Bone*, 14 (4), 625–634.

Argetsinger, LS, Campbell, GS, Yang, X, Witthuhn, BA, Silvennoinen, O, Ihle, JN, and Carter-Su’, C, 1993. Identification of JAK2 As a Growth Hormone Receptor-Associated Tyrosine Kinase. *Cell*, 74, 237–244.

Aspden, RM, 2003. Mechanical Testing of Bone Ex Vivo. *In*: *Bone Research*

Protocols. New Jersey: Humana Press, 369–380.

Aubin, JE, 1998. Bone stem cells. *J Cell Biochem*, 72 (S30–31), 73–82.

Bachrach, LK, 2001. Acquisition of optimal bone mass in childhood and adolescence. *Trends Endocrinol. Metab.*, 12 (1), 22–8.

Backeljauw, PF, Kuntze, J, Frane, J, Calikoglu, AS, and Chernausek, SD, 2013. Adult and near-adult height in patients with severe insulin-like growth factor-I deficiency after long-term therapy with recombinant human insulin-like growth factor-I. *Horm Res Paediat*, 80 (1), 47–56.

Backeljauw, PF, Miller, BS, Dutailly, P, Houchard, A, Lawson, E, Hale, DE, Reiner, B, Sperling, MA, and MS316 Study Group, 2015. Recombinant human growth hormone plus recombinant human insulin-like growth factor-1 coadministration therapy in short children with low insulin-like growth factor-1 and growth hormone sufficiency: results from a randomized, multicenter, open-label, paral. *Horm Res Paediat*, 83 (4), 268–79.

Barkan, AL, DeMott-Friberg, R, and Samuels, MH, 2000. Growth hormone (GH) secretion in primary adrenal insufficiency: effects of cortisol withdrawal and patterned replacement on GH pulsatility and circadian rhythmicity. *Pituitary*, 3 (3), 175–179.

Barker, DJP, 2004. The developmental origins of adult disease. *J Am Coll Nutr*, 23 (6 Suppl), 588S–595S.

Baron, J, Huang, Z, Oerter, KE, Bacher, JD, and Cutler, GB, 1992. Dexamethasone acts locally to inhibit longitudinal bone growth in rabbits. *Am J Physiol*, 263 (3 Pt 1), E489-92.

Barton, ER, Morris, L, Musaro, A, Rosenthal, N, Sweeney, HL, and Lee Sweeney, H, 2002. Muscle-specific expression of insulin-like growth factor I counters muscle decline in mdx mice. *J Cell Biol*, 157 (1), 137–147.

Baudy, AR, Reeves, EKM, Damsker, JM, Heier, C, Garvin, LM, Dillingham, BC, McCall, J, Rayavarapu, S, Wang, Z, Vandermeulen, JH, Sali, A, Jahnke, V, Duguez, S, DuBois, D, Rose, MC, Nagaraju, K, and Hoffman, EP, 2012. Δ-9,11 modification of glucocorticoids dissociates nuclear factor-κB inhibitory efficacy from glucocorticoid response element-associated side effects. *J Pharmacol Exp Ther*, 343 (1), 225–32.

Baxter, R, 1988. Characterization of the Acid-Labile Subunit of the Growth Hormone-Dependent Insulin-Like Growth Factor Binding Protein Complex*. *J*

Clin Endocrinol Metab, 67 (2), 265–272.

Beamer, WG, Donahue, LR, Rosen, CJ, and Baylink, DJ, 1996. Genetic variability in adult bone density among inbred strains of mice. *Bone*, 18 (5), 397–403.

Bell, JM, Shields, MD, Watters, J, Hamilton, A, Beringer, T, Elliott, M, Quinlivan, R, Tirupathi, S, and Blackwood, B, 2017. Interventions to prevent and treat corticosteroid-induced osteoporosis and prevent osteoporotic fractures in Duchenne muscular dystrophy. *Cochrane Database Syst Rev*, 1, CD010899.

Bello, L, Gordish-Dressman, H, Morgenroth, LP, Henricson, EK, Duong, T, Hoffman, EP, Cnaan, A, McDonald, CM, and CINRG Investigators, 2015. Prednisone/prednisolone and deflazacort regimens in the CINRG Duchenne Natural History Study. *Neurology*, 85 (12), 1048–1055.

Vande Berg, BC, Malghem, J, Lecouvet, FE, Devogelaer, J-P, Maldague, B, and Houssiau, FA, 1999. Fat conversion of femoral marrow in glucocorticoid-treated patients: A cross-sectional and longitudinal study with magnetic resonance imaging. *Arthritis Rheum*, 42 (7), 1405–1411.

Bergström, I, Isaksson, H, Koskela, A, Tuukkanen, J, Ohlsson, C, Andersson, G, and Windahl, SH, 2018. Prednisolone treatment reduces the osteogenic effects of loading in mice. *Bone*, 112, 10–18.

Bethel, M, Chitteti, BR, Srour, EF, and Kacena, MA, 2013. The changing balance between osteoblastogenesis and adipogenesis in aging and its impact on hematopoiesis. *Curr Osteoporos Rep*, 11 (2), 99–106.

Bianchi, ML, Mazzanti, A, Galbiati, E, Saraifoger, S, Dubini, A, Cornelio, F, and Morandi, L, 2003. Bone mineral density and bone metabolism in Duchenne muscular dystrophy. *Osteoporos Int*, 14 (9), 761–767.

Bianchi, ML, Biggar, D, Bushby, K, Rogol, AD, Rutter, MM, and Tseng, B, 2011. Endocrine aspects of Duchenne muscular dystrophy. *Neuromuscul Disord*, 21 (4), 298–303.

Biggar, WD, Harris, VA, Eliasoph, L, and Alman, B, 2006. Long-term benefits of deflazacort treatment for boys with Duchenne muscular dystrophy in their second decade. *Neuromuscul Disord*, 16 (4), 249–255.

Birnkrant, DJ, Bushby, K, Bann, CM, Alman, BA, Apkon, SD, Blackwell, A, Case, LE, Cripe, L, Hadjiyannakis, S, Olson, AK, Sheehan, DW, Bolen, J, Weber, DR, Ward, LM, and DMD Care Considerations Working Group, 2018. Diagnosis and management of Duchenne muscular dystrophy, part 2: respiratory, cardiac,

bone health, and orthopaedic management. *Lancet Neurol*, 17 (4), 347–361.

Birnkrant, DJ, Bushby, K, Bann, CM, Apkon, SD, Blackwell, A, Brumbaugh, D, Case, LE, Clemens, PR, Hadjiyannakis, S, Pandya, S, Street, N, Tomezsko, J, Wagner, KR, Ward, LM, Weber, DR, and DMD Care Considerations Working Group, 2018. Diagnosis and management of Duchenne muscular dystrophy, part 1: diagnosis, and neuromuscular, rehabilitation, endocrine, and gastrointestinal and nutritional management. *Lancet Neurol*, 17 (3), 251–267.

Blain, AM, Greally, E, McClorey, G, Manzano, R, Betts, CA, Godfrey, C, O'Donovan, L, Coursindel, T, Gait, MJ, Wood, MJ, MacGowan, GA, and Straub, VW, 2018. Peptide-conjugated phosphodiamidate oligomer-mediated exon skipping has benefits for cardiac function in mdx and Cmah-/-mdx mouse models of Duchenne muscular dystrophy. *PLoS One*, 13 (6), e0198897.

Blodgett, FM, Burgin, L, Iezzoni, D, Gribetz, D, and Talbot, NB, 1956. Effects of Prolonged Cortisone Therapy on the Statural Growth, Skeletal Maturation and Metabolic Status of Children. *New Engl J Med*, 254 (14), 636–641.

Bodor, M and McDonald, CM, 2013. Why short stature is beneficial in Duchenne muscular dystrophy. *Muscle Nerve*, 48 (3), 336–42.

Bonifati, MD, Ruzza, G, Bonometto, P, Berardinelli, A, Gorni, K, Orcesi, S, Lanzi, G, and Angelini, C, 2000. A multicenter, double-blind, randomized trial of deflazacort versus prednisone in Duchenne muscular dystrophy. *Muscle Nerve*, 23 (9), 1344–1347.

Bothwell, JE, Gordon, KE, Dooley, JM, MacSween, J, Cummings, EA, and Salisbury, S, 2003. Vertebral fractures in boys with Duchenne muscular dystrophy. *Clin Pediatr*, 42 (4), 353–356.

Bouvard, B, Audran, M, Legrand, E, and Chappard, D, 2009. Ultrastructural characteristics of glucocorticoid-induced osteoporosis. *Osteoporos Int*, 20 (6), 1089–1092.

Bouxsein, ML, Boyd, SK, Christiansen, BA, Guldberg, RE, Jepsen, KJ, and Müller, R, 2010. Guidelines for assessment of bone microstructure in rodents using micro-computed tomography. *J Bone Min Res*, 25 (7), 1468–1486.

Boyce, BF and Xing, L, 2007. The RANKL/RANK/OPG pathway. *Curr Osteoporos Rep*, 5 (3), 98–104.

Braat, E, Hoste, L, De Waele, L, Gheysens, O, Vermeersch, P, Goffin, K, Pottel, H, Goemans, N, and Levtchenko, E, 2015. Renal function in children and

adolescents with Duchenne muscular dystrophy. *Neuromuscul Disord*, 25 (5), 381–7.

Breur, GJ, Vanenkevort, BA, Farnum, CE, and Wilsman, NJ, 1991. Linear relationship between the volume of hypertrophic chondrocytes and the rate of longitudinal bone growth in growth plates. *J Orthop Res*, 9 (3), 348–359.

Bruker, 2017. Analysis of bone by micro-CT General information. *Bruker Micro CT Acad*, 1–41.

Brumsen, C, Hamdy, NA, and Papapoulos, SE, 1997. Long-term effects of bisphosphonates on the growing skeleton. Studies of young patients with severe osteoporosis. *Med*, 76 (4), 266–283.

Bucay, N, Sarosi, I, Dunstan, CR, Morony, S, Tarpley, J, Capparelli, C, Scully, S, Tan, HL, Xu, W, Lacey, DL, Boyle, WJ, and Simonet, WS, 1998. osteoprotegerin-deficient mice develop early onset osteoporosis and arterial calcification. *Genes Dev*, 12 (9), 1260–8.

Buckner, JL, Bowden, SA, and Mahan, JD, 2015. Optimizing Bone Health in Duchenne Muscular Dystrophy. *Int J Endocrinol*, 2015, 928385.

Bucuvalas, JC, Chernausek, SD, Alfaro, MP, Krug, SK, Ritschel, W, and Wilmott, RW, 2001. Effect of insulin like growth factor-1 treatment in children with cystic fibrosis. *J Pediatr Gastroenterol Nutr*, 33 (5), 576–581.

Bulfield, G, Siller, WG, Wight, PA, and Moore, KJ, 1984. X chromosome-linked muscular dystrophy (mdx) in the mouse. *Proc Natl Acad Sci U S A*, 81 (4), 1189–92.

Bushby, K, Muntoni, F, Urtizberea, A, Hughes, R, and Griggs, R, 2004. Report on the 124th ENMC International Workshop. Treatment of Duchenne muscular dystrophy; defining the gold standards of management in the use of corticosteroids. 2-4 April 2004, Naarden, The Netherlands. *Neuromuscul Disord*, 14 (8–9), 526–534.

Bushby, K, Finkel, R, Birnkrant, DJ, Case, LE, Clemens, PR, Cripe, L, Kaul, A, Kinnett, K, McDonald, C, Pandya, S, Poysky, J, Shapiro, F, Tomezsko, J, and Constantin, C, 2010. Diagnosis and management of Duchenne muscular dystrophy, part 2: implementation of multidisciplinary care. *Lancet Neurol*, 9 (2), 177–189.

Bushby, K and Griggs, R, 2011. FOR-DMD. Finding the Optimum Regimen for Duchenne Muscular Dystrophy. An NIH Funded Trial of Steroids [online].

Available from: http://www.parentprojectmd.org.

Canalis, E, Bilezikian, JP, Angeli, A, and Giustina, A, 2004. Perspectives on glucocorticoid-induced osteoporosis. *Bone*, 34 (4), 593–598.

Canalis, E, 2005. The Fate of Circulating Osteoblasts. *New Engl J Med*, 352 (19), 2014–2016.

Canalis, E, Mazziotti, G, Giustina, A, and Bilezikian, JP, 2007. Glucocorticoid-induced osteoporosis: pathophysiology and therapy. *Osteoporos Int*, 18 (10), 1319–1328.

Caplan, AI, 1991. Mesenchymal stem cells. *J Orthop Res*, 9 (5), 641–650.

Cawthorn, WP *et al.*, 2014. Bone Marrow Adipose Tissue Is an Endocrine Organ that Contributes to Increased Circulating Adiponectin during Caloric Restriction. *Cell Metab*, 20 (2), 368–375.

Cawthorn, WP, Scheller, EL, Parlee, SD, Pham, HA, Learman, BS, Redshaw, CMH, Sulston, RJ, Burr, AA, Das, AK, Simon, BR, Mori, H, Bree, AJ, Schell, B, Krishnan, V, and MacDougald, OA, 2016. Expansion of Bone Marrow Adipose Tissue During Caloric Restriction Is Associated With Increased Circulating Glucocorticoids and Not With Hypoleptinemia. *Endocrinology*, 157 (2), 508–521.

Chamberlain, JS, Metzger, J, Reyes, M, Townsend, D, and Faulkner, JA, 2007. Dystrophin-deficient mdx mice display a reduced life span and are susceptible to spontaneous rhabdomyosarcoma. *FASEB J*, 21 (9), 2195–2204.

Chandrasekharan, K, Yoon, JH, Xu, Y, deVries, S, Camboni, M, Janssen, PML, Varki, A, and Martin, PT, 2010. A human-specific deletion in mouse Cmah increases disease severity in the mdx model of Duchenne muscular dystrophy. *Sci Transl Med*, 2 (42), 42ra54.

Chen, G, Deng, C, and Li, Y-P, 2012. TGF-β and BMP Signaling in Osteoblast Differentiation and Bone Formation. *Int J Biol Sci*, 8 (2), 272–288.

Chen, Q, Shou, P, Zheng, C, Jiang, M, Cao, G, Yang, Q, Cao, J, Xie, N, Velletri, T, Zhang, X, Xu, C, Zhang, L, Yang, H, Hou, J, Wang, Y, and Shi, Y, 2016. Fate decision of mesenchymal stem cells: adipocytes or osteoblasts? *Cell Death Differ*, 23 (7), 1128–1139.

Chia, DJ, 2014. Minireview: mechanisms of growth hormone-mediated gene regulation. *Mol Endocrinol*, 28 (7), 1012–25.

Chou, HH, Takematsu, H, Diaz, S, Iber, J, Nickerson, E, Wright, KL, Muchmore, EA,

Nelson, DL, Warren, ST, and Varki, A, 1998. A mutation in human CMP-sialic acid hydroxylase occurred after the Homo-Pan divergence. *Proc Natl Acad Sci U S A*, 95 (20), 11751–6.

Chrysis, D, Ritzen, EM, and Sävendahl, L, 2003. Growth retardation induced by dexamethasone is associated with increased apoptosis of the growth plate chondrocytes. *J Endocrinol*, 176 (3), 331–337.

Cittadini, A, Comi, LI, Longobardi, S, Petretta, VR, Casaburi, C, Passamano, L, Merola, B, Durante-Mangonid, E, and Politano, LSL, 2003. A preliminary randomized study of growth hormone administration in Becker and Duchenne muscular dystrophies. *Eur Heart J*, 24 (7), 664–672.

Clark, RG, Mortensen, DL, and Carlsson, LMS, 1995. Insulin-like growth factor-1 and growth hormone (GH) have distinct and overlapping anabolic effects in GH-deficient rats. *Endocrine*, 3 (4), 297–304.

Clarke, B, 2008. Normal bone anatomy and physiology. *Clin J Am Soc Nephrol*, 3 Suppl 3 (Suppl 3), S131-9.

Clemmons, DR, 1993. IGF binding proteins and their functions. *Mol Reprod Dev*, 35 (4), 368–375.

Cohen, J, Blethen, S, Kuntze, J, Smith, SL, Lomax, KG, and Mathew, PM, 2014. Managing the child with severe primary insulin-like growth factor-1 deficiency (IGFD): IGFD diagnosis and management. *Drugs R D*, 14 (1), 25–9.

Coley, WD, Bogdanik, L, Vila, MC, Yu, Q, Van Der Meulen, JH, Rayavarapu, S, Novak, JS, Nearing, M, Quinn, JL, Saunders, A, Dolan, C, Andrews, W, Lammert, C, Austin, A, Partridge, TA, Cox, GA, Lutz, C, and Nagaraju, K, 2016. Effect of genetic background on the dystrophic phenotype in *mdx* mice. *Hum Mol Genet*, 25 (1), 130–145.

Conklin, LS *et al.*, 2018. Phase IIa trial in Duchenne muscular dystrophy shows vamorolone is a first-in-class dissociative steroidal anti-inflammatory drug. *Pharmacol Res*, 136, 140–150.

Connolly, AM, Keeling, RM, Mehta, S, Pestronk, A, and Sanes, JR, 2001. Three mouse models of muscular dystrophy : the natural history of strength and fatigue in dystrophin- , dystrophin / utrophin- , and laminin a 2-deficient mice. *Neuromuscul Disord*, 11 (8), 703–712.

Cooper, KL, Oh, S, Sung, Y, Dasari, RR, Kirschner, MW, and Tabin, CJ, 2013. Multiple phases of chondrocyte enlargement underlie differences in skeletal

proportions. *Nature*, 495 (7441), 375–378.

Cowin, SC and Cardoso, L, 2015. Blood and interstitial flow in the hierarchical pore space architecture of bone tissue. *J Biomech*, 48 (5), 842–54.

Crockett, JC, Rogers, MJ, Coxon, FP, Hocking, LJ, and Helfrich, MH, 2011. Bone remodelling at a glance. *J Cell Sci*, 124 (Pt 7), 991–8.

Crofton, PM, Ahmed, SF, Wade, JC, Stephen, R, Elmlinger, MW, Ranke, MB, Kelnar, CJH, and Wallace, WHB, 1998. Effects of Intensive Chemotherapy on Bone and Collagen Turnover and the Growth Hormone Axis in Children with Acute Lymphoblastic Leukemia. *J Clin Endocrinol Metab*, 83 (9), 3121–3129.

D'Ercole, AJ, Applewhite, GT, and Underwood, LE, 1980. Evidence that somatomedin is synthesized by multiple tissues in the fetus. *Dev Biol*, 75 (2), 315–28.

Daftary, AS, Crisanti, M, Kalra, M, Wong, B, and Amin, R, 2007. Effect of long-term steroids on cough efficiency and respiratory muscle strength in patients with Duchenne muscular dystrophy. *Pediatrics*, 119 (2), e320-4.

Damsker, JM, Dillingham, BC, Rose, MC, Balsley, MA, and Heier, CR, 2013. VBP15, a Glucocorticoid Analogue, Is Effective at Reducing Allergic Lung Inflammation in Mice. *PLoS One*, 8 (5), 63871.

Dankwa, S, Lim, C, Bei, AK, Jiang, RHY, Abshire, JR, Patel, SD, Goldberg, JM, Moreno, Y, Kono, M, Niles, JC, and Duraisingh, MT, 2016. Ancient human sialic acid variant restricts an emerging zoonotic malaria parasite. *Nat Commun*, 7, 11187.

Davey, HW, Wilkins, RJ, and Waxman, DJ, 1999. STAT5 Signaling in Sexually Dimorphic Gene Expression and Growth Patterns. *Am J Hum Genet*, 65 (4), 959–965.

Deconinck, AE, Rafael, JA, Skinner, JA, Brown, SC, Potter, AC, Metzinger, L, Watt, DJ, Dickson, JG, Tinsley, JM, Davies, KE, and Holloway, R, 1997. Utrophin-dystrophin-deficient mice as a model for Duchenne muscular dystrophy. *Cell*, 90 (4), 717–727.

Deconinck, N and Dan, B, 2007. Pathophysiology of Duchenne Muscular Dystrophy: Current Hypotheses. *Pediatr Neurol*, 36 (1), 1–7.

Delaissé, J-M, Andersen, TL, Engsig, MT, Henriksen, K, Troen, T, and Blavier, L, 2003. Matrix metalloproteinases (MMP) and cathepsin K contribute differently to osteoclastic activities. *Microsc Res Tech*, 61 (6), 504–513.

Delany, AM, Durant, D, and Canalis, E, 2001. Glucocorticoid Suppression of IGF I Transcription in Osteoblasts. *Mol Endocrinol*, 15 (10), 1781–1789.

Dempster, DW, Compston, JE, Drezner, MK, Glorieux, FH, Kanis, JA, Malluche, H, Meunier, PJ, Ott, SM, Recker, RR, and Parfitt, AM, 2013. Standardized nomenclature, symbols, and units for bone histomorphometry: A 2012 update of the report of the ASBMR Histomorphometry Nomenclature Committee. *J Bone Min Res*, 28 (1), 2–17.

Devlin, MJ, 2011. Why does starvation make bones fat? *Am J Hum Biol*, 23 (5), 577–585.

Dobie, R, MacRae, VE, Huesa, C, van't Hof, R, Ahmed, SF, and Farquharson, C, 2014. Direct stimulation of bone mass by increased GH signalling in the osteoblasts of Socs2-/- mice. *J Endocrinol*, 223 (1), 93–106.

Dobie, R, Ahmed, SF, Staines, KA, Pass, C, Jasim, S, MacRae, VE, and Farquharson, C, 2015. Increased linear bone growth by GH in the absence of SOCS2 is independent of IGF-1. *J Cell Physiol*, 230 (11), 2796–2806.

Dorchies, OM, Reutenauer-Patte, J, Dahmane, E, Ismail, HM, Petermann, O, Patthey-Vuadens, O, Comyn, SA, Gayi, E, Piacenza, T, Handa, RJ, Décosterd, LA, and Ruegg, UT, 2013. The Anticancer Drug Tamoxifen Counteracts the Pathology in a Mouse Model of Duchenne Muscular Dystrophy. *Am J Pathol*, 182 (2), 485–504.

Drachman, DB, Toyka, K V, and Myer, E, 1974. Prednisone in Duchenne muscular dystrophy. *Lancet*, 2 (7894), 1409–1412.

Eastell, R, Reid, DM, Compston, J, Cooper, C, Fogelman, I, Francis, RM, Hosking, DJ, Purdie, DW, Ralston, SH, Reeve, J, Russell, RGG, Stevenson, JC, and Torgerson, DJ, 1998. A UK Consensus Group on management of glucocorticoid-induced osteoporosis: an update. *J Intern Med*, 244 (4), 271–292.

Eberwine, J, 1999. Glucocorticoid and Mineralocorticoid Receptors as Transcription Factors. *In*: G. Siegel et al., eds. *Basic Neurochemistry: Molecular, Cellular and Medical Aspects*. Philidelphia: Lippincott-Raven.

Eckstein, F, Weusten, A, Schmidt, C, Wehr, U, Wanke, R, Rambeck, W, Wolf, E, and Mohan, S, 2004. Longitudinal in vivo effects of growth hormone overexpression on bone in transgenic mice. *J Bone Miner Res*, 19 (5), 802–10.

Eiholzer, U, Boltshauser, E, Frey, D, Molinari, L, and Zachmann, M, 1988. Short

stature: a common feature in Duchenne muscular dystrophy. *Eur J Pediatr*, 147 (6), 602–605.

El-Hajj Fuleihan, G, Muwakkit, S, Arabi, A, Daouk, LE, Ghalayini, T, Chaiban, J, and Abboud, M, 2012. Predictors of bone loss in childhood hematologic malignancies: a prospective study. *Osteoporos Int*, 23 (2), 665–674.

Elraiyah, T, Gionfriddo, MR, and Murad, MH, 2015. Acting on black box warnings requires a GRADE evidence table and an implementation guide: the case of teriparatide. *J Clin Epidemiol*, 68 (6), 698–702.

Emery, AE, 1991. Population frequencies of inherited neuromuscular diseases--a world survey. *Neuromuscul Disord*, 1 (1), 19–29.

Emons, J, Chagin, AS, Sävendahl, L, Karperien, M, and Wit, JM, 2011. Mechanisms of Growth Plate Maturation and Epiphyseal Fusion. *Horm Res Paediat*, 75 (6), 383–391.

Escolar, DM *et al.*, 2011. Randomized, blinded trial of weekend vs daily prednisone in Duchenne muscular dystrophy. *Neurology*, 77 (5), 444–452.

Espina, B, Liang, M, Russell, RGG, and Hulley, PA, 2008. Regulation of bim in glucocorticoid-mediated osteoblast apoptosis. *J Cell Physiol*, 215 (2), 488–496.

Everts, V, Delaissé, JM, Korper, W, Jansen, DC, Tigchelaar-Gutter, W, Saftig, P, and Beertsen, W, 2002. The Bone Lining Cell: Its Role in Cleaning Howship's Lacunae and Initiating Bone Formation. *J Bone Min Res*, 17 (1), 77–90.

Fairclough, RJ, Bareja, A, and Davies, KE, 2011. Progress in therapy for Duchenne muscular dystrophy. *Exp Physiol*, 96 (11), 1101–1113.

Farnum, CE, Lee, R, O'Hara, K, and Urban, JPG, 2002. Volume increase in growth plate chondrocytes during hypertrophy: the contribution of organic osmolytes. *Bone*, 30 (4), 574–81.

Feber, J *et al.*, 2012. Skeletal findings in children recently initiating glucocorticoids for the treatment of nephrotic syndrome. *Osteoporos Int*, 23 (2), 751–760.

Ferron, M, Hinoi, E, Karsenty, G, and Ducy, P, 2008. Osteocalcin differentially regulates β cell and adipocyte gene expression and affects the development of metabolic diseases in wild-type mice. *Proc Natl Acad Sci*, 105 (13), 5266–5270.

Fielder, PJ, Mortensen, DL, Mallet, P, Carlsson, B, Baxter, RC, and Clark, RG, 1996. Differential Long-Term Effects of Insulin-Like Growth Factor-I (IGF-I), Growth Hormone (GH), and IGF-I Plus GH on Body Growth and IGF Binding

Proteins in Hypophysectomized Rats. *Endocrinology*, 137 (5), 1913–20.

Florencio-Silva, R, Sasso, GR da S, Sasso-Cerri, E, Simões, MJ, and Cerri, PS, 2015. Biology of Bone Tissue: Structure, Function, and Factors That Influence Bone Cells. *Biomed Res Int*, 1–17.

Frost, HM, 1990. Skeletal structural adaptations to mechanical usage (SATMU): 2. Redefining Wolff's Law: The remodeling problem. *Anat Rec*, 226 (4), 414–422.

Frost, HM, 2003. Bone's mechanostat: A 2003 update. *Anat Rec*, 275A (2), 1081–1101.

Fryburg, DA, 1994. Insulin-like growth factor I exerts growth hormone- and insulin-like actions on human muscle protein metabolism. *Am J Physiol*, 267 (2 Pt 1), E331-6.

van Gaalen, SM, Kruyt, MC, Geuze, RE, de Bruijn, JD, Alblas, J, and Dhert, WJA, 2010. Use of Fluorochrome Labels in In Vivo Bone Tissue Engineering Research. *Tissue Eng Part B Rev*, 16 (2), 209–17.

Gao, X, Tang, Y, Amra, S, Sun, X, Cui, Y, Cheng, H, Wang, B, and Huard, J, 2019. Systemic investigation of bone and muscle abnormalities in dystrophin/utrophin double knockout mice during postnatal development and the mechanisms. *Hum Mol Genet*, epub.

Gazzerro, E and Canalis, E, 2006. Skeletal actions of insulin-like growth factors. *Expert Rev Endocrinol Metab*, 1 (1), 47–56.

Gennari, L, Merlotti, D, Valleggi, F, Martini, G, and Nuti, R, 2007. Selective Estrogen Receptor Modulators for Postmenopausal Osteoporosis. *Drugs Aging*, 24 (5), 361–379.

Girgis, CM, Sher, D, and Seibel, MJ, 2010. Atypical femoral fractures and bisphosphonate use. *N Engl J Med*, 362 (19), 1848–1849.

Girotra, M, Rubin, MR, and Bilezikian, JP, 2007. The use of parathyroid hormone in the treatment of osteoporosis. *Rev Endocr Metab Disord*, 7 (1–2), 113–121.

Giustina, A, Mazziotti, G, and Canalis, E, 2008. Growth hormone, insulin-like growth factors, and the skeleton. *Endocr Rev*, 29 (5), 535–559.

Glatt, V, Canalis, E, Stadmeyer, L, and Bouxsein, ML, 2007. Age-Related Changes in Trabecular Architecture Differ in Female and Male C57BL/6J Mice. *J Bone Min Res*, 22 (8), 1197–1207.

Gordon, KE, Dooley, JM, Sheppard, KM, MacSween, J, and Esser, MJ, 2011. Impact of bisphosphonates on survival for patients with Duchenne muscular

dystrophy. *Pediatrics*, 127 (2), e353-8.

Govoni, KE, Lee, SK, Chung, Y-S, Behringer, RR, Wergedal, JE, Baylink, DJ, and Mohan, S, 2007. Disruption of insulin-like growth factor-I expression in type IIαI collagen-expressing cells reduces bone length and width in mice. *Physiol Genomics*, 30 (3), 354–362.

Grahnemo, L, Jochems, C, Andersson, A, Engdahl, C, Ohlsson, C, Islander, U, and Carlsten, H, 2015. Possible role of lymphocytes in glucocorticoid-induced increase in trabecular bone mineral density. *J Endocrinol*, 224 (1), 97–108.

Gray, SK, McGee-Lawrence, ME, Sanders, JL, Condon, KW, Tsai, C-J, and Donahue, SW, 2012. Black bear parathyroid hormone has greater anabolic effects on trabecular bone in dystrophin-deficient mice than in wild type mice. *Bone*, 51 (3).

Green, H, Morikawa, M, and Nixon, T, 1985. A dual effector theory of growth-hormone action. *Differentiation*, 29 (3), 195–8.

Gregorevic, P, Plant, DR, Leeding, KS, Bach, LA, and Lynch, GS, 2002. Improved contractile function of the mdx dystrophic mouse diaphragm muscle after insulin-like growth factor-I administration. *Am J Pathol*, 161 (6), 2263–2272.

Gregorevic, P, Plant, DR, and Lynch, GS, 2004. Administration of insulin-like growth factor-I improves fatigue resistance of skeletal muscles from dystrophicmdx mice. *Muscle Nerve*, 30 (3), 295–304.

Griggs, RC, Moxley, RT, Mendell, JR, Fenichel, GM, Brooke, MH, Miller, PJ, Mandel, S, Florence, J, Schierbecker, J, and Kaiser, KK, 1990. Randomized, double-blind trial of mazindol in Duchenne dystrophy. *Muscle Nerve*, 13 (12), 1169–1173.

Grinspoon, S, Baum, H, Lee, K, Anderson, E, Herzog, D, and Klibanski, A, 1996. Effects of short-term recombinant human insulin-like growth factor I administration on bone turnover in osteopenic women with anorexia nervosa. *J Clin Endocrinol Metab*, 81 (11), 3864–3870.

Grounds, M, 2014. TREAT-NMD SOP No. DMD_M.1.2.007 Quantification of histopathology in Haemotoxylin and Eosin stained muscle sections [online]. Available from: http://www.treat-nmd.eu/research/preclinical/dmd-sops/.

Gutpell, KM, Hrinivich, WT, and Hoffman, LM, 2015. Skeletal Muscle Fibrosis in the mdx / utrn + / - Mouse Validates Its Suitability as a Murine Model of Duchenne Muscular Dystrophy. *PLoS One*, 3, 1–13.

Hadjidakis, D and Androulakis, I, 2006. Bone Remodeling. *Ann N Y Acad Sci*, 1092 (1), 385–396.

Hales, CN and Barker, DJ, 2001. The thrifty phenotype hypothesis. *Br Med Bull*, 60, 5–20.

Harada, SI, Balena, R, Rodan, GA, and Rodan, SB, 1995. The role of prostaglandins in bone formation. *Connect Tissue Res*, 31 (4), 279–82.

Hartman, ML, Veldhuis, JD, and Thorner, MO, 1993. Normal Control of Growth Hormone Secretion. *Horm Res*, 40 (1–3), 37–47.

Hedlund, M, Tangvoranuntakul, P, Takematsu, H, Long, JM, Housley, GD, Kozutsumi, Y, Suzuki, A, Wynshaw-Boris, A, Ryan, AF, Gallo, RL, Varki, N, and Varki, A, 2007. N-glycolylneuraminic acid deficiency in mice: implications for human biology and evolution. *Mol Cell Biol*, 27 (12), 4340–4346.

Heier, CR *et al.*, 2013. VBP15, a novel anti-inflammatory and membrane-stabilizer, improves muscular dystrophy without side effects. *EMBO Mol Med*, 5 (10), 1569–85.

Helliwell, TR, Man, NT, Morris, GE, and Davies, KE, 1992. The dystrophin-related protein, utrophin, is expressed on the sarcolemma of regenerating human skeletal muscle fibres in dystrophies and inflammatory myopathies. *Neuromuscul Disord*, 2 (3), 177–84.

Hennedige, AA, Jayasinghe, J, Khajeh, J, and Macfarlane, T V., 2013. Systematic Review on the Incidence of Bisphosphonate Related Osteonecrosis of the Jaw in Children Diagnosed with Osteogenesis Imperfecta. *J Oral Maxillofac Res*, 4 (4), e1.

Henneicke, H, Gasparini, SJ, Brennan-Speranza, TC, Zhou, H, and Seibel, MJ, 2014. Glucocorticoids and bone: Local effects and systemic implications. *Trends Endocrinol Metab*, 25 (4), 197–211.

Herrington, J and Carter-Su, C, 2001. Signaling pathways activated by the growth hormone receptor. *Trends Endocrinol Metab*, 12 (6), 252–7.

Herrmann, M, Henneicke, H, Street, J, Modzelewski, J, Kalak, R, Buttgereit, F, Dunstan, CR, Zhou, H, and Seibel, MJ, 2009. The challenge of continuous exogenous glucocorticoid administration in mice. *Steroids*, 74 (2), 245–249.

Hofbauer, LC, Khosla, S, Dunstan, CR, Lacey, DL, Boyle, WJ, and Riggs, BL, 2000. The Roles of Osteoprotegerin and Osteoprotegerin Ligand in the Paracrine Regulation of Bone Resorption. *J Bone Miner Res*, 15 (1), 2–12.

Hofbauer, LC, Zeitz, U, Schoppet, M, Skalicky, M, Schuler, C, Stolina, M, Kostenuik, PJ, Erben, RG, Schüler, C, Stolina, M, Kostenuik, PJ, Erben, RG, Schuler, C, Stolina, M, Kostenuik, PJ, and Erben, RG, 2009. Prevention of glucocorticoid-induced bone loss in mice by inhibition of RANKL. *Arthritis Rheum*, 60 (5), 1427–1437.

Hoffman, EP, Reeves, E, Damsker, J, Nagaraju, K, McCall, JM, Connor, EM, and Bushby, K, 2012. Novel approaches to corticosteroid treatment in Duchenne muscular dystrophy. *Phys Med Rehabil Clin N Am*, 23 (4), 821–8.

Hoffman, EP, Riddle, V, Siegler, MA, Dickerson, D, Backonja, M, Kramer, WG, Nagaraju, K, Gordish-Dressman, H, Damsker, JM, and McCall, JM, 2018. Phase 1 trial of vamorolone, a first-in-class steroid, shows improvements in side effects via biomarkers bridged to clinical outcomes. *Steroids*, 134, 43–52.

Hong, J-H, Hwang, ES, McManus, MT, Amsterdam, A, Tian, Y, Kalmukova, R, Mueller, E, Benjamin, T, Spiegelman, BM, Sharp, PA, Hopkins, N, and Yaffe, MB, 2005. TAZ, a Transcriptional Modulator of Mesenchymal Stem Cell Differentiation. *Science (80-)*, 309 (5737), 1074–1078.

Houston, DA, Staines, KA, Macrae, VE, and Farquharson, C, 2016. Culture of Murine Embryonic Metatarsals: A Physiological Model of Endochondral Ossification Video Link. *J Vis Exp*, 54978 (11810).

Huang, P, Cheng, G, Lu, H, Aronica, M, Ransohoff, RM, and Zhou, L, 2011. Impaired respiratory function in mdx and mdx/utrn+/− mice. *Muscle Nerve*, 43 (2), 263–267.

Huizenga, NATM, Koper, JW, de Lange, P, Pols, HAP, Stolk, RP, Burger, H, Grobbee, DE, Brinkmann, AO, de Jong, FH, and Lamberts, SWJ, 1998. A Polymorphism in the Glucocorticoid Receptor Gene May Be Associated with an Increased Sensitivity to Glucocorticoids in Vivo. *J Clin Endocrinol Metab*, 83 (1), 144–151.

Hunziker, EB, 1994. Mechanism of longitudinal bone growth and its regulation by growth plate chondrocytes. *Microsc Res Tech*, 28 (6), 505–519.

Hunziker, EB, Wagner, J, and Zapf, J, 1994. Differential effects of insulin-like growth factor I and growth hormone on developmental stages of rat growth plate chondrocytes in vivo. *J Clin Invest*, 93 (3), 1078–1086.

Hutchison, MR, Bassett, MH, and White, PC, 2007. Insulin-Like Growth Factor-I and Fibroblast Growth Factor, But Not Growth Hormone, Affect Growth Plate

Chondrocyte Proliferation. *Endocrinology*, 148 (7), 3122–3130.

Ibbotson, KJ, Orcutt, CM, D'Souza, SM, Paddock, CL, Arthur, JA, Jankowsky, ML, and Boyce, RW, 2009. Contrasting effects of parathyroid hormone and insulin-like growth factor I in an aged ovariectomized rat model of postmenopausal osteoporosis. *J Bone Miner Res*, 7 (4), 425–432.

Iida-Klein, A, Lu, SS, Yokoyama, K, Dempster, DW, Nieves, JW, and Lindsay, R, 2003. Precision, accuracy, and reproducibility of dual X-ray absorptiometry measurements in mice in vivo. *J Clin Densitom*, 6 (1), 25–33.

Isaac, C, Wright, A, Usas, A, Li, H, Tang, Y, Mu, X, Greco, N, Dong, Q, Vo, N, Kang, J, Wang, B, and Huard, J, 2013. Dystrophin and utrophin "double knockout" dystrophic mice exhibit a spectrum of degenerative musculoskeletal abnormalities. *J Orthop Res*, 31 (3), 343–349.

Iwamoto, J, Matsumoto, H, Takeda, T, Sato, Y, Liu, X, and Yeh, JK, 2008. Effects of Vitamin K2 and Risedronate on Bone Formation and Resorption, Osteocyte Lacunar System, and Porosity in the Cortical Bone of Glucocorticoid-Treated Rats. *Calcif Tissue Int*, 83 (2), 121–128.

James, KA, Cunniff, C, Apkon, SD, Mathews, K, Lu, Z, Holtzer, C, Pandya, S, Ciafaloni, E, and Miller, L, 2015. Risk Factors for First Fractures Among Males With Duchenne or Becker Muscular Dystrophy. *J Pediatr Orthop*, 35 (6), 640–644.

Janssen, JA, 2009. Advantages and disadvantages of GH/IGF-I combination treatment. *Rev Endocr Metab Disord*, 10 (2), 157–162.

Jarukamjorn, K, Sakuma, T, Jaruchotikamol, A, Ishino, Y, Oguro, M, and Nemoto, N, 2006. Modified expression of cytochrome P450 mRNAs by growth hormone in mouse liver. *Toxicology*, 219 (1–3), 97–105.

Jia, D, O'Brien, CA, Stewart, SA, Manolagas, SC, and Weinstein, RS, 2006. Glucocorticoids act directly on osteoclasts to increase their life span and reduce bone density. *Endocrinology*, 147 (12), 5592–5599.

Jilka, RL, 2013. The relevance of mouse models for investigating age-related bone loss in humans. *Journals Gerontol - Ser A Biol Sci Med Sci*, 68 (10), 1209–1217.

Jones, JI and Clemmons, DR, 1995. Insulin-Like Growth Factors and Their Binding Proteins: Biological Actions. *Endocr Rev*, 16 (1), 3–34.

Joseph, J, Cho, D, and Doles, J, 2018. Metabolomic Analyses Reveal Extensive

Progenitor Cell Deficiencies in a Mouse Model of Duchenne Muscular Dystrophy. *Metabolites*, 8 (4), 61.

Joseph, S, McCarrison, S, and Wong, SC, 2016. Skeletal Fragility in Children with Chronic Disease. *Horm Res Paediat*, 86 (2), 71–82.

Joseph, S, Wang, C, Bushby, K, Guglieri, M, Horrocks, I, Straub, V, Ahmed, SF, and Wong, SC, 2019. Fractures and Linear Growth in a Nationwide Cohort of Boys With Duchenne Muscular Dystrophy With and Without Glucocorticoid Treatment. *JAMA Neurol*.

Joseph, S, Wang, C, Di Marco, M, Horrocks, I, Abu-Arafeh, I, Baxter, A, Cordeiro, N, McLellan, L, McWilliam, K, Naismith, K, Stephen, E, Ahmed, SF, and Wong, SC, 2019. Fractures and bone health monitoring in boys with Duchenne muscular dystrophy managed within the Scottish Muscle Network. *Neuromuscul Disord*, 29 (1), 59–66.

Judex, S, Garman, R, Squire, M, Donahue, L-R, and Rubin, C, 2004. Genetically Based Influences on the Site-Specific Regulation of Trabecular and Cortical Bone Morphology. *J Bone Min Res*, 19 (4), 600–606.

Jux, C, Leiber, K, Hügel, U, Blum, W, Ohlsson, C, Klaus, G, and Mehls, O, 1998. Dexamethasone impairs growth hormone (GH)-stimulated growth by suppression of local insulin-like growth factor (IGF)-I production and expression of GH- and IGF-I-receptor in cultured rat chondrocytes. *Endocrinology*, 139 (7), 3296–305.

Kanis, JA, Johansson, H, Oden, A, Johnell, O, de Laet, C, Melton, LJ, Tenenhouse, A, Reeve, J, Silman, AJ, Pols, HA, Eisman, JA, McCloskey, E V, and Mellstrom, D, 2004. A Meta-Analysis of Prior Corticosteroid Use and Fracture Risk. *J Bone Min Res*, 19 (6), 893–899.

Kao, K-T, Joseph, S, Capaldi, N, Brown, S, Di Marco, M, Dunne, J, Horrocks, I, Shepherd, S, Ahmed, SF, and Wong, SC, 2019. Skeletal disproportion in glucocorticoid-treated boys with Duchenne muscular dystrophy. *Eur J Pediatr*, 1–8.

Karsenty, G and Wagner, EF, 2002. Reaching a genetic and molecular understanding of skeletal development. *Dev Cell*, 2 (4), 389–406.

Karsenty, G, Kronenberg, HM, and Settembre, C, 2009. Genetic Control of Bone Formation. *Annu Rev Cell Dev Biol*, 25 (1), 629–648.

Kasukawa, Y, Baylink, DJ, Guo, R, and Mohan, S, 2003. Evidence that sensitivity to

growth hormone (GH) is growth period and tissue type dependent: studies in GH-deficient lit/lit mice. *Endocrinology*, 144 (9), 3950–7.

Kavaler, S, Morinaga, H, Jih, A, Fan, W, Hedlund, M, Varki, A, and Kim, JJ, 2011. Pancreatic -cell failure in obese mice with human-like CMP-Neu5Ac hydroxylase deficiency. *FASEB J*, 25 (6), 1887–1893.

Kember, NF and Sissons, HA, 1976. Quantitative histology of the human growth plate. *J Bone Joint Surg Br*, 58–B (4), 426–35.

Kim, H-J, Zhao, H, Kitaura, H, Bhattacharyya, S, Brewer, JA, Muglia, LJ, Ross, FP, and Teitelbaum, SL, 2006. Glucocorticoids suppress bone formation via the osteoclast. *J Clin Invest*, 116 (8), 2152–60.

Kim, H-JH-JH-J *et al.*, 2007. Glucocorticoids and the Osteoclast. *Ann N Y Acad Sci*, 1116 (1), 335–339.

Kim, H, Barton, E, Muja, N, Yakar, S, Pennisi, P, and LeRoith, D, 2005. Intact Insulin and Insulin-Like Growth Factor-I Receptor Signaling Is Required for Growth Hormone Effects on Skeletal Muscle Growth and Function *in Vivo*. *Endocrinology*, 146 (4), 1772–1779.

King, CS, Weir, EC, Gundberg, CW, Fox, J, and Insogna, KL, 1996. Effects of continuous glucocorticoid infusion on bone metabolism in the rat. *Calcif Tissue Int*, 59 (3), 184–191.

King, WM, Ruttencutter, R, Nagaraja, HN, Matkovic, V, Landoll, J, Hoyle, C, Mendell, JR, and Kissel, JT, 2007. Orthopedic outcomes of long-term daily corticosteroid treatment in Duchenne muscular dystrophy. *Neurology*, 68 (19), 1607–1613.

Klaus, G, Jux, C, Fernandez, P, Rodriguez, J, Himmele, R, and Mehls, O, 2000. Suppression of growth plate chondrocyte proliferation by corticosteroids. *Pediatr Nephrol*, 14 (7), 612–5.

Ko, J-Y, Chuang, P-C, Chen, M-W, Ke, H-C, Wu, S-L, Chang, Y-H, Chen, Y-S, and Wang, F-S, 2013. MicroRNA-29a ameliorates glucocorticoid-induced suppression of osteoblast differentiation by regulating β-catenin acetylation. *Bone*, 57 (2), 468–475.

Kogianni, G and Noble, BS, 2007. The biology of osteocytes. *Curr Osteoporos Rep*, 5 (2), 81–86.

Komori, T, 2009. Regulation of Osteoblast Differentiation by Runx2. Springer, Boston, MA, 43–49.

Krogsgaard, MR, Thamsborg, G, and Lund, B, 1996. Changes in bone mass during low dose corticosteroid treatment in patients with polymyalgia rheumatica: a double blind, prospective comparison between prednisolone and deflazacort. *Ann Rheum Dis*, 55 (2), 143–146.

Kupfer, SR, Underwood, LE, Baxter, RC, and Clemmons, DR, 1993. Enhancement of the anabolic effects of growth hormone and insulin-like growth factor I by use of both agents simultaneously. *J Clin Invest*, 91 (2), 391–396.

Kwek, EB, Goh, SK, Koh, JS, Png, MA, and Howe, TS, 2008. An emerging pattern of subtrochanteric stress fractures: a long-term complication of alendronate therapy? *Injury*, 39 (2), 224–231.

Kwon, D-N, Chang, B-S, and Kim, J-H, 2014. MicroRNA dysregulation in liver and pancreas of CMP-Neu5Ac hydroxylase null mice disrupts insulin/PI3K-AKT signaling. *Biomed Res Int*, 2014, 236385.

Kwon, D-N, Choi, Y-J, Cho, S-G, Park, C, Seo, HG, Song, H, and Kim, J-H, 2015. CMP-Neu5Ac Hydroxylase Null Mice as a Model for Studying Metabolic Disorders Caused by the Evolutionary Loss of Neu5Gc in Humans. *Biomed Res Int*, 2015, 1–16.

Lai, H-CC, FitzSimmons, SC, Allen, DB, Kosorok, MR, Rosenstein, BJ, Campbell, PW, and Farrell, PM, 2000. Risk of Persistent Growth Impairment after Alternate-Day Prednisone Treatment in Children with Cystic Fibrosis. *N Engl J Med*, 342 (12), 851–859.

Lane, NE, Yao, W, Balooch, M, Nalla, RK, Balooch, G, Habelitz, S, Kinney, JH, and Bonewald, LF, 2006. Glucocorticoid-Treated Mice Have Localized Changes in Trabecular Bone Material Properties and Osteocyte Lacunar Size That Are Not Observed in Placebo-Treated or Estrogen-Deficient Mice. *J Bone Min Res*, 21 (3), 466–476.

Laron, Z, 2001. Insulin-like growth factor 1 (IGF-1): a growth hormone. *Mol Pathol*, 54 (5), 311–6.

Larson, CM and Henderson, RC, 2000. Bone mineral density and fractures in boys with Duchenne muscular dystrophy. *J Pediatr Orthop*, 20 (1), 71–74.

Lebel, DE, Corston, JA, McAdam, LC, Biggar, WD, and Alman, BA, 2013. Glucocorticoid treatment for the prevention of scoliosis in children with Duchenne muscular dystrophy: long-term follow-up. *J Bone Jt Surg Am*, 95 (12), 1057–1061.

Lefaucheur, JP and Sebille, A, 1995. Basic fibroblast growth factor promotes in vivo muscle regeneration in murine muscular dystrophy. *Neurosci Lett*, 202 (1–2), 121–4.

Lin, S, Huang, J, Liang, ZZ, Liu, Y, Liu, G, Li, N, Wang, K, Liyi, ZZ, Wu, T, Qin, L, Liao, C, Qin, L, and Li, G, 2014. Glucocorticoid-Induced Osteoporosis in Growing Rats. *Calcif Tissue Int*, 95 (4), 362–373.

Lindahl, A, Nilsson, A, and Isaksson, OGP, 1987. Effects of growth hormone and insulin-like growth factor-I on colony formation of rabbit epiphyseal chondrocytes at different stages of maturation. *J Endocrinol*, 115 (2), 263–271.

Livak, KJ and Schmittgen, TD, 2001. Analysis of Relative Gene Expression Data Using Real-Time Quantitative PCR and the 2−ΔΔCT Method. *Methods*, 25 (4), 402–408.

LoCascio, V, Bonucci, E, Imbimbo, B, Ballanti, P, Adami, S, Milani, S, Tartarotti, D, and DellaRocca, C, 1990. Bone loss in response to long-term glucocorticoid therapy. *Bone Miner*, 8 (1), 39–51.

Loftus, J, Allen, R, Hesp, R, David, J, Reid, DM, Wright, DJ, Green, JR, Reeve, J, Ansell, BM, and Woo, PM, 1991. Randomized, double-blind trial of deflazacort versus prednisone in juvenile chronic (or rheumatoid) arthritis: a relatively bone-sparing effect of deflazacort. *Pediatrics*, 88 (3), 428–436.

Loveridge, N, Farquharson, C, and Scheven, BA, 1990. Endogenous mediators of growth. *Proc Nutr Soc*, 49 (3), 443–50.

Luca, AM, 2014. TREAT-NMD SOP No.DMD_M.2.2.001 Use of grip strength meter to assess the limb strength of mdx mice [online]. Available from: http://www.treat-nmd.eu/research/preclinical/dmd-sops/.

Lupu, F, Terwilliger, JD, Lee, K, Segre, G V., and Efstratiadis, A, 2001. Roles of growth hormone and insulin-like growth factor 1 in mouse postnatal growth. *Dev Biol*, 229 (1), 141–162.

Lynch, GS, Hinkle, RT, Chamberlain, JS, Brooks, S V, and Faulkner, JA, 2001. Force and power output of fast and slow skeletal muscles from mdx mice 6-28 months old. *J Physiol*, 535 (Pt 2), 591–600.

Mackie, EJ, Tatarczuch, L, and Mirams, M, 2011. The skeleton: a multi-functional complex organ. The growth plate chondrocyte and endochondral ossification. *J Endocrinol*, 211 (2), 109–121.

Maes, C and Kronenberg, HM, 2016. Bone Development and Remodeling. *In*:

Endocrinology: Adult and Pediatric. W.B. Saunders, 1038–1062.e8.

Manzur, AY, Kuntzer, T, Pike, M, and Swan, A, 2008. Glucocorticoid corticosteroids for Duchenne muscular dystrophy. *Cochrane Database Syst Rev*, (1), CD003725.

Masternak, MM, Panici, JA, Wang, F, Wang, Z, and Spong, A, 2010. The effects of growth hormone (GH) treatment on GH and insulin/IGF-1 signaling in long-lived ames dwarf mice. *Journals Gerontol - Ser A Biol Sci Med Sci*, 65 (1), 24–30.

Matsumoto, M, Awano, H, Lee, T, Takeshima, Y, Matsuo, M, and Iijima, K, 2017. Patients with Duchenne muscular dystrophy are significantly shorter than those with Becker muscular dystrophy, with the higher incidence of short stature in Dp71 mutated subgroup. *Neuromuscul Disord*, 27 (11), 1023–1028.

Matthews, E, Brassington, R, Kuntzer, T, Jichi, F, and Manzur, AY, 2016. Corticosteroids for the treatment of Duchenne muscular dystrophy. *In*: E. Matthews, ed. *Cochrane Database Syst Rev*. Chichester, UK, UK: John Wiley & Sons, Ltd, CD003725.

Mauras, N, George, D, Evans, J, Milov, D, Abrams, S, Rini, A, Welch, S, and Haymond, MW, 2002. Growth hormone has anabolic effects in glucocorticosteroid-dependent children with inflammatory bowel disease: a pilot study. *Metabolism*, 51 (1), 127–135.

Mavalli, MD, DiGirolamo, DJ, Fan, Y, Riddle, RC, Campbell, KS, van Groen, T, Frank, SJ, Sperling, MA, Esser, KA, Bamman, MM, and Clemens, TL, 2010. Distinct growth hormone receptor signaling modes regulate skeletal muscle development and insulin sensitivity in mice. *J Clin Invest*, 120 (11), 4007–20.

Mayo, AL, Craven, BC, McAdam, LC, and Biggar, WD, 2012. Bone health in boys with Duchenne Muscular Dystrophy on long-term daily deflazacort therapy. *Neuromuscul Disord*, 22 (12), 1040–1045.

Mazziotti, G and Giustina, A, 2013. Glucocorticoids and the regulation of growth hormone secretion. *Nat Rev Endocrinol*, 9 (5), 265–276.

McAdam, LC, Mayo, AL, Alman, BA, and Biggar, WD, 2012. The Canadian experience with long-term deflazacort treatment in Duchenne muscular dystrophy. *Acta Myol*, 31 (1), 16–20.

McClung, MR, 2017. Sclerostin antibodies in osteoporosis: latest evidence and therapeutic potential. *Ther Adv Musculoskelet Dis*, 9 (10), 263–270.

Mcdonald, AA, Hebert, SL, Kunz, MD, Ralles, SJ, and Mcloon, LK, 2015. Disease

course in mdx : utrophin + / − mice : comparison of three mouse models of Duchenne muscular dystrophy. *Physiol Rep*, 3 (4), 1–22.

McDonald, CM, Abresch, RT, Carter, GT, Fowler Jr., WM, Johnson, ER, Kilmer, DD, and Sigford, BJ, 1995. Profiles of neuromuscular diseases. Duchenne muscular dystrophy. *Am J Phys Med Rehabil*, 74 (5 Suppl), S70-92.

McDonald, CM, Han, JJ, Mah, JK, and Carter, GT, 2012. Corticosteroids and Duchenne muscular dystrophy: does earlier treatment really matter? *Muscle Nerve*, 45 (6), 777–779.

Merlini, L, Granata, C, Ballestrazzi, A, Cornelio, F, Tassoni, P, Tugnoli, S, and Cacciari, E, 1988. Growth hormone evaluation in Duchenne muscular dystrophy. *Ital J Neurol Sci*, 9 (5), 471–475.

Merlini, L, Gennari, M, Malaspina, E, Cecconi, I, Armaroli, A, Gnudi, S, Talim, B, Ferlini, A, Cicognani, A, and Franzoni, E, 2012. Early corticosteroid treatment in 4 Duchenne muscular dystrophy patients: 14-year follow-up. *Muscle Nerve*, 45 (6), 796–802.

Messina, MF, Aguennouz, M, Arrigo, T, Rodolico, C, Valenzise, M, Musumeci, O, Vita, G, Lanzano, N, and De Luca, F, 2008. Novel SHOX gene mutation in a short boy with Becker muscular dystrophy: double trouble in two adjacent genes. *Horm Res*, 69 (2), 124–128.

Milad, N, White, Z, Tehrani, AY, Sellers, S, Rossi, FMV, and Bernatchez, P, 2017. Increased plasma lipid levels exacerbate muscle pathology in the mdx mouse model of Duchenne muscular dystrophy. *Skelet Muscle*, 7 (1), 19.

Misof, BM, Roschger, P, Mcmillan, HJ, Ma, J, Klaushofer, K, Rauch, F, and Ward, LM, 2016. Histomorphometry and Bone Matrix Mineralization Before and After Bisphosphonate Treatment in Boys With Duchenne Muscular Dystrophy : A Paired Transiliac Biopsy Study. *J Bone Min Res*, 31 (5), 1–10.

Montgomery, E, Pennington, C, Isales, CM, and Hamrick, MW, 2005. Muscle-bone interactions in dystrophin-deficient and myostatin-deficient mice. *Anat Rec A Discov Mol Cell Evol Biol*, 286 (1), 814–822.

Morgenroth, VH, Hache, LP, and Clemens, PR, 2012. Insights into bone health in Duchenne muscular dystrophy. *Bonekey Rep*, 1 (November 2011), 1–11.

Moxley, RT, Pandya, S, Ciafaloni, E, Fox, DJ, and Campbell, K, 2010. Change in natural history of Duchenne muscular dystrophy with long-term corticosteroid treatment: implications for management. *J Child Neurol*, 25 (9), 1116–1129.

Mueller, K, Cortesi, R, Modrowski, D, and Marie, PJ, 1994. Stimulation of trabecular bone formation by insulin-like growth factor I in adult ovariectomized rats. *Am J Physiol Metab*, 267 (1), E1–E6.

Muller, J, Vayssiere, N, Royuela, M, Leger, ME, Muller, A, Bacou, F, Pons, F, Hugon, G, and Mornet, D, 2001. Comparative evolution of muscular dystrophy in diaphragm, gastrocnemius and masseter muscles from old male mdx mice. *J Muscle Res Cell Motil*, 22 (2), 133–9.

Muntoni, F, Mateddu, A, Marchei, F, Clerk, A, and Serra, G, 1993. Muscular weakness in the mdx mouse. *J Neurol Sci*, 120 (1), 71–7.

Mushtaq, T and Ahmed, SF, 2002. The impact of corticosteroids on growth and bone health. *Arch Dis Child*, 87 (2), 93–96.

Mustafy, T, Benoit, A, Londono, I, Moldovan, F, and Villemure, I, 2018. Can repeated in vivo micro-CT irradiation during adolescence alter bone microstructure, histomorphometry and longitudinal growth in a rodent model? *PLoS One*, 13 (11), e0207323.

Nagel, BH, Mortier, W, Elmlinger, M, Wollmann, HA, Schmitt, K, and Ranke, MB, 1999. Short stature in Duchenne muscular dystrophy: a study of 34 patients. *Acta Paediatr*, 88 (1), 62–65.

Nakagaki, WR, Bertran, CA, Matsumura, CY, Santo-Neto, H, and Camilli, JA, 2011. Mechanical, biochemical and morphometric alterations in the femur of mdx mice. *Bone*, 48 (2), 372–379.

Nakashima, T, Hayashi, M, Fukunaga, T, Kurata, K, Oh-hora, M, Feng, JQ, Bonewald, LF, Kodama, T, Wutz, A, Wagner, EF, Penninger, JM, and Takayanagi, H, 2011. Evidence for osteocyte regulation of bone homeostasis through RANKL expression. *Nat Med*, 17 (10), 1231–1234.

Nereo, NE, Fee, RJ, and Hinton, VJ, 2003. Parental stress in mothers of boys with duchenne muscular dystrophy. *J Pediatr Psychol*, 28 (7), 473–484.

Newton, R and Holden, NS, 2007. Separating transrepression and transactivation: a distressing divorce for the glucocorticoid receptor? *Mol Pharmacol*, 72 (4), 799–809.

Norstedt, G and Palmiter, R, 1984. Secretory rhythm of growth hormone regulates sexual differentiation of mouse liver. *Cell*, 36 (4), 805–12.

Novotny, SA, Warren, GL, Lin, AS, Guldberg, RE, Baltgalvis, KA, and Lowe, DA, 2011. Bone is functionally impaired in dystrophic mice but less so than skeletal

muscle. *Neuromuscul Disord*, 21 (3), 183–193.

Novotny, SA, Warren, GL, Lin, AS, Guldberg, RE, Baltgalvis, KA, and Lowe, DA, 2012. Prednisolone treatment and restricted physical activity further compromise bone of mdx mice. *J Musculoskelet Neuronal Interact*, 12 (1), 16–23.

Nystedt, J, Anderson, H, Hirvonen, T, Impola, U, Jaatinen, T, Heiskanen, A, Blomqvist, M, Satomaa, T, Natunen, J, Saarinen, J, Lehenkari, P, Valmu, L, and Laine, J, 2009. Human CMP- N -Acetylneuraminic Acid Hydroxylase (CMAH) is a Novel Stem Cell Marker Linked to Stem Cell-Specific Mechanisms. *Stem Cells*, 28 (2), 258–67.

Odgaard, A and Gundersen, HJ, 1993. Quantification of connectivity in cancellous bone, with special emphasis on 3-D reconstructions. *Bone*, 14 (2), 173–82.

Ogoshi, T, Hagino, H, Fukata, S, Tanishima, S, Okano, T, and Teshima, R, 2008. Influence of glucocorticoid on bone in 3-, 6-, and 12-month-old rats as determined by bone mass and histomorphometry. *Mod Rheumatol*, 18 (6), 552–561.

Oh, C-D and Chun, J-S, 2003. Signaling mechanisms leading to the regulation of differentiation and apoptosis of articular chondrocytes by insulin-like growth factor-1. *J Biol Chem*, 278 (38), 36563–71.

Ohnaka, K, Tanabe, M, Kawate, H, Nawata, H, and Takayanagi, R, 2005. Glucocorticoid suppresses the canonical Wnt signal in cultured human osteoblasts. *Biochem Biophys Res Commun*, 329 (1), 177–181.

Okerblom, JJ, Schwarz, F, Olson, J, Fletes, W, Ali, SR, Martin, PT, Glass, CK, Nizet, V, and Varki, A, 2017. Loss of CMAH during human evolution primed the monocyte-macrophage lineage toward a more inflammatory and phagocytic state. *J Immunol*, 198 (6), 2366–2373.

Olgaard, K, Storm, T, van Wowern, N, Daugaard, H, Egfjord, M, Lewin, E, and Brandi, L, 1992. Glucocorticoid-induced osteoporosis in the lumbar spine, forearm, and mandible of nephrotic patients: a double-blind study on the high-dose, long-term effects of prednisone versus deflazacort. *Calcif Tissue Int*, 50 (6), 490–497.

Ortega, N, Behonick, DJ, and Werb, Z, 2004. Matrix remodeling during endochondral ossification. *Trends Cell Biol*, 14 (2), 86–93.

Owen, HC, Miner, JN, Ahmed, SF, and Farquharson, C, 2007. The growth plate

sparing effects of the selective glucocorticoid receptor modulator, AL-438. *Mol Cell Endocrinol*, 264 (1–2), 164–170.

Owen, HC, Ahmed, SF, and Farquharson, C, 2009. Chondrocyte p21(WAF1/CIP1) expression is increased by dexamethasone but does not contribute to dexamethasone-induced growth retardation in vivo. *Calcif Tissue Int*, 85 (4), 326–334.

Pappa, H, Thayu, M, Sylvester, F, Leonard, M, Zemel, B, and Gordon, C, 2011. Skeletal health of children and adolescents with inflammatory bowel disease. *J Pediatr Gastroenterol Nutr*, 53 (1), 11–25.

Parfitt, AM, Drezner, MK, Glorieux, FH, Kanis, JA, Malluche, H, Meunier, PJ, Ott, SM, and Recker, RR, 2009. Bone histomorphometry: Standardization of nomenclature, symbols, and units: Report of the ASBMR histomorphometry nomenclature committee. *J Bone Min Res*, 2 (6), 595–610.

Parker, EA, Hegde, A, Buckley, M, Barnes, KM, Baron, J, and Nilsson, O, 2007. Spatial and temporal regulation of GH-IGF-related gene expression in growth plate cartilage. *J Endocrinol*, 194 (1), 31–40.

Pass, C, MacRae, VE, Huesa, C, Faisal Ahmed, S, and Farquharson, C, 2012. SOCS2 is the critical regulator of GH action in murine growth plate chondrogenesis. *J Bone Min Res*, 27 (5), 1055–1066.

Patsch, JM, Li, X, Baum, T, Yap, SP, Karampinos, DC, Schwartz, A V, and Link, TM, 2013. Bone marrow fat composition as a novel imaging biomarker in postmenopausal women with prevalent fragility fractures. *J Bone Miner Res*, 28 (8), 1721–1728.

Patschan, D, Loddenkemper, K, and Buttgereit, F, 2001. Molecular mechanisms of glucocorticoid-induced osteoporosis. *Bone*, 29 (6), 498–505.

Pereira, RC, Delany, AM, and Canalis, E, 2002. Effects of cortisol and bone morphogenetic protein-2 on stromal cell differentiation: correlation with CCAAT-enhancer binding protein expression. *Bone*, 30 (5), 685–691.

Pettit, AR, Ji, H, von Stechow, D, Müller, R, Goldring, SR, Choi, Y, Benoist, C, and Gravallese, EM, 2001. TRANCE/RANKL knockout mice are protected from bone erosion in a serum transfer model of arthritis. *Am J Pathol*, 159 (5), 1689–99.

Pittenger, MF, Mackay, AM, Beck, SC, Jaiswal, RK, Douglas, R, Mosca, JD, Moorman, MA, Simonetti, DW, Craig, S, and Marshak, DR, 1999. Multilineage

potential of adult human mesenchymal stem cells. *Science*, 284 (5411), 143–7.

Playford, MP, Bicknell, D, Bodmer, WF, and Macaulay, VM, 2000. Insulin-like growth factor 1 regulates the location, stability, and transcriptional activity of beta-catenin. *Proc Natl Acad Sci U S A*, 97 (22), 12103–8.

Price, WA, Stiles, AD, Moats-Staats, BM, and D'Ercole, AJ, 1992. Gene expression of insulin-like growth factors (IGFs), the type 1 IGF receptor, and IGF-binding proteins in dexamethasone-induced fetal growth retardation. *Endocrinology*, 130 (3), 1424–1432.

Radley-Crabb, HG, Fiorotto, ML, and Grounds, MD, 2011. The different impact of a high fat diet on dystrophic mdx and control C57Bl/10 mice. *PLoS Curr*, 3, RRN1276.

Radley-Crabb, HG, Marini, JC, Sosa, HA, Castillo, LI, Grounds, MD, and Fiorotto, ML, 2014. Dystropathology increases energy expenditure and protein turnover in the Mdx mouse model of Duchenne muscular dystrophy. *PLoS One*, 9 (2), e89277.

Rapaport, D, Colletto, GM, Vainzof, M, Duaik, MC, and Zatz, M, 1991. Short stature in Duchenne muscular dystrophy. *Growth Regul*, 1 (1), 11–15.

Rapisarda, R, Muntoni, F, Gobbi, P, and Dubowitz, V, 1995. Duchenne muscular dystrophy presenting with failure to thrive. *Arch Dis Child*, 72 (5), 437–438.

Rauch, A *et al.*, 2010. Glucocorticoids suppress bone formation by attenuating osteoblast differentiation via the monomeric glucocorticoid receptor. *Cell Metab*, 11 (6), 517–531.

Rauch, F, Travers, R, Plotkin, H, and Glorieux, FH, 2002. The effects of intravenous pamidronate on the bone tissue of children and adolescents with osteogenesis imperfecta. *J Clin Invest*, 110 (9), 1293–1299.

Reeves, EKM, Hoffman, EP, Nagaraju, K, Damsker, JM, and McCall, JM, 2013. VBP15: preclinical characterization of a novel anti-inflammatory delta 9,11 steroid. *Bioorg Med Chem*, 21 (8), 2241–9.

Reinwald, S and Burr, D, 2008. Review of nonprimate, large animal models for osteoporosis research. *J Bone Min Res*, 23 (9), 1353–1368.

Rich, SM and Ayala, FJ, 2000. Population structure and recent evolution of Plasmodium falciparum. *Proc Natl Acad Sci*, 97 (13), 6994–7001.

Ricotti, V, Ridout, DA, Scott, E, Quinlivan, R, Robb, SA, Manzur, AY, and Muntoni, F, 2013. Long-term benefits and adverse effects of intermittent versus daily

glucocorticoids in boys with Duchenne muscular dystrophy. *J Neurol Neurosurg Psychiatry*, 84 (6), 698–705.

Ricotti, V, Spinty, S, Roper, H, Hughes, I, Tejura, B, Robinson, N, Layton, G, Davies, K, Muntoni, F, and Tinsley, J, 2016. Safety, Tolerability, and Pharmacokinetics of SMT C1100, a 2-Arylbenzoxazole Utrophin Modulator, following Single- and Multiple-Dose Administration to Pediatric Patients with Duchenne Muscular Dystrophy. *PLoS One*, 11 (4), e0152840.

Roberts, S, Narisawa, S, Harmey, D, Millán, JL, and Farquharson, C, 2007. Functional Involvement of PHOSPHO1 in Matrix Vesicle-Mediated Skeletal Mineralization. *J Bone Miner Res*, 22 (4), 617–627.

Robey, PG, 2008. Noncollagenous Bone Matrix Proteins. *In*: *Principles of Bone Biology*. Academic Press, 335–349.

Rochefort, GY, Pallu, S, and Benhamou, CL, 2010. Osteocyte: the unrecognized side of bone tissue. *Osteoporos Int*, 21 (9), 1457–1469.

Rosen, CJ, Ackert-Bicknell, C, Rodriguez, JP, and Pino, AM, 2009. Marrow fat and the bone microenvironment: developmental, functional, and pathological implications. *Crit Rev Eukaryot Gene Expr*, 19 (2), 109–24.

Rufo, A, Del Fattore, A, Capulli, M, Carvello, F, De Pasquale, L, Ferrari, S, Pierroz, D, Morandi, L, De Simone, M, Rucci, N, Bertini, E, Bianchi, ML, De Benedetti, F, and Teti, A, 2011. Mechanisms inducing low bone density in Duchenne muscular dystrophy in mice and humans. *J Bone Min Res*, 26 (8), 1891–1903.

Ruifrok, AC and Johnston, DA, 2001. Quantification of histochemical staining by color deconvolution. *Anal Quant Cytol Histol*, 23, 291–299.

Rutter, MM, Collins, J, Rose, SR, Woo, JG, Sucharew, H, Sawnani, H, Hor, KN, Cripe, LH, and Wong, BL, 2012. Growth hormone treatment in boys with Duchenne muscular dystrophy and glucocorticoid-induced growth failure. *Neuromuscul Disord*, 22 (12), 1046–1056.

Rutter, MM, Collins, J, Backeljauw, PF, Horn, P, Taylor, MD, Hu, SY, Blum, S, Morehart, P, Sawnani, H, and Wong, BL, 2013. P.11.15 Recombinant human insulin-like growth factor-I (IGF-I) therapy in Duchenne Muscular Dystrophy (DMD): A 6-month prospective randomized controlled trial. *Neuromuscul Disord*, 23 (9–10), 803.

Salmon, W and Daughaday, W, 1957. A hormonally controlled serum factor which stimulates sulfate incorporation by cartilage in vitro. *J Lab Clin Med*, 49 (6),

825–36.

Sarrazin, E, Hagen, M Von Der, Schara, U, Von Au, K, Kaindl, AM, von der Hagen, M, Schara, U, Von Au, K, Kaindl, AM, Hagen, M Von Der, Schara, U, Von Au, K, and Kaindl, AM, 2014. Growth and psychomotor development of patients with Duchenne muscular dystrophy. *Eur J Paediatr Neurol*, 18 (1), 38–44.

Sbrocchi, AM, Forget, S, Laforte, D, Azouz, EM, and Rodd, C, 2010. Zoledronic acid for the treatment of osteopenia in pediatric Crohn's disease. *Pediatr Int*, 52 (5), 754–761.

Sbrocchi, AM, Rauch, F, Jacob, P, McCormick, A, McMillan, HJ, Matzinger, MA, and Ward, LM, 2012. The use of intravenous bisphosphonate therapy to treat vertebral fractures due to osteoporosis among boys with Duchenne muscular dystrophy. *Osteoporos Int*, 23 (11), 2703–2711.

Scheller, EL, Troiano, N, Vanhoutan, JN, Bouxsein, MA, Fretz, JA, Xi, Y, Nelson, T, Katz, G, Berry, R, Church, CD, Doucette, CR, Rodeheffer, MS, Macdougald, OA, Rosen, CJ, and Horowitz, MC, 2014. Use of osmium tetroxide staining with microcomputerized tomography to visualize and quantify bone marrow adipose tissue in vivo. *Methods Enzymol*, 537, 123–39.

Scheller, EL, Doucette, CR, Learman, BS, Cawthorn, WP, Khandaker, S, Schell, B, Wu, B, Ding, S-Y, Bredella, MA, Fazeli, PK, Khoury, B, Jepsen, KJ, Pilch, PF, Klibanski, A, Rosen, CJ, and Macdougald, OA, 2015. Region-specific variation in the properties of skeletal adipocytes reveals regulated and constitutive marrow adipose tissues. *Nat Commun*, 6 (1), 7808.

Scheller, EL, Cawthorn, WP, Burr, AA, Horowitz, MC, and MacDougald, OA, 2016. Marrow Adipose Tissue: Trimming the Fat. *Trends Endocrinol Metab*, 27 (6), 392–403.

Schertzer, JD, Ryall, JG, Lynch, GS, Jonathan, D, Ryall, JG, and Lynch, GS, 2018. Systemic administration of IGF-I enhances oxidative status and reduces contraction-induced injury in skeletal muscles of mdx dystrophic mice, 499–505.

Schindelin, J, Arganda-Carreras, I, Frise, E, Kaynig, V, Longair, M, Pietzsch, T, Preibisch, S, Rueden, C, Saalfeld, S, Schmid, B, Tinevez, J-Y, White, DJ, Hartenstein, V, Eliceiri, K, Tomancak, P, and Cardona, A, 2012. Fiji: an open-source platform for biological-image analysis. *Nat Methods*, 9 (7), 676–682.

Selbach, M, Schwanhäusser, B, Thierfelder, N, Fang, Z, Khanin, R, and Rajewsky,

N, 2008. Widespread changes in protein synthesis induced by microRNAs. *Nature*, 455, 58–63.

Shanmugam, M, Govindarajan, R, and J. Sinal, C, 2018. Bone Marrow Adipose Tissue and Skeletal Health. *Curr Osteoporos Rep*, 16, 11914–18.

Shavlakadze, T, White, J, Hoh, JFY, Rosenthal, N, and Grounds, MD, 2004. Targeted expression of insulin-like growth factor-1 reduces early myofiber necrosis in dystrophic mdx mice. *Mol Ther*, 10 (5), 829–843.

Sheng, MH-C, Zhou, X-D, Bonewald, LF, Baylink, DJ, and Lau, K-HW, 2013. Disruption of the insulin-like growth factor-1 gene in osteocytes impairs developmental bone growth in mice. *Bone*, 52 (1), 133–144.

Shi, C, Huang, P, Kang, H, Hu, B, Qi, J, Jiang, M, Zhou, H, Guo, L, and Deng, L, 2015. Glucocorticoid inhibits cell proliferation in differentiating osteoblasts by microRNA-199a targeting of WNT signaling. *J Mol Endocrinol*, 54 (3), 325–337.

Shi, S, de Gorter, DJJ, Hoogaars, WMH, 't Hoen, PAC, and ten Dijke, P, 2013. Overactive bone morphogenetic protein signaling in heterotopic ossification and Duchenne muscular dystrophy. *Cell Mol Life Sci*, 70 (3), 407–23.

Simon, D, Fernando, C, Czernichow, P, and Prieur, A-M, 2002. Linear growth and final height in patients with systemic juvenile idiopathic arthritis treated with longterm glucocorticoids. *J Rheumatol*, 29 (6), 1296–300.

Sims, NA, Clément-Lacroix, P, Da Ponte, F, Bouali, Y, Binart, N, Moriggl, R, Goffin, V, Coschigano, K, Gaillard-Kelly, M, Kopchick, J, Baron, R, and Kelly, PA, 2000. Bone homeostasis in growth hormone receptor–null mice is restored by IGF-I but independent of Stat5. *J Clin Invest*, 106 (9), 1095–1103.

Sinha, KM and Zhou, X, 2013. Genetic and molecular control of osterix in skeletal formation. *J Cell Biochem*, 114 (5), 975–84.

Sinnesael, M, Boonen, S, Claessens, F, Gielen, E, and Vanderschueren, D, 2011. Testosterone and the male skeleton: a dual mode of action. *J Osteoporos*, 2011, 240328.

Smink, JJ, Koster, JG, Gresnigt, MG, Rooman, R, Koedam, JA, and Van Buul-Offers, SC, 2002. IGF and IGF-binding protein expression in the growth plate of normal, dexamethasone-treated and human IGF-II transgenic mice. *J Endocrinol*, 175 (1), 143–53.

Smink, JJ, Gresnigt, MG, Hamers, N, Koedam, JA, Berger, R, and Van Buul-Offers, SC, 2003. Short-term glucocorticoid treatment of prepubertal mice decreases

growth and IGF-I expression in the growth plate. *J Endocrinol*, 177 (3), 381–8.

Söderpalm, A-C, Magnusson, P, Åhlander, A-C, Karlsson, J, Kroksmark, A-K, Tulinius, M, and Swolin-Eide, D, 2007. Low bone mineral density and decreased bone turnover in Duchenne muscular dystrophy. *Neuromuscul Disord*, 17 (11–12), 919–928.

Sommerfeldt, DW and Rubin, CT, 2001. Biology of bone and how it orchestrates the form and function of the skeleton. *Eur Spine J*, 10 (Suppl 2), S86-95.

Song, B, Estrada, KD, and Lyons, KM, 2009. Smad signaling in skeletal development and regeneration. *Cytokine Growth Factor Rev*, 20 (5–6), 379–388.

Song, Y-HH, Song, JL, Delafontaine, P, and Godard, MP, 2013. The therapeutic potential of IGF-I in skeletal muscle repair. *Trends Endocrinol Metab*, 24 (6), 310–319.

Srinivasan, R, Rawlings, D, Wood, CL, Cheetham, T, Moreno, ACJ, Mayhew, A, Eagle, M, Guglieri, M, Straub, V, Owen, C, Bushby, K, and Sarkozy, A, 2016. Prophylactic oral bisphosphonate therapy in duchenne muscular dystrophy, 54 (1), 79–85.

Van Staa, TP, Leufkens, HGM, Abenhaim, L, Zhang, B, and Cooper, C, 2000. Use of oral corticosteroids and risk of fractures. *J Bone Min Res*, 15 (6), 993–1000.

Van Staa, TP, Leufkens, HGM, and Cooper, C, 2002. The Epidemiology of Corticosteroid-Induced Osteoporosis: a Meta-analysis. *Osteoporos Int*, 13, 777–87.

Stewart, PM, 2007. The adrenal cortex. *In*: H. Kronenberg et al., eds. *Williams Textbook of Endocrinology*. Saunders Elsevier.

Strakova, J, Kamdar, F, Kulhanek, D, Razzoli, M, Garry, DJ, Ervasti, JM, Bartolomucci, A, and Townsend, D, 2018. Integrative effects of dystrophin loss on metabolic function of the mdx mouse. *Sci Rep*, 8 (1), 13624.

Sundström, K, Cedervall, T, Ohlsson, C, Camacho-Hübner, C, and Sävendahl, L, 2014. Combined treatment with GH and IGF-I: additive effect on cortical bone mass but not on linear bone growth in female rats. *Endocrinology*, 155 (12), 4798–807.

Szigyarto, CA-K and Spitali, P, 2018. Biomarkers of Duchenne muscular dystrophy: current findings. *Degener Neurol Neuromuscul Dis*, 8, 1–13.

Tahimic, CGT, Wang, Y, and Bikle, DD, 2013. Anabolic effects of IGF-1 signaling on

the skeleton. *Front Endocrinol (Lausanne)*, 4 (6), 1–14.

Takarada, T, Hinoi, E, Nakazato, R, Ochi, H, Xu, C, Tsuchikane, A, Takeda, S, Karsenty, G, Abe, T, Kiyonari, H, and Yoneda, Y, 2013. An analysis of skeletal development in osteoblast-specific and chondrocyte-specific runt-related transcription factor-2 (Runx2) knockout mice. *J Bone Miner Res*, 28 (10), 2064–2069.

Takata, S and Yasui, N, 2001. Disuse osteoporosis. *J Med Invest*, 48 (3–4), 147–56.

Taylor, CR and Levenson, RM, 2006. Quantification of immunohistochemistry-issues concerning methods, utility and semiquantitative assessment. *Histopathology*, 49 (4), 411–424.

Teitelbaum, SL, 2007. Osteoclasts: What Do They Do and How Do They Do It? *Am J Pathol*, 170 (2), 427–435.

Tencerova, M and Kassem, M, 2016. The Bone Marrow-Derived Stromal Cells: Commitment and Regulation of Adipogenesis. *Front Endocrinol (Lausanne)*, 7 (127), 1–12.

Thiele, S, Ziegler, N, Tsourdi, E, De Bosscher, K, Tuckermann, JP, Hofbauer, LC, and Rauner, M, 2012. Selective glucocorticoid receptor modulation maintains bone mineral density in mice. *J Bone Min Res*, 27 (11), 2242–2250.

Tomlinson, PB, Joseph, C, and Angioi, M, 2015. Effects of vitamin D supplementation on upper and lower body muscle strength levels in healthy individuals. A systematic review with meta-analysis. *J Sci Med Sport*, 18 (5), 575–80.

Truett, GE, Heeger, P, Mynatt, RL, Truett, AA, Walker, JA, and Warman, ML, 2000. Preparation of PCR-quality mouse genomic DNA with hot sodium hydroxide and tris (HotSHOT). *Biotechniques*, 29 (1), 52, 54.

Turk, R, Sterrenburg, E, Meijer, E de, Ommen, G-J van, Dunnen, J den, and Hoen, P ’t, 2005. Muscle regeneration in dystrophin-deficient mdx mice studied by gene expression profiling. *BMC Genomics*, 6, 98.

Umlawska, W and Prusek-Dudkiewicz, A, 2010. Growth retardation and delayed puberty in children and adolescents with juvenile idiopathic arthritis. *Arch Med Sci*, 6 (1), 19–23.

Vasikaran, S, Eastell, R, Bruyère, O, Foldes, AJ, Garnero, P, Griesmacher, A, McClung, M, Morris, HA, Silverman, S, Trenti, T, Wahl, DA, Cooper, C, Kanis, JA, and IOF-IFCC Bone Marker Standards Working Group, 2011. Markers of

bone turnover for the prediction of fracture risk and monitoring of osteoporosis treatment: a need for international reference standards. *Osteoporos Int*, 22 (2), 391–420.

Veilleux, L-N and Rauch, F, 2017. Muscle-Bone Interactions in Pediatric Bone Diseases. *Curr Osteoporos Rep*, 15 (5), 425–32.

Verschure, PJ, van Marle, J, Joosten, LA, and van den Berg, WB, 1995. Chondrocyte IGF-1 receptor expression and responsiveness to IGF-1 stimulation in mouse articular cartilage during various phases of experimentally induced arthritis. *Ann Rheum Dis*, 54 (8), 645–53.

Wagner, KR, Lechtzin, N, and Judge, DP, 2007. Current treatment of adult Duchenne muscular dystrophy. *Biochim Biophys Acta - Mol Basis Dis*, 1772 (2), 229–237.

Wallace, RJ, Mori, H, Simon, BR, Parlee, SD, Bree, AJ, Krishnan, V, Zhang, B, Scheller, EL, Learman, BS, MacDougald, OA, Cawthorn, WP, and Sulston, RJ, 2016. Increased Circulating Adiponectin in Response to Thiazolidinediones: Investigating the Role of Bone Marrow Adipose Tissue. *Front Endocrinol (Lausanne)*, 7 (September), 1–17.

Walsh, LJ, Wong, CA, Pringle, M, and Tattersfield, AE, 1996. Use of oral corticosteroids in the community and the prevention of secondary osteoporosis: a cross sectional study. *BMJ*, 313 (7053), 344–6.

Wang, F-S, Chung, P-C, Lin, C-L, Chen, M-W, Ke, H-J, Chang, Y-H, Chen, Y-S, Wu, S-L, Ko, J-Y, and Ko, J-Y, 2013. MicroRNA-29a Protects Against Glucocorticoid-Induced Bone Loss and Fragility in Rats by Orchestrating Bone Acquisition and Resorption. *Arthritis Rheum*, 65 (6), 1530–1540.

Wang, J, Zhou, J, Cheng, CM, Kopchick, JJ, and Bondy, CA, 2004. Evidence supporting dual, IGF-I-independent and IGF-I-dependent, roles for GH in promoting longitudinal bone growth. *J Endocrinol*, 180 (2), 247–55.

Weber, DR, Hadjiyannakis, S, Mcmillan, HJ, Noritz, G, and Ward, LM, 2018. Obesity and Endocrine Management of the Patient With Duchenne Muscular Dystrophy. *Pediatrics*, 142, e20180333.

Weinstein, RS, Jilka, RL, Parfitt, AM, and Manolagas, SC, 1998. Inhibition of Osteoblastogenesis and Promotion of Apoptosis of Osteoblasts and Osteocytes by Glucocorticoids Potential Mechanisms of Their Deleterious Effects on Bone. *J Clin Invest*, 102 (2), 274–282.

Weinstein, RS and Manolagas, SC, 2000. Apoptosis and osteoporosis. *Am J Med*, 108 (2), 153–64.

Weinstein, RS, Chen, J-R, Powers, CC, Stewart, SA, Landes, RD, Bellido, T, Jilka, RL, Parfitt, AM, and Manolagas, SC, 2002. Promotion of osteoclast survival and antagonism of bisphosphonate-induced osteoclast apoptosis by glucocorticoids. *J Clin Invest*, 109 (8), 1041–8.

West, NA, Yang, ML, Weitzenkamp, DA, Andrews, J, Meaney, FJ, Oleszek, J, Miller, LA, Matthews, D, and DiGuiseppi, C, 2013. Patterns of Growth in Ambulatory Males with Duchenne Muscular Dystrophy. *J Pediatr*, 163 (6), 1759–1763.e1.

Westendorf, JJ, Kahler, RA, and Schroeder, TM, 2004. Wnt signaling in osteoblasts and bone diseases. *Gene*, 341, 19–39.

Wheater, G, Elshahaly, M, Tuck, SP, Datta, HK, and van Laar, JM, 2013. The clinical utility of bone marker measurements in osteoporosis. *J Transl Med*, 11, 201.

Willmann, R, Possekel, S, Dubach-powell, J, Meier, T, and Ruegg, MA, 2009. Neuromuscular Disorders Mammalian animal models for Duchenne muscular dystrophy, 19, 241–249.

Wong, SC, Dobie, R, Altowati, MA, Werther, GA, Farquharson, C, and Ahmed, SF, 2016. Growth and the growth hormone-insulin like growth factor 1 axis in children with chronic inflammation: Current Evidence, Gaps in Knowledge, and Future Directions. *Endocr Rev*, 37 (1), 62–110.

Wong, SC *et al.*, 2019. 236th ENMC International Workshop Bone Protective Therapy In Duchenne Muscular Dystrophy: Determining The Feasibility And Standards Of Clinical Trials. *Neuromuscul Disord*, 29 (1), 59–66.

Wood, C, Stenson, C, and Embleton, N, 2015. The developmental origins of osteoporosis. *Curr Genomics*, 16 (6).

Wood, CL, Straub, V, Guglieri, M, Bushby, K, and Cheetham, T, 2015. Short stature and pubertal delay in Duchenne muscular dystrophy. *Arch Dis Child*, 101 (1), 101–106.

Wood, CL, Cheetham, T, Guglieri, M, Bushby, K, Owen, C, Johnstone, H, and Straub, V, 2015. Testosterone Treatment of Pubertal Delay in Duchenne Muscular Dystrophy. *Neuropediatrics*, 46 (6), 371–376.

Wood, CL, Marini Bettolo, C, Bushby, K, Straub, V, Rawlings, D, Sarkozy, A, Owen,

C, and Cheetham, TD, 2016. Bisphosphonate use in Duchenne Muscular Dystrophy - Why, when to start and when to stop? *Expert Opin Orphan Drugs*, 4 (4).

Wood, CL, Soucek, O, Wong, SC, Zaman, F, Farquharson, C, Savendahl, L, and Ahmed, SF, 2018. Animal models to explore the effects of glucocorticoids on skeletal growth and structure. *J Endocrinol*, 236 (1), R69–R91.

Wu, Y, Sun, H, Yakar, S, and LeRoith, D, 2009. Elevated levels of insulin-like growth factor (IGF)-I in serum rescue the severe growth retardation of IGF-I null mice. *Endocrinology*, 150 (9), 4395–403.

Xia, X, Kar, R, Gluhak-Heinrich, J, Yao, W, Lane, NE, Bonewald, LF, Biswas, SK, Lo, WK, and Jiang, JX, 2010. Glucocorticoid-induced autophagy in osteocytes. *J Bone Min Res*, 25 (11), 2479–2488.

Xiong, J, Onal, M, Jilka, RL, Weinstein, RS, Manolagas, SC, and O'Brien, CA, 2011. Matrix-embedded cells control osteoclast formation. *Nat Med*, 17 (10), 1235–1241.

Yakar, S, Liu, J-L, Stannard, B, Butler, A, Accili, D, Sauer, B, and Leroith, D, 1999. Normal growth and development in the absence of hepatic insulin-like growth factor I. *Dev Biol*, 96, 7324–7329.

Yakar, S, Rosen, CJ, Beamer, WG, Ackert-Bicknell, CL, Wu, Y, Liu, J-L, Ooi, GT, Setser, J, Frystyk, J, Boisclair, YR, and LeRoith, D, 2002. Circulating levels of IGF-1 directly regulate bone growth and density. *J Clin Invest*, 110 (6), 771–81.

Yao, W, Cheng, Z, Busse, C, Pham, A, Nakamura, MC, and Lane, NE, 2008. Glucocorticoid excess in mice results in early activation of osteoclastogenesis and adipogenesis and prolonged suppression of osteogenesis: A longitudinal study of gene expression in bone tissue from glucocorticoid- treated mice. *Arthritis Rheum*, 58 (6), 1674–1686.

Yao, W, Dai, W, Jiang, L, Lay, EY-A, Zhong, Z, Ritchie, RO, Li, X, Ke, H, and Lane, NE, 2016. Sclerostin-antibody treatment of glucocorticoid-induced osteoporosis maintained bone mass and strength. *Osteoporos Int*, 27 (1), 283–294.

Yeung, DKW, Griffith, JF, Antonio, GE, Lee, FKH, Woo, J, and Leung, PC, 2005. Osteoporosis is associated with increased marrow fat content and decreased marrow fat unsaturation: A proton MR spectroscopy study. *J Magn Reson Imaging*, 22 (2), 279–285.

Yoon, S-H, Sugamori, KS, Grynpas, MD, and Mitchell, J, 2018. Effect of 25-

HydroxyVitamin D Deficiency and Its Interaction with Prednisone Treatment on Musculoskeletal Health in Growing Mdx Mice. *Calcif Tissue Int*, 103 (3), 311–323.

Yoon, S-H, Grynpas, M, and Mitchell, J, 2019. Intermittent PTH treatment improves bone and muscle in glucocorticoid treated Mdx mice: A model of Duchenne Muscular Dystrophy. *Bone*, 121, 232–242.

Yoon, S, Chen, J, Grynpas, MD, and Mitchell, J, 2016. Prophylactic pamidronate partially protects from glucocorticoid-induced bone loss in the mdx mouse model of Duchenne muscular dystrophy. *Bone*, 90, 168–180.

Zak, M, Müller, J, and Karup Pedersen, F, 1999. Final Height, Armspan, Subischial Leg Length and Body Proportions in Juvenile Chronic Arthritis. *Horm Res Paediatr*, 52 (2), 80–85.

Zalavras, C, Shah, S, Birnbaum, MJ, and Frenkel, B, 2003. Role of apoptosis in glucocorticoid-induced osteoporosis and osteonecrosis. *Crit Rev Eukaryot Gene Expr*, 13 (2–4), 221–35.

Zatz, M, Rapaport, D, Vainzof, M, Rocha, JM, Pavanello Rde, C, Colletto, GM, and Peres, CA, 1988. Relation between height and clinical course in Duchenne muscular dystrophy. *Am J Med Genet*, 29 (2), 405–410.

Zezulak, KM and Green, H, 1986. The generation of insulin-like growth factor-1--sensitive cells by growth hormone action. *Science (80-)*, 233 (4763), 551–553.

Zhang, M, Xuan, S, Bouxsein, ML, von Stechow, D, Akeno, N, Faugere, MC, Malluche, H, Zhao, G, Rosen, CJ, Efstratiadis, A, and Clemens, TL, 2002. Osteoblast-specific Knockout of the Insulin-like Growth Factor (IGF) Receptor Gene Reveals an Essential Role of IGF Signaling in Bone Matrix Mineralization. *J Biol Chem*, 277 (46), 44005–44012.

Zhao, G, Monier-Faugere, M-C, Langub, MC, Geng, Z, Nakayama, T, Pike, JW, Chernausek, SD, Rosen, CJ, Donahue, L-R, Malluche, HH, Fagin, JA, and Clemens, TL, 2000. Targeted Overexpression of Insulin-Like Growth Factor I to Osteoblasts of Transgenic Mice: Increased Trabecular Bone Volume without Increased Osteoblast Proliferation. *Endocrinology*, 141 (7), 2674–2682.

Zhou, L, Rafael-Fortney, JA, Huang, P, Zhao, XS, Cheng, G, Zhou, X, Kaminski, HJ, Liu, L, and Ransohoff, RM, 2008. Haploinsufficiency of utrophin gene worsens skeletal muscle inflammation and fibrosis in mdx mice. *J Neurol Sci*, 264 (1–2), 106–11.

CHAPTER 9

Appendices

9 Appendices

Appendix I- Primer sequences

Utrophin primer sequences

Primer number (from Jax.org)	Primer type	Sequence 5' --> 3'
10791	Mutant forward	CGC TTC CTC GTG CTT TAC GGT AT
12402	Common	AAG ATT TGC AGA CCG GAA GA
14702	Wildtype forward	TGT CAT TCT CTG AGG CCT TTC

cmah primer sequences (kindly supplied by Professor Straub)

Primer name	Primer sequences	Predicted band size
Common forward	5’ TCC CAG ACC AGG AGG AGT TA	
Wild type reverse	5’ CTT CCA GTT GTG CTT TGT GC	297 bp (wild type)
Mutant reverse	5’ GTC AGG AAA CAG CAC CAA CA	~400 bp (*cmah*)

Appendix II- SOP for grip strength meter

1. Assemble the meter by fixing electronics onto main stand with counter weight at back
2. Screw prehension adaptor to instrument
3. Insert the grid and secure with side screw
4. Plug power supply adapter on meter and mains
5. Turn machine on
6. Press zero and ensure the VLI reading is +/-0.4g or less. If not, briefly press zero again.
7. Hold mouse by the tail above the grid
8. Move mouse down until its front legs grab the grid in approximately the middle
9. While animal is grasping, lower it to almost horizontal position
10. Smoothly pull animal in axis of sensor until grip is released (needs to be held for approx. 3 s)
11. Maximum force developed is large number on screen (should measure in grams)

Good practice points (According to TREAT-NMD SOP)

- Repeat on each mouse up to 5 times, approximately 1 minute apart
- Use best reading or a mean of values
- Measurements must be discarded if the animal uses only one paw or also uses its hind paws, turns backwards during the pull, or leaves the bar without resistance
- Need to measure bodyweight in parallel so that strength/BW can be calculated
- Perform the test blinded and using same operator each time if possible

Expected values

- Usually wild type and *mdx* mice have fore limb strength values that are about five to seven times their body weight
- Values for absolute strength generally range from 0.09 to 0.120 kg at 4-5 weeks of age and may reach 0.150 to 0.200 kg at 12-15 weeks. The increment in normalized strength values is usually 0.95 to 1.5 after 4 weeks.

Appendix III- Protocols

Protocol for haematoxylin and eosin staining

Slides were prepared for histology according to the following protocol:

- Dewax paraffin sections – incubate slides at 60oC for 20minutes.
- Dewax sections – Xylene wash for 3 minutes (repeat x3).
- Rehydrate sections – 100% ethanol for 3 minutes (repeat x2).
- Rehydrate sections – 70% ethanol for 3 minutes.
- Rinse – double distilled water for 1-3 minutes.
- Stain - Haematoxylin for 30 seconds.
- Stain - Remove excess stain in tap water (until nuclei turn blue).
- Stain - 70% ethanol for 3 minutes.
- Stain - Eosin for 15 seconds (omit this step for haematoxylin only staining).
- Dehydrate – 100% ethanol for 3 minutes (repeat x3).
- Clear – Xylene wash for 3 minutes (repeat x3).
- Mount - DPX mountant and coverslip.

Protocol for toluidine blue staining

- Place in a 0.04% Toluidine blue solution for 10 minutes.
- Rinse gently with 3 changes of deionized water (for 30s each)
- Counterstain with 0.02% Fast Green solution for 3 minutes
- Rinse gently with 2 changes of deionized water for 30 seconds each
- Dehydrate briefly in 3 changes of 95% ethanol and 2 changes of 100% ethanol for 30 seconds each.
- Clear in 3 changes of xylene
- Cover-slip and allow to dry

Protocol for Goldner's Trichrome Staining

- Prepare solutions:

  Solution 1 – Wiegert's haematoxylin

  1. Mix equal parts Solutions A and B immediately before staining. Mix well.

  Solution 2 – Ponceau de Xylidine-acid fuchsin stock

  1. Add 2ml glacial acetic acid to 98 ml dH_2O

2. Dissolve 1.5g Ponceau de Xylidine and 0.5g acid fuchsin

Solution 3 – Azophloxine stock

1. Add 0.6ml glacial acetic acid to 99.4ml dH_2O
2. Dissolve 0.5g azophloxine

Solution 4 – Red solution

1. Make up 80ml 0.2% acetic acid
2. Add 12ml Solution 2 and 8ml Solution 3

Solution 5 – Orange solution

1. Dissolve 3g phosphomolybdic acid and 2g Orange G in 500ml dH_2O

Solution 6 – Green solution

1. Add 1ml glacial acetic acid to 499ml dH_2O
2. Dissolve 1g light green

- Dewax to water
- Stain in Solution 1 for 10min
- Differentiate in 1% acid alcohol for 15s
- Wash well under agitation for 10min
- Stain in Red solution (Solution 4) for 5min
- Rinse in 1% acetic acid
- Stain in Orange solution (Solution 5) for 10min
- Rinse in 1% acetic acid
- Stain in Green solution (Solution 6) for 5 min
- Rinse in dH_2O
- Blot dry
- Quick mount

Appendix IV- Genes in Qiagen osteogenesis gene array (ECM: extra cellular matrix)

Symbol	Description	Classification
Acvr1	Activin A receptor, type 1	Osteoblast differentiation, Ossification, Bone mineralisation
Ahsg	Alpha-2-HS-glycoprotein	Ossification, Bone mineralisation, ECM protease inhibitor
Alpl	Alkaline phosphatase, liver/bone/kidney	Skeletal development, ECM
Anxa5	Annexin A5	Ca ion regulation
Bglap	Bone gamma carboxyglutamate protein	Ossification, Osteoclast differentiation, Osteoblast differentiation, Bone mineralisation, Ca ion regulation, Cell adhesion
Bgn	Biglycan	ECM
Bmp1	Bone morphogenetic protein 1	Cartilage condensation, Ossification, Cell-cell adhesion
Bmp2	Bone morphogenetic protein 2	Ossification, Osteoblast differentiation, Bone mineralisation
Bmp3	Bone morphogenetic protein 3	Ossification
Bmp4	Bone morphogenetic protein 4	Ossification, Osteoblast differentiation, Bone mineralisation
Bmp5	Bone morphogenetic protein 5	Ossification
Bmp6	Bone morphogenetic protein 6	Ossification, Osteoblast differentiation, Bone mineralisation
Bmp7	Bone morphogenetic protein 7	Ossification, Osteoblast differentiation, Bone mineralisation
Bmpr1a	Bone morphogenetic protein receptor, type 1A	Ossification, Osteoblast differentiation, Bone mineralisation, Cell-cell adhesion
Bmpr1b	Bone morphogenetic protein receptor, type 1B	Cartilage condensation, Ossification, Osteoblast differentiation, Bone mineralisation
Bmpr2	Bone morphogenic protein receptor, type II (serine/threonine kinase)	Ossification, Osteoblast differentiation, Bone mineralisation
Cd36	CD36 antigen	ECM adhesion
Cdh11	Cadherin 11	Ossification, Ca ion regulation, Cell-cell adhesion
Chrd	Chordin	Ossification, Osteoblast differentiation
Col10a1	Collagen, type X, alpha 1	Ossification, ECM
Col14a1	Collagen, type XIV, alpha 1	Osteoblast differentiation, ECM, Cell-cell adhesion
Col1a1	Collagen, type I, alpha 1	ECM
Col1a2	Collagen, type I, alpha 2	ECM
Col2a1	Collagen, type II, alpha 1	Cartilage condensation, Ossification, ECM, Cell-cell adhesion
Col3a1	Collagen, type III, alpha 1	ECM, ECM adhesion
Col4a1	Collagen, type IV, alpha 1	ECM
Col5a1	Collagen, type V, alpha 1	ECM, Cell adhesion
Comp	Cartilage oligomeric matrix protein	Skeletal development, Ca ion reg, Cell adhesion
Csf1	Colony stimulating factor 1 (macrophage)	Ossification, Osteoclast differentiation, ECM adhesion

Csf2	Colony stimulating factor 2 (granulocyte-macrophage)	Growth factors
Csf3	Colony stimulating factor 3 (granulocyte)	Growth factors
Ctsk	Cathepsin K	Ossification, ECM proteases
Dlx5	Distal-less homeobox 5	Ossification, Osteoblast differentiation
Egf	Epidermal growth factor	Ca ion reg, Growth factors
Fgf1	Fibroblast growth factor 1	Growth factors
Fgf2	Fibroblast growth factor 2	Ossification, Osteoblast differentiation, Ca ion reg, Growth factors
Fgfr1	Fibroblast growth factor receptor 1	Skeletal development
Fgfr2	Fibroblast growth factor receptor 2	Ossification, Bone mineralisation
Flt1	FMS-like tyrosine kinase 1	ECM
Fn1	Fibronectin 1	Cell adhesion
Gdf10	Growth differentiation factor 10	Ossification, Osteoblast differentiation, Growth factors
Gli1	GLI-Kruppel family member GLI1	Ossification, Osteoblast differentiation, Transcription factors
Icam1	Intercellular adhesion molecule 1	Cell-cell adhesion,
Igf1	Insulin-like growth factor 1	Ossification, Osteoblast differentiation, Bone mineralisation, Growth factors
Igf1r	Insulin-like growth factor I receptor	Ossification
Ihh	Indian hedgehog	Ossification, Osteoblast differentiation, Cell-cell adhesion

Appendix V Trabecular μCT data adjusted for length

Mouse type	Unadjusted at 3 weeks	Adjusted for length
Tissue volume, in mm^3 (SD)		
WT	1.48 (0.27)	1.42 (0.30)
mdx	1.24 (0.09)	1.17 (0.11)
mdx:utr	1.17 (0.09)	1.13 (0.59)
mdx:cmah	1.03 (0.22) ***	0.99 (0.22) ***
Bone volume, in mm^3 (SD)		
WT	0.11 (0.03)	0.10 (0.03)
mdx	0.08 (0.02)	0.07 (0.02)
mdx:utr	0.08 (0.01)	0.08 (0.01)
mdx:cmah	0.08 (0.02)	0.08 (0.02)
BV/TV % (SD)		
WT	6.78 (0.79)	6.90 (0.78)
mdx	6.55 (1.17)	6.29 (1.03)
mdx:utr	6.82 (1.10)	6.95 (1.09)
mdx:cmah	8.30 (1.15)	8.37 (1.28)
Trabecular thickness, in mm (SD)		
WT	0.03 (0.003)	0.03 (0.003)
mdx	0.03 (0.002)	0.03 (0.002)
mdx:utr	0.03 (0.002)	0.03 (0.002)
mdx:cmah	0.03 (0.001)	0.03 (0.002)
Trabecular separation, in mm (SD)		
WT	0.30 (0.05)	0.30 (0.04)
mdx	0.37 (0.07)	0.38 (0.06)
mdx:utr	0.36 (0.03)	0.36 (0.03)
mdx: cmah	0.29 (0.46)	0.28 (0.05)
Trabecular number, in 1/mm (SD)		
WT	2.04 (0.15)	2.08 (0.19)
mdx	2.08 (0.42)	1.98 (0.35)
mdx:utr	2.06 (0.38)	2.11 (0.38)
mdx:cmah	2.66 (0.45) *	2.70 (0.48)*
Structural Model Index (SD)		
WT	2.32 (0.08)	2.32 (0.08)
mdx	2.20 (0.10)	2.21 (0.09)
mdx:utr	2.15 (0.10) *	2.15 (0.10)*
mdx:cmah	2.19 (0.09)	2.18 (0.09)
Connectivity (SD)		
WT	618.9 (121.4)	595.4 (114.0)
mdx	516.5 (147.2)	465.2 (157.5)
mdx:utr	429.6 (108.8)	421.8 (99.4)
mdx:cmah	561.8 (72.5)	551.5 (68.0)

Cortical μCT data adjusted for length

Mouse type	Unadjusted values (3 wks)	Adjusted for tibial length
Cortical tissue area, mm^2 (SD)		
WT	0.62 (0.09)	0.62 (0.09)
mdx	0.56 (0.05)	0.56 (0.05)
mdx:utr	0.54 (0.06)	0.54 (0.06)
mdx:cmah	0.54 (0.07)	0.54 (0.07)
Periosteal perimeter, in mm (SD)		
WT	3.01 (0.22)	3.01 (0.22)
mdx	2.85 (0.13)	2.83 (0.14)
mdx:utr	2.81 (0.18)	2.82 (0.18)
mdx:cmah	2.78 (0.20)	2.79 (0.20)
Cortical bone area, mm^2 (SD)		
WT	0.29 (0.07)	0.30 (0.07)
mdx	0.25 (0.03)	0.25 (0.03)
mdx:utr	0.25 (0.03)	0.25 (0.03)
mdx:cmah	0.22 (0.03) *	0.22 (0.03) *
Endosteal perimeter, in mm (SD)		
WT	2.20 (0.11)	2.21 (0.10)
mdx	2.19 (0.11)	2.17 (0.12)
mdx:utr	2.08 (0.09)	2.09 (0.09)
mdx:cmah	2.15 (0.19)	2.15 (0.19)
Cortical tissue volume, in mm^3 (SD)		
WT	0.45 (0.20)	0.44 (0.20)
mdx	0.34 (0.16)	0.32 (0.14)
mdx:utr	0.45 (0.14)	0.43 (0.13)
mdx:cmah	0.48 (0.06)	0.46 (0.06)
Cortical bone volume, in mm^3 (SD)		
WT	0.22 (0.11)	0.21 (0.11)
mdx	0.15 (0.07)	0.14 (0.06)
mdx:utr	0.20 (0.06)	0.19 (0.06)
mdx:cmah	0.20 (0.03)	0.19 (0.03)
Cortical bone fraction (%) (SD)		
WT	46.62 (4.55)	46.58 (4.56)
mdx	44.56 (3.30)	44.57 (3.34)
mdx:utr	45.76 (1.02)	45.71 (1.04)
mdx:cmah	41.46 (4.50)	41.36 (4.52)
Cortical thickness, in mm (SD)		
WT	0.50 (0.08)	0.49 (0.10)
mdx	0.46 (0.08)	0.45 (0.09)

mdx:utr	0.48 (0.07)	0.48 (0.08)
mdx:cmah	0.54 (0.04)	0.54 (0.04)
Mean polar moment of inertia (SD)		
WT	0.05 (0.02)	0.05 (0.02)
mdx	0.04 (0.01)	0.03 (0.01)
mdx:utr	0.03 (0.01)	0.03 (0.01)
mdx:cmah	0.03 (0.01)	0.03 (0.01)
Mean eccentricity (SD)		
WT	0.57 (0.10)	0.56 (0.11)
mdx	0.47 (0.11)	0.43 (0.11)
mdx:utr	0.61 (0.10)	0.60 (0.09)
mdx:cmah	0.58 (0.10)	0.57 (0.09)

Appendix VI Publications

REVIEW

Animal models to explore the effects of glucocorticoids on skeletal growth and structure

Claire L Wood[1], Ondrej Soucek[2,3], Sze C Wong[4], Farasat Zaman[3], Colin Farquharson[1], Lars Savendahl[3] and S Faisal Ahmed[4]

[1]Division of Developmental Biology, Roslin Institute, University of Edinburgh, Edinburgh, UK
[2]Department of Paediatrics, 2nd Faculty of Medicine, Charles University in Prague and Motol University Hospital, Prague, Czech Republic
[3]Department of Women's and Children's Health, Karolinska Institutet and Pediatric Endocrinology Unit, Karolinska University Hospital, Stockholm, Sweden
[4]Developmental Endocrinology Research Group, School of Medicine, University of Glasgow, Glasgow, UK

Correspondence should be addressed to S F Ahmed: Faisal.ahmed@glasgow.ac.uk

Abstract

Glucocorticoids (GCs) are effective for the treatment of many chronic conditions, but their use is associated with frequent and wide-ranging adverse effects including osteoporosis and growth retardation. The mechanisms that underlie the undesirable effects of GCs on skeletal development are unclear, and there is no proven effective treatment to combat them. An *in vivo* model that investigates the development and progression of GC-induced changes in bone is, therefore, important and a well-characterized pre-clinical model is vital for the evaluation of new interventions. Currently, there is no established animal model to investigate GC effects on skeletal development and there are pros and cons to consider with the different protocols used to induce osteoporosis and growth retardation. This review will summarize the literature and highlight the models and techniques employed in experimental studies to date.

Key Words
- glucocorticoids
- growth
- mouse
- murine
- osteoporosis
- skeletal development

Journal of Endocrinology (2018) **236**, R69–R91

Introduction and background

It is estimated that, at any one time, over 250,000 people are exposed to systemic glucocorticoids (GCs); approximately 10% of children will require GCs at some stage during their childhood (Mushtaq & Ahmed 2002) and 5% of the population aged 80 years or over have used GCs in the past (Kanis *et al.* 2004). Long-term GCs are effective in many conditions, such as inflammatory bowel disease (Pappa *et al.* 2011), chronic renal disorders (Olgaard *et al.* 1992), lung conditions, haematological malignancies (El-Hajj Fuleihan *et al.* 2012) and connective tissue disease, and in some, such as Duchenne muscular dystrophy (DMD) (Matthews *et al.* 2016), they are the mainstay of long-term treatment. Unfortunately, GCs are associated with frequent and wide-ranging side effects, many of which are dose related and associated with considerable morbidity. Of these, two of the potentially most serious and challenging to manage are glucocorticoid-induced osteoporosis (GIO) and growth retardation. Osteoporosis is characterized by a reduction in bone mass and loss of bone microarchitecture, leading to impaired bone strength and increased fracture risk (Reinwald & Burr 2008). GIO is the most prevalent type of secondary osteoporosis and accounts for about 25% of cases (Eastell *et al.* 1998). It is associated with considerable morbidity and mortality; a reduction in bone mineral density (BMD) of up to 40% can occur with GC therapy, and it is estimated that up to half of those on long-term GC therapy will experience fractures (Reid 1997). In those with DMD, 75% are predicted to have a vertebral fracture after 8 years of GC therapy (Bothwell *et al.* 2003), and this

http://joe.endocrinology-journals.org
https://doi.org/10.1530/JOE-17-0361

event is often followed by loss of ambulation (McDonald *et al.* 2002). The General Practice Research Database has shown that daily prednisolone doses of as little as 2.5 mg can cause an increased risk of fracture (Van Staa *et al.* 2000). A recent meta-analysis also showed that there is only weak evidence for the use of common osteoporosis drugs in the prevention of fractures (Amiche *et al.* 2016), suggesting that there is great need for pre-clinical work to inform the development of new therapies.

As healthy children have high rates of bone growth, their skeleton is particularly vulnerable to the adverse effects of GCs on bone formation. GC-induced growth retardation was first described 60 years ago after an equivalent cortisone dose of only 1.5 mg/kg/day (Blodgett *et al.* 1956) and can be considerable; by 15 years of age, boys with DMD who are treated with deflazacort are 21 cm shorter on average than untreated boys (Biggar *et al.* 2006). GC-induced growth retardation can also occur following GC exposure by several alternative routes including inhaled GC in asthma (Allen *et al.* 1994) and intra-articular GC injections in juvenile arthritis (Umlawska & Prusek-Dudkiewicz 2010). GC-induced growth retardation is dose dependent and alternate-day or weekend dosing is associated with less growth retardation (Escolar *et al.* 2011, Ricotti *et al.* 2013). In children, although compensatory catch-up growth may occur after cessation of GC therapy (Crofton *et al.* 1998), prolonged exposure may reduce the potential for catch-up (Simon *et al.* 2002).

Skeletal development

The foetal skeleton develops in two distinct ways; intramembranous ossification occurs within flat bones including the skull and facial bones, whereas endochondral ossification accounts for the linear development of the long bones such as the femur and tibia. Appositional growth also occurs, whereby bone lining the medullary cavity is reabsorbed and new bone tissue is laid down beneath the periosteum, thus increasing bone diameter. This can still occur even after longitudinal growth ceases. In this review, we shall focus on endochondral ossification, which is driven by the actions of the chondrocytes within the epiphyseal growth plate and is the process responsible for bone formation and longitudinal growth of the majority of the skeleton. During the initial, patterning phase of skeletal development, mesenchymal cells condense into tissue elements at specific sites that form the structure of future bones (Karsenty & Wagner 2002). By 5-week gestation in humans, these pre-cartilaginous anlagen reflect the shape, size, position and number of skeletal elements that will be present in the mature skeleton (Javaid & Cooper 2002). Following this, differentiation to either chondrocytes or osteoblasts occurs within the condensations. Chondrocytes within each element organize into growth plates and move through their associated orderly pattern of resting, proliferative and hypertrophic phases (Mackie *et al.* 2011). Once they reach the hypertrophic phase, chondrocytes promote invasion of blood vessels and the production of an extracellular matrix (ECM) that is rich in type II collagen, aggrecan, cytokines and vascular growth factors, which facilitates vascular invasion and gradual mineralization of the ECM surrounding the hypertrophic chondrocyte. The cartilaginous ECM is gradually replaced by a bony ECM (rich in type I collagen), when apoptosis of the hypertrophic chondrocytes occurs and osteoblasts invade the cartilaginous scaffold. As osteoblasts lay down new bone, to form the periosteum, the primary ossification centre expands towards the ends of the cartilage model. In long bones, a secondary ossification centre subsequently forms at each end of the bone, leaving a cartilaginous growth plate in between the two ossification centres. Growth is orchestrated at the growth plates but at puberty, bony bridges form between the ossification centres, resulting in the cessation of growth due to the fusion of the growth plate and its replacement by bone. After birth, a continuing cycle of modelling (or remodelling in adults when it occurs without a change in bone shape) occurs, and there is a fine balance between bone formation and bone resorption to ensure that bone can sense and adapt to alterations in functional, metabolic and mechanical demands.

GCs and their mechanisms

GC-induced osteoporosis

The aetiology of GC-induced osteoporosis is complex and a detailed review of the underlying mechanisms as recently reported (Henneicke *et al.* 2014) is beyond the scope of the current review. Instead, we will summarise the key mechanisms and the differing effects of GCs in osteoblasts, osteoclasts and osteocytes. There are two distinct phases of GC-induced bone loss, resulting from the suppressive effects of GCs on both osteoblastogenesis and osteoclastogenesis. The initial acute period of increased bone resorption is followed by a more indolent phase of bone loss caused by a reduction in bone formation

http://joe.endocrinology-journals.org
https://doi.org/10.1530/JOE-17-0361

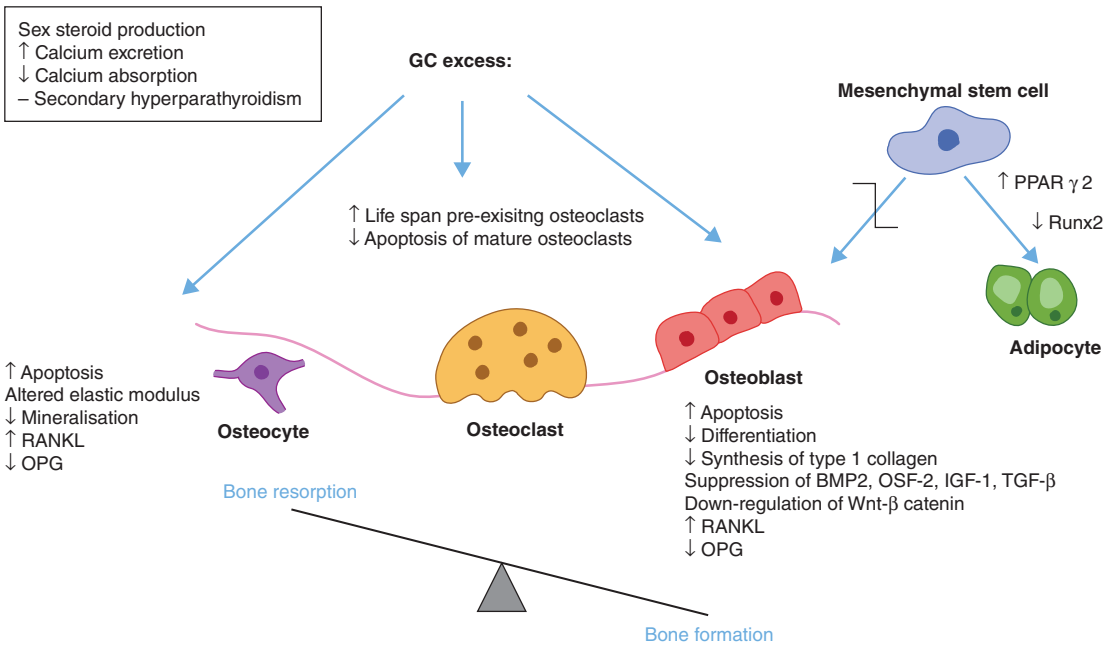

Figure 1
Systemic consequences of exogenous glucocorticoids and effects on different bone cells and adipocytes. BMP2, bone morphogenetic protein 2; IGF-1, insulin-like growth factor-1; Legend-RANKL, receptor activator of nuclear factor kappa-B ligand; OPG, osteoprotegrin; OSF-2, osteoblast-specific factor-2; TGF-β, transforming growth factor beta.

(Canalis *et al.* 2004). Indirect effects of GCs on the skeleton such as decreased calcium absorption, increased renal calcium clearance, reduced growth hormone (GH) secretion and suppression of sex steroid metabolism were previously thought to play a fundamental role, but the main mechanisms underlying GIO are now known to result from the direct effect of GCs on the resident bone cells, see Fig. 1.

Glucocorticoids and mineralocorticoids act through corticosteroid receptors – the mineralocorticoid receptor (MR) and the glucocorticoid receptor (GR). These receptors have often been referred to as Type 1 and Type 2 corticosteroid receptors, respectively (Eberwine 1999, Stewart 2007). The GR is expressed in many bone cells, including osteoblasts, osteoclasts and osteocytes (Bouvard *et al.* 2009) and also in chondrocytes within the growth plate. Once GCs bind to the GR in the cytoplasm, the GR translocates to the nucleus, where it acts as a transcription factor and modifies gene expression, via the GC-response element, either by causing transactivation or transrepression. Transactivation accounts for most of the GC-associated adverse effects and *in vitro* and murine studies demonstrate that selective GR modulators can alter the extent of these adverse effects (Owen *et al.* 2007, Thiele *et al.* 2012). However, studies using transgenic mice with a GR gene mutation that prevents dimerization and therefore transactivation still have reduced bone formation. This suggests that transrepression is probably also at least partly responsible (Rauch *et al.* 2010). Polymorphism of the GR gene is associated with varying susceptibility to GCs (Huizenga *et al.* 1998), which may in part explain the heterogeneity in GC-associated fracture rates in humans.

MicroRNAs (miRNAs) are endogenous RNAs made up of 18–25 nucleotides that interact with messenger RNA to change protein expression. Recent work has shown that several miRNAs have differential expression in GC-treated bone. For example, a reduction in miRNA-29a expression, which interacts with Wnt signalling components and Dkk-1 during osteoblast differentiation was associated with GC-associated bone loss. Gain of miRNA-29a function by a miRNA-29a precursor (Wang *et al.* 2013) attenuated the deleterious effects of GC treatment on bone mass, microarchitecture and biomechanical strength.

Effects of GC on osteoblasts

The chronic bone loss in GIO predominantly results from the ability of GCs to decrease both the number and functionality of osteoblasts. Osteoblasts and adipocytes are both derived from mesenchymal stem cells. By changing the fate of osteoprogenitor cells, GCs effectively reduce the pool of cells that can become mature, differentiated

osteoblasts and bone marrow stromal cells are instead directed along the adipogenesis pathway. This has been shown to occur via the transactivation of CCAAT/enhancer binding protein in murine stromal cells (Pereira *et al.* 2002), which increases expression of peroxisome proliferator-activated receptor gamma 2 (PPARγ2) and suppresses the expression of Runx2 (Canalis *et al.* 2004, 2007). GCs may, therefore, increase bone marrow adipose tissue at the expense of mature osteoblasts and cancellous bone (Weinstein & Manolagas 2000). Outside of bone, GCs also promote preadipocyte conversion to mature adipocytes and thus cause hyperplasia of adipose tissue. A 2-fold increase in cancellous adipocyte area in GC-treated mice compared to placebo has been reported, alongside a significant increase in adipocyte production in bone marrow cultures (Weinstein & Manolagas 2000). The exact mechanism(s) by which the reduction in osteoblastogenesis occurs is unclear; however, it is known that GCs cause suppression of bone anabolic factors such as bone morphogenetic proteins (Pereira *et al.* 2002), osteoblast-specific factor 2 (OSF-2) and insulin-like growth factor 1 (IGF-1) (Jones & Clemmons 1995) and TGF-β that activates osteoblastic transcription factors such as Runx2 and β-catenin. In cultured human osteoblasts, exogenous GC administration also results in the suppression of the canonical Wnt-β-catenin signalling pathway, which prevents osteoblast apoptosis and encourages progression through the osteoblast cell cycle and thus proliferation (Ohnaka *et al.* 2005). Furthermore, murine GC exposure has been shown to upregulate sclerostin gene expression, which antagonises Wnt stimulation of osteoblast differentiation (Yao *et al.* 2016). Using a transgenic mouse line, GCs have also been shown to suppress interleukin 11 expression, which further inhibits osteoblast differentiation (Rauch *et al.* 2010). In addition to inhibiting osteoblast differentiation, GCs also prevent bone matrix synthesis by inhibiting osteoblast-driven synthesis of type I collagen, which forms most of the ECM (Canalis 2005) and osteocalcin. GC administration to mice has also been shown to induce osteoblast apoptosis and suppress terminal differentiation (Weinstein *et al.* 1998).

Effects of GC on osteoclasts and osteocytes

Osteoclasts are derived from haematopoetic stem cells and resorb bone by creating an acidic environment and producing collagen-degrading enzymes. GCs exert an early direct effect on osteoclasts by increasing both their number and activity, with a corresponding increase in bone resorption, seen after only 7 days of GC treatment in mice (Jia *et al.* 2006). This overall increase in osteoclast number occurs despite a reduction in osteoclast production in the bone marrow, suggesting that GC treatment increases the lifespan of pre-existing osteoclasts. However, the longer term role of the osteoclast in glucocorticoid-induced osteoporosis remains controversial; despite an initial increase in bone resorption, prolonged GC excess appears to suppress osteoclast number and function. For example, after 4 weeks of prednisolone treatment in mice, bone resorption fell to or below normal levels (Weinstein *et al.* 1998). GCs also directly block the induction of cytoskeletal changes in the osteoclast required for the resorptive capabilities of the cell (Kim *et al.* 2007). There is also evidence that GCs suppress the proliferation of osteoclast precursors (Kim *et al.* 2006) However, GC also cause an increase in receptor activator of nuclear factor kappa beta ligand (RANKL) (Hofbauer *et al.* 2009), which is produced by both osteoblasts and osteocytes (Nakashima *et al.* 2011, Xiong *et al.* 2011) and downregulation of osteoprotegrin (OPG), which is a decoy receptor for RANKL. This skews the ratio of RANKL: OPG towards osteoclastogenesis. Overall, the long-term effect of exogenous GCs on osteoclastogenesis still requires clarification, but it appears that the osteoblast is the main target of exogenous GCs.

Osteocytes are terminally differentiated osteoblasts that play an important role in the repair of bone micro-damage. GCs alter the osteocyte-canalicular network by changing the elastic modulus surrounding the lacunae of osteocytes and cause reduced mineralisation (Lane *et al.* 2006). Autophagy may be responsible for these observed localised osteocyte perilacunar changes, occurring as a self-protection mechanism during GC treatment (Xia *et al.* 2010). High-dose GC therapy in several animal and human models has also been shown to induce osteocyte apoptosis (Zalavras *et al.* 2003).

GC-induced growth retardation

The growth-suppressing effects of GCs are multifactorial and result from both systemic and local actions on all types of bone cell. The GH/IGF-1 axis is the main determinant of postnatal longitudinal growth, and GH and IGF-1 have interdependent roles in growth regulation. The rate of longitudinal bone growth is principally controlled through the regulation of chondrocyte proliferation, differentiation and hypertrophy at the growth plate (Wong *et al.* 2016). GH promotes chondrocyte differentiation, the secretion of IGF-1 by liver cells and the amplification

of local IGF-1 synthesis by chondrocytes, which induces clonal expansion of chondrocyte columns within the growth plate (Zezulak & Green 1986).

GCs also affect the expression of various components of the GH/IGF-1 axis (Price *et al.* 1992, Jux *et al.* 1998, Klaus *et al.* 2000, Smink *et al.* 2002). Seven days of dexamethasone treatment in prepubertal mice reduced gene expression of IGF-1 throughout chondrocytes in all phases within the growth plate (Smink *et al.* 2003*a*) as well as causing a significant increase in the number of apoptotic cells within the hypertrophic zone. Different mechanisms of GC-induced apoptosis have been proposed such as activation of caspase 3 and suppression of Bcl-2 (Chrysis *et al.* 2003, Espina *et al.* 2008). GCs block the activation of GH and IGF-1 receptors in chondrocytes as well as reducing IGF-1 and GH receptor expression by chondrocytes (Wong *et al.* 2016). Glucocorticoids also impair IGF-1 signalling, mainly via the phosphoinositide 3-kinase pathway within the growth plate. Furthermore, GCs suppress prostaglandin E2 synthesis (Harada *et al.* 1995) as well as vascular endothelial growth factor expression in chondrocytes, thus preventing blood vessel invasion of the ossification centre, which is crucial for degradation of the ECM and subsequent ossification and growth (Smink *et al.* 2003*a*). The intrinsic effect of GC on the mouse growth plate was evident when a local dexamethasone infusion significantly reduced tibial growth compared to the contralateral limb (Baron *et al.* 1992). GCs also act systemically to inhibit the pulsatile secretion of GH from the anterior pituitary gland by increasing somatostatin tone (Mazziotti & Giustina 2013).

Animal models of GIO- and GC-induced growth retardation

It is essential to utilise animal models that show similar pathology to the human disease process that is under scrutiny, in order to effectively carry out pre-clinical studies and test novel compounds. GCs may lead to some localized changes in bone strength that are similar to other causes of osteoporosis, but they also display some unique effects which explains why GC exposure is associated with a higher risk of fracture at equivalent BMD and hence reinforcing the need for an appropriate animal model to specifically investigate GIO (Lane 2005, Xia *et al.* 2010). In addition, the search continues to find selective GR agonists that possess the anti-inflammatory benefits of traditional GCs without the associated adverse effects (Sundahl *et al.* 2015). Suitable pre-clinical models are also vital to this process.

It remains a challenge, however, to find an appropriate animal model for pre-clinical studies of skeletal development as there is no single animal model that exactly mimics the human pathology. Whilst larger animals such as primates and dogs may have the most similar reproductive, anatomical and physiological characteristics, there are ethical issues to consider as well as difficulties with their maintenance and costs (Reinwald & Burr 2008). Sheep, rabbits, and pigs have also been developed as large animal models of GIO in previous studies (Scholz-Ahrens *et al.* 2007, Baofeng *et al.* 2010, Ding *et al.* 2010) but these too have limitations. The following section will discuss the various animal models used to investigate both GIO and GC-induced growth retardation.

Animal species used for GC-induced osteoporosis models

Different animal species have been used to explore the effect of GCs on the development of osteoporosis and to search for substances that prevent the observed deleterious effects. The inquiry performed on PubMed, with 'osteoporosis', 'glucocorticoids' and 'animal name' used as MeSH terms, retrieved 70 papers for rats, 34 for mice, 16 for rabbits, 11 for sheep, 5 for pigs and 3 papers for zebrafish. Although the popularity of rats is related to their established position in postmenopausal osteoporosis research, as evidenced by FDA guidelines (Thompson *et al.* 1995), murine models are increasingly used nowadays. Mice are considered to be an appropriate pre-clinical model of GIO. They share more than 95% of the human genome and can be readily genetically manipulated to simulate specific human diseases. It is also possible to control for the variability found in humans and undertake experiments that would otherwise be impossible in humans. They also have the added advantage of being relatively easy and cost-effective to maintain. The adult mammalian skeleton undergoes a continuous remodelling cycle and some of the early pre-clinical studies using different species failed to appreciate this. More recent work has shown that the mouse shows a similar pattern to human GIO, with an early phase of osteoclast mediated bone resorption, followed by a more indolent phase of decreased osteoblastogenesis and bone formation (Yao *et al.* 2008). Unlike in humans, however, mice lack osteons (or the Haversian system) in cortical bone and therefore remodelling within this structure does not occur as it does in humans (Jilka 2013). Marked effects on bone structural parameters caused by GCs are more

http://joe.endocrinology-journals.org
https://doi.org/10.1530/JOE-17-0361

Table 1 Animal models of glucocorticoid-induced osteoporosis.

Species	Sex + age	GC type, duration, administration, dose	Body Weight (compared to baseline)	Bone site	Bone imaging technique
Mice, FVB	F, 3 week	Dex, 28 days working day SC 14.3 µg/mouse/day	NA	Fem	uCT
Mice, ICR	M, 6–8 week	Dex, 28 days, daily IP inj., 2.5 mg/kg/day	No change in GC group, +15% in controls	Tib	Histomorph, (tib), pQCT (tib diaphysis)
Mice, mod Swiss Webster backgrnd	M, 2 month	Pred, 21 days, sc pellet, 0.8, 2.8 and 4.0 mg/kg/day	–20% in GC groups, +24% in controls	Fem LS	Histomorph, (L4, fem shaft); uCT (L5, distal fem)
Mice, Swiss Webster	M, 2 month	Pred, 21 days, sc pellet, 3.3 mg/kg/day	–20% in GC group; +25% in controls	Fem LS	Histomorph (L4, L5, fem diaphysis); uCT (fem diaphysis, L5)
Mice, WT littermates of transgenic offspring	M, 8 week	Cort, 28 days, sc pellet, NA	NA	Tib LS	Histomorph(prox tibia); uCT (L3, tibia)
Mice, CD1 Swiss White	M, 7–9 week	Cort, 28 days, sc pellet, 15 mg/kg/day	NA	Tib LS	uCT (L3, tibia)
Mice, C57BL/6J + 129/SvJ	F + M, 9 week	Cort, 28 days sc pellet every week NA	+27% in GC groups; +3% in controls	Tib	QCT
Mice, C57BL/6	F, 8–10 week	Dex, 17 days working day IP 88 µg/mouse/day	NA	Fem	pQCT
Mice, C57BL/6J	F, 3 month	Dex, 84 days thrice week IM 2.1 mg/kg/day	NA (at end GC group +22% vs controls)	Tib	Histomorph,;CT
Mice, Swiss Webster	M, 3 month	Pred, 28 days, sc pellet, 1.4, 2.8 and 5.6 mg/kg/day	NA	F	Histomorph
Mice, C57BL/6	F, 4 month	Pred, 28 days sc pellet 1.4, 2.1 mg/kg/day	No change	Fem LS	Histomorph (LS) DXA (LS; fem) uCT (LS)
Mice, Swiss Webster	M, 4 month	Pred, 28 days, sc pellet, 2.1 mg/kg/day	NA	LS	Histomorph(L5); DXA (L? *in vivo*)
Mice, Swiss Webster	F, 5 month	Pred, 10 days sc pellet 2.1 mg/kg/day	NA	LS	Histomorph, DXA
Mice, Swiss Webster	M, 5 month	Pred, 28 days, sc pellet, 5.0 mg/kg/day	No change by end (–15% after 2 weeks in GC gp)	Tib	Histomorph, ; uCT
Mice, C57BL/6	M, 6 month	Pred, 56 days, sc pellet, 2.8 mg/kg/day	NA	Fem LS	uCT (L3, femoral diaphysis)
Mice, C57BL/6	M, 6 month	Pred, 28 days, sc pellet, 2.1 mg/kg/day	NA	LS	Histomorph, (L1–L4); uCT (L5); DXA (L1–L4 *in vivo*)
Mice, Swiss Webster	M, 6 month	Pred, 56 days, sc pellet, 5.0 mg/kg/day	NA	Fem	uCT
Mice, BALB/c	F, 7 month	Dex, 14 & 21 days daily IP 1.0, 5.0, 10 mg/kg/day	No change	Fem Tib LS	Histomorph (Fem, Tib, L5) uCT (Fem, Tib, LS)
Mice, Swiss Webster	M, 6 month	Pred, 21 days, sc pellet, 1.4 mg/kg/day	–10% after 1 week, regained initial weight by study end (no diff GC vs control by end)	LS	Histomorph(L5); uCT (L5)

http://joe.endocrinology-journals.org
https://doi.org/10.1530/JOE-17-0361

Histomorphometry (GC vs controls)	**μCT** (GC vs control)	**DXA** (GC vs control)	**Bone strength testing** (GC vs control)	**Ref**
NA	BV/TV: no diff	NA	NA	Postnov *et al.* (2009)
BV/TV–45%	pQCT: no difference in vBMD, Cortical Thickness–57%	NA	NA	Du *et al.* (2011)
MS/BS–50%, BFR/BS–65% in highest GC group only	BV/TV–22% in highest GC group only	NA	Axial compression (L6), 4-point-bend test (fem) L6: Max Load –48% and –61% in 2 higher doses GC gps, resp; no diff at fem	Yao *et al.* (2016)
L5: MS/BS –46%, BFR/BS –60%; Fem: diaphyseal endocortex: BFR/BS –91%, diaphyseal periosteum –92%	L5: BV/TV –32%; distal fem: BV/TV: no diff	NA	Axial compression (L6), 3-point-bend test (femur) Max Load: L6: –24%, fem: no diff	Dai *et al.* (2015)
Zero endocortical BFR/BS at tib	L3: BV/TV: no diff; tibial metaphysis: BV/TV: no diff; tib diaphysis: Cortical thickness: no diff	NA	3-point-bend test (tib) Max Load: no diff	Henneicke *et al.* (2011)
NA	L3: BV/TV–33%; tibia: BV/TV–56%	NA	NA	Herrmann *et al.* (2009)
NA	Trab BMD: –12% F, –21% M BV/TV –20% F, –27%M cort vBMD decreased, but not cort thickness/bone area	NA	NA	Tamura *et al.* (2015)
NA	Trab vBMD :+30%, Cort thickness: –9%	NA	NA	Grahnemo *et al.* (2015)
NA	BV/TV–47%	NA	NA	Cheng *et al.* (2015)
MS/BS –40–60% (in two highest GC doses)	NA	NA	Axial compression (L6)	Jia *et al.* (2011)
MS/BS: no diff, BFR/BS: –36%	BV/TV: no diff Cort thickness: –22%	LS: aBMD: –5% Fem: no diff	Axial compression (LS) No diff	Sato *et al.* (2016)
BV/TV–66%	NA	aBMD change from baseline–9% in GC gp and–4% in controls, (sig diff between grps)	NA	Li *et al.* (2016)
BV/TV: –23%, MS/BS: –86%, BFR/BS: –90%	NA	aBMD: –18%	Axial compression (LS) Max Load: –34%	Plotkin *et al.* (2011)
BV/TV –22%, MS/BS –61%, BFR/BS –75%	BV/TV no difference	NA	NA	Bouvard *et al.* (2013)
NA	L3: BV/TV–25%; femoral diaphysis: Cortical thickness –20%	NA	NA	Fumoto *et al.* (2014)
BFR/BS–49%	BV/TV not diff	aBMD–11%	Axial compression (L6)	Weinstein *et al.* (2011)
NA	BV/TV no difference (–30% at day 28)	NA	NA	Yao *et al.* (2008)
Fem: BV/TV: no diff, Fem: MS/BS: –62%, Fem: BFR/BS: –74% (at mid GC dose)	Fem BV/TV: +11%; LS: no diff	NA	NA	McLaughlin *et al.* (2002)
BV/TV –19%, MS/BS–31%, BFR/BS–80%	BV/TV–22%	NA	Axial compression (L3) Max Load: no dif	Lane *et al.* (2005)

(Continued)

http://joe.endocrinology-journals.org
https://doi.org/10.1530/JOE-17-0361

Table 1 Continued.

Species	Sex + age	GC type, duration, administration, dose	Body Weight (compared to baseline)	Bone site	Bone imaging technique
Mice, Swiss Webster	M, 7 month	Pred, 27 days, sc pellet, 0.7 and 2.1 mg/kg/day	NA (tendency to lower weights in GC grps by end)	Fem LS	Histomorph (L?, femur), DXA (L? *in vivo*)
Mice, Black Swiss +129SvJ	M, 7 month	Pred, 28 days sc pellet, 2.1 mg/kg/day	NA	Fem LS	Histomorph,(LS, Fem); pQCT (LS, Fem)
Rabbits, Japanese white	F, 6 month	MP, 28 days, daily IM inj., 2.0 mg/kg/day	−9% in both control and GC groups	Fem LS	DXA (fem head and shaft), uCT (fem, L4)
Rabbits, New Zealand white	F, 8 month	MP, 56 days, daily IM inj., 1.0 mg/kg/day	No change	LS	DXA (L3–L4 *in vivo*), uCT (L3–4)
Rabbits, New Zealand white	F, 8 month	MP, 28 days, daily IM inj., 1.5 mg/kg/day	No change (no details were shown)	LS Knee	DXA (L3–L4, knee)
Rabbits, New Zealand white	M, 8 month	Dex, 84 days, twice a week IM inj., 0.9 mg/kg/day	Slight increase in all groups (no numbers shown)	LS	Histomorph (L3), DXA (L3–L4)
Rats, Wistar	M, 2 month	Pred, 42 days, oral gavage every second day, 15 mg/kg/day	NA	Tib	pQCT (tibial diaphysis)
Rats, Sprague–Dawley	F, 3 month	Dex, 84 days, twice a week IM inj., 0.7 mg/kg/day	No change	Multi sites	DXA (head, upper limb, fem, trunk, rib, pelvis, spine, whole body)
Rats, Sprague–Dawley	F, 3 month	MP, 56 days, thrice a week SC inj., 2.1 mg/kg/day	No change	Tib Fem	Histomorph,(tib diaphysis); DXA (fem)
Rats, Sprague–Dawley	M, 3 months	Pred, 90 days, daily oral gavage, 1.5, 3.0 and 6.0 mg/kg/day	+33% in GC groups; +62% in controls	Tib Fem LS	Histomorph (fem, tibia); DXA (fem, L5); uCT (L6)
Rats, Wistar	F, 3, 6, 12 month	Pred, 28 days, daily SC inj., 2.0 and 20 mg/kg/day	+9%, +3% No change in controls; +5%, no change, −8% in high GC group (3, 6, 12-month old mice, resp.)	Tib	pQCT (tib metaphysis and diaphysis)
Rats, Sprague–Dawley	F, 6 month	MP, 30 days, thrice a week SC inj, 3.0 mg/kg/day	No change (no details shown)	Tib Total Body	Histomorph(tib)DXA (total body)
Rats, Sprague–Dawley	F, 8 month	MP, 60 days, daily SC inj, 30 mg/kg/day	NA	Fem	DXA
Rats, Wistar	M, 8 month	MP, 42 days, weekly SC inj, 1.0 mg/kg/day	NA	Femur LS	Histomorph (distal fem); DXA (L2–L4 *in vivo*)
Rats, Sprague–Dawley	M, NA 200–225 g	Dex, 19 days, continuous pump infusion, 16.3 µg/rat/day	+8% in GC group, +52% in controls	Fem	Histomorph

Histomorphometry (GC vs controls)	**μCT** (GC vs control)	**DXA** (GC vs control)	**Bone strength testing** (GC vs control)	**Ref**
BV/TV–39%, MS/BS–26%, BFR/BS–53% (in higher GC group only)	NA	aBMD change from base –3, –7, –9% in controls, lower, higher GC dose groups, respectively (sig diff between higher GC vs control)	NA	Weinstein *et al.* (1998)
LS: BV/TV: –31% LS: BFR/BS: 84% Fem: no difference	pQCT: vBMD no diff	NA	Axial compression (LS); 3-point bend test (femur) Max Load: LS: –29%, Fem: no diff	Hofbauer *et al.* (2009)
NA	Osteonecrosis after 8 weeks (4-week treatment +4-week wash out) in fem head	aBMD: femoral head –33%; fem shaft–22%	NA	Lin *et al.* (2016)
NA	BV/TV–17%	aBMD–25%	Axial compression (L3–4) Max Load–19%, no diff in Stiffness	Baofeng *et al.* (2010)
NA	NA	aBMD: spine–9%; knee–19%	NA	Castañeda *et al.* (2008)
BV/TV–39%	NA	aBMD–27%	Axial compression (L4) Max Load–38%, Stiffness–34%	Yongtao *et al.* (2014)
NA	Cortical vBMD –2%, Cortical thickness: no diff, SSI–25%	NA	NA	Yokote *et al.* (2008)
NA	NA	aBMD: spine–18%	NA	Jiang *et al.* (2016)
MS/BS–60%, BFR/BS–76%	NA	aBMD–5%	NA	Iwamoto *et al.* (2008)
tib: BV/TV: no diff, MS/BS–27% (high GC gp only), BFR/BS–52% (all combined); fem: BV/TV: no diff, MS/BS–39% (comb), BFR/BS–38% (comb)	BV/TV: no difference	aBMD: fem: –8%; L5: no diff	Axial compression (L5), 3-point-bend test (fem) Max Load: fem: –7% (no diff with lowest dose), L5: –22%; Stiffness: fem: –17% (no diff with lowest dose), L5: data not shown	Lin *et al.* (2014)
NA	Trab vBMD higher/lower/not diff (3/6/12-month old), Cortical vBMD unchanged in either group (only % changes from baseline given)	NA	NA	Ogoshi *et al.* (2008)
BV/TV–11%, MS/BS–13%, BFR/BS–18%	NA	aBMD–8%	NA	Dalle Carbonare *et al.* (2007)
NA	NA	aBMD–9%	3-point-bend test (femur) Max Load–27%	Bitto *et al.* (2009)
BV/TV –34%	NA	aBMD –1% in controls, –10% in GC (sig diff between gps)	NA	Wimalawansa & Simmons (1998)
BV/TV–50%	NA	NA	NA	King *et al.* (1996)

aBMD, areal bone mineral density; BFR/BV, bone formation rate/bone surface; BV/TV, bone volume/tissue volume; Cort, corticosterone; Dex, dexamethasone; DXA, dual x-ray absorptiometry; F, female; Fem, femur; GC, glucocorticoid; Histomorph, histomorphometry; LS, lumbar spine, M, male; MAR, mineral apposition rate; MP, methylprednisolone; MS/BS, mineralizing surface/bone Surface; NA, not available; Pred, prednisolone; pQCT, peripheral quantitative CT; QCT, quantitative CT; Tib, tibia; uCT, micro-CT; vBMD, volumetric BMD.

http://joe.endocrinology-journals.org
https://doi.org/10.1530/JOE-17-0361

frequently observed in younger animals, but in order to avoid complications in bone measurements due to loss of weight caused by GC, it has been suggested that skeletally mature animals should be used to investigate GIO. Gene knockout and transgenic approaches have also established the usefulness of the mouse in determining which genes are critical for bone turnover (Rauch *et al.* 2010). The mouse has also been used effectively in other models of bone loss, such as androgen or oestrogen loss and ageing (Pogoda *et al.* 2005). However, with regard to bone density and quality, dogs appear to be most similar to humans and rats the least (Aerssens *et al.* 1998). Interestingly, *in vivo* and *in vitro* bone mineral imaging as well as scale mineralization studies in zebrafish were described as a very simple alternative to explore alterations in mineralization pathways to GC challenge (Barrett *et al.* 2006).

Techniques to measure GIO

Osteoporosis is defined as an alteration of bone structure leading to increased fragility and fracture rate. In humans, clinically significant fractures and inappropriately low BMD serve as diagnostic criteria for osteoporosis. There is no such consensus on criteria defining osteoporosis in animal models. As spontaneous fractures do not occur in most animal models, unlike in humans, suitable proxy outcome measures need to be utilized. The following methods have been used to describe changes in bone health after GC exposure:

Bone histomorphometry

Traditional methods to assess changes in bone structure include the evaluation of histological sections of mineralized bone. In basic osteoporosis research, lumbar vertebral bodies and long-bone (typically, femoral and tibial) metaphyses are examined to investigate trabecular (cancellous) bone changes, whereas cortical bone alterations are assessed within the diaphysis of long bones. In addition to the primary static measures, so-called dynamic parameters can also be calculated using the primary measures assessed on bone histological sections after appropriate fluorochrome labelling.

Dual-energy x-ray absorptiometry

Dual-energy x-ray absorptiometry (DXA) is widely used for BMD evaluation in the clinical as well as research setting. DXA assesses areal BMD (aBMD=bone mineral content/bone area). The precision of *in vivo* DXA scans has been shown to be very good in mice (coefficients of variation <2%) at total body (excluding head), lumbar spine (L4–L5), whole femur and whole tibia sites (Iida-Klein *et al.* 2003). This enables longitudinal BMD observations to be used in murine osteoporosis studies. However, in studies, DXA scans have often been performed on different skeletal sites *ex vivo* as an outcome measure (Table 1). The main drawback of DXA is that there is no information on bone structure or quality. Bone mass increases with body mass, therefore, smaller and younger animals will have lower BMD compared to larger and older ones, but not necessarily more fragile bones. Since experimental drugs, such as GCs, may affect body weight or growth (as discussed later), size should be taken into account to prevent the introduction of bias regarding the effect on BMD. However, bone size adjustments are rarely undertaken in murine osteoporosis studies (none of the studies listed in Table 1).

Peripheral quantitative computerized tomography and micro-computerized tomography

By using peripheral quantitative computerized tomography (pQCT), true volumetric BMD can be assessed, that, together with bone architecture and geometry, allows for calculation of bone strength and structural indices. These indices correlate very well with whole bone strength when tested *ex vivo* (Siu *et al.* 2003, Kokoroghiannis *et al.* 2009). Micro-computerized tomography (μCT) is normally used at a resolution of 1–10 μm in rodents (Bouxsein *et al.* 2010). Major advantages compared to 2D histological sections are the 3D nature of the data, so that real mineralized bone matrix volumes in whole bone tissue volumes (BV/TV) can be assessed, faster data acquisition and larger bone region under investigation.

Biomechanical testing and biochemical markers of bone metabolism

Although the primary aim may be focused at the molecular, cellular, tissue or whole bone organ level, the crucial clinically relevant outcome of the numerous papers focusing on osteoporosis research is to increase bone strength and reduce fracture risk. Bone tissue is a complex and metabolically active structure and, at the organ level, bone continuously adapts to mechanical loading and other environmental factors to mitigate the stress and sustain its function. Therefore, none of the

http://joe.endocrinology-journals.org
https://doi.org/10.1530/JOE-17-0361

above mentioned parameters alone can sufficiently mirror actual bone health. Biomechanical testing is the only method capable of verifying whether a treatment may cause or prevent bone fragility. In laboratory animals, bone competence is usually tested through axial compression of the vertebral bodies or three-point bending of long bones (Jepsen *et al.* 2015).

Distinct biochemical markers in serum/plasma are also used to follow disease or drug-mediated changes in bone formation (Glendenning 2011).

GC type and dose to induce osteoporosis

Prednisolone (or prednisone), methylprednisolone and dexamethasone are the most frequent synthetic GC used in osteoporosis animal models (Table 1). However, they have distinct differences in potency. Although the following order from the most to least potent is in agreement with several studies (i.e., dexamethasone > methylprednisolone > prednisolone/prednisone > hydrocortisone/corticosterone), the relative efficacy may vary based on the assay or method of evaluation (Meikle & Tyler 1977, Tanaka *et al.* 1994, Buttgereit *et al.* 2002). The relative efficacy and potency of GC may also depend on the system studied, for example the potency for effects on bone metabolism may be quite different to those on glucose and fat metabolism (Ahmed *et al.* 2002, Wallace *et al.* 2003). In addition, it is not yet clear whether genomic or non-genomic pathways play the major role in GIO (Hartmann *et al.* 2016). Altered bone structure was observed in two-month-old male mice treated with 15 mg/kg/day of corticosterone (Herrmann *et al.* 2009), but only 2.8 mg/kg/day of methylprednisolone was needed to induce similar changes in mice of same age and sex (Yao *et al.* 2016). Therefore, methylprednisolone appears to be more potent than corticosterone in osteoporosis induction. Another study showed decreases in bone density, bone formation rate and bone strength in 6-month-old C57BL/6 male mice treated with prednisolone 2.1 mg/kg/day over 28 days, but the same dose was not sufficient to induce significant changes in female mice (Weinstein *et al.* 2011). By contrast, the same prednisolone dose was used in female mice of similar age, but different strain (i.e., Swiss Webster), and significant decreases were observed in bone density, bone formation and bone strength after only 10 days (Plotkin *et al.* 2011). This highlights that sex- as well as strain-specific efficacy may be present with different GCs. Controlling for sex (male), strain (Swiss Webster) and route of administration (slow release subcutaneous pellets), 3-month-old mice required 5.6 mg/kg/day of prednisolone, the highest dose tested, to induce a significant decrease in mineralizing surface/bone surface (MS/BS) and bone strength (Jia *et al.* 2011) whereas a decrease in MS/BS and BMD was observed in 7-month-old mice challenged with 2.1 mg/kg/day of prednisolone (Weinstein *et al.* 1998). Therefore, mouse age and pubertal status may be an additional factor influencing the potency of the tested GCs. In humans a dose of dexamethasone of 1 mg is equivalent to 6 mg of prednisolone, therefore consideration of the dose used relative to clinical application is important.

It is also important when investigating GIO to describe the impact on both trabecular and cortical bone as there are discrepancies between data obtained at different sites, see Table 1.

Route of administration in GIO models

Osteoporosis is induced by systemic administration of GC. Many studies implemented regular intramuscular, intraperitoneal or subcutaneous injections, but single implantation of slow release subcutaneous pellet or oral gavage have also been used (Table 1). In rats of the same strain and age, daily oral gavage of GCs over a 90 day period (Lin *et al.* 2014) led to similar adverse effects on bone (as assessed by histomorphometry and aBMD) as thrice weekly subcutaneous injections of GC over 56 days (Iwamoto *et al.* 2008). By contrast, a much shorter period of intervention is necessary to induce osteoporosis with daily injections (Ogoshi *et al.* 2008) or continuous infusion through subcutaneously implanted osmotic pumps (King *et al.* 1996). Daily injections are stressful for the animals, which may negatively influence the outcome and ethical regulations in some countries may not allow multiple repeated injections over a long time period. For example, the injection of carrier alone (PEG 400) caused a 3-fold increase in serum corticosterone levels in mice, compared to a 5–10 fold increase induced by an intraperitoneal injection of 10 mg corticosterone/kg body weight, 1 h after injection (Herrmann *et al.* 2009). This technique of administration would also not be acceptable to most patients in the clinical trial setting. Micro-osmotic pumps were found to have a large variation in residual volumes 21 days after implantation. With a filling volume of 250 µL, residual volumes containing active drug ranged from 50 to 180 µL, which indicated major differences in the flow-rate of individual pumps (Herrmann *et al.* 2009). Subcutaneous insertion of slow release pellets containing

http://joe.endocrinology-journals.org
https://doi.org/10.1530/JOE-17-0361

corticosterone leads to more consistent drug levels as compared to subcutaneous injections of corticosterone. Oral gavage seems to be less effective compared to daily injections or slow release subcutaneous pellets, but has the most translational relevance, as this would be the most accepted method of GC administration in the clinical setting. Whilst slow release pellet insertion may reduce unnecessary repetition of periodical injections over the study period their safety and efficacy needs further validation.

Animal models of GC-induced growth retardation

It is likely that different animal models are required to investigate GIO and growth retardation. Poor choice of model may result in misinterpretation of results and limited translational promise. For example, the young growing rat does not show any bone loss or changes in microarchitecture of trabecular bone and modelling is the prevailing activity; therefore, it is a poor model for human GIO (until at least 9 months of age when the transition to remodelling occurs). It does appear, however, to be a good model to mimic the growth retardation seen in children exposed to GC (Lelovas *et al.* 2008). For growth studies, the age and status of sexual maturity at the time of growth plate closure must also be considered. Unlike humans, bone acquisition and longitudinal bone growth continue in mice and rats after sexual maturity. Linear bone growth in rodents increases during the largest proportion of life expectancy in comparison with other species (Kilborn *et al.* 2002). Humans and primates (showing the second highest ratios of age at growth plate closure to life expectancy), cows and sheep are also considered adults at the age when growth plate closure occurs. By contrast, rabbits, dogs and cats would be described as very young adults at the time of physis closure. In mice, whilst the highest growth phase is from weaning until sexual maturation, body weight continues to increase in the mouse up to the end of the 52nd week and long-bone growth continues slowly after puberty (Jilka 2013). By contrast, New Zealand white rabbits begin sexual maturation at approximately 2 months of age and undergo epiphyseal fusion by approximately 6 months of age. Therefore, in order to induce growth retardation and allow for subsequent catch-up growth in one study, GC challenge was commenced when the rabbits were 5 weeks of age (Weise *et al.* 2001). Nevertheless, using rabbits at a young age proved problematic for Kugelberg and coworkers who were unable to sex them at 3 weeks of age and therefore had to use both males and females in their study (Kugelberg *et al.* 2005). This is important as imprinting (Jansson *et al.* 1985) by androgen secretion of the neonatal rodent brain has been shown to result in sex differentiation of body growth and, therefore, it is also important to consider which sex of animal is most relevant to the research question.

Techniques to assess bone growth rate

When studying mammalian growth, simple gross parameters such as weight, body or tail length have historically been used as proxies for growth rates (Hughes & Tanner 1970), and are still routinely recorded when assessing growth in pre-clinical studies. These measurements can be very inaccurate, however, and dependent on other confounding factors (Melin *et al.* 2005). X-ray determination of the length of different long bones with the aid of anatomical landmarks (Weber *et al.* 1968) is a simple but more accurate proxy. Recent advances in imaging also mean that tibial/femoral length can be accurately measured using micro (μ)CT. This is often performed in conjunction with other measures of trabecular and cortical bone structure (Waarsing *et al.* 2004, Bouxsein *et al.* 2010). In addition, *in vivo* μCT is a non-invasive imaging technique that allows longitudinal bone growth to be evaluated over a period of weeks or months in the same animals and would therefore be well suited for monitoring GC-induced growth retardation. This can be a cost-effective and ethical method as it reduces the number of animals required for a study and also minimizes intra-subject variability. Potential drawbacks include the dose of ionizing radiation delivered through multiple scans and the potential for radiation associated tissue effects on the growing skeleton (Klinck *et al.* 2008, Laperre *et al.* 2011). Inclusion of a non-irradiated contralateral limb would clarify the magnitude of this potential issue. Also, by administering fluorescent labels (Owen *et al.* 2009) at known time intervals, the bone formation rate (BFR) at the chondro-osseous junction can be assessed visually under UV light, without the need for further staining or decalcification (Dobie *et al.* 2015). In addition to the methods used to assess the growth rate of the entire bone, measures of the tibial epiphyseal growth plate width have been used for over 50 years as a reliable proxy indicator of growth rate (Interlichia *et al.* 2010).

More recently, a number of investigators have used *ex vivo* models such as rodent metatarsals in culture

(Mårtensson *et al.* 2004, Mushtaq *et al.* 2004). For example, when fetal mouse metatarsals were cultured for up to 10 days with either daily or alternate-day dexamethasone at 10^{-6}M, dexamethasone-treated bones paralleled control bone growth rate until day 8 when their rate of growth decreased resulting in a total length that was significantly reduced from controls at days 8 and 10 (Mushtaq *et al.* 2004).

It is well established that the rate of linear bone growth is dependent on growth plate chondrocyte proliferation, matrix turnover and changes in chondrocyte shape and size (Hunziker & Schenk 1989, Farquharson & Jefferies 2000). Advances in quantitative histology now enable the growth plate to be scrutinized in greater detail to assess the contribution of the different chondrocyte activities to overall growth rate. Whilst quantitative histology techniques were developed in the 1970s to assess the relationship between cell division in growth cartilage and overall bone growth, chondrocyte proliferation is now routinely quantified by the immunohistochemical detection of BrdU incorporation into proliferating cells in tissue sections of the growth plate (Farquharson & Loveridge 1990). Cell death of hypertrophic chondrocytes within the growth plate is also required for physiological bone growth and the TUNEL assay allows the detection and quantification of apoptotic cells within a population of chondrocytes (Kyrylkova *et al.* 2012).

GC type and dose to induce growth retardation

The inquiry was performed on PubMed, with 'growth retardation' or 'growth', 'glucocorticoids' and 'animal name' used as MeSH terms. When summarising the data, we have not included studies where only gross body measurement parameters were taken as a subset of a larger study. Studies where only an abstract was available were also excluded. Where the same groups have published multiple work using the same species and methodology, only the initial data has been represented in Table 2.

As shown in Table 2, dexamethasone was the most frequently used GC in the growth retardation models that we reviewed. Method of administration and dosage varied greatly, consistent with the GIO models. Rodents were used in the majority of studies. Four of the studies administered subcutaneous injections of dexamethasone to mice of between 3 and 5 weeks of age. All used daily injections, except for one, where a 5-times weekly regimen was followed (Rooman *et al.* 1999). The length of course varied from 7 to 28 days and the dose used varied from approximately 0.02 mg/kg/day to 5 mg/kg/day. In one of the studies, where three varying doses were used, the lowest dose of 0.2 µg (approximately 0.02 mg/kg/day) did not cause significant growth reduction, but both the 2 µg and 20 µg doses caused similar growth retardation (Rooman *et al.* 1999). No differing side effects were reported in the two groups. When a dose of 2 mg/kg/day was used, body weight was reduced only in males and femur length only in females, whilst a significant reduction in body weight was demonstrated by day 3 using 5 mg/kg/day in females in a different study (Owen *et al.* 2009). It would, therefore, appear that there is a sex difference in response to GCs and that an optimal dose would be greater than 2 mg/kg/day to ensure significant growth retardation in both sexes. However, the rapid catabolic response with a reduction in body weight by day 3 seen with a dose of 5 mg/kg/day would suggest the need for close monitoring (Owen *et al.* 2009).

We reviewed 8 studies using rats, usually either Wistar or Sprague–Dawley and up to 4 months of age at study induction. All except two studies used only male rats. Length of course varied greatly from 4 to 90 days. In one of the studies using prednisolone, 10 mg/kg/day was originally chosen (after a previous study by the same authors demonstrated no effect on cortical bone using 5 mg/kg/day (Ortoft *et al.* 1992)) but after observing unexpectedly high weight loss, the dose was decreased to 5 mg/kg/day. Using 5 mg/kg/day they were able to demonstrate reduced longitudinal bone growth of the lumbar vertebrae. This highlights one of the problems of using body weight as a reflection of growth. GC can show a dual metabolic effect on body weight, depending on the dosage, method of administration and length of treatment. High dosages can cause a catabolic effect and loss in body weight whereas lower dosages can cause an increase in appetite and associated weight gain (as frequently seen in humans). For example, 1 mg/kg single dose of dexamethasone given to piglets caused accelerated growth at 18 days of age (Carroll 2001). Piglets are also noted to have a metabolic response to GCs that closely mimics the response observed in infants and children receiving long-term GC therapy (Ward *et al.* 1998). One of the studies using Wistar rats demonstrated inhibition of growth after only 10 days of either inhaled budesonide or fluticasone (Kemer *et al.* 2015), even at a dose of only 50 µg. This is particularly relevant when considering that

http://joe.endocrinology-journals.org
https://doi.org/10.1530/JOE-17-0361

Table 2 Animal models of glucocorticoid-induced growth retardation.

Species	Sex + age	GC duration, method, dose	Measurement	Bone site	Results	Ref
FVB Mice	F, 3 weeks	Dex, 5 days a week for 4 weeks, daily SC inj, 0.2, 2 or 20 µg/animal/day (approx. 0.02 mg–2 mg/kg/day)	BW, snout-tail length under anaesthesia weekly After cull, organs weighed, tib dissected, length measured using digital caliper Tib dissected-GP width	tib	• Dex at 2 and 20 µg/day caused reduction in:wt of tib, humerus and lumbar vertebra (only vertebra sig) • wt of organs esp. liver/ muscle • total width of GP (mainly due to reduction in proliferative zone) Tibia length only slightly affected. No change in hypertrophic zone	Rooman *et al.* (1999)
FVB mice	F, 3 weeks	Dex, 7 days, daily SC inj, 20 µg/day (approx. 2 mg/kg/day)	BW Nose-tail length Tibiae dissected-GP width and zones TUNEL assay	tib	Dex caused reduction in:- total body weight (16.7 vs 13.6 g) length gain (1.9 vs 1.3 cm) tib GP width (dec in width of proliferative zone) number of prolif chondrocytes Inc in number of apoptotic chondrocytes	Smink *et al.* (2003*a*)
BL6 and BL6 (P21$^{-/-}$) mice	F, 4 weeks	Dex, 7 days, daily SC inj, 5 mg/kg/day	Daily BW, nose-rump body length on days 1 and 7 Digital caliper measurement of tib and organ weights after dissection.GP zone widths. Calcein labelling to measure MAR	tib	• Dex treatment caused reduction in:BW by D3 and CRL by D7 (8.2 vs 7.6 cm) • liver, spleen and tibia Wt • GP width (esp in PZ and HZ) • MAR	Owen *et al.* (2009)
Homozygous Bax-deficient and C57BL6 mice	Both, 30–32 days	Dex, 28 days, daily SC inj, 2 mg/kg	Body weight Bones measured weekly by X-ray BrdU histology, TUNEL assay	fem	Dex caused reduction in: fem growth (by 47% in female, 50% in males BW (only significant in males) chondrocyte proliferation and chondrocyte column density Inc no. apoptotic chondrocytes	Zaman *et al.* (2012)
Wistar rats	Both, 10 days	Budesonide 10 days, inhaled, 50 or 200 µg Fluticasone propionate 10 days, inhaled, 50 or 250 µg	BW change during study period Tib dissected-GP zone widths, proliferation and apoptosis rates using Ki-67 and Tdt markers		Lowest weight gain in high-dose fluticasone group All GP zone widths lower than controls (only significant at higher doses, more marked in high-dose fluticasone than budesonide) Proliferative cell rates sig lower than controls Apoptosis in hypertophic zone of high-dose fluticasone group almost doubled	Kemer *et al.* (2015)

Sprague–Dawley rats	M, 23 days	Dex, 24 days, daily intraperitoneal inj, 40 μg/kg/day	BW bi-weekly Nose-anal length prior to cull		• Dex caused reduction in: final BW (118 vs 106 g) • nose-anal length (18.5 vs 17.8 cm) • growth rate (7.4 vs 6.1 g/day)	Tulipano *et al.* (2007)
Long-Evans rats	M, 37 days	Cortisone, 4 days, daily SC inj, 1 mg/25 g BW/day	BW, tail length Right tib measured after cull, with calipers. GP Width measured	tib	• Cortisone treatment showed reduction in:tail + tib length • BW velocity Wider epiphyseal GP width seen	Mosier and Jansons (1989)
Sprague–Dawley rats	M, 7 weeks	Dex, 7 days, daily SC inj, 5 mg/kg/day	BW Growth rate by calcein labelling of tibia TUNEL assay	tib	Dex caused reduction in: BW (23% loss vs 32% gain in controls. growth rate (68 /207 μm day) chondrocyte column density 4-fold increase in apoptosis in THCs	Chrysis *et al.* (2003)
Wistar rats	F, 2 months	Methylpred, 90 days, daily SC inj, variable dose-1, 3, 6 or 9 mg/kg/day	BW weekly. Nose-tail length, length of R lower extremity weekly for 4 weeks, then fortnightly using sliding caliper. Calcein/tetracycline labelling of GP sections from prox tib after dissection.	fem, tib	• Dose-dependent decrease in:weight gain • nose-tail length • fem and tib lengths (even at 1 mg/kg/day) • growth at the prox epiphyseal GP • muscle mass Effect seen after 1 week, persisted for study duration	Ortoft *et al.* (1998*b*)
Sprague–Dawley rats	M, 3 months	Pred, 90 days, oral gavage, varied-1.5/3.0/6.0 mg/kg/day	BW weekly Calcein/tetracycline labelling to measure MAR and longitudinal growth rate	fem, tib	• Pred caused dose-dependent reduction in:BW (11.4, 14.7 and 19.2% with pred at 1.5/3.0/6.0 mg/kg/day respectively) • fem metaphyseal growth rate 6.0 mg/kg/day caused reduction in periosteal MAR of tib cortex	Lin *et al.* (2014)
Wistar rats	M, 3 months	Corticosterone, 3 weeks, daily SC inj, 10 mg/day (approx 40 mg/kg/day)	BW TUNEL assay Tib dissected-GP width	tib	• Corticosterone caused reduction in:BW velocity • GP width Increased apoptosis of terminal hypertrophic chondrocytes	Silvestrini *et al.* (2000)

(Continued)

http://joe.endocrinology-journals.org
https://doi.org/10.1530/JOE-17-0361

http://joe.endocrinology-journals.org
https://doi.org/10.1530/JOE-17-0361

Table 2 Continued.

Species	Sex + age	GC duration, method, dose	Measurement	Bone site	Results	Ref
Wistar rats	F,105 days	Pred, 80 days, daily SC inj, 5 mg/kg/day (initially 10 mg/kg/day-Dec due to s/e)	BW Height of L5 vertebrae	LS	Longitudinal bone growth of L5 arrested	Ortoft *et al.* (1998*a*)
New Zealand white rabbits	Both, 3 weeks	Dex, 8 weeks, eye drops, 20 µL 10 times daily over 13 h period. Gp 1-all doses, group 2-alt doses. Ave daily dose 0.24–0.62 mg/kg/day	BW and crown-rump length weekly Fem length measured after cull by micrometre	fem	• Dex caused dose-dependent reduction in:crown-rump length • fem length • BW gain	Kugelberg *et al.* (2005)
New Zealand white rabbits	M, 4 weeks	Dex, local infusion into one proximal tibial GP, over 7 days, 80 ng/µL, 1 µL/h	Serial radiographs of pinned tibia	tib	Dex caused reduction in: epiphyseal growth rate compared with contralateral side Most marked at days 5–8. Recovered by day 21	Baron *et al.* (1992)
New Zealand white rabbits	M, 5 weeks	Dex, 5 weeks, daily SC inj, 0.5 mg/kg per day	Fem length measurement using digital caliper Oxytetracycline labelling of longitudinal growth. Fem dissected-GP width/zones Chondrocyte prolif rate	fem	Dex caused reduction in: fem length heights of the total GP, prolif and hypertrophic zones BW gain	Weise *et al.* (2001)
Large Polish White piglets	Both, 2 days	Dex, 12 days, IM inj every 2nd day, 0.5 mg/kg of birthwt	BW at start and end of study Length of fem, hum (technique not specified)	fem, hum	• Dex treatment caused reduction in:BW • Femoral and humerus bone length (not significant)	Śliwa *et al.* (2005)
Yorkshire piglets	M, 4–5 days	Dex, 15 days, bd by orogastric gavage, Tapering-5 days each of 0.5, 0.3 and 0.2 mg/kg/day	Body weight, snout to rump length, fem length using single photon absorptiometry	fem	• Dex caused reduction in:length by day 6 and BW by day 11 Growth velocity reduction persisted only with 0.3 and 0.5 mg/kg/day	Ward *et al.* (1998)
Cross-bred piglets (Landrace × Yorkshire)	F, 6 weeks	Pred, 5 days, oral, 5 mg/kg/day	Tib dissected-GP width. TUNEL assay	tib	• Pred caused reduction in:total GP widths to 81% of controls, proliferative zone • trab bone length 7-fold chondrocytes in hypertrophic zone inc in apoptotic	Smink *et al.* (2003*b*)

BD, twice daily; BW, birthweight; Dex, dexamethasone; F, female; Fem, femur; GP, Growth plate; IM, intramuscular; Inj, injection; LS, lumbar spine; M, male; MAR, mineral apposition rate; Pred, prednisolone; SC, SC; S/E, side effects; tib, tibia.

inhaled GCs are the treatment of choice for persistent asthma symptoms in both children and adults.

Decreased bone growth has been demonstrated even at concentrations as low as 1 mg/kg/day in a study of rats, where doses of up to 9 mg/kg/day of methylprednisolone were used (Ortoft *et al.* 1998*a*). In this study there was no discernible dose-specific side effects although serum insulin levels were reduced in all groups. These authors also noted that the catabolic effect of 9 mg/kg/day of methylprednisolone (Ortoft *et al.* 1998*b*) by daily subcutaneous injection was less than that noted when a 5 mg of depot prednisolone was used in rats of a similar age (Ortoft *et al.* 1998*a*). This suggests that routes of administration must also be considered.

Three studies were reviewed which used rabbits; each of these used dexamethasone, but via a different method of administration (eye drops, local infusion and daily subcutaneous injection) therefore they cannot be directly compared. However, all studies reported significant reductions in growth within the dexamethasone-treated groups. All rabbits were aged 5 weeks or less at study induction and all were aged 11 weeks or less at time of cull. In the only pre-clinical model to use a topical method of GC administration, significant effects on growth were demonstrated (Kugelberg *et al.* 2005).

Three studies used piglets, all of whom were less than 7 weeks of age at the end of the study. Again a variety of routes of GC administration were used. It would appear that a dose of 0.25 mg/kg/day of dexamethasone is insufficient to induce bone growth retardation in young piglets (Śliwa *et al.* 2005). In a similar study, a reduction in growth velocity persisted only when piglets were dosed with 0.3 mg/kg/day and above (Ward *et al.* 1998) and when prednisolone, at an equivalent dexamethasone dose of 0.75 mg/kg/day was used, a significant change in growth plate histology was seen (Smink *et al.* 2003*b*).

It appears that higher equivalent doses of GCs are used in rodents compared to larger mammals such as rabbits and piglets. In young mice, an optimal dose of dexamethasone when administered by daily subcutaneous injection seems to be between 2 and 5 mg/kg/day. This review demonstrates that there are a varied number of different methods that can be employed effectively to cause GC-induced growth retardation. However, unlike the review of GIO, we found no studies using implantable pellets or osmotic mini-pumps that measured growth parameters and therefore further studies are required to clarify their effectiveness of these delivery routes in causing growth retardation. Having highlighted the pitfalls of using the gross parameter body weight as a marker of growth; we propose that any future studies should also use other confirmatory parameters of growth such as bone length measurements, BFR or growth plate histology.

Genetically engineered animal models

Global deletion of GR is lethal and mice die of respiratory failure due to lung atelectasis on the first day of life (Cole *et al.* 1995) therefore it is not possible to create a complete GR-knockout model. However, tissue-specific genetically modified mouse models can be useful to tease out the effect of GCs on interlinked reactions between the different types of bone cells. For example, deleting osteoblast-specific GR conferred protection from GIO, whilst deleting osteoclast-derived GR had no effect (Rauch *et al.* 2010). Development of col 2.3 and col 3.6 hydroxysteroid dehydrogenase (HSD)2 transgenic mouse models that activate 11β-HSD2 in osteoblasts showed decreased vertebral trabecular and femoral cortical bone mass, without any change in serum GC levels (Liu *et al.* 2004), thus implicating a role for endogenous GC signalling within the osteoblast for optimal bone mass acquisition.

Conclusion

In this review, we have demonstrated that there are specific outcome measures that should be assessed when investigating either GIO or GC-induced growth retardation. We carried out a literature review with the aim of determining the most appropriate animal model to use when demonstrating the effects of GC on growth and bone structure, but results are too heterogeneous to enable one specific model to be advocated over another in all situations. However, there is sufficient evidence to recommend that investigation of GC-induced growth retardation in mice should be performed using dexamethasone 2–5 mg/kg/day by daily subcutaneous injection, and the outcome measures should include serial lengths (using consistent measuring technique) and/or growth plate width and BFR; the measurement of body weight for assessing linear growth is too inaccurate. When investigating GIO, there is insufficient evidence to recommend one specific mode of delivery over another, but in most studies, a dose of prednisolone 2–5 mg/kg/day in mice has been sufficient. Recommended

http://joe.endocrinology-journals.org
https://doi.org/10.1530/JOE-17-0361

outcome measures include volumetric BMD (by pQCT or μCT rather than by DXA for greater accuracy) and bone biomechanical testing to mimic fracture rate in clinical studies.

Declaration of interest

Diurnal research grant, Novo Nordisk-data monitoring board and educational meetings, Kyowa Kirin, consultancy (S F A).

Funding

C W, S F A and C F are supported by the Medical Research Council (MRC) (MR/N020588/1). S C W and S F A are supported by the Chief Scientist Office (CSO) (CAF/DMD/14/01). L S is supported by the Swedish Research Council project 2015-02406. O S is partly supported by an ESPE Research Fellowship, sponsored by Novo Nordisk A/S. F Z is supported by funding from the Swedish Research Council, Swedish Society for Medical Research, Swedish Childhood Cancer Foundation, Sällskapet Barnavård, HKH Kronprinsessan Lovisas Förening för Barnasjukvård/Stiftelsen Axel Tielmans Minnesfond. We are grateful to the Biotechnology and Biological Sciences Research Council (BBSRC) for Institute Strategic Programme Grant Funding (BB/J004316/1; BBS/E/D/20221657) to CF.

Author contribution statement

All authors drafted the outline for the manuscript. C W and O S wrote the first draft. S F A, C F, S C W, L S and F Z revised and approved the final version.

References

Aerssens J, Boonen S, Lowet G & Dequeker J 1998 Interspecies differences in bone composition, density, and quality: potential implications for in vivo bone research. *Endocrinology* **139** 663–670. (https://doi.org/10.1210/endo.139.2.5751)

Ahmed SF, Tucker P, Mushtaq T, Wallace AM, Williams DM & Hughes IA 2002 Short-term effects on linear growth and bone turnover in children randomized to receive prednisolone or dexamethasone. *Clinical Endocrinology* **57** 185–191. (https://doi.org/10.1046/j.1365-2265.2002.01580.x)

Allen DB, Mullen M & Mullen B 1994 A meta-analysis of the effect of oral and inhaled corticosteroids on growth. *Journal of Allergy and Clinical Immunology* **93** 967–976. (https://doi.org/10.1016/S0091-6749(94)70043-5)

Amiche MA, Albaum JM, Tadrous M, Pechlivanoglou P, Lévesque LE, Adachi JD, Cadarette SM, Article O, Amiche MA, Albaum JM, *et al.* 2016 Efficacy of osteoporosis pharmacotherapies in preventing fracture among oral glucocorticoid users : a network. *Osteoporosis International* **27** 1989–1998. (https://doi.org/10.1007/s00198-015-3476-4)

Baofeng L, Zhi Y, Bei C, Guolin M, Qingshui Y & Jian L 2010 Characterization of a rabbit osteoporosis model induced by ovariectomy and glucocorticoid. *Acta Orthopaedica* **81** 396–401. (https://doi.org/10.3109/17453674.2010.483986)

Baron J, Huang Z, Oerter KE, Bacher JD & Cutler GB 1992 Dexamethasone acts locally to inhibit longitudinal bone growth in rabbits. *American Journal of Physiology* **263** E489–E492.

Barrett R, Chappell C, Quick M & Fleming A 2006 A rapid, high content, in vivo model of glucocorticoid-induced osteoporosis. *Biotechnology Journal* **1** 651–655. (https://doi.org/10.1002/biot.200600043)

Biggar WD, Harris VA, Eliasoph L & Alman B 2006 Long-term benefits of deflazacort treatment for boys with Duchenne muscular dystrophy in their second decade. *Neuromuscular Disorders* **16** 249–255. (https://doi.org/10.1016/j.nmd.2006.01.010)

Bitto A, Burnett B, Polito F, Levy R, Marini H, Di Stefano V, Irrera N, Armbruster M, Minutoli L, Altavilla D, *et al.* 2009 Genistein aglycone reverses glucocorticoid-induced osteoporosis and increases bone breaking strength in rats: a comparative study with alendronate. *British Journal of Pharmacology* **156** 1287–1295. (https://doi.org/10.1111/j.1476-5381.2008.00100.x)

Blodgett FM, Burgin L, Iezzoni D, Gribetz D & Talbot NB 1956 Effects of prolonged cortisone therapy on the statural growth, skeletal maturation and metabolic status of children. *New England Journal of Medicine* **254** 636–641. (https://doi.org/10.1056/NEJM195604052541402)

Bothwell JE, Gordon KE, Dooley JM, MacSween J, Cummings EA & Salisbury S 2003 Vertebral fractures in boys with Duchenne muscular dystrophy. *Clinical Pediatrics* **42** 353–356. (https://doi.org/10.1177/000992280304200408)

Bouvard B, Audran M, Legrand E & Chappard D 2009 Ultrastructural characteristics of glucocorticoid-induced osteoporosis. *Osteoporosis International* **20** 1089–1092. (https://doi.org/10.1007/s00198-009-0864-7)

Bouvard B, Gallois Y, Legrand E, Audran M & Chappard Glucocor D 2013 Glucocorticoids reduce alveolar and trabecular bone in mice. *Joint Bone Spine* **80**. (https://doi.org/10.1016/j.jbspin.2012.01.009)

Bouxsein ML, Boyd SK, Christiansen BA, Guldberg RE, Jepsen KJ & Müller R 2010 Guidelines for assessment of bone microstructure in rodents using micro-computed tomography. *Journal of Bone and Mineral Research* **25** 1468–1486. (https://doi.org/10.1002/jbmr.141)

Buttgereit F, da Silva JAP, Boers M, Burmester G-R, Cutolo M, Jacobs J, Kirwan J, Köhler L, Van Riel P, Vischer T, *et al.* 2002 Standardised nomenclature for glucocorticoid dosages and glucocorticoid treatment regimens: current questions and tentative answers in rheumatology. *Annals of the Rheumatic Diseases* **61** 718–722. (https://doi.org/10.1136/ard.61.8.718)

Canalis E 2005 The fate of circulating osteoblasts. *New England Journal of Medicine* **352** 2014–2016. (https://doi.org/10.1056/NEJMe058080)

Canalis E, Bilezikian JP, Angeli A & Giustina A 2004 Perspectives on glucocorticoid-induced osteoporosis. *Bone* **34** 593–598. (https://doi.org/10.1016/j.bone.2003.11.026)

Canalis E, Mazziotti G, Giustina A & Bilezikian JP 2007 Glucocorticoid-induced osteoporosis: pathophysiology and therapy. *Osteoporosis International* **18** 1319–1328. (https://doi.org/10.1007/s00198-007-0394-0)

Carroll JA 2001 Dexamethasone treatment at birth enhances neonatal growth in swine. *Domestic Animal Endocrinology* **21** 97–109. (https://doi.org/10.1016/S0739-7240(01)00107-2)

Castañeda S, Calvo E, Largo R, González-González R, de la Piedra C, Díaz-Curiel M & Herrero-Beaumont G 2008 Characterization of a new experimental model of osteoporosis in rabbits. *Journal of Bone and Mineral Metabolism* **26** 53–59. (https://doi.org/10.1007/s00774-007-0797-1)

Cheng Y, Wang W-L & Liang J-J 2015 Genistein attenuates glucocorticoid-induced bone deleterious effects through regulation Eph/ephrin expression in aged mice. *International Journal of Clinical and Experimental Pathology* **8** 394–403.

Chrysis D, Ritzen EM & Sävendahl L 2003 Growth retardation induced by dexamethasone is associated with increased apoptosis of the growth plate chondrocytes. *Journal of Endocrinology* **176** 331–337. (https://doi.org/10.1677/joe.0.1760331)

Cole TJ, Blendy JA, Monaghan AP, Krieglstein K, Schmid W, Aguzzi A, Fantuzzi G, Hummler E, Unsicker K & Schütz G 1995 Targeted

disruption of the glucocorticoid receptor gene blocks adrenergic chromaffin cell development and severely retards lung maturation. *Genes and Development* **9** 1608–1621. (https://doi.org/10.1101/gad.9.13.160)

Crofton PM, Ahmed SF, Wade JC, Stephen R, Elmlinger MW, Ranke MB, Kelnar CJH & Wallace WHB 1998 Effects of intensive chemotherapy on bone and collagen turnover and the growth hormone axis in children with acute lymphoblastic leukemia. *Journal of Clinical Endocrinology and Metabolism* **83** 3121–3129. (https://doi.org/10.1210/jcem.83.9.5133)

Dai W, Jiang L, Lay Y-AE, Chen H, Jin G, Zhang H, Kot A, Ritchie RO, Lane NE & Yao W 2015 Prevention of glucocorticoid induced bone changes with beta-ecdysone. *Bone* **74** 48–57. (https://doi.org/10.1016/j.bone.2015.01.001)

Dalle Carbonare L, Bertoldo F, Valenti MT, Zordan S, Sella S, Fassina A, Turco G, Realdi G, Lo Cascio V & Giannini S 2007 Risedronate prevents the loss of microarchitecture in glucocorticoid-induced osteoporosis in rats. *Journal of Endocrinological Investigation* **30** 739–746. (https://doi.org/10.1007/BF03350811)

Ding M, Cheng L, Bollen P, Schwarz P & Overgaard S 2010 Glucocorticoid induced osteopenia in cancellous bone of sheep. *Spine* **35** 363–370. (https://doi.org/10.1097/BRS.0b013e3181b8e0ff)

Dobie R, Ahmed SF, Staines KA, Pass C, Jasim S, MacRae VE & Farquharson C 2015 Increased linear bone growth by GH in the absence of SOCS2 is independent of IGF-1. *Journal of Cellular Physiology* **230** 2796–2806. (https://doi.org/10.1002/jcp.25006)

Du J, Cheng B, Zhu X & Ling C 2011 Ginsenoside Rg1, a novel glucocorticoid receptor agonist of plant origin, maintains glucocorticoid efficacy with reduced side effects. *Journal of Immunology* **187** 942–950. (https://doi.org/10.4049/jimmunol.1002579)

Eastell R, Reid DM, Compston J, Cooper C, Fogelman I, Francis RM, Hosking DJ, Purdie DW, Ralston SH, Reeve J, *et al*. 1998 A UK Consensus Group on management of glucocorticoid-induced osteoporosis: an update. *Journal of Internal Medicine* **244** 271–292. (https://doi.org/10.1046/j.1365-2796.1998.00408.x)

Eberwine J 1999 Glucocorticoid and mineralocorticoid receptors as transcription factors. In *Basic Neurochemistry: Molecular, Cellular and Medical Aspects*, 6th edition. Eds G Siegel, BA Granoff & RW Albers. Philidelphia, PA, USA: Lippincott-Raven.

El-Hajj Fuleihan G, Muwakkit S, Arabi A, Daouk LE, Ghalayini T, Chaiban J & Abboud M 2012 Predictors of bone loss in childhood hematologic malignancies: a prospective study. *Osteoporosis International* **23** 665–674. (https://doi.org/10.1007/s00198-011-1605-2)

Escolar DM, Hache LP, Clemens PR, Cnaan A, McDonald CM, Viswanathan V, Kornberg AJ, Bertorini TE, Nevo Y, Lotze T, *et al*. 2011 Randomized, blinded trial of weekend vs daily prednisone in Duchenne muscular dystrophy. *Neurology* **77** 444–452. (https://doi.org/10.1212/WNL.0b013e318227b164)

Espina B, Liang M, Russell RGG & Hulley PA 2008 Regulation of bim in glucocorticoid-mediated osteoblast apoptosis. *Journal of Cellular Physiology* **215** 488–496. (https://doi.org/10.1002/jcp.21335)

Farquharson C & Jefferies D 2000 Chondrocytes and longitudinal bone growth: the development of tibial dyschondroplasia. *Poultry Science* **79** 994–1004. (https://doi.org/10.1093/ps/79.7.994)

Farquharson C & Loveridge N 1990 Cell proliferation within the growth plate of long bones assessed by bromodeoxyuridine uptake and its relationship to glucose 6-phosphate dehydrogenase activity. *Bone and Mineral* **10** 121–130. (https://doi.org/10.1016/0169-6009(90)90087-V)

Fumoto T, Ishii K, Ito M, Berger S, Schütz G & Ikeda K 2014 Mineralocorticoid receptor function in bone metabolism and its role in glucocorticoid-induced osteopenia. *Biochemical and Biophysical Research Communications* **447** 407–412. (https://doi.org/10.1016/j.bbrc.2014.03.149)

Glendenning P 2011 Markers of bone turnover for the prediction of fracture risk and monitoring of osteoporosis treatment: a need for international reference standards. *Osteoporosis International* **22** 391–420.

Grahnemo L, Jochems C, Andersson A, Engdahl C, Ohlsson C, Islander U & Carlsten H 2015 Possible role of lymphocytes in glucocorticoid-induced increase in trabecular bone mineral density. *Journal of Endocrinology* **224** 97–108. (https://doi.org/10.1530/JOE-14-0508)

Harada SI, Balena R, Rodan GA & Rodan SB 1995 The role of prostaglandins in bone formation. *Connective Tissue Research* **31** 279–282. (https://doi.org/10.3109/03008209509010823)

Hartmann K, Koenen M, Schauer S, Wittig-Blaich S, Ahmad M, Baschant U & Tuckermann JP 2016 Molecular actions of glucocorticoids in cartilage and bone during health, disease, and steroid therapy. *Physiological Reviews* **96** 409–447. (https://doi.org/10.1152/physrev.00011.2015)

Henneicke H, Herrmann M, Kalak R, Brennan-Speranza TC, Heinevetter U, Bertollo N, Day RE, Huscher D, Buttgereit F, Dunstan CR, *et al*. 2011 Corticosterone selectively targets endocortical surfaces by an osteoblast-dependent mechanism. *Bone* **49** 733–742. (https://doi.org/10.1016/j.bone.2011.06.013)

Henneicke H, Gasparini SJ, Brennan-Speranza TC, Zhou H & Seibel MJ 2014 Glucocorticoids and bone: local effects and systemic implications. *Trends in Endocrinology and Metabolism* **25** 197–211. (https://doi.org/10.1016/j.tem.2013.12.006)

Herrmann M, Henneicke H, Street J, Modzelewski J, Kalak R, Buttgereit F, Dunstan CR, Zhou H & Seibel MJ 2009 The challenge of continuous exogenous glucocorticoid administration in mice. *Steroids* **74** 245–249. (https://doi.org/10.1016/j.steroids.2008.11.009)

Hofbauer LC, Zeitz U, Schoppet M, Skalicky M, Schuler C, Stolina M, Kostenuik PJ, Erben RG, Schüler C, Stolina M, *et al*. 2009 Prevention of glucocorticoid-induced bone loss in mice by inhibition of RANKL. *Arthritis and Rheumatism* **60** 1427–1437. (https://doi.org/10.1002/art.24445)

Hughes PC & Tanner JM 1970 A longitudinal study of the growth of the black-hooded rat: methods of measurement and rates of growth for skull, limbs, pelvis, nose-rump and tail lengths. *Journal of Anatomy* **106** 349–370.

Huizenga NATM, Koper JW, de Lange P, Pols HAP, Stolk RP, Burger H, Grobbee DE, Brinkmann AO, de Jong FH & Lamberts SWJ 1998 A polymorphism in the glucocorticoid receptor gene may be associated with an increased sensitivity to glucocorticoids in vivo. *Journal of Clinical Endocrinology and Metabolism* **83** 144–151. (https://doi.org/10.1210/jcem.83.1.4490)

Hunziker EB & Schenk RK 1989 Physiological mechanisms adopted by chondrocytes in regulating longitudinal bone growth in rats. *Journal of Physiology* **414** 55–71. (https://doi.org/10.1113/jphysiol.1989.sp017676)

Iida-Klein A, Lu SS, Yokoyama K, Dempster DW, Nieves JW & Lindsay R 2003 Precision, accuracy, and reproducibility of dual X-ray absorptiometry measurements in mice in vivo. *Journal of Clinical Densitometry* **6** 25–33.

Interlichia JP, Williams NG, Rodgers BDBD, Greenspan FS, Li CH, Simpson ME, Evans HM, Smeets T, van Buul-Offers S, Rodgers BDBD, *et al*. 2010 A rapid, valid and inexpensive assay for measuring epiphyseal plates in mouse tibia. *Growth Hormone and IGF Research* **20** 171–173. (https://doi.org/10.1016/j.ghir.2009.10.004)

Iwamoto J, Matsumoto H, Takeda T, Sato Y, Liu X & Yeh JK 2008 Effects of vitamin K2 and risedronate on bone formation and resorption, osteocyte lacunar system, and porosity in the cortical bone of glucocorticoid-treated rats. *Calcified Tissue International* **83** 121–128. (https://doi.org/10.1007/s00223-008-9146-1)

Jansson J, Ekberg S, Isaksson J, Mode A & Gustafsson J 1985 Imprinting of growth hormone secretion, body growth, and hepatic steroid metabolism by neonatal testosterone. *Endocrinology* **117** 1881–1889. (https://doi.org/10.1210/endo-117-5-1881)

Javaid MKK & Cooper C 2002 Prenatal and childhood influences on osteoporosis. *Best Practice and Research* **16** 349–367. (https://doi.org/10.1053/beem.2002.0199)

Jepsen KJ, Silva MJ, Vashishth D, Guo XE & van der Meulen MC 2015 Establishing biomechanical mechanisms in mouse models: practical guidelines for systematically evaluating phenotypic changes in the diaphyses of long bones. *Journal of Bone and Mineral Research* **30** 951–966. (https://doi.org/10.1002/jbmr.2539)

Jia D, O'Brien CA, Stewart SA, Manolagas SC & Weinstein RS 2006 Glucocorticoids act directly on osteoclasts to increase their life span and reduce bone density. *Endocrinology* **147** 5592–5599. (https://doi.org/10.1210/en.2006-0459)

Jia J, Yao W, Guan M, Dai W, Shahnazari M, Kar R, Bonewald L, Jiang JX & Lane NE 2011 Glucocorticoid dose determines osteocyte cell fate. *FASEB Journal* **25** 3366–3376. (https://doi.org/10.1096/fj.11-182519)

Jiang Y, Gou H, Wang S, Zhu J, Tian S & Yu L 2016 Effect of pulsed electromagnetic field on bone formation and lipid metabolism of glucocorticoid-induced osteoporosis rats through canonical Wnt signaling pathway. *Evidence-Based Complementary and Alternative Medicine* **2016** 1–13. (https://doi.org/10.1155/2016/4927035)

Jilka RL 2013 The relevance of mouse models for investigating age-related bone loss in humans. *Journals of Gerontology* **68** 1209–1217. (https://doi.org/10.1093/gerona/glt046)

Jones JI & Clemmons DR 1995 Insulin-like growth factors and their binding proteins: biological actions. *Endocrine Reviews* **16** 3–34. (https://doi.org/10.1210/edrv-16-1-3)

Jux C, Leiber K, Hügel U, Blum W, Ohlsson C, Klaus G & Mehls O 1998 Dexamethasone impairs growth hormone (GH)-stimulated growth by suppression of local insulin-like growth factor (IGF)-I production and expression of GH- and IGF-I-receptor in cultured rat chondrocytes. *Endocrinology* **139** 3296–3305. (https://doi.org/10.1210/endo.139.7.6099)

Kanis JA, Johansson H, Oden A, Johnell O, de Laet C, Melton LJ, Tenenhouse A, Reeve J, Silman AJ, Pols HA, *et al.* 2004 A meta-analysis of prior corticosteroid use and fracture risk. *Journal of Bone and Mineral Research* **19** 893–899. (https://doi.org/10.1359/JBMR.040134)

Karsenty G & Wagner EF 2002 Reaching a genetic and molecular understanding of skeletal development. *Developmental Cell* **2** 389–406. (https://doi.org/10.1016/S1534-5807(02)00157-0)

Kemer S, Karademir F, Aydemir G, Kucukodaci Z, Pirgon O, Genc FA & Aydinoz S 2015 Effects of inhaled corticosteroids on the growth plates of infant rats. *Fetal and Pediatric Pathology* **34** 223–232. (https://doi.org/10.3109/15513815.2015.1042606)

Kilborn SH, Trudel G & Uhthoff H 2002 Review of growth plate closure compared with age at sexual maturity and lifespan in laboratory animals. *Contemporary Topics in Laboratory Animal Science* **41** 21–26.

Kim H-J, Zhao H, Kitaura H, Bhattacharyya S, Brewer JA, Muglia LJ, Ross FP & Teitelbaum SL 2006 Glucocorticoids suppress bone formation via the osteoclast. *Journal of Clinical Investigation* **116** 2152–2160. (https://doi.org/10.1172/JCI28084)

Kim H-J, Zhao H, Kitura H, Bhattacharyya S, Brewer JA, Muglia LJ, Patrick Ross F & Teitelbaum SL 2007 Glucocorticoids and the Osteoclast. *Annals of the New York Academy of Sciences* **1116** 335–339. (https://doi.org/10.1196/annals.1402.057)

King CS, Weir EC, Gundberg CW, Fox J & Insogna KL 1996 Effects of continuous glucocorticoid infusion on bone metabolism in the rat. *Calcified Tissue International* **59** 184–191. (https://doi.org/10.1007/s002239900107)

Klaus G, Jux C, Fernandez P, Rodriguez J, Himmele R & Mehls O 2000 Suppression of growth plate chondrocyte proliferation by corticosteroids. *Pediatric Nephrology* **14** 612–615. (https://doi.org/10.1007/s004670000344)

Klinck RJ, Campbell GM & Boyd SK 2008 Radiation effects on bone architecture in mice and rats resulting from in vivo micro-computed tomography scanning. *Medical Engineering and Physics* **30** 888–895. (https://doi.org/10.1016/j.medengphy.2007.11.004)

Kokoroghiannis C, Charopoulos I, Lyritis G, Raptou P, Karachalios T & Papaioannou N 2009 Correlation of pQCT bone strength index with mechanical testing in distraction osteogenesis. *Bone* **45** 512–516. (https://doi.org/10.1016/j.bone.2009.05.021)

Kugelberg M, Shafiei K, Ohlsson C, Sävendahl L & Zetterström C 2005 Glucocorticoid eye drops inhibit growth in the newborn rabbit. *Acta Paediatrica* **94** 1096–1101. (https://doi.org/10.1080/08035250510028731)

Kyrylkova K, Kyryachenko S, Leid M & Kioussi C 2012 Detection of apoptosis by TUNEL assay. In *Odontogenesis: Methods in Molecular Biology (Methods and Protocols)*, **887** 41–47. Ed. C Kioussi. Clifton, NJ, USA: Humana Press. (https://doi.org/10.1007/978-1-61779-860-3_5)

Lane NE 2005 New observations on bone fragility with glucocorticoid treatment. Results from an in vivo animal model. *Journal of Musculoskeletal and Neuronal Interactions* **5** 331–332.

Lane NE, Yao W, Balooch M, Nalla RK, Balooch G, Habelitz S, Kinney JH & Bonewald LF 2006 Glucocorticoid-treated mice have localized changes in trabecular bone material properties and osteocyte lacunar size that are not observed in placebo-treated or estrogen-deficient mice. *Journal of Bone and Mineral Research* **21** 466–476. (https://doi.org/10.1359/JBMR.051103)

Laperre K, Depypere M, van Gastel N, Torrekens S, Moermans K, Bogaerts R, Maes F & Carmeliet G 2011 Development of micro-CT protocols for in vivo follow-up of mouse bone architecture without major radiation side effects. *Bone* **49** 613–622. (https://doi.org/10.1016/j.bone.2011.06.031)

Lelovas PP, Xanthos TT, Thoma SE, Lyritis GP & Dontas IA 2008 The laboratory rat as an animal model for osteoporosis research. *Comparative Medicine* **58** 424–430.

Li X, Zhou Z, Zhang Y & Yang H 2016 IL-6 contributes to the defective osteogenesis of bone marrow stromal cells from the vertebral body of the glucocorticoid-induced osteoporotic mouse. *PLoS ONE* **11** e0154677. (https://doi.org/10.1371/journal.pone.0154677)

Lin S, Huang J, Liang ZZ, Liu Y, Liu G, Li N, Wang K, Liyi ZZZZZ, Wu T, Qin L, *et al.* 2014 Glucocorticoid-Induced Osteoporosis in Growing Rats. *Calcified Tissue International* **95** 362–373. (https://doi.org/10.1007/s00223-014-9899-7)

Lin T, Liu J, Yang S, Liu X, Feng X & Fu D 2016 Relation between the development of osteoporosis and osteonecrosis following glucocorticoid in a rabbit model. *Indian Journal of Orthopaedics* **50** 406. (https://doi.org/10.4103/0019-5413.185606)

Liu F, Woitge HW, Braut A, Kronenberg MS, Lichtler AC, Mina M & Kream BE 2004 Expression and activity of osteoblast-targeted Cre recombinase transgenes in murine skeletal tissues. *International Journal of Developmental Biology* **48** 645–653. (https://doi.org/10.1387/ijdb.041816fl)

Mackie EJ, Tatarczuch L & Mirams M 2011 The skeleton: a multi-functional complex organ. The growth plate chondrocyte and endochondral ossification. *Journal of Endocrinology* **211** 109–121. (https://doi.org/10.1530/JOE-11-0048)

Mårtensson K, Chrysis D & Sävendahl L 2004 Interleukin-1β and TNF-α act in synergy to inhibit longitudinal growth in fetal rat metatarsal bones. *Journal of Bone and Mineral Research* **19** 1805–1812. (https://doi.org/10.1359/JBMR.040805)

Matthews E, Brassington R, Kuntzer T, Jichi F & Manzur AY 2016 Corticosteroids for the treatment of Duchenne muscular dystrophy. In *Cochrane Database of Systematic Reviews*, CD003725. Ed E Matthews. Chichester, UK: John Wiley & Sons, Ltd. (https://doi.org/10.1002/14651858.CD003725.pub4)

Mazziotti G & Giustina A 2013 Glucocorticoids and the regulation of growth hormone secretion. *Nature Reviews Endocrinology* **9** 265–276. (https://doi.org/10.1038/nrendo.2013.5)

McDonald DG, Kinali M, Gallagher AC, Mercuri E, Muntoni F, Roper H, Jardine P, Jones DH & Pike MG 2002 Fracture prevalence in Duchenne

muscular dystrophy. *Developmental Medicine and Child Neurology* **44** 695–698. (https://doi.org/10.1111/j.1469-8749.2002.tb00272.x)

McLaughlin F, Mackintosh J, Hayes BP, McLaren A, Uings IJ, Salmon P, Humphreys J, Meldrum E & Farrow SN 2002 Glucocorticoid-induced osteopenia in the mouse as assessed by histomorphometry, microcomputed tomography, and biochemical markers. *Bone* **30** 924–930. (https://doi.org/10.1016/S8756-3282(02)00737-8)

Meikle AW & Tyler FH 1977 Potency and duration of action of glucocorticoids. Effects of hydrocortisone, prednisone and dexamethasone on human pituitary-adrenal function. *American Journal of Medicine* **63** 200–207. (https://doi.org/10.1016/0002-9343(77)90233-9)

Melin AD, Bergmann PJ & Russell AP 2005 Mammalian postnatal growth estimates: the influence of weaning on the choice of a comparative metric. *Journal of Mammalogy* **86** 1042–1049. (https://doi.org/10.1644/1545-1542(2005)86[1042:MPGETI]2.0.CO;2)

Mosier HD & Jansons RA 1989 Rats stunted by high-dose glucocorticoid treatment are capable of undergoing catch-up growth after fasting. *Pediatric Research* **25** 373–376. (https://doi.org/10.1203/00006450-198904000-00013)

Mushtaq T & Ahmed SF 2002 The impact of corticosteroids on growth and bone health. *Archives of Disease in Childhood* **87** 93–96. (https://doi.org/10.1136/ADC.87.2.93)

Mushtaq T, Bijman P, Ahmed SF & Farquharson C 2004 Insulin-like growth factor-I augments chondrocyte hypertrophy and reverses glucocorticoid-mediated growth retardation in fetal mice metatarsal cultures. *Endocrinology* **145** 2478–2486. (https://doi.org/10.1210/en.2003-1435)

Nakashima T, Hayashi M, Fukunaga T, Kurata K, Oh-hora M, Feng JQ, Bonewald LF, Kodama T, Wutz A, Wagner EF, *et al.* 2011 Evidence for osteocyte regulation of bone homeostasis through RANKL expression. *Nature Medicine* **17** 1231–1234. (https://doi.org/10.1038/nm.2452)

Ogoshi T, Hagino H, Fukata S, Tanishima S, Okano T & Teshima R 2008 Influence of glucocorticoid on bone in 3-, 6-, and 12-month-old rats as determined by bone mass and histomorphometry. *Modern Rheumatology* **18** 552–561. (https://doi.org/10.1007/s10165-008-0096-2)

Ohnaka K, Tanabe M, Kawate H, Nawata H & Takayanagi R 2005 Glucocorticoid suppresses the canonical Wnt signal in cultured human osteoblasts. *Biochemical and Biophysical Research Communications* **329** 177–181. (https://doi.org/10.1016/j.bbrc.2005.01.117)

Olgaard K, Storm T, van Wowern N, Daugaard H, Egfjord M, Lewin E & Brandi L 1992 Glucocorticoid-induced osteoporosis in the lumbar spine, forearm, and mandible of nephrotic patients: a double-blind study on the high-dose, long-term effects of prednisone versus deflazacort. *Calcified Tissue International* **50** 490–497. (https://doi.org/10.1007/BF00582160)

Ortoft G, Oxlund H, Jørgensen PH & Andreassen TT 1992 Glucocorticoid treatment or food deprivation counteract the stimulating effect of growth hormone on rat cortical bone strength. *Acta Paediatrica* **81** 912–917. (https://doi.org/10.1111/j.1651-2227.1992.tb12134.x)

Ortoft G, Oxlund H & Andreassen TT 1998*a* Administration of a glucocorticoid with depot effect counteracts the stimulating effect of growth hormone on cancellous and cortical bone of the vertebral body in rats. *Calcified Tissue International* **63** 14–21.

Ortoft G, Grønbaek H & Oxlund H 1998*b* Growth hormone administration can improve growth in glucocorticoid-injected rats without affecting the lymphocytopenic effect of the glucocorticoid. *Growth Hormone and IGF Research* **8** 251–264.

Owen HC, Miner JN, Ahmed SF & Farquharson C 2007 The growth plate sparing effects of the selective glucocorticoid receptor modulator, AL-438. *Molecular and Cellular Endocrinology* **264** 164–170. (https://doi.org/10.1016/j.mce.2006.11.006)

Owen HC, Ahmed SF & Farquharson C 2009 Chondrocyte p21(WAF1/CIP1) expression is increased by dexamethasone but does not contribute to dexamethasone-induced growth retardation in vivo. *Calcified Tissue International* **85** 326–334. (https://doi.org/10.1007/s00223-009-9276-0)

Pappa H, Thayu M, Sylvester F, Leonard M, Zemel B & Gordon C 2011 Skeletal health of children and adolescents with inflammatory bowel disease. *Journal of Pediatric Gastroenterology and Nutrition* **53** 11–25. (https://doi.org/10.1097/MPG.0b013e31821988a3)

Pereira RC, Delany AM & Canalis E 2002 Effects of cortisol and bone morphogenetic protein-2 on stromal cell differentiation: correlation with CCAAT-enhancer binding protein expression. *Bone* **30** 685–691. (https://doi.org/10.1016/S8756-3282(02)00687-7)

Plotkin LII, Bivi N & Bellido T 2011 A bisphosphonate that does not affect osteoclasts prevents osteoblast and osteocyte apoptosis and the loss of bone strength induced by glucocorticoids in mice. *Bone* **49** 122–127. (https://doi.org/10.1016/j.bone.2010.08.011)

Pogoda P, Priemel M, Schilling AF, Gebauer M, Catalfi-Lehnen P, Barvencik F, Beil T, Miinch C, Rupprecht M, Miildner C, *et al.* 2005 Mouse models in skeletal physiology and osteoporosis: experiences and data on 14 839 cases from the Hamburg Mouse Archives. *Journal of Bone and Mineral Metabolism* **23** 97–102. (https://doi.org/10.1007/BF03026332)

Postnov A, Schutter T, Sijbers J, Karperien M & Clerck N 2009 Glucocorticoid-induced osteoporosis in growing mice is not prevented by simultaneous intermittent PTH treatment. *Calcified Tissue International* **85** 530–537. (https://doi.org/10.1007/s00223-009-9301-3)

Price WA, Stiles AD, Moats-Staats BM & D'Ercole AJ 1992 Gene expression of insulin-like growth factors (IGFs), the type 1 IGF receptor, and IGF-binding proteins in dexamethasone-induced fetal growth retardation. *Endocrinology* **130** 1424–1432. (https://doi.org/10.1210/endo.130.3.1371449)

Rauch A, Seitz S, Baschant U, Schilling AF, Illing A, Stride B, Kirilov M, Mandic V, Takacz A, Schmidt-Ullrich R, *et al.* 2010 Glucocorticoids suppress bone formation by attenuating osteoblast differentiation via the monomeric glucocorticoid receptor. *Cell Metabolism* **11** 517–531. (https://doi.org/10.1016/j.cmet.2010.05.005)

Reid IR 1997 Glucocorticoid osteoporosis – mechanisms and management. *European Journal of Endocrinology* **137** 209–217. (https://doi.org/10.1530/eje.0.1370209)

Reinwald S & Burr D 2008 Review of nonprimate, large animal models for osteoporosis research. *Journal of Bone and Mineral Research* **23** 1353–1368. (https://doi.org/10.1359/jbmr.080516)

Ricotti V, Ridout DA, Scott E, Quinlivan R, Robb SA, Manzur AY & Muntoni F 2013 Long-term benefits and adverse effects of intermittent versus daily glucocorticoids in boys with Duchenne muscular dystrophy. *Journal of Neurology, Neurosurgery, and Psychiatry* **84** 698–705. (https://doi.org/10.1136/jnnp-2012-303902)

Rooman R, Koster G, Bloemen R, Gresnigt R & van Buul-Offers SC 1999 The effect of dexamethasone on body and organ growth of normal and IGF-II-transgenic mice. *Journal of Endocrinology* **163** 543–552. (https://doi.org/10.1677/joe.0.1630543)

Sato AY, Cregor M, Delgado-Calle J, Condon KW, Allen MR, Peacock M, Plotkin LI & Bellido T 2016 Protection from glucocorticoid-induced osteoporosis by anti-catabolic signaling in the absence of SOST/sclerostin. *Journal of Bone and Mineral Research* **31** 1791–1802. (https://doi.org/10.1002/jbmr.2869)

Scholz-Ahrens KE, Delling G, Stampa B, Helfenstein A, Hahne H-J, Acil Y, Timm W, Barkmann R, Hassenpflug J, Schrezenmeir J, *et al.* 2007 Glucocorticosteroid-induced osteoporosis in adult primiparous Gottingen miniature pigs: effects on bone mineral and mineral metabolism. *AJP: Endocrinology and Metabolism* **293** E385–E395. (https://doi.org/10.1152/ajpendo.00627.2006)

Silvestrini G, Ballanti P, Patacchioli FR, Mocetti P, Di Grezia R, Wedard BM, Angelucci L & Bonucci E 2000 Evaluation of apoptosis and the glucocorticoid receptor in the cartilage growth plate and

metaphyseal bone cells of rats after high-dose treatment with corticosterone. *Bone* **26** 33–42. (https://doi.org/10.1016/S8756-3282(99)00245-8)

Simon D, Fernando C, Czernichow P & Prieur A-M 2002 Linear growth and final height in patients with systemic juvenile idiopathic arthritis treated with longterm glucocorticoids. *Journal of Rheumatology* **29** 1296–1300.

Siu WS, Qin L & Leung KS 2003 pQCT bone strength index may serve as a better predictor than bone mineral density for long bone breaking strength. *Journal of Bone and Mineral Metabolism* **21** 316–322. (https://doi.org/10.1007/s00774-003-0427-5)

Śliwa E, Kowalik S, Tatara MR, Majcher P, Krupski W & Studziński T 2005 Effects of dexamethasone on physical properties and mineral density of long bones in piglets. *Bulletin of the Veterinary Institute in Pulawy* **49** 97–100.

Smink JJ, Koster JG, Gresnigt MG, Rooman R, Koedam JA & Van Buul-Offers SC 2002 IGF and IGF-binding protein expression in the growth plate of normal, dexamethasone-treated and human IGF-II transgenic mice. *Journal of Endocrinology* **175** 143–153. (https://doi.org/10.1677/joe.0.1750143)

Smink JJ, Gresnigt MG, Hamers N, Koedam JA, Berger R & Van Buul-Offers SC 2003*a* Short-term glucocorticoid treatment of prepubertal mice decreases growth and IGF-I expression in the growth plate. *Journal of Endocrinology* **177** 381–388. (https://doi.org/10.1677/joe.0.1770381)

Smink JJ, Buchholz IM, Hamers N, van Tilburg CM, Christis C, Sakkers RJB, de Meer K, van Buul-Offers SC & Koedam JA 2003*b* Short-term glucocorticoid treatment of piglets causes changes in growth plate morphology and angiogenesis. *Osteoarthritis and Cartilage* **11** 864–871. (https://doi.org/10.1016/S1063-4584(03)00187-0)

Van Staa TP, Leufkens HGM, Abenhaim L, Zhang B & Cooper C 2000 Use of oral corticosteroids and risk of fractures. *Journal of Bone and Mineral Research* **15** 993–1000. (https://doi.org/10.1359/jbmr.2000.15.6.993)

Stewart PM 2007 The adrenal cortex. In *Williams Textbook of Endocrinology*, 11th edition. Eds H Kronenberg, S Melmed, K Polonsky & PR Larsen. Philadelphia, PA, USA: Saunders Elsevier.

Sundahl N, Bridelance J, Libert C, De Bosscher K & Beck IM 2015 Selective glucocorticoid receptor modulation: new directions with non-steroidal scaffolds. *Pharmacology and Therapeutics* **152** 28–41. (https://doi.org/10.1016/j.pharmthera.2015.05.001)

Tamura Y, Kawao N, Yano M, Okada K, Okumoto K, Chiba Y, Matsuo O & Kaji H 2015 Role of plasminogen activator inhibitor-1 in glucocorticoid-induced diabetes and osteopenia in mice. *Diabetes* **64** 2194–2206. (https://doi.org/10.2337/db14-1192)

Tanaka H, Hirano F, Nomura Y, Miura T, Makino Y, Fukawa E & Makino I 1994 Relative glucocorticoid potency revisited. *Rheumatology International* **14** 9–12. (https://doi.org/10.1007/BF00302665)

Thiele S, Ziegler N, Tsourdi E, De Bosscher K, Tuckermann JP, Hofbauer LC & Rauner M 2012 Selective glucocorticoid receptor modulation maintains bone mineral density in mice. *Journal of Bone and Mineral Research* **27** 2242–2250. (https://doi.org/10.1002/jbmr.1688)

Thompson DD, Simmons HA, Pirie CM & Ke HZ 1995 FDA Guidelines and animal models for osteoporosis. *Bone* **17** 125S–133S.

Tulipano G, Taylor JE, Halem HA, Datta R, Dong JZ, Culler MD, Bianchi I, Cocchi D & Giustina A 2007 Glucocorticoid inhibition of growth in rats: partial reversal with the full-length ghrelin analog BIM-28125. *Pituitary* **10** 267–274. (https://doi.org/10.1007/s11102-007-0054-6)

Umlawska W & Prusek-Dudkiewicz A 2010 Growth retardation and delayed puberty in children and adolescents with juvenile idiopathic arthritis. *Archives of Medical Science* **6** 19–23. (https://doi.org/10.5114/aoms.2010.13501)

Waarsing J, Day J, van der Linden J, Ederveen A, Spanjers C, De Clerck N, Sasov A, Verhaar JA & Weinans H 2004 Detecting and tracking local changes in the tibiae of individual rats: a novel method to analyse longitudinal in vivo micro-CT data. *Bone* **34** 163–169. (https://doi.org/10.1016/j.bone.2003.08.012)

Wallace AM, Tucker P, Williams DM, Hughes IA & Ahmed SF 2003 Short-term effects of prednisolone and dexamethasone on circulating concentrations of leptin and sex hormone-binding globulin in children being treated for acute lymphoblastic leukaemia. *Clinical Endocrinology* **58** 770–776. (https://doi.org/10.1046/j.1365-2265.2003.01790.x)

Wang F-S, Chung P-C, Lin C-L, Chen M-W, Ke H-J, Chang Y-H, Chen Y-S, Wu S-L & Ko J-Y 2013 MicroRNA-29a protects against glucocorticoid-induced bone loss and fragility in rats by orchestrating bone acquisition and resorption. *Arthritis and Rheumatism* **65** 1530–1540. (https://doi.org/10.1002/art.37948)

Ward WE, Donovan SM & Atkinson SA 1998 Dexamethasone-induced abnormalities in growth and bone metabolism in piglets are partially attenuated by growth hormone with no synergistic effect of insulin-like growth factor-I. *Pediatric Research* **44** 215–221. (https://doi.org/10.1203/00006450-199808000-00013)

Weber JC, VanHuss WD & Mostosky U V 1968 Determination of bone length in vivo. *Research Quarterly* **39** 223–224.

Weinstein RS & Manolagas SC 2000 Apoptosis and osteoporosis. *American Journal of Medicine* **108** 153–164. (https://doi.org/10.1016/S0002-9343(99)00420-9)

Weinstein RS, Jilka RL, Parfitt AM & Manolagas SC 1998 Inhibition of osteoblastogenesis and promotion of apoptosis of osteoblasts and osteocytes by glucocorticoids potential mechanisms of their deleterious effects on bone. *Journal of Clinical Investigation* **102** 274–282. (https://doi.org/10.1172/JCI2799)

Weinstein RS, O'Brien CA, Almeida M, Zhao H, Roberson PK, Jilka RL & Manolagas SC 2011 Osteoprotegerin prevents glucocorticoid-induced osteocyte apoptosis in mice. *Endocrinology* **152** 3323–3331. (https://doi.org/10.1210/en.2011-0170)

Weise M, De-Levi S, Barnes KM, Gafni RI, Abad V & Baron J 2001 Effects of estrogen on growth plate senescence and epiphyseal fusion. *PNAS* **98** 6871–6876. (https://doi.org/10.1073/pnas.121180498)

Wimalawansa SJ & Simmons DJ 1998 Prevention of corticosteroid-induced bone loss with alendronate. *Proceedings of the Society for Experimental Biology and Medicine* **217** 162–167. (https://doi.org/10.3181/00379727-217-44218)

Wong SC, Dobie R, Altowati MA, Werther GA, Farquharson C & Ahmed SF 2016 Growth and the growth hormone-insulin like growth factor 1 axis in children with chronic inflammation: current evidence, gaps in knowledge, and future directions. *Endocrine Reviews* **37** 62–110. (https://doi.org/10.1210/er.2015-1026)

Xia X, Kar R, Gluhak-Heinrich J, Yao W, Lane NE, Bonewald LF, Biswas SK, Lo WK & Jiang JX 2010 Glucocorticoid-induced autophagy in osteocytes. *Journal of Bone and Mineral Research* **25** 2479–2488. (https://doi.org/10.1002/jbmr.160)

Xiong J, Onal M, Jilka RL, Weinstein RS, Manolagas SC & O'Brien CA 2011 Matrix-embedded cells control osteoclast formation. *Nature Medicine* **17** 1235–1241. (https://doi.org/10.1038/nm.2448)

Yao W, Cheng Z, Busse C, Pham A, Nakamura MC & Lane NE 2008 Glucocorticoid excess in mice results in early activation of osteoclastogenesis and adipogenesis and prolonged suppression of osteogenesis: a longitudinal study of gene expression in bone tissue from glucocorticoid-treated mice. *Arthritis and Rheumatism* **58** 1674–1686. (https://doi.org/10.1002/art.23454)

Yao W, Dai W, Jiang L, Lay EY-A, Zhong Z, Ritchie RO, Li X, Ke H & Lane NE 2016 Sclerostin-antibody treatment of glucocorticoid-induced osteoporosis maintained bone mass and strength. *Osteoporosis International* **27** 283–294. (https://doi.org/10.1007/s00198-015-3308-6)

Yokote Y, Kimura E, Kimura M & Kozono Y 2008 Biomechanical analysis of combined treatment of high calcium and bisphosphonate in tibia of steroid-treated growing-phase rats. *Dental Materials Journal* **27** 647–653. (https://doi.org/10.4012/dmj.27.647)

Yongtao Z, Kunzheng W, Jingjing Z, Hu S, Jianqiang K, Ruiyu L & Chunsheng W 2014 Glucocorticoids activate the local renin–angiotensin system in bone: possible mechanism for glucocorticoid-induced osteoporosis. *Endocrine* **47** 598–608. (https://doi.org/10.1007/s12020-014-0196-z)

Zalavras C, Shah S, Birnbaum MJ & Frenkel B 2003 Role of apoptosis in glucocorticoid-induced osteoporosis and osteonecrosis. *Critical Reviews in Eukaryotic Gene Expression* **13** 221–235. (https://doi.org/10.1615/CritRevEukaryotGeneExpr.v13.i24.140)

Zaman F, Chrysis D, Huntjens K, Fadeel B, Sävendahl L, Mushtaq T, Ahmed S, Yeh T, Lin YY, Lin H, *et al.* 2012 Ablation of the pro-apoptotic protein bax protects mice from glucocorticoid-induced bone growth impairment. *PLoS ONE* **7** e33168. (https://doi.org/10.1371/journal.pone.0033168)

Zezulak KM & Green H 1986 The generation of insulin-like growth factor-1 – sensitive cells by growth hormone action. *Science* **233** 551–553. (https://doi.org/10.1126/science.3726546)

Received in final form 5 October 2017
Accepted 17 October 2017
Accepted preprint published online 17 October 2017

Bone protective agents in children

Claire Louise Wood,[1,2] S Faisal Ahmed[3]

[1]Division of Developmental Biology, University of Edinburgh Roslin Institute, Roslin, Midlothian, UK
[2]John Walton Muscular Dystrophy Research Centre, Institute of Genetic Medicine, Newcastle upon Tyne, UK
[3]Developmental Endocrinology Research Group, School of Medicine, University of Glasgow, Glasgow, UK

Correspondence to
Professor S Faisal Ahmed, Developmental Endocrinology Research Group, School of Medicine, University of Glasgow, Royal Hospital for Children, 1345 Govan Road, Glasgow G51 4TF, UK;
faisal.ahmed@glasgow.ac.uk

Received 14 July 2017
Revised 25 September 2017
Accepted 28 September 2017
Published Online First
24 October 2017

ABSTRACT

Evaluation of bone health in childhood is important to identify children who have inadequate bone mineralisation and who may benefit from interventions to decrease their risk of osteoporosis and subsequent fracture. There are no bone protective agents that are licensed specifically for the prevention and treatment of osteoporosis in children. In this review, we discuss the mechanism of action and use of bisphosphonates and other new and established bone protective agents in children.

INTRODUCTION

Healthy bone is metabolically active and undergoes continuous modelling and remodelling during childhood to maintain the balance between bone formation and bone resorption. The size and shape of the skeleton changes rapidly during modelling in childhood and adolescence and approximately 90% of bone mass is accrued during the first 18 years of life.[1] If this finely tuned process is disturbed, then osteoporosis can result. Osteoporosis is defined as a skeletal disorder characterised by compromised bone strength and predisposing a person to an increased risk of fracture[2] and the importance of correctly diagnosing osteoporosis in children has been highlighted by the International Society for Clinical Densitometry (ISCD).[3] The finding of one or more vertebral fracture is indicative of osteoporosis in the absence of local disease or high energy trauma. In the absence of vertebral compression, a diagnosis of osteoporosis is indicated by the presence of both a clinically significant fracture history and bone mineral density (BMD) z-score ≤2.0.[3] Skeletal fragility in children may be primary, due to an intrinsic bone abnormality (usually genetic in origin) or secondary as a result of an underlying medical condition or its treatment. Examples of conditions that can result in primary skeletal fragility include osteogenesis imperfecta, idiopathic juvenile osteoporosis and osteoporosis pseudoglioma syndrome. In most but not all cases, this skeletal fragility is associated with reduced BMD and will also satisfy the ISCD definition of osteoporosis. Secondary osteoporosis is more common and has been reported in several chronic conditions in children (see table 1). It may arise due to a combination of factors including the inflammatory process itself, suboptimal nutrition, reduced lean body mass, decreased physical activity, delayed puberty or due to treatment for the underlying condition, particularly glucocorticoids (GC).[4]

Although there are several bone-protective agents currently used in adults with osteoporosis (see table 2), none is licensed specifically for the prevention or treatment of osteoporosis in childhood. For children with chronic illness, treatment of the underlying condition should be the mainstay of osteoporosis prevention and treatment.

BISPHOSPHONATES

In children, bone protective therapy has often been delivered using antiresorptive therapy, and in particular, bisphosphonates (BPs). Because a detailed review of the use of BPs in every chronic childhood condition is not possible within this article, we will focus on three examples:

1. Osteogenesis imperfecta (OI)—an example of primary skeletal fragility
2. Cerebral palsy (CP)—secondary osteoporosis related to immobility
3. Duchenne muscular dystrophy (DMD)—secondary osteoporosis associated with GC use.

BPs were the first pharmacological agent to be used in children with fragility fractures.[5] Although BPs have now been widely used in adults with a range of conditions, their use in children has been more limited, in part because of concerns regarding the effects on the growing skeleton.[6] They are so called because they have two phosphonate groups, which enable them to bind to bone. They reduce osteoclast activity primarily by promoting osteoclast apoptosis and so inhibiting bone resorption. BPs also reduce overall bone turnover because bone resorption is coupled to bone formation. However, because osteoblast activity at the periosteal surface is unaffected, an overall increase in bone formation in the growing skeleton and potential reshaping of existing vertebral fractures can still occur, despite the low turnover state.[7] The newer, nitrogen-containing BPs (eg, alendronate, zoledronate, risedronate and pamidronate) work by inhibiting the enzymes within osteoclasts that are involved in the farnesyl pyrophosphate synthase and mevalonate pathways, which are important for varying aspects of osteoclast function and also inducing osteoclast apoptosis.[7] Although they have poor oral absorption, BPs have an extremely long half-life; a study of pamidronate in paediatric OI found that 2 years after cessation of treatment, bone mineral content (BMC) z-scores remained above pretreatment levels[8] and urinary excretion of pamidronate has been detected up to 8 years later.[9] This has potential implications for females of reproductive age as rodent studies have shown that BPs can cross the placenta and accumulate in the fetal skeleton causing decreased bone growth and deaths in the offspring.[10] There is, however, no evidence to date that prior BP exposure or even BP exposure during pregnancy is associated with reproductive toxicity.[11]

To cite: Wood CL, Ahmed SF. *Arch Dis Child* 2018;**103**:503–508.

Table 1 Examples of conditions associated with skeletal fragility and/or osteoporosis in children

Primary: the result of a specific condition (usually genetic in origin) causing increased skeletal fragility	**Secondary:** the result of a medical condition or medication used to treat it (children with chronic illness often have multiple risk factors)
Osteogenesis imperfecta	Medications, eg, glucocorticoids used in asthma, arthritis, Duchenne muscular dystrophy
Idiopathic juvenile osteoporosis	Nutritional problems, eg, Crohn's disease, anorexia nervosa
Osteoporosis pseudoglioma syndrome	Reduced mobility, eg, cerebral palsy and neuromuscular conditions
	Conditions causing delayed puberty or insufficient production of sex hormones
	Chronic illness such as thyroid disease, leukaemia

GC, glucocorticoids; GH, growth hormone; IGF-1, insulin-like growth factor 1; PTH, parathyroid hormone.

Osteogenesis imperfecta

BPs were first used in children to treat OI (the most common primary disorder of bone fragility) in 198[12] and are now the mainstay of treatment in this condition. The main effect of BPs in children with OI appears to be an increase in cortical bone width (a growth-dependent process that in turn improves mechanical strength) and trabecular number. The primary aim of BP treatment in OI is to reduce fracture frequency. Despite there being some evidence from a recent Cochrane review[13] that included 14 studies and 819 participants to show that either oral or cyclical intravenous BPs increase BMD in children with OI, the authors were unable to demonstrate reliable evidence of improvements in overall clinical status (reduced pain, improved growth or functional mobility). Also, while several studies independently reported a decreased fracture risk, the review could not show a consistent reduction in fracture rate after use of either oral or intravenous BP. There is growing interest in the use of oral BPs in OI, particularly in those with milder phenotypes, as they may be more cost-effective and easier to use than intravenous alternatives.[14 15] As yet, there does not appear to be sufficient evidence to favour oral agents above intravenous BPs in the acute treatment phase or in those with severe OI.[16]

Secondary osteoporosis

Although BPs are now used for bone protection in many other childhood conditions, much of the justification for their use in other chronic diseases has been extrapolated from evidence in OI. A systematic review has concluded that there is insufficient evidence to recommend BPs as standard therapy for secondary osteoporosis in children because the link between increasing BMD and reducing fracture risk remains unproven.[17] The efficacy of BP therapy on BMD appears to depend on the age at time of treatment and the amount of bone growth remaining. Generally, they appear to be a safe and effective therapy in cases of severe bone loss, although the long-term effect of inhibition of bone turnover remains unknown. BPs may also ameliorate pain in certain circumstances,[18] but further work is needed to clarify this.[5]

BPs in cerebral palsy

CP is a heterogeneous group of non-progressive disorders of motor function and posture. Some patients with CP have a significant reduction in mobility and bone mass quickly diminishes without adequate bone loading. By 10 years of age, over 95% of those with non-ambulatory severe CP have osteopaenia[19] and fractures are 20% more likely in those who are non-ambulatory. First-line measures should include optimising vitamin D and calcium levels and the encouragement of weight-bearing activity. Vibration therapies have also been used, although there is only limited evidence of their effectiveness. A recent meta-analysis[20] assessing the effect of BPs on increasing BMD in children with CP found that the lumbar spine and femoral BMD z-scores were significantly higher after BP treatment compared with pretreatment values, but only one randomised controlled trial met the inclusion criteria. Furthermore, it remains unclear whether this translates to a reduction in fracture incidence, which is important when the annual fracture incidence in children with moderate-to-severe CP is 4%.[21] In addition, oromotor dysfunction and gastro-oesophageal reflux are often present in CP which may preclude the use of oral BPs.

Table 2 Drugs that are used in children and their mechanism of action

Agents that have been used in clinical practice in children and may have a beneficial effect on bone health	**Main mechanisms of action**
Vitamin D and calcium	Vitamin D regulates calcium and phosphate absorption which are the main mineral component of bone
Bisphosphonates	Reduce osteoclast activity so inhibiting bone resorption. Also reduce overall bone turnover as resorption is coupled to formation
Sex steroids	Oestrogen decreases osteoclast number and activity so reducing resorption. Also increases GH levels, which is anabolic to bone. Testosterone stimulates osteoblastogenesis directly and also acts indirectly through aromatisation to oestradiol and the anabolic effects of androgens on muscle mass
Recombinant human GH and IGF-1	GH stimulates osteoblast and preosteoblast proliferation directly and also indirectly through IGF-1 to increase bone formation. Also stimulates osteoclast differentiation, so overall increases bone remodelling. May also exert their effects through effects on mineral metabolism, alterations in glucocorticoid metabolism and anabolic effects on muscle mass
New therapies that are not in clinical practice in children but may have a beneficial effect on bone health	
Cathepsin K inhibitors	Prevents type 1 collagen degradation and reduces bone resorption
RANKL inhibitors	Prevents osteoclastogenesis and thus reduces bone resorption
Sclerostin antibodies	Prevents antagonism of Wnt signalling pathway by sclerostin, thus promoting osteoblast function and bone formation
Recombinant human PTH	Stimulates new bone formation when given intermittently by increasing osteoblastogenesis and osteoblast survival

GC, glucocorticoids; GH, growth hormone; IGF-1, insulin-like growth factor 1; PTH, parathyroid hormone; RANKL, receptor activator of nuclear factor-k-B ligand.

BPs in DMD

Long-term GC use has dramatically improved the disease course in DMD.[22] GC are normally commenced once muscle function begins to plateau, usually at about 5 years of age and are

continued through to adulthood. Growth retardation[23] and fragility fractures are important problems in DMD; it is predicted that after 100 months of GC therapy, 75% of boys will sustain a vertebral fracture.[24] Although BPs are frequently used, there is no consensus regarding timing of initiation, drug regimen or cessation of treatment. Prophylactic BP in DMD in those receiving GC has been reported to be associated with increased survival.[25] While BPs may be associated with an improvement in back pain and some vertebral reshaping, provided that the child is still growing, they do not completely prevent the development of new vertebral fractures.[26] Recent data from transiliac biopsies in boys with DMD have also shown that while BPs appear to be effective early in GC-induced bone loss, long-term use may further dampen remodelling.[27] A recent Cochrane review concluded that there was no strong evidence to guide the use of any therapy to prevent or treat GC-induced osteoporosis in boys with DMD.[28] Therefore, before considering prophylactic BP use, the potential risks must be weighed up against the benefits including consideration of the potential adverse effects of BP therapy and a decision made regarding the most appropriate time to use them.[29]

Adverse effects of BP therapy

BPs are generally well tolerated in children,[30] but as little is known of the long-term consequences of BP treatment, all patients should be regularly reviewed, looking in particular for evidence of adverse effects. An acute phase response to the initiation of intravenous BP therapy is very common, with short-lived fever and flu-like symptoms. Hypophosphataemia and hypocalcaemia can also occur.[31] Delayed bone healing after osteotomy in OI has also been described with BP use.[32] There are also three rare, but potentially serious adverse events that may be related to long-term exposure to BPs:

1. Osteonecrosis of the jaw: BP-associated osteonecrosis of the jaw (ONJ) is defined as, 'an area of exposed bone in the maxillofacial region that does not heal within 8 weeks, in a patient who is receiving or has been exposed to a BP and has not had radiation therapy to the craniofacial region'.[33] ONJ appears to be more common in adults using intravenous BPs,[34] and it has not yet been reported in a child.[35] Most cases have been documented in those receiving doses higher than prescribed for osteoporosis (eg, for malignancy) and in patients on therapy for >2 years. Experts have suggested doing any invasive dental procedures before starting treatment or suspending therapy for 3 or more months before and after such procedures, where possible,[36] although there is no evidence to support these recommendations.
2. Atypical femoral fractures: although atypical subtrochanteric femur fractures (AFF) are very rare and account for <1% of all hip/femoral fractures, they have been predominantly reported in patients taking BPs[37] and have recently been associated with BP use in a child.[38] Because BPs act by reducing bone turnover, it is possible that by preventing remodelling and effectively 'freezing' the skeleton, they allow tiny cracks to form and stress fractures to develop. AFFs occur at sites of high tensional stress, such as the lateral cortex of the proximal femoral shaft. It is also thought that those taking concomitant GCs in addition to BPs or with a genetic disposition to fracture may have a further increased risk. A large Swedish observational study of femoral fractures in postmenopausal women[39] showed that fracture rate decreased rapidly after drug withdrawal, therefore intermittent use may be favourable and a BP 'holiday' in children on long-term BPs could be considered.
3. Iatrogenic osteopetrosis: in 2003, the first case of BP-induced osteopetrosis (or marble bone disease) was described in a boy aged 12 years who had received pamidronate infusions for the previous 3 years for idiopathic bone pain and osteopaenia.[40] Abnormal oversuppression of bone remodelling (with a histological absence of osteoclasts on bone surfaces) was still present when he was followed up 7 years after cessation of BP.

Vitamin D and calcium

Vitamin D is essential for skeletal health and regulates calcium and phosphate absorption.[41] Vitamin D deficiency may be associated with decreased BMC and increased risk of rickets.[42] Children with chronic diseases are more prone to vitamin D deficiency for a variety of reasons including malabsorption, limited sunlight exposure, nutritional restrictions and the use of medications such as anticonvulsants and GCs, therefore prevention of vitamin D deficiency should be routinely considered in those with chronic illnesses. The mean dietary intake of vitamin D in children may only be about 100 IU/day[43] and therefore in the UK, the Scientific Advisory Committee for Nutrition has recommended a reference nutrient intake (RNI) of 400 IU/day for children.[43] This requirement may be even higher in those with chronic illnesses.[44] Adequate dietary calcium to meet the RNI should also be advised and supplementation considered if this is unlikely to be reached. There is no clear evidence that calcium supplementation in excess of the RNI has additional benefits on bone density while there are significant associated risks of excessive total calcium intake. Vitamin D and calcium levels should be optimised prior to the initiation of BP therapy to prevent BP-induced hypocalcaemia and maximise efficacy.

GH and IGF-1

While there is ample evidence that the GH-IGF-1 pathway has direct effects on bone mass and strength in experimental models,[45] the effect of recombinant human GH (rhGH) on bone health in children is debatable.[46] In addition to a direct effect on osteoblast activity, it is possible that the anabolic effects of rhGH may also be mediated through an effect on lean mass,[47] alterations in PTH sensitivity[48] or even modulation of the 11-β-hydroxysteroid dehydrogenase shuttle, which is responsible for the inactivation of cortisol to cortisone.[49] Given that both rhGH and rhIGF-1 are licensed for use in children with growth disorders and in light of data from children and adults with chronic inflammation, there is potential for these anabolic agents to improve growth potential, muscle strength and bone mass in many cases of primary and secondary osteoporosis. However, before using these pharmacological agents for this purpose, an improved understanding of their effects on linear growth and bone mass, and the underlying mechanisms through which they exert their effects on bone, is imperative.

Recombinant parathyroid hormone

Teriparatide is a form of recombinant human PTH and is unique because unlike BPs, it stimulates new bone formation. It is approved for use in adults with osteoporosis and over half a million adults with severe osteoporosis have received this drug.[50] Furthermore, its anabolic effect on bone has opened up the possibility of using it in combination or sequentially with antiresorptive agents such BPs.[51] However, experimental studies have shown that almost half of the rats exposed to the highest doses

developed osteosarcoma.[52] Despite there being many differences which make humans less susceptible than rats,[53] this risk is still of particular concern to the paediatric and adolescent population where osteosarcoma is most prevalent. However, over the last decade, there have been increasing reports of the use of recombinant PTH for intractable hypocalcaemia associated with hypoparathyroidism in children.[54]

Sex steroids

Growth and pubertal development are often impaired in chronic disease and the pubertal process and associated GH surge are vital to increase bone size and bone mineral accrual. Androgen deficiency is a recognised risk factor for osteoporosis and fracture and evidence suggests that early initiation of androgen therapy is associated with improved BMD in adults.[55] However, precocious puberty or treatment with high doses of either oestrogen or testosterone can paradoxically cause premature fusion of the epiphyses and a subsequent reduction in final height.[56] Oxandrolone, an anabolic steroid that is only weakly androgenic and does not aromatise, has been studied in children with severe burns. It has been reported to increase bone mass,[57] but is often not readily available. Physiological oestrogen replacement given transdermally (so not to inhibit IGF-1 production) alongside cyclical progesterone has also been shown to increase bone mineral accrual in teenagers with anorexia[58] and the American College of Sports Medicine recommends that oral contraceptives be considered in amenorrhoeic athletes over 16 years of age if BMD is declining despite sufficient weight gain.[59]

Alternative agents for consideration

Receptor activator of nuclear factor-k-B ligandinhibitors

Denosumab is a monoclonal antibody to the receptor activator of nuclear factor-k-B ligand (RANKL), a key mediator of osteoclast activity. It is given subcutaneously and targets the RANKL (figure 1), thus inhibiting osteoclast-mediated bone resorption and increasing BMD. There is extensive data to show its efficacy in postmenopausal osteoporosis[60] and it has also been used in a group of children with OI.[61] However, its efficacy and side-effect profile is not clearly understood in children and there may be an increased risk of calcium dysregulation, so further studies are warranted.[62]

Sclerostin antibody

Sclerostin is produced by osteocytes (figure 1) and probably acts as antagonist of the Wnt signalling pathway to inhibit bone formation, although the exact mechanism remains unclear.[63] Neutralisation of sclerostin using monoclonal antibodies in a mouse model of OI, resulted in improved bone mass and reduced long bone fragility[64] and early clinical studies in adults have shown similar results.[65] Sclerostin antibodies have also been used to prevent GC-induced trabecular and cortical bone loss in mouse models of GC-induced osteoporosis.[66]

Cathepsin K inhibitors

Cathepsin K is a cysteine protease that is highly expressed by osteoclasts and degrades type 1 collagen[67] (figure 1). Cathepsin K inhibitors are thought to reduce bone resorption while also increasing the number of cells of osteoclast lineage and therefore not suppressing bone formation to the same degree as BPs. Cathepsin K inhibitors such as odanacatib have shown promising efficacy data,[68] but an increased risk of atrial fibrillation and stroke in adult phase III trials has meant that marketing of these agents has now been halted.

CONCLUSION

Alongside consideration of pharmacological approaches to maximise bone accrual, optimising nutritional factors and encouraging activity, within the constraints of the disease process are also important. Timely pubertal assessment should be performed in those with chronic disease and where appropriate, puberty induced. Optimal management includes regular screening to identify those at risk of fracture and then aiming to treat earlier, rather than waiting for fragility fractures to occur, particularly in those who have little potential for spontaneous recovery.

There is still limited evidence for the use of bone protective agents in most childhood conditions and although BPs are commonly used, evidence for their efficacy remains limited. Most studies are small and only have limited follow-up and there is no consensus on the length of BP treatment regimens and dosage in children. Long-term safety needs to be assessed by large-scale trials with extended follow-up; the rarity of many conditions under study may necessitate international collaborative efforts. Many studies also use change

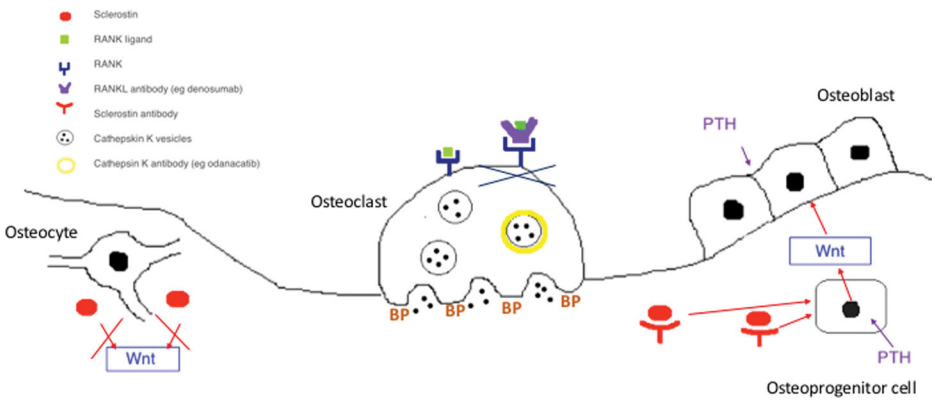

Figure 1 Schematic diagram to show the mechanism of action of bone protective agents. Bisphosphonates (BPs) act at the osteoclast to reduce bone resorption. Recombinant parathyroid hormone (PTH), eg, teriparatide promotes bone formation. Sclerostin is secreted by osteocytes; sclerostin antibody binds to circulating sclerostin and so enables Wnt signalling of osteoprogenitors and osteoblasts. Receptor activator of nuclear factor-k-B ligand (RANKL) antibodies (eg, denosumab) target the RANK ligand and prevent bone resorption at the osteoclast. Cathepsin K inhibitors (eg, odanacatib) prevent release of enzymes that degrade collagen at the osteoclast.

in BMD as primary outcome but the extent of correlation with this and subsequent fracture rate remain unclear and age-appropriate reference ranges are not commonly available for very young children. As antiresorptives result in a low bone-turnover state with an associated reduction in bone formation and hence reduced overall bone remodelling, it would clearly be advantageous to find safe and effective anabolic agents to use in the paediatric population, either alone or in combination and this must remain a research priority.

Contributors CW wrote the first draft, SFA edited and approved the final version.

Funding CW and SFA: Medical Research Council and Muscular Dystrophy UK MR/N020588/1, SFA: Chief Scientist Office CAF/DMD/14/01.

Competing interests SFA: diurnal research grant, Novo Nordisk (data monitoring board and educational meetings), Kyowa Kirin (consultancy).

Provenance and peer review Commissioned; externally peer reviewed.

REFERENCES

1 Bachrach LK. Acquisition of optimal bone mass in childhood and adolescence. *Trends Endocrinol Metab* 2001;12:22–8.
2 NIH Consensus Development Panel on Osteoporosis revention Diagnosis, and therapy. Osteoporosis prevention, diagnosis, and therapy. *JAMA* 2001;285:785–95.
3 Crabtree NJ, Arabi A, Bachrach LK, *et al*. Dual-energy X-ray absorptiometry interpretation and reporting in children and adolescents: the revised 2013 ISCD Pediatric Official Positions. *J Clin Densitom* 2014;17:225–42.
4 Joseph S, McCarrison S, Wong SC. Skeletal Fragility in Children with Chronic Disease. *Horm Res Paediatr* 2016;86:71–82.
5 Glorieux FH, Bishop NJ, Plotkin H, *et al*. Cyclic administration of pamidronate in children with severe osteogenesis imperfecta. *N Engl J Med* 1998;339:947–52.
6 Brumsen C, Hamdy NA, Papapoulos SE. Long-term effects of bisphosphonates on the growing skeleton. Studies of young patients with severe osteoporosis. *Medicine* 1997;76:266–83.
7 Russell RG, Watts NB, Ebetino FH, *et al*. Mechanisms of action of bisphosphonates: similarities and differences and their potential influence on clinical efficacy. *Osteoporos Int* 2008;19:733–59.
8 Rauch F, Munns C, Land C, *et al*. Pamidronate in children and adolescents with osteogenesis imperfecta: effect of treatment discontinuation. *J Clin Endocrinol Metab* 2006;91:1268–74.
9 Papapoulos SE, Cremers SC. Prolonged bisphosphonate release after treatment in children. *N Engl J Med* 2007;356:1075–6.
10 Graepel P, Bentley P, Fritz H, *et al*. Reproduction toxicity studies with pamidronate. *Arzneimittelforschung* 1992;42:654–67.
11 Green SB, Pappas AL. Effects of maternal bisphosphonate use on fetal and neonatal outcomes. *Am J Health Syst Pharm* 2014;71:2029–36.
12 Devogelaer JP, Malghem J, Maldague B, *et al*. Radiological manifestations of bisphosphonate treatment with APD in a child suffering from osteogenesis imperfecta. *Skeletal Radiol* 1987;16:360–3.
13 Dwan K, Phillipi CA, Steiner RD, *et al*. Bisphosphonate therapy for osteogenesis imperfecta. *Cochrane Database Syst Rev* 2014;7:Cd005088.
14 Unal E, Abaci A, Bober E, *et al*. Efficacy and safety of oral alendronate treatment in children and adolescents with osteoporosis. *J Pediatr Endocrinol Metab* 2006;19:523–8.
15 Bishop N, Adami S, Ahmed SF, *et al*. Risedronate in children with osteogenesis imperfecta: a randomised, double-blind, placebo-controlled trial. *Lancet* 2013;382:1424–32.
16 Ward LM, Rauch F, Whyte MP, *et al*. Alendronate for the treatment of pediatric osteogenesis imperfecta: a randomized placebo-controlled study. *J Clin Endocrinol Metab* 2011;96:355–64.
17 Ward L, Tricco AC, Phuong P, *et al*. Bisphosphonate therapy for children and adolescents with secondary osteoporosis. *Cochrane Database Syst Rev* 2007:CD005324.
18 Aström E, Söderhäll S. Beneficial effect of long term intravenous bisphosphonate treatment of osteogenesis imperfecta. *Arch Dis Child* 2002;86:356–64.
19 Henderson RC, Lark RK, Kecskemethy HH, *et al*. Bisphosphonates to treat osteopenia in children with quadriplegic cerebral palsy: a randomized, placebo-controlled clinical trial. *J Pediatr* 2002;141:644–51.
20 Kim MJ, Kim SN, Lee IS, *et al*. Effects of bisphosphonates to treat osteoporosis in children with cerebral palsy: a meta-analysis. *J Pediatr Endocrinol Metab* 2015;28:1343–50.
21 Mergler S, Evenhuis HM, Boot AM, *et al*. Epidemiology of low bone mineral density and fractures in children with severe cerebral palsy: a systematic review. *Dev Med Child Neurol* 2009;51:773–8.
22 Moxley RT, Pandya S, Ciafaloni E, *et al*. Change in natural history of Duchenne muscular dystrophy with long-term corticosteroid treatment: implications for management. *J Child Neurol* 2010;25:1116–29.
23 Wood CL, Straub V, Guglieri M, *et al*. Short stature and pubertal delay in duchenne muscular dystrophy. *Arch Dis Child* 2016;101:101–6.
24 Bothwell JE, Gordon KE, Dooley JM, *et al*. Vertebral fractures in boys with duchenne muscular dystrophy. *Clin Pediatr* 2003;42:353–6.
25 Gordon KE, Dooley JM, Sheppard KM, *et al*. Impact of bisphosphonates on survival for patients with Duchenne muscular dystrophy. *Pediatrics* 2011;127:e353–e358.
26 Srinivasan R, Rawlings D, Wood CL, *et al*. Prophylactic oral bisphosphonate therapy in duchenne muscular dystrophy. *Muscle Nerve* 2016;54:79–85.
27 Misof BM, Roschger P, McMillan HJ, *et al*. Histomorphometry and bone matrix mineralization before and after bisphosphonate treatment in boys with duchenne muscular dystrophy: a paired transiliac biopsy study. *J Bone Miner Res* 2016;31:1060–9.
28 Bell JM, Shields MD, Watters J, *et al*. Interventions to prevent and treat corticosteroid-induced osteoporosis and prevent osteoporotic fractures in Duchenne muscular dystrophy. *Cochrane Database Syst Rev* 2017;1:CD010899.
29 Wood CL, Marini Bettolo C, Bushby K, *et al*. Bisphosphonate use in Duchenne Muscular Dystrophy – why. *when to start and when to stop? Expert Opin Orphan Drugs* 2016;4:407–16.
30 Batch JA, Couper JJ, Rodda C, *et al*. Use of bisphosphonate therapy for osteoporosis in childhood and adolescence. *J Paediatr Child Health* 2003;39:88–92.
31 George S, Weber DR, Kaplan P, *et al*. Short-term safety of zoledronic acid in young patients with bone disorders: an extensive institutional experience. *J Clin Endocrinol Metab* 2015;100:4163–71.
32 Munns CF, Rauch F, Zeitlin L, *et al*. Delayed osteotomy but not fracture healing in pediatric osteogenesis imperfecta patients receiving pamidronate. *J Bone Miner Res* 2004;19:1779–86.
33 Khosla S, Burr D, Cauley J, *et al*. Bisphosphonate-associated osteonecrosis of the jaw: report of a task force of the American Society for Bone and Mineral Research. *J Bone Miner Res* 2007;22:1479–91.
34 Silverman SL, Landesberg R. Osteonecrosis of the jaw and the role of bisphosphonates: a critical review. *Am J Med* 2009;122:S33–S45.
35 Hennedige AA, Jayasinghe J, Khajeh J, *et al*. Systematic review on the incidence of bisphosphonate related osteonecrosis of the jaw in children diagnosed with osteogenesis imperfecta. *J Oral Maxillofac Res* 2013;4:e1.
36 Malden N, Beltes C, Lopes V. Dental extractions and bisphosphonates: the assessment, consent and management, a proposed algorithm. *Br Dent J* 2009;206:93–8.
37 Girgis CM, Sher D, Seibel MJ. Atypical femoral fractures and bisphosphonate use. *N Engl J Med* 2010;362:1848–9.
38 van de Laarschot DM, Zillikens MC. Atypical femur fracture in an adolescent boy treated with bisphosphonates for X-linked osteoporosis based on PLS3 mutation. *Bone* 2016;91:148–51.
39 Schilcher J, Koeppen V, Aspenberg P, *et al*. Risk of atypical femoral fracture during and after bisphosphonate use. *N Engl J Med* 2014;371:974–6.
40 Whyte MP, Wenkert D, Clements KL, *et al*. Bisphosphonate-induced osteopetrosis. *N Engl J Med* 2003;349:457–63.
41 Tomlinson PB, Joseph C, Angioi M. Effects of vitamin D supplementation on upper and lower body muscle strength levels in healthy individuals. A systematic review with meta-analysis. *J Sci Med Sport* 2015;18:575–80.
42 Pearce SH, Cheetham TD. Diagnosis and management of vitamin D deficiency. *BMJ* 2010;340:b5664.
43 SACN. Vitamin D and Health report. 2016.
44 Wood CL, Cheetham TD. Vitamin D: increasing supplement use among at-risk groups (NICE guideline PH56). *Arch Dis Child Educ Pract Ed* 2016;101:43–5.
45 Ahmed SF, Farquharson C. The effect of GH and IGF1 on linear growth and skeletal development and their modulation by SOCS proteins. *J Endocrinol* 2010;206:249–59.
46 Högler W, Shaw N. Childhood growth hormone deficiency, bone density, structures and fractures: scrutinizing the evidence. *Clin Endocrinol* 2010;72:281–9.
47 Schweizer R, Martin DD, Schönau E, *et al*. Muscle function improves during growth hormone therapy in short children born small for gestational age: results of a peripheral quantitative computed tomography study on body composition. *J Clin Endocrinol Metab* 2008;93:2978–83.
48 White HD, Ahmad AM, Durham BH, *et al*. PTH circadian rhythm and PTH target-organ sensitivity is altered in patients with adult growth hormone deficiency with low BMD. *J Bone Miner Res* 2007;22:1798–807.
49 Stewart PM, Toogood AA, Tomlinson JW. Growth hormone, insulin-like growth factor-I and the cortisol-cortisone shuttle. *Horm Res* 2001;56 Suppl 1(Suppl 1):1–6.
50 Hodsman AB, Bauer DC, Dempster DW, *et al*. Parathyroid hormone and teriparatide for the treatment of osteoporosis: a review of the evidence and suggested guidelines for its use. *Endocr Rev* 2005;26:688–703.

51 Whitmarsh T, Treece GM, Gee AH, *et al*. Mapping bone changes at the proximal femoral cortex of postmenopausal women in response to alendronate and teriparatide alone, combined or sequentially. *J Bone Miner Res* 2015;30:1309–18.
52 Vahle JL, Sato M, Long GG, *et al*. Skeletal changes in rats given daily subcutaneous injections of recombinant human parathyroid hormone (1-34) for 2 years and relevance to human safety. *Toxicol Pathol* 2002;30:312–21.
53 Subbiah V, Madsen VS, Raymond AK, *et al*. Of mice and men: divergent risks of teriparatide-induced osteosarcoma. *Osteoporos Int* 2010;21:1041–5.
54 Winer KK, Zhang B, Shrader JA, *et al*. Synthetic human parathyroid hormone 1-34 replacement therapy: a randomized crossover trial comparing pump versus injections in the treatment of chronic hypoparathyroidism. *J Clin Endocrinol Metab* 2012;97:391–9.
55 Katznelson L, Finkelstein JS, Schoenfeld DA, *et al*. Increase in bone density and lean body mass during testosterone administration in men with acquired hypogonadism. *J Clin Endocrinol Metab* 1996;81:4358–65.
56 Crawford JD. Treatment of tall girls with estrogen. *Pediatrics* 1978;62:1189–95.
57 Reeves PT, Herndon DN, Tanksley JD, *et al*. Five-year outcomes after long-term oxandrolone adminstration in severely burned children: a randomized clinical trial. *Shock* 2016;45:367–74.
58 Misra M, Katzman D, Miller KK, *et al*. Physiologic estrogen replacement increases bone density in adolescent girls with anorexia nervosa. *J Bone Miner Res* 2011;26:2430–8.
59 Nattiv A, Loucks AB, Manore MM, *et al*. The Female Athlete Triad. *Med Sci Sport Exerc* 2007;39:1867–82.
60 Cummings SR, San Martin J, McClung MR, *et al*. Denosumab for prevention of fractures in postmenopausal women with osteoporosis. *N Engl J Med* 2009;361:756–65.
61 Hoyer-Kuhn H, Netzer C, Koerber F, *et al*. Two years' experience with denosumab for children with osteogenesis imperfecta type VI. *Orphanet J Rare Dis* 2014;9:145.
62 Setsu N, Kobayashi E, Asano N, *et al*. Severe hypercalcemia following denosumab treatment in a juvenile patient. *J Bone Miner Metab* 2016;34:118–22.
63 MacNabb C, Patton D, Hayes JS, *et al*. Sclerostin antibody therapy for the treatment of osteoporosis: clinical prospects and challenges. *J Osteoporos* 2016;2016:1–22.
64 Sinder BP, Eddy MM, Ominsky MS, *et al*. Sclerostin antibody improves skeletal parameters in a Brtl/+ mouse model of osteogenesis imperfecta. *J Bone Miner Res* 2013;28:73–80.
65 Recker RR, Benson CT, Matsumoto T, *et al*. A randomized, double-blind phase 2 clinical trial of blosozumab, a sclerostin antibody, in postmenopausal women with low bone mineral density. *J Bone Miner Res* 2015;30:216–24.
66 Yao W, Dai W, Jiang L, *et al*. Sclerostin-antibody treatment of glucocorticoid-induced osteoporosis maintained bone mass and strength. *Osteoporos Int* 2016;27:283–94.
67 Duong leT, Leung AT, Langdahl B. Cathepsin K inhibition: a new mechanism for the treatment of osteoporosis. *Calcif Tissue Int* 2016;98:381–97.
68 Bone HG, Dempster DW, Eisman JA, *et al*. Odanacatib for the treatment of postmenopausal osteoporosis: development history and design and participant characteristics of LOFT, the Long-Term Odanacatib Fracture Trial. *Osteoporos Int* 2015;26:699–712.

REVIEW

Bones and muscular dystrophies: what do we know?

Claire L. Wood[a,b] *and Volker Straub*[a]

Purpose of review
Muscle and bone are intrinsically linked, and therefore, it is not surprising that many muscular dystrophies are associated with impaired bone health and increased risk of osteoporosis. Osteoporotic fracture is an important and preventable cause of morbidity and mortality. This article will firstly review the general causes of impaired bone health in muscular dystrophies and then focus on the evidence available for the diagnosis and treatment of osteoporosis in specific conditions.

Recent findings
With the exception of DMD, there is a paucity of data regarding bone health in muscular dystrophies. However, it appears that in common with all types of muscular dystrophies that cause a significant level of muscle weakness and disability there is an increased risk of falls, fractures and decreased vitamin D levels. A better understanding of the extent of the impaired bone health and underlying causes could help to identify potential new therapeutic agents and aid clinical care.

Summary
It would be prudent for clinicians to assess fracture risk in their muscular dystrophy patients and if appropriate, arrange surveillance and recommend vitamin D supplementation. Additionally, fracture should be considered in any patient presenting with new-onset bone pain.

Keywords
muscle–bone interaction, muscular dystrophies, osteoporosis

INTRODUCTION

Muscular dystrophy is the term given to a rare and highly heterogeneous group of genetic muscle diseases, characterized by progressive skeletal muscle wasting and weakness from congenital through to adult-onset. As many muscular dystrophies are extremely rare, information about bone health in the individual conditions remains sparse. However, there are many causes in common across the group.

CAUSES OF IMPAIRED BONE HEALTH IN MUSCULAR DYSTROPHIES

Bone mineral density (BMD) in adulthood depends predominantly on growth and mineralization of the skeleton and the resultant peak bone mass achieved and then, to a lesser extent, on the subsequent loss. In healthy individuals, 80% of bone mass is accrued by 18 years of age [1] and a reduced peak BMD in childhood has been proposed as one of the strongest predictors of later life fractures [2]. Healthy bone is metabolically active and undergoes continuous remodelling to maintain the balance between bone formation and bone resorption. If this finely tuned process is disturbed, then osteoporosis can result. Osteoporosis is characterized by the depletion of bone mineral mass, combined with bone microarchitecture deterioration, enhanced bone fragility and a resultant increased fracture risk [3]; a 10% loss of vertebral bone mass can double the risk of a vertebral fracture [4].

Genetic predisposition only accounts for up to 50% of the variance in bone mass. Other important influences on bone health include lifestyle and sociodemographic factors (such as alcohol and tobacco use), nutrient intakes (including vitamin

[a]The John Walton Muscular Dystrophy Research Centre and MRC Centre for Neuromuscular Diseases, Institute of Genetic Medicine, Newcastle University and [b]Roslin Institute, Edinburgh University, Edinburgh, UK

Correspondence to Volker Straub, The John Walton Muscular Dystrophy Research Centre and MRC Centre for Neuromuscular Diseases, Institute of Genetic Medicine, Newcastle University, Centre for Life, Newcastle Upon Tyne NE1 3BZ, UK. Tel: +44 191 241 8617;
e-mail: volker.straub@ncl.ac.uk

Curr Opin Neurol 2018, 31:000–000
DOI:10.1097/WCO.0000000000000603

KEY POINTS

- Bone health and fracture risk should be assessed and vitamin D supplementation recommended in all patients with muscular dystrophy.
- With the exception of DMD, there is a paucity of data regarding bone health in muscular dystrophies.
- There is limited evidence for the use of any interventions to prevent or treat osteoporosis in this cohort.
- Consider fracture in any patient presenting with new-onset bone pain.

D and calcium intake), physical activity and bone stress, and comorbidities and drug treatments. Although impaired bone health in muscular dystrophies has been recognized for almost 80 years [5], it is only relatively recently that the importance of assessment and diagnosis of osteoporosis in these conditions has been recognized [6]. It is likely that several co-existing factors are responsible for the impaired bone health in muscular dystrophies:

The muscle–bone interaction

Bone and muscle are intrinsically linked and the mechanostat model [7] is a widely accepted theory; normal bone mineral accrual depends on a regulatory circuit sensing the bone deformations that are produced by muscle contractions to regulate osteocyte activity and modulate bone strength. The muscle weakness and reduced mobility that result from muscular dystrophies, and in particular those which are congenital or paediatric-onset, cause reduced loading forces on the bone, diminished bone growth and mineral accrual and result in osteopaenic/osteoporotic bone and low-trauma fractures, fractures that result from mechanical forces that would not ordinarily result in fracture [8,9]. A concise review has recently been published about the muscle–bone interaction [10▪]. In particular, once a patient becomes nonambulatory, and no dynamic or gravitational bone loading occurs, bone resorption exceeds bone formation; often termed disuse osteoporosis [11]. In support of this, retrospective data from the the Muscular Dystrophy Surveillance, Tracking and Research (MDSTAR) network combining Duchenne muscular dystrophy (DMD) and Becker muscular dystrophy patients, shows that full-time wheelchair use increased the risk of first fracture by 75% for every 3 months of use [12].

The myotendinous junction (MTJ) is also a major site of force transfer in skeletal muscle. There are two independent transsarcolemmal linkage systems present at the MTJ, the dystrophin–glycoprotein complex and the a7ß1 integrin complex. Therefore, if a muscular dystrophy involves a mutation encoding for components of this linkage then MTJ function will be impaired, further contributing to abnormal bone loading. Examples include DMD, Becker muscular dystrophy and limb girdle muscular dystrophies (LGMD)2I. However, even if two muscular dystrophies appear to be phenotypically very similar, for example, Becker muscular dystrophy and LGMD2I, they can have very different contractile properties [13]. Costameres are also important for the conduction of force during muscle contraction [14]. The lateral force generated through these is impaired in a number of muscular dystrophies, therefore directly reducing bone loading.

Glucocorticoids

Glucocorticoids (GCs) are currently the mainstay of treatment in DMD and are the only pharmacological intervention proven to stabilize muscle strength for at least a number of years. They are offered before muscle function starts to decline and overall slow the progression of disease [15▪▪]. Therefore, by adulthood, in addition to the effects of the muscular dystrophy itself, most patients with DMD have also been on high-dose GCs for over 10 years.

The combination of progressive myopathy and osteotoxic GC therapy in DMD contributes to significant growth retardation [16] and fragility fractures [17], which can be very challenging to manage. GC are not widely used in other muscular dystrophies, and in fact have been shown to be ineffective in some, such as dysferlinopathy [18].

Glucocorticoid-induced osteoporosis is associated with considerable morbidity and even mortality; a reduction in BMD of up to 40% can occur with glucocorticoid therapy, and it is estimated that up to half of those on long-term glucocorticoid therapy will experience fractures [19]. The use of glucocorticoid within the previous 6 months increased the risk of fracture three-fold and osteoporotic fracture by almost five-fold compared with nonexposed patients in a retrospective cohort study of patients with muscular dystrophies [6]. Data suggests that the greatest bone loss is experienced in the first year of treatment [20] and particularly in trabecular bone [19], but ongoing loss continues with prolonged treatment [21].

Vitamin D deficiency

Vitamin D is essential for skeletal health and regulates calcium absorption, and may also have

Table 1. Evidence for bone involvement and published data on bone health in muscular dystrophies

Disease	Primary bone involvement	Specific secondary risk factors for bone involvement	DXA data	Guidelines for monitoring bone health
DMD	Impaired osteoblast function [33,48] Activation of NFKB pathway and increased osteoclastogenesis	Glucocorticoid use Delayed puberty Inflammation and cytokine release	Many studies, including: LS BMD decreased compared with controls, further decreased when nonambulatory [39] GC dose and motor function correlated with BMD [49] LS BMD greater in BP-treated cohort of patients [50]	At each clinic visit [40▪▪]: ask about back pain/fractures At initial visit (with follow-up as required): serum calcium, phosphate, magnesium, alkaline phosphatase, parathyroid hormone Annually: calcium/vitamin D intake and vitamin D level Spine BMD by DXA Lateral thoracolumbar spine X-ray (1–2 yearly on GC, 2–3 yearly if not) Do lumbar spine X-ray if back pain or at least 0.5 SD decline in LS BMD *z*-score/12m)
FSHD	Not known	Increased incidence of vitamin D insufficiency	BMD not uniformly reduced but moderately correlated with strength and function [42▪]	No published guidelines
LGMD	Not known	Increased fall risk Greater than expected levels of vitamin D insufficiency [43]	None found	No information re monitoring bone health in guidelines [44]
Myotonic dystrophy	Not known	Testicular atrophy and hypogonadism Instability causing increased falls and fracture risk Increased incidence of vitamin D insufficiency	BMD comparable with control population [47▪]	No information regarding bone health in guidelines [51]

DMD, Duchenne muscular dystrophy; FSHD, facioscapulohumeral muscular dystrophy; LGMD, limb girdle muscular dystrophies.

an additional role in muscle strength [22]. Low vitamin D levels in patients with muscular dystrophies are likely to be multifactorial and may result from reduced sunlight exposure (especially in nonambulant patients), reduced oral motor function [23] and obesity. Vitamin D absorption is also reduced by glucocorticoid use, and so it is, recommended that vitamin D levels are checked routinely in DMD before commencing glucocorticoid and annually thereafter (Table 1; [24]). Adequate dietary calcium to meet the reference nutrient intake should also be advised and supplementation considered if this is unlikely to be reached [25].

Instability and fall risk

Postural abnormalities are found in almost all patients with muscular dystrophies and the abnormal vertebral load further contributes to an abnormality of bone loading; the resulting impairment of balance further increases fracture risk. Muscle instability also plays an indirect role in bone health, via an increased fall risk. For example, it has been shown that people with myotonic dystrophy fall 10 times more frequently than their healthy counterparts [26].

Effects of chronic disease and inflammation

The inflammatory process and cytokine release associated with muscular dystrophies may also contribute further to low bone density, as is demonstrated in other chronic diseases [27]. In particular in DMD, the activation of the NF-KB pathway may also cause altered muscle metabolism and activation of osteoclastogenesis [28].

Pubertal delay and hypogonadism

Testosterone acts via its conversion to 5-alpha dihydrotestosterone or oestradiol to enhance osteoblast differentiation and action and reduce osteoclast activity. Puberty is a crucial time for bone mineral accrual and pubertal timing is an important determinant of peak bone mass. Puberty is often delayed in many childhood chronic conditions and is almost universally delayed or absent in glucocorticoid-treated DMD [16,29]. Over half of patients were

found to have low testosterone levels when total and free serum levels were measured in 59 men with different dystrophinopathies [30].

Genetic defects associated with both muscle function and bone activity

It is possible that in certain neuromuscular conditions, the genetic defect may also have additional deleterious effects on bone health, or interact with other markers of osteoporosis [31], but this has not been studied in detail. For example, in spinal muscular atrophy, an interaction between osteoclast-stimulating factor (OSF) and survival motor neuron (SMN) protein may occur, thus causing an additional increase in bone resorption [32]. Studies of the dystrophin deficient mouse model for DMD (*mdx*) have also suggested a reduced bone mass and strength and higher osteoclast number and bone resorption rate, independent of glucocorticoid use [33–35]. These findings have been demonstrated prior to the onset of significant muscle weakness in young mice, therefore suggesting an intrinsic bone abnormality in addition to the reduced bone loading.

Whilst the above factors are likely to be common to most of the muscular dystrophies, the next section highlights the disease-specific evidence and guidance available on bone health.

Becker muscular dystrophy

Becker muscular dystrophy is caused by a reduction, rather than complete absence of dystrophin expression, thus resulting in a less severe phenotype compared with DMD. There is limited evidence regarding the increased fracture risk in Becker muscular dystrophy, but it follows that as disease progression occurs and muscle weakness worsens, osteopaenia/osteoporosis may occur [12].

Congenital muscular dystrophies

There does not appear to be any published data regarding bone health in congenital muscular dystrophies, probably because of the heterogeneity and rarity of the individual conditions. These individuals are at high risk of osteoporosis; however, because of the chronicity and severity of the muscle weakness and resultant effects on bone accrual.

Duchenne muscular dystrophy

DMD is the most common and best characterized form of muscular dystrophy and affects 1 in 4000 live male births [36]. As quality of life and survival rates continue to improve, bone health has become an increasingly important issue [37]. The presence of fractures in the DMD population and the risk factors for osteoporosis have been well documented [17,38,39] and the recently updated standards of care for DMD include comprehensive information for the monitoring of bone health (Table 1) [40▪▪]. Bone pain and fractures (long bone and vertebral) are common and can occur after minimal or no trauma. It has been predicted that by 100 months of high-dose daily glucocorticoid therapy as many as 75% will have at least one vertebral fracture [41]. Loss of ambulation occurs in up to half after their first fracture.

Facioscapulohumeral muscular dystrophy

A recent cross-sectional study of 94 adults from two sites aimed to determine whether BMD is reduced in individuals with facioscapulohumeral muscular dystrophy (FSHD) and whether or not BMD and fractures correlate with muscle strength or function [42▪]. They found that 30% had insufficient vitamin D levels, with reduced levels from the US cohort compared with Australia, possibly explained by latitude. The disease severity score, BMD, muscle strength and functionality were not uniformly reduced and were all highly variable, but whole-body and regional BMD were found to be moderately correlated with strength and function. Their conclusion was that effective treatment plans must be tailored based on individual BMD and strength to prevent fractures and promote optimal bone health.

Limb girdle muscular dystrophies

LGMDs are a genetically heterogeneous group of diseases characterized by muscle weakness and wasting in the arms and legs. A recent cross-sectional survey endeavoured to determine the risk factors for osteoporosis, falls and fractures in various muscle conditions, including LGMD. The data suggested an increased risk of falls in LGMD patients and osteoporosis in nonambulatory patients with myopathies and increased prevalence of vitamin D insufficiency with decreased levels in 55% of patients with LGMD. However, the authors stated that, 'Their conclusions were limited by the low number of participants with different myopathies, cross-sectional design and retrospective nature and that larger, multicentre study of patients with limb girdle muscular dystrophies seems to be warranted' [43]. The recently published guidelines do not provide any evidence regarding monitoring for osteoporosis with bone-density testing. [44]

Myotonic dystrophy

Myotonic dystrophy type 1 (DM1) is the most common adult-onset muscular dystrophy, whereas type

2 (DM2) is rarer and tends to have a milder phenotype with later onset of symptoms. Severe cases of DM1 may also present in childhood and congenital forms can occur. Approximately 80% of patients with myotonic dystrophy will develop primary hypogonadism, which often occurs later in adulthood and is frequently associated with low testosterone levels [45]. Although hypogonadism is usually associated with low BMD, a study of 32 myotonic dystrophy patients found lower vitamin D levels compared with the control group but comparable BMD scores when measured using dual energy X-ray absorptiometry (DXA) of the femoral neck [46]. There appears to be an increased fracture risk in DM1 patients regardless of BMD, because of the higher fall rate compared with some other muscular dystrophies [6]. A web-based survey of 573 adults with DM1 [47▪] found they had a 2.3 times increased risk of falling compared with a healthy adult over 65 years of age, although like any voluntary, questionnaire-based study, this will be subject to significant recall bias. Seventeen percent had sustained a fracture in the previous 12 months, with the ankle and foot accounting for the majority of fractures, but there was no data available regarding bone density.

INVESTIGATIONS INTO BONE HEALTH

When reviewing patients with muscular dystrophies, consideration should be given to their bone health and where available, guidelines followed to further assess their risk of osteoporosis. In the rarer dystrophies, where there are no clinical guidelines available, assessment of individual risk factors should be used to determine which, if any of the below investigations are performed, either as screening tools or as a response to bone pain or reduced function.

Fracture incidence

Fracture is the most clinically relevant endpoint when assessing bone health. Fractures are an important cause of morbidity and reduction in quality of life. Some can occur after minimal trauma, or even just on handling. Death because of fat embolism after long-bone fracture has also been reported in DMD [52]. The pathogenesis of fragility fracture is multifactorial. Assessment of fracture risk depends not only on BMD but also on several other factors including bone remodelling, morphology and architecture and muscle function and balance. Using fracture incidence as a proxy for bone health has important limitations. Firstly, the fracture pattern in muscular dystrophies is likely to differ from the healthy population. For example, lower participation in sports activities will lead to fewer upper extremity fractures. Falls also contribute to an increased risk of lower extremity fracture and particularly femoral fracture, which are otherwise rare in the young population. It is likely that vertebral fractures in DMD are under-diagnosed and any acute back pain or focal tenderness as well as sudden deterioration in mobility should warrant further investigation. Vertebral fractures usually cause change in the shape of the vertebrae and scoring systems such as the Genant semi-quantitative method [53] can be useful to determine the severity of vertebral fractures. In this method, fracture severity is assessed solely by determining the extent of vertebral height reduction and morphological change; type of deformity (such as wedge or compression) is not used to determine fracture grade.

Dual energy X-ray absorptiometry

Current standards of care recommend assessment of spinal BMD by DXA on an annual basis in DMD. Evidence for its use is less clear in the other muscular dystrophies (Table 1). The exact correlation between BMD and fracture risk remains unclear, although it probably remains the best clinically available proxy for fracture risk. Models like the Fracture Risk Assessment Tool (FRAX) can be useful in combination with DXA to predict fracture risk in adults [54], but this cannot be used in children. Furthermore, interpretation of DXA results in DMD patients can be technically challenging because of their small size, body composition and the possibility of contractures and spinal instrumentation. Appropriate software to enable size adjustment and longitudinal readings for the patients are essential for accurate interpretation of risk. Vertebral fractures can also cause spuriously high BMD readings because a given bone volume has effectively been compressed into a smaller area.

Bone turnover markers

Bone turnover markers can be useful in addition to BMD to estimate fracture risk and to determine response to therapy and treatment adherence, but have limited use in children because of variations in normal range. Markers of bone formation include bone-specific alkaline phosphatase, osteocalcin (which is the most abundant noncollagenous protein in the extracellular matrix) and P1NP (a propeptide of type 1 collagen). The most frequently used markers of resorption are C-telopeptide (CTX) and N-telopeptide (NTX), which are released from the C-terminal and N-terminal ends of type 1 collagen,

respectively. CTX is recommended by the National Osteoporosis Foundation as the reference marker of bone resorption [55]. Many bone turnover markers, however, are not readily available in clinical practice, thus limiting their use.

Spinal X-ray

The new standards of care in DMD place an increased emphasis on the use of spinal X-ray as a surveillance tool to try and improve detection of vertebral fracture (Table 1). Newer methods of vertebral fracture assessment are also being developed, including the use of lateral DXA images [56], which may reduce the necessity for spinal X-rays in the future.

Other imaging modalities

Peripheral quantitative computed tomography, MRI and ultrasound have currently only been used in the research setting when investigating bone health in muscular dystrophies. A novel study using ultrasound to comparing muscle and bone parameters in DMD, Becker, LGMD and FSHD found that Becker and DMD patients had significantly lower bone health scores [57]. There were no observed differences in LGMD and FSHD, but the authors felt that this may be because of sample sizes or limitations of ultrasound as a measurement technique because it cannot provide absolute measure of BMD, bone mineral content, or bone geometry or distinguish between cortical and trabecular bone. These limitations preclude its clinical use.

POTENTIAL TREATMENT STRATEGIES

There are very limited treatment strategies currently available for the treatment of osteoporosis associated with muscle diseases. The impaired osteoblast function described in both the *mdx* mouse and patients with DMD suggest that an anabolic bone treatment would be optimal, but there are no current options clinically available. A recent Cochrane review [58▪▪] concluded that, 'We know of no evidence from high-quality randomised controlled trials (RCTs) about the efficacy of interventions to prevent or treat corticosteroid-induced osteoporosis and prevent osteoporotic fragility fractures in DMD in children and adults.'

The next section focuses on some of the therapies that are currently in use, with examples highlighting their use in DMD.

Bisphosphonates

There is limited evidence for the use of bisphosphonates in DMD and their use varies by centre; some advocate prophylactic bisphosphonate use whereas in other institutions, they are reserved for the treatment of fractures and there is no consensus regarding timing of initiation, drug regimen or cessation of treatment. The efficacy of BP therapy on BMD appears to depend on the age at time of treatment and the amount of bone growth remaining [59]. Generally, they appear to be a well tolerated and effective therapy in cases of severe bone loss, although the long-term effect of inhibition of bone turnover remains unknown [60–62].

Prophylactic bisphosphonates in DMD in those receiving Glucocorticoid has been reported to be associated with increased survival [63] but evidence from this study should be interpreted with caution as it was a retrospective review of only 16 patients, 12 of whom were on intravenous bisphosphonates. Although bisphosphonates are frequently used to treat osteoporosis in DMD, they do not primarily affect osteoblast function and their use does not prevent the development of new vertebral fractures [64]. Sbrocchi *et al.* [65] found that using intravenous bisphosphonate therapy to treat vertebral fractures in DMD was associated with an improvement in back pain and stabilization/improvement in vertebral height ratios of previous vertebral fractures, but that it did not completely prevent the development of new vertebral fractures. A retrospective review of patients treated with risedronate for a mean of 3.6 years showed significantly less vertebral fractures in the treated cohort compared with a control group [50]. The lumbar spine (age and size adjusted) BMD *z*-scores also remained unchanged in treated patients, and were significantly greater than in the untreated cohort [50]. Recent work utilizing trans-iliac biopsy samples, however, suggests that caution needs to be taken before prophylactic bisphosphonates are used, particularly in a condition such as DMD, where there are additional risk factors for ongoing bone turnover suppression including myopathy and GCs [48]. They found that bone turnover was already low before the initiation of bisphosphonates and then as expected, the anti-resorptive bisphosphonate treatment decreased bone formation indices further. An unexpected drop in trabecular bone volume, however, was also noted and unlike in osteogenesis imperfecta, no structural improvements were seen.

In view of the risk of fracture in children with DMD and the impact of fracture on health and long-term mobility, prophylactic use of bisphosphonates may, therefore, be beneficial [65–67] but the method of administration and when to start, stop or pause treatment remains unclear [68]. It is likely that bisphosphonates are effective in the initial period of glucocorticoid-induced bone loss when

there is increased bone remodelling but become less responsive as osteoclast function reduces with prolonged treatment and bone remodelling ceases. After this time, bisphosphonates may further dampen bone remodelling and instead compromise skeletal quality, predisposing to fracture.

Parathyroid hormone

High levels of parathyroid hormone (PTH) stimulate osteoclastic bone resorption but intermittent low-dose PTH can stimulate osteoblast function by increasing PGE_2 and TGF-β release from bone [69]. This could, therefore, be a useful anabolic agent to counteract the adverse effects of GCs in osteoblasts. However, recombinant parathyroid hormone treatment using teriparatide requires daily subcutaneous injections and is currently contraindicated in children with a 'black box' warning, limiting its use to 2-year duration in adults [70] because of the risk of osteosarcoma.

Testosterone

The use of testosterone therapy in DMD has recently been reviewed [29] and it appears to be well tolerated in adolescents with DMD but our evaluation of practice found that neither growth nor pubertal developmental were optimal and few patients had adult endogenous testosterone levels posttreatment. There remains much variability in clinical practice regarding whether oral, topical or intramuscular preparations are used, and the age at initiation and duration of treatment vary greatly by centre. The importance of testosterone in the maintenance of muscle mass as well as bone density is critical, and testosterone supplementation should be considered when hypogonadism is present in adults with muscular dystrophies.

Vitamin D and calcium

There are multiple risk factors and evidence for vitamin D deficiency in this population as discussed above and so vitamin D supplementation should routinely be recommended to all patients with a muscular dystrophy. Whilst an adequate dietary calcium is required to satisfy reference intake levels, there is no evidence in the DMD population to indicate that additional calcium will have a beneficial impact on bone health. Patients with DMD are at risk of hypercalciuria and additional calcium may simply increase susceptibility to nephrocalcinosis [71].

CONCLUSION

With the exception of DMD, there is a paucity of data regarding bone health in muscular dystrophies. A better understanding of the extent of the impaired bone health and underlying causes could help to identify potential new therapeutic agents and aid clinical care. However, it appears that in common with all types of muscular dystrophies that cause a significant level of muscle weakness and disability, there is an increased risk of falls, fractures and decreased vitamin D levels. It would, therefore, be prudent for clinicians to assess fracture risk in their muscular dystrophy patients and if appropriately arrange surveillance and recommend vitamin D supplementation. Additionally, fracture should be considered in any patient presenting with new-onset bone pain.

Acknowledgements

Diagnostic facilities at the John Walton Muscular Dystrophy Research Centre are supported by the Nationally Commissioned Highly Specialised Service (HSS) for Neuromuscular Diseases (NHS England). The authors would like to thank Dr Timothy Cheetham, consultant paediatric endocrinologist, for his support of the service. The Newcastle University John Walton Muscular Dystrophy Research Centre is part of the Institute of Genetic Medicine and the Newcastle upon Tyne Hospitals NHS Foundation Trust.

Financial support and sponsorship

C.L.W. is supported by a MRC/MDUK clinical research fellowship (MR/N020588/1). Writing of the manuscript was not financially supported.

Conflicts of interest

There are no conflicts of interest.

REFERENCES AND RECOMMENDED READING

Papers of particular interest, published within the annual period of review, have been highlighted as:

- ■ of special interest
- ■■ of outstanding interest

1. Bachrach LK. Acquisition of optimal bone mass in childhood and adolescence. Trends Endocrinol Metab 2001; 12:22–28.
2. Wood CL, Stenson C, Embleton N. The developmental origins of osteoporosis. Curr Genomics 2015; 16:411–418.
3. NIH Consensus Development Panel on Osteoporosis Prevention, Diagnosis, Therapy. Osteoporosis prevention, diagnosis, and therapy. JAMA 2001; 285:785–795.
4. Klotzbuecher CM, Ross PD, Landsman PB, *et al.* Patients with prior fractures have an increased risk of future fractures: a summary of the literature and statistical synthesis. J Bone Miner Res 2000; 15:721–739.
5. Maybarduk P, Levine M. Osseous atrophy associated with progressive muscular dystrophy. Am J Dis Child 1941; 61:565–576.
6. Pouwels S, de Boer A, Leufkens HGM, *et al.* Risk of fracture in patients with muscular dystrophies. Osteoporos Int 2014; 25:509–518.

7. Frost HM. Bone's mechanostat: a 2003 update. Anat Rec A Discov Mol Cell Evol Biol 2003; 275:1081–1101.
8. Feber J, Gaboury I, Ni A, *et al.,* Canadian STOPP Consortium. Skeletal findings in children recently initiating glucocorticoids for the treatment of nephrotic syndrome. Osteoporos Int 2012; 23:751–760.
9. Matthews E, Brassington R, Kuntzer T, *et al.* Corticosteroids for the treatment of Duchenne muscular dystrophy. Cochrane Database of Syst Rev 2016; CD003725..
10. Veilleux L-N, Rauch F. Muscle-bone interactions in pediatric bone diseases.
■ Curr Osteoporos Rep 2017; 15:425–432.

A concise review detailing the importance of the muscle–bone interaction.

11. Takata S, Yasui N. Disuse osteoporosis. J Med Invest 2001; 48:147–156.
12. James KA, Cunniff C, Apkon SD, *et al.* Risk factors for first fractures among males with duchenne or becker muscular dystrophy. J Pediatr Orthop 2015; 35:640–644.
13. Løkken N, Hedermann G, Thomsen C, *et al.* Contractile properties are disrupted in Becker muscular dystrophy, but not in limb girdle type 2I. Ann Neurol 2016; 80:466–471.
14. Pardo JV, Siliciano JD, Craig SW. A vinculin-containing cortical lattice in skeletal muscle: transverse lattice elements mark sites of attachment between myofibrils and sarcolemma. Proc Natl Acad Sci U S A 1983; 80:1008–1012.
15. Birnkrant DJ, Bushby K, Bann CM, *et al.,* DMD Care Considerations Working
■■ Group. Diagnosis and management of Duchenne muscular dystrophy, part 1: diagnosis, and neuromuscular, rehabilitation, endocrine, and gastrointestinal and nutritional management. Lancet Neurol 2018; 17:251–267.

Part 1 of the recently updated standards of care, providing a comprehensive overview of the management of DMD.

16. Wood CL, Straub V, Guglieri M, *et al.* Short stature and pubertal delay in Duchenne muscular dystrophy. Arch Dis Child 2015; 101:101–106.
17. King WM, Ruttencutter R, Nagaraja HN, *et al.* Orthopedic outcomes of long-term daily corticosteroid treatment in Duchenne muscular dystrophy. Neurology 2007; 68:1607–1613.
18. Walter MC, Reilich P, Thiele S, *et al.* Treatment of dysferlinopathy with deflazacort: a double-blind, placebo-controlled clinical trial. Orphanet J Rare Dis 2013; 8:26.
19. Reid IR. Glucocorticoid osteoporosis–mechanisms and management. Eur J Endocrinol 1997; 137:209–217.
20. Laan RF, Buijs WC, van Erning LJ, *et al.* Differential effects of glucocorticoids on cortical appendicular and cortical vertebral bone mineral content. Calcif Tissue Int 1993; 52:5–9.
21. LoCascio V, Ballanti P, Milani S, *et al.* A histomorphometric long-term longitudinal study of trabecular bone loss in glucocorticoid-treated patients: prednisone versus deflazacort. Calcif Tissue Int 1998; 62:199–204.
22. Tomlinson PB, Joseph C, Angioi M. Effects of vitamin D supplementation on upper and lower body muscle strength levels in healthy individuals. A systematic review with meta-analysis. J Sci Med Sport 2015; 18:575–580.
23. Tilton AH, Miller MD, Khoshoo V. Nutrition and swallowing in pediatric neuromuscular patients. Semin Pediatr Neurol 1998; 5:106–115.
24. Patschan D, Loddenkemper K, Buttgereit F. Molecular mechanisms of glucocorticoid-induced osteoporosis. Bone 2001; 29:498–505.
25. British Nutrition Foundation Nutrition Bulletin 2005; 30:237-277.
26. Wiles CM, Busse ME, Sampson CM, *et al.* Falls and stumbles in myotonic dystrophy. J Neurol Neurosurg Psychiatry 2006; 77:393–396.
27. Joseph S, McCarrison S, Wong SC. Skeletal fragility in children with chronic disease. Horm Res Paediatr 2016; 86:71–82.
28. Morgenroth VH, Hache LP, Clemens PR. Insights into bone health in Duchenne muscular dystrophy. Bonekey Rep 2012; 1:1–11.
29. Wood CL, Cheetham TD, Guglieri M, *et al.* Testosterone treatment of pubertal delay in Duchenne muscular dystrophy. Neuropediatrics 2015; 46:371–376.
30. Al-Harbi TM, Bainbridge LJ, McQueen MJ, *et al.* Hypogonadism is common in men with myopathies. J Clin Neuromuscul Dis 2008; 9:397–401.
31. Estrada K, Styrkarsdottir U, Evangelou E, *et al.* Genome-wide meta-analysis identifies 56 bone mineral density loci and reveals 14 loci associated with risk of fracture. Nat Genet 2012; 44:491–501.
32. Kurihara N, Menaa C, Maeda H, *et al.* Osteoclast-stimulating factor interacts with the spinal muscular atrophy gene product to stimulate osteoclast formation. J Biol Chem 2001; 276:41035–41039.
33. Rufo A, Del Fattore A, Capulli M, *et al.* Mechanisms inducing low bone density in Duchenne muscular dystrophy in mice and humans. J Bone Min Res 2011; 26:1891–1903.
34. Novotny SA, Warren GL, Lin AS, *et al.* Bone is functionally impaired in dystrophic mice but less so than skeletal muscle. Neuromuscul Disord 2011; 21:183–193.
35. Nakagaki WR, Bertran CA, Matsumura CY, *et al.* Mechanical, biochemical and morphometric alterations in the femur of mdx mice. Bone 2011; 48:372–379.
36. Mendell JR, Shilling C, Leslie ND, *et al.* Evidence-based path to newborn screening for Duchenne muscular dystrophy. Ann Neurol 2012; 71: 304–313.
37. Buckner JL, Bowden SA, Mahan JD. Optimizing bone health in duchenne muscular dystrophy. Int J Endocrinol 2015; 2015:928385.
38. McAdam LC, Mayo AL, Alman BA, *et al.* The Canadian experience with long-term deflazacort treatment in Duchenne muscular dystrophy. Acta Myol 2012; 31:16–20.
39. Larson CM, Henderson RC. Bone mineral density and fractures in boys with Duchenne muscular dystrophy. J Pediatr Orthop 2000; 20:71–74.
40. Birnkrant DJ, Bushby K, Bann CM, *et al.* Diagnosis and management of
■■ Duchenne muscular dystrophy, part 2: respiratory, cardiac, bone health, and orthopaedic management. Lancet Neurol 2018; 17:347–361.

Part 2 of the recently updated standards of care, providing a comprehensive overview of the management of DMD.

41. Bothwell JE, Gordon KE, Dooley JM, *et al.* Vertebral fractures in boys with Duchenne muscular dystrophy. Clin Pediatr (Phila) 2003; 42:353–356.
42. Chagarlamudi H, Corbett A, Stoll M, *et al.* Bone health in facioscapulohumeral
■ muscular dystrophy: a cross-sectional study. Muscle Nerve 2017; 56: 1108–1113.

The first published study investigating bone health in FSHD.

43. Danckworth F, Karabul N, Posa A, *et al.* Risk factors for osteoporosis, falls and fractures in hereditary myopathies and sporadic inclusion body myositis - a cross sectional survey. Mol Genet Metab Rep 2014; 1:85–97.
44. Narayanaswami P, Weiss M, Selcen D, *et al.,* Guideline Development Subcommittee of the American Academy of Neurology; Practice Issues Review Panel of the American Association of Neuromuscular & Electrodiagnostic Medicine. Evidence-based guideline summary: diagnosis and treatment of limb-girdle and distal dystrophies: report of the Guideline Development Subcommittee of the American Academy of Neurology and the Practice Issues Review Panel of the American Association of Neuromuscular & Electrodiagnostic Medicine. Neurology 2014; 83:1453–1463.
45. Vazquez JA, Pinies JA, Martul P, *et al.* Hypothalamic-pituitary-testicular function in 70 patients with myotonic dystrophy. J Endocrinol Invest 1990; 13:375–379.
46. Terracciano C, Rastelli E, Morello M, *et al.* Vitamin D deficiency in myotonic dystrophy type 1. J Neurol 2013; 260:2330–2334.
47. Jiménez-Moreno AC, Raaphorst J, Babačić H, *et al.* Falls and resulting
■ fractures in myotonic dystrophy: results from a multinational retrospective survey. Neuromuscul Disord 2018; 28:229–235.

Recent data showing an increased risk of falls in myotonic dystrophy.

48. Misof BM, Roschger P, Mcmillan HJ, *et al.* Histomorphometry and bone matrix mineralization before and after bisphosphonate treatment in boys with Duchenne muscular dystrophy: a paired transiliac biopsy study. J Bone Min Res 2016; 31:1–10.
49. Bianchi ML, Mazzanti A, Galbiati E, *et al.* Bone mineral density and bone metabolism in Duchenne muscular dystrophy. Osteoporos Int 2003; 14:761–767.
50. Srinivasan R, Rawlings D, Wood CL, *et al.* Prophylactic oral bisphosphonate therapy in duchenne muscular dystrophy. Muscle Nerve 2016; 54:79–85.
51. Turner C, Hilton-Jones D. The myotonic dystrophies: diagnosis and management. J Neurol Neurosurg Psychiatry 2010; 81:358–367.
52. Feder D, Koch ME, Palmieri B, *et al.* Fat embolism after fractures in Duchenne muscular dystrophy: an underdiagnosed complication? A systematic review. Ther Clin Risk Manag 2017; 13:1357–1361.
53. Genant HK, Wu CY, van Kuijk C, Nevitt MC. Vertebral fracture assessment using a semiquantitative technique. J Bone Min Res 1993; 8:1137–1148.
54. Kanis JA, Johnell O, Oden A, *et al.* FRAX and the assessment of fracture probability in men and women from the UK. Osteoporos Int 2008; 19:385–397.
55. Vasikaran S, Eastell R, Bruyère O, *et al.,* IOF-IFCC Bone Marker Standards Working Group. Markers of bone turnover for the prediction of fracture risk and monitoring of osteoporosis treatment: a need for international reference standards. Osteoporos Int 2011; 22:391–420.
56. Blake GM, Rea JA, Fogelman I. Vertebral morphometry studies using dual-energy x-ray absorptiometry. Semin Nucl Med 1997; 27:276–290.
57. Morse CI, Smith J, Denny A, *et al.* Bone health measured using quantitative ultrasonography in adult males with muscular dystrophy. J Musculoskelet Neuronal Interact 2016; 16:339–347.
58. Bell JM, Shields MD, Watters J, *et al.* Interventions to prevent and treat
■■ corticosteroid-induced osteoporosis and prevent osteoporotic fractures in Duchenne muscular dystrophy. Cochrane Database Syst Rev 2017; CD010899.

A recent Cochrane review highlighting the lack of treatment options available to prevent or treat corticosteroid-induced osteoporosis in DMD.

59. Brumsen C, Hamdy NA, Papapoulos SE, *et al.* Long-term effects of bisphosphonates on the growing skeleton. Studies of young patients with severe osteoporosis. Medicine (Baltimore) 1997; 76:266–283.
60. Kwek EB, Goh SK, Koh JS, *et al.* An emerging pattern of subtrochanteric stress fractures: a long-term complication of alendronate therapy? Injury 2008; 39:224–231.
61. Girgis CM, Sher D, Seibel MJ. Atypical femoral fractures and bisphosphonate use. N Engl J Med 2010; 362:1848–1849.
62. Hennedige AA, Jayasinghe J, Khajeh J, Macfarlane TV, *et al.* Systematic review on the incidence of bisphosphonate related osteonecrosis of the jaw in children diagnosed with osteogenesis imperfecta. J Oral Maxillofac Res 2013; 4:e1.
63. Gordon KE, Dooley JM, Sheppard KM, *et al.* Impact of bisphosphonates on survival for patients with Duchenne muscular dystrophy. Pediatrics 2011; 127:e353–e358.

64. Rauch F, Travers R, Plotkin H, Glorieux FH. The effects of intravenous pamidronate on the bone tissue of children and adolescents with osteogenesis imperfecta. J Clin Invest 2002; 110:1293–1299.

65. Sbrocchi AM, Rauch F, Jacob P, *et al.* The use of intravenous bisphosphonate therapy to treat vertebral fractures due to osteoporosis among boys with Duchenne muscular dystrophy. Osteoporos Int 2012; 23:2703–2711.

66. Houston C, Mathews K, Shibli-Rahhal A. Bone density and alendronate effects in Duchenne muscular dystrophy patients. Muscle Nerve 2014; 49:506–511.

67. Palomo Atance E, Ballester Herrera MJ, Marquez de La Plata MA, *et al.* Alendronate treatment of osteoporosis secondary to Duchenne muscular dystrophy. An Pediatr 2011; 74:122–125.

68. Wood CL, Marini Bettolo C, Bushby K, *et al.* Bisphosphonate use in Duchenne muscular dystrophy - why, when to start and when to stop? Expert Opin Orphan Drugs 2016; 4:407–416.

69. Girotra M, Rubin MR, Bilezikian JP. The use of parathyroid hormone in the treatment of osteoporosis. Rev Endocr Metab Disord 2007; 7:113–121.

70. Elraiyah T, Gionfriddo MR, Murad MH. Acting on black box warnings requires a GRADE evidence table and an implementation guide: the case of teriparatide. J Clin Epidemiol 2015; 68:698–702.

71. Braat E, Hoste L, De Waele L, *et al.* Renal function in children and adolescents with Duchenne muscular dystrophy. Neuromuscul Disord 2015; 25: 381–387.

Treatment of Duchenne muscular dystrophy: first small steps

Published Online
July 17, 2017
http://dx.doi.org/10.1016/S0140-6736(17)31669-0

See Online/Articles
http://dx.doi.org/10.1016/S0140-6736(17)31611-2

Duchenne muscular dystrophy (DMD) is a progressive and life-limiting X-linked recessive disorder caused by mutations in the *DMD* gene that result in reduced or absent dystrophin production. Dystrophin is part of the dystrophin–glycoprotein complex, which acts as a scaffold between the actin cytoskeleton and the extracellular matrix and, as such, maintains muscle fibre integrity. Absence of dystrophin causes progressive and irreversible tissue damage, resulting in muscle fibrosis and fatty replacement. Despite DMD being the focus of intensive research for decades, there is still no cure for the approximately 250 000 people with this disorder worldwide.

Ataluren has been marketed under the trade name Translarna by PTC Therapeutics (South Plainfield, NJ, USA). The drug allows ribosomal readthrough of premature stop codons, thus enabling production of functional dystrophin that might ameliorate disease progression.[1] Roughly 10–15% of patients with DMD have an underlying nonsense mutation in the *DMD* gene[2] and so could potentially benefit from treatment with ataluren.

In *The Lancet*, Craig McDonald and colleagues[3] present the results of a phase 3, multicentre, randomised, double-blind, placebo-controlled trial (ACT DMD) that assessed the ability of ataluren to stabilise ambulation, with a focus on a prespecified subgroup of patients with ambulatory decline. The primary endpoint of change in 6-min walk distance (6MWD) from baseline to week 48, with a hypothesis of a difference of at least 30 m between ataluren-treated and placebo-treated patients, did not differ significantly between groups in the intention-to-treat population (difference 13·0 m [SE 10·4], 95% CI −7·4 to 33·4; p=0·213). However, a benefit of ataluren was observed in the subgroup of patients with a baseline 6MWD of 300 m or more to less than 400 m (difference *vs* placebo 42·9 m [SE 15·9], 95% CI 11·8–74·0; p=0·007).

ACT DMD is a follow-on trial[4] and was driven by the need to provide confirmatory efficacy data before full marketing authorisation of ataluren. In 2016, the European Medicines Agency gave conditional approval for the drug to be used and, once data demonstrating its ability to stabilise ambulation were obtained, the National Institute for Health and Care Excellence (NICE) agreed reimbursement within a managed access agreement for the treatment of ambulant patients with DMD aged 5 years or older.[5] Ataluren has not had a smooth passage through to marketing authorisation, with the initial extension of the phase 2b study halted by the data safety monitoring board because of poor efficacy before subgroup analysis (NCT00847379). The clinical trial in non-ambulatory patients was likewise terminated prematurely (NCT01009294).

The present trial highlights the potential difficulties that can arise when selecting a primary outcome in clinical studies. The 6MWD is regarded as one of the gold-standard outcome measures in DMD trials, but there are several limitations to its use. McDonald and colleagues explain that the 6MWD is effort dependent and hence has restricted sensitivity in patients with higher baseline function, and shows substantial interpatient variability in patients with lower baseline function.[3,6] A difference of 30 m in the 6MWD has been suggested to be clinically meaningful.[7] In McDonald and colleagues' trial, a change of only 13 m favouring ataluren was recorded overall, but a much larger change of 43 m was recorded in the prespecified subgroup of patients with a baseline 6MWD of 300 m or more to less than 400 m—ie, those already in the decline phase of the disease.[3] Interventions that have a beneficial effect before the decline phase of DMD are desirable, but the 6MWD does not seem to be an optimal primary outcome measure in this group of

Allen J Schaben/Contributor/Getty

patients. Alternative objective and non-invasive markers are needed, and research into the use of muscle MRI and other biomarkers is ongoing.[8–10]

The ACT DMD study is an excellent example of the extensive international, multicentre, collaborative approach that is essential given the rare nature of DMD. The study also relies on core sets of outcome measures and adheres to international care standards.[8] However, at best, the results show the acceptable short-term safety profile of ataluren and evidence of efficacy in a small subset of patients with DMD. Further research is needed, and indeed is already underway, to establish the longer-term safety profile and efficacy of this drug (NCT02090959). In the meantime, it is perhaps a reflection of the paucity of treatments for one of the most common fatal genetic diseases diagnosed in childhood that NICE have agreed to fund a drug that costs in excess of £200 000 per patient per year on the basis of secondary trial outcomes.

A wide variety of different therapeutic approaches are being trialled in patients with DMD, several of which are mutation specific. These approaches include the use of compounds facilitating the upregulation of dystrophin analogues (NCT02858362); exon-skipping techniques with antisense oligonucleotides to convert an out-of-frame mutation into an in-frame mutation, thus allowing partial dystrophin expression;[11] and the use of selective steroid receptor modulators (NCT02760264). In the meantime, ACT DMD and the use of ataluren provide a glimmer of hope for the 15% of patients with a nonsense mutation and are the first small steps towards effective treatment of this patient population, hopefully with more to follow.

*Claire L Wood, Tim Cheetham
The John Walton Muscular Dystrophy Research Centre, Institute of Genetic Medicine, International Centre for Life (CLW) and Department of Paediatric Endocrinology, Royal Victoria Infirmary (TC), Newcastle University, Newcastle upon Tyne NE1 3BZ, UK
claire.wood@newcastle.ac.uk

We declare no competing interests.

1 Welch EM, Barton ER, Zhuo J, et al. PTC124 targets genetic disorders caused by nonsense mutations. *Nature* 2007; **447:** 87–91.
2 Aartsma-Rus A, Ginjaar IB, Bushby K. The importance of genetic diagnosis for Duchenne muscular dystrophy. *J Med Genet* 2016; **53:** 145–51.
3 McDonald CM, Campbell C, Erazo R, et al; the Clinical Evaluator Training Group, the ACT DMD Study Group. Ataluren in patients with nonsense mutation Duchenne muscular dystrophy (ACT DMD): a multicentre, randomised, double-blind, placebo-controlled, phase 3 trial. *Lancet* 2017; published online July 17. http://dx.doi.org/10.1016/S0140-6736(17)31611-2.
4 Bushby K, Finkel R, Wong B, et al; PTC124-GD-007-DMD Study Group. Ataluren treatment of patients with nonsense mutation dystrophinopathy. *Muscle Nerve* 2014; **50:** 477–87.
5 National Institute for Health and Care Excellence. Ataluren for treating Duchenne muscular dystrophy with a nonsense mutation in the dystrophin gene. July, 2016. https://www.nice.org.uk/guidance/hst3 (accessed June 8, 2017).
6 Mcdonald CM, Henricson EK, Abresch RT, et al. The 6-minute walk test and other endpoints in Duchenne muscular dystrophy: longitudinal natural history observations over 48 weeks from a multicenter study. *Muscle Nerve* 2013; **48:** 343–56.
7 Lynn S, Aartsma-Rus A, Bushby K, et al. Measuring clinical effectiveness of medicinal products for the treatment of Duchenne muscular dystrophy. *Neuromuscul Disord* 2015; **25:** 96–105.
8 Straub V, Balabanov P, Bushby K, et al. Stakeholder cooperation to overcome challenges in orphan medicine development: the example of Duchenne muscular dystrophy. *Lancet Neurol* 2016; **15:** 882–90.
9 Hathout Y, Seol H, Han MH, Zhang A, Brown KJ, Hoffman E. Clinical utility of serum biomarkers in Duchenne muscular dystrophy. *Clin Proteomics* 2016; **13:** 9.
10 Hollingsworth KG, Garrood P, Eagle M, Bushby K, Straub V. Magnetic resonance imaging in Duchenne muscular dystrophy: longitudinal assessment of natural history over 18 months. *Muscle Nerve* 2013; **48:** 586–88.
11 Wood MJ. To skip or not to skip: that is the question for Duchenne muscular dystrophy. *Mol Ther* 2013; **21:** 2131–32.